ORTHOGONAL COLLOCATION AS A METHOD OF ANALYSIS IN CHEMICAL REACTION ENGINEERING

by

NOBLE BRADFORD FERGUSON

A dissertation submitted in partial fulfillment

of the requirements for the degree of

DOCTOR OF PHILOSOPHY

UNIVERSITY OF WASHINGTON

1971

Approved by Bruce A. Finlayson

Department Chemical Engineer

Date July 30, 1971

UNIVERSITY OF WASHINGTON

Date: July 16, 1971

We have carefully read the dissertation entitled Orthogonal Collocation as a Method of Analysis in Chemical Reaction Engineering

submitted by Noble Bradford Ferguson in partial fulfillment of the requirements of the degree of Doctor of Philosophy in Chemical Engineering and recommend its acceptance. In support of this recommendation we present the following joint statement of evaluation to be filed with the dissertation.

The thesis concerns approximate solution of nonlinear ordinary and partial differential equations arising in chemical reactor analysis. The first chapter presents the results of computations and compares the collocation method to other methods of analysis. Stability and convergence of the method are proved. The most significant results are those in the next chapter on error bounds. Prior to this time, with most numerical solutions it was rarely possible to specify the error, although sometimes an error is estimated from the numerical calculations. Mr. Ferguson derives rigorous error bounds so that after finding an approximate solution an upper bound on the error can be derived even though an exact solution is not known. Several example calculations are done and demonstrate that the bounds can be within 0.01 per cent or smaller. The final chapter applies the methods to an engineering problem, the analysis of a catalytic muffler to reduce air pollution from automobiles. In this chapter the candidate demonstrates his ability to incorporate engineering intuition to provide a mathematical model with the minimum sophistication necessary.

DISSERTATION READING COMMITTEE: Bruce A Finlayson

Norman F. Sather

Lewis T. Fan

In presenting this disseration in partial fulfillment of the requirements for the doctoral degree at the University of Washington, I agree that the Library shall make its copies freely available for inspection. I further agree that extensive copying of this dissertation is allowable only for scholarly purposes. Requests for copying or reproduction of this dissertation may be referred to University Microfilms, 300 North Zeeb Road. Ann Arbor, Michigan 48106, to whom the author has granted "the right to reproduce and sell (a) copies of the manuscript in microform and/or (b) printed copies of the manuscript made from microform."

Signature Nelda B. Ferguson

Date July 30, 1971

TABLE OF CONTENTS

LIST OF TABLES

LIST OF FIGURES

NOTATION

(Any equation that is referenced is preceded by the letter for the chapter in which it occurs.)

a	geometry factor, for example eq. A11
a_i or $a_i^{(n)}$	expansion coefficients
A	frequency factor of the rate constant, k
A_{ji}	matrix element, for example eq. A14, representing the Lagrange interpolation coefficient for the first derivative operator
a^{ij}	coefficient matrix of eq. B12 which couples the derivatives
a_o	uniform ellipticity constant for a^{ij}
A/F	air-to-fuel ratio of mixture into automobile engine
b_i or $b_i^{(n)}$	expansion coefficients
B_{ji}	matrix element, for example eq. A15, representing the Lagrange interpolation coefficient for the Laplacian operator
b	transformation parameter, for example eq. B13
$\partial\Omega$	boundary of Ω
c	concentration or heat capacity
c_i	expansion coefficients
C_{ji}	matrix element, for example eq. A12
$\tilde{c}_i$	approximate solution at the i-th collocation point
c_1, c_2	positive numbers of eq. B68
$\underline{c}$	vector function
dv	differential element of integration
d_p	particle diamter

D_t	tube diameter
D, D_i	spatial domains
D_{ji}	matrix elements, for example eq. A13
d_i	expansion coefficients as defined in Table B16
D_s^e	effective mass diffusivity in a catalyst particle
D_{NO-N_2}	binary diffusion coefficient for nitric oxide and nitrogen
e_i	i-th component of numerical integration error for system of differential equations
E_1, E_2, E_3	defined by eq. A57
E	activation energy in the definition of the Arrhenius type rate constant
$E^{(n+1)}$	quadrature error for a scheme using n interior quadrature points and 1 boundary point
f	friction factor or function
f_i	expansion function
F	volumetric flow rate
FTP	Federal Test Procedure
g(t)	function of eqs. A27 and A49
g_i	mass fraction of the i-th component or constant of eq. B16
G	mass flux or Green's function
∇	"grad" operator
h(t)	function of eqs. A26 and A50
h_t	heat transfer coefficient
H_n	subspace, for example eq. B4
h_{ot}	over-all heat transfer coefficient

ΔH_i^s	heat of adsorption
ΔH_{RXN}	heat of reaction
[I]	identity matrix
k	a rate constant or a numerical parameter
k_1, k_2	constants defined in eq. A18
k_o, k_1	constants defined in eqs. A26-27
k_s^e	effective solid thermal conductivity
k_j	parameter of eq. B76
k_o, k_j	constants of eq. B20
K_A, K_B	adsorption equilibrium constants
k_g^{NO}	mass transfer coefficient for nitric oxide
k_r^e	effective thermal conductivity (radial component) in a packed bed
K_1, K_2	constants defined by eq. B28
K_i	differential operator of eq. B65
K_i^*	adjoint operator of K_i
ℓ_j	parameter of eq. B76
$L_i(x^2)$	Lagrange interpolation polynomial
L	length parameter
$\bar{m}$	mass average molecular weight
m_i	molecular weight of i-th component
m	number of collocation points (in method of least squares)
M	Lipschitz constant
$\bar{M}$	constant defined by eq. B25

$m(t)$	a priori upper bound for the solution to the transient heat balance for a nonisothermal chemical reaction
$[M]$	a matrix notation
n	number of collocation points or expansion functions, or n-th order chemical reaction
$\|(\cdot)\|_\infty =$	$\max \|(\cdot)\|$
$\|(\cdot)\|^2_{L_2} =$	$\int_D (\cdot)^2 \, dv$
Nu	Nussalt number
N_1	inverse of the dimensionless thermal conductivity
N_2	inverse of the dimensionless mass diffusivity
N_{ij}	defined in eq. B41
$N_j =$	$\sum_i M^2_{ji}$
$N =$	$\sqrt{\max_{\underline{x}} \underline{v} \cdot \underline{v}}$
$\|(\cdot)\|$	a general norm
NO_x	a mixture of the nitric oxides, primarily nitric oxide(NO) and nitrous oxide (NO_2)
$O(\cdot)$	Landau symbol
p_A, p_B	partial pressures of components A and B
Δp	pressure drop
P_{TOTAL}	pressure (absolute), total, eq. C6
P_{i-1}	orthogonal polynomial, (i-1)-th order in the independent variable
Pr	Prandtl number

Pe_z^m	axial mass Peclet number
Pe_z^h	axial heat Peclet number
Q_{ji}	matrix element, defined in eq. A14
r_i	i-th collocation point
r	radial coordinate or constant in eq. B3
Δr	radial increment
$\|r_j\|$	j-th over-all rate expression
R	operator
$R(\tilde{u})$	residual function
R_p	particle radius
R_g	ideal-gas constant
Re	particle Reynolds number, eq. C8
S_T	external surface area of particles in the reactor
Sc	Schmidt number
Sh	Sherwood number
t	time variable
t'	upper limit of time variable considered
Δt	time increment (or step size)
T	temperature or upper limit of time considered
$\tilde{T}_i$	approximate solution at the i-th collocation point
u	exact solution of differential equation
u_i	expansion functions
$\tilde{u}_i$	approximate solution at the i-th collocation point
$\tilde{u}$	approximate solution

$\underline{u}$	vector function
v	function
$\underline{v}$	vector function, for example velocity function in eq. B63
$\langle v \rangle$	a vector notation
V, V_{TOTAL}	total reactor volume
V_i	volume of i-th mixing cell
$w(x)$ or $w_i(x)$	weight functions
$W_j^{(n+1)}$	j-th quadrature weight-coefficient of a scheme using n interior points and 1 boundary point
x, $\underline{x}$	spatial coordinates
x_j	j-th collocation point
Δx	spatial increment (or step size)
y	exact solution of a differential equation
$\tilde{y}^{(1)}$ or $\tilde{y}^{(2)}$	approximate solutions
z	axial coordinate in tubular, packed-bed reactor

Greek letters:

$\alpha_1, \alpha_2, \alpha_3, \alpha_4$	dimensionless equilibrium constants of eqs. B52-53
α	constant of eq. B3, of eq. B35, or eq. B63
β	dimensionless heat of reaction
β_j	constant of eq. B64
γ	dimensionless activation energy
γ_j	constant of eq. B64

$\delta(\underline{x} - \underline{x}_j)$	Dirac delta function
δ_{ij}	Kronecker delta
δ_j	constant of eq. B64
ϵ	void fraction, reactor
ϵ_p	particle void fraction
ϵ_j	j-th error component of the approximate solution to a system of equations
ξ	effectiveness factor
λ_i	i-th eigenvalue
Ω	spatial domain
ϕ	Thiele modulus
$\phi(r)$	function of eq. B48
$\psi(r)$	function of eq. B48
ρ	density
θ_i	auxilliary function introduced in section B5.
$\mu(\cdot)$	spectral radius of a matrix

Subscripts:

ref	reference point
x	first partial derivative with respect to x
t	first partial derivative with respect to t
xx	second partial derivative with respect to x
,j	partial derivative with respect to j-th spatial coordinate
A, B, C	different species of mass balance
i, j, k	indices

i	i-th mixing cell
p	particle
s	solid
g	gas
f	fluid
t	tube

Superscripts:

g	gas
s	solid

ACKNOWLEDGMENT

The scholarly advice and understanding provided by Dr. B. A. Finlayson has been a continual benefit to my course of study at the University of Washington. It is with deep respect that I acknowledge his guidance.

INTRODUCTION

While the approximate methods of solving differential equations receive occasional consideration in texts and in the literature these methods continue to be viewed with a certain amount of curiosity. This is due partly to the association of specific methods with specific problems, for example the integral method is frequently associated with the boundary-layer equations. Quite often these associations are presented in such a way (unintentionally) as to obscure the manner in which the method can be generalized and applied to additional problems. If one considers the use of these methods in solving nonlinear differential equations one often finds that the resulting mathematics is unduly complicated (as compared to other means of solution). The objective of this study is to provide an extensive development of an approximate method which has a great deal of potential and to derive new error bounds for the purpose of assessing the accuracy of such an approximate solution.

In Chapter A we show how the method of orthogonal collocation, an approximate method of solution, is easily generalized for application to many different types of nonlinear ordinary and parabolic partial differential equations. Unlike many other approximate methods of solution, the method of orthogonal collocation is quite easy to apply to nonlinear problems, for example the method reduces a semi-linear parabolic partial differential equation to a system of first-order ordinary differential equations. We illustrate the application of this method by

analyzing different nonlinear differential equations common to reaction engineering. Briefly, the numerical illustrations indicate that, for nonlinear parabolic partial differential equations, the method requires only $\frac{1}{4}$ to $\frac{1}{40}$ the computation time required to obtain a solution of comparable accuracy (estimated) with a finite difference scheme. We develop several new features for the method with respect to its use and prove that the convergence of the solution obtained by Galerkin's method is sufficient to guarantee the convergence of the solution obtained by the method of orthogonal collocation. This last fact allows one to prove convergence of the method of orthogonal collocation (in many cases) by simply using the available convergence proofs for Galerkin's method.

While a method of solving differential equations may be easy to use for many types of problems, one does not generally know anything about the accuracy of the approximate solution (we are referring to a rigorous assessment of the error). With an error bound one is able to compare the accuracy obtained using different approximate methods, using different expansion functions (when the approximate solution is assumed to have the form of a linear combination of know functions and unknown expansion coefficients), or using different numbers of expansion functions. In Chapter B we derive several new pointwise and mean-square error bounds for nonlinear, second-order ordinary differential equations and semi-linear parabolic partial differential equations. These results are valid for systems of equations. By means of example, we show that

the method of orthogonal collocation, using only three collocation points, provides approximate solutions which are pointwise accurate to within 0.01%. The error bounds represent a significant advancement in the field of approximate methods of solution.

In Chapter C we analyze a packed-bed reactor for the conversion of nitric oxide to nitrogen and carbon dioxide. The reactant stream is, for this problem, the exhaust from an automobile. We use the method of orthogonal collocation at various stages of the analysis. Based on available data, the reactor is modelled by a series of four mixing-cells in which the reaction occurs heterogeneously. The completed model simulates the conversion of nitric oxide under the transient operating conditions prescribed by the Federal Test Procedure. The analysis of the transient model indicates that the thermal inertia of the solid packing is an extremely important variable.

CHAPTER A

Collocation as a Method of Analysis

The method of collocation is a means of obtaining an approximate solution to a differential equation. This method is particularly useful for nonlinear ordinary differential equations and nonlinear parabolic partial differential equations, as demonstrated in this chapter. Briefly, the method requires the approximate solution to satisfy the differential equation exactly at a few selected points (collocation points) in the domain of the independent variable(s). When these points are chosen as the roots of an appropriate orthogonal polynomial, the method is referred to as orthogonal collocation. We have assumed that the approximate solution has the form of a linear combination of functions and these are referred to as expansion functions.

The following section illustrates, by means of a simple nonlinear ordinary differential equation, the use of the method of collocation. One must choose the expansion functions and the collocation points. The accuracy can be estimated by increasing the number of points and noting any changes in the approximate solution. One should not accept a questionable approximate solution.

Current evidence indicates that the method of orthogonal collocation is a substantial improvement over the simpler method of collocation. The method of orthogonal collocation transforms an ordinary differential equation into a system of n algebraic equations

where n is the number of collocation points. This system of equations can be written with the values of the approximate solution at the collocation points as the unknown quantities. We have found that one set of orthogonal polymials gives better results for problems with the solution specified on the boundary and that a different set gives better results when the solution is unspecified on the boundary.

When the method of orthogonal collocation is applied to nonlinear parabolic partial differential equations of the form $u_t = f(u_{xx}, u_x, u, x, t)$, one obtains a system of n first order ordinary differential equations with time as the independent variable. This system can be integrated using one of the familiar techniques: a Runge-Kutta method or a predictor-corrector method. We chose the improved Euler method (without iterations). We examine the numerical stability and prove a rather simple stability criterion. We have shown that the convergence of the approximate solution obtained by Galerkin's method is a sufficient condition for the convergence of the approximate solution obtained by the method of orthogonal collocation. This is a very useful result because it allows one to use directly the proven convergence theorems. The method of orthogonal collocation is applied to the transient mass and energy balances describing a nonisothermal chemical reaction. These applications indicate that the resulting computation times are from $\frac{1}{4}$ to $\frac{1}{40}$ the time required for an explicit finite difference method. The ease of applying the method of orthogonal collocation, the estimated

accuracy, and the reduced computation times indicate that the method has an extremely high potential as a tool for numerical analysis of such equations.

1. Introduction

When the exact solution, u, of a differential equation,

$$R[u] = 0 \tag{1}$$

is approximated by a linear combination of n specified functions, u_i, no set of n coefficients will, in general, result in the approximate solution,

$$\tilde{u} = \sum_{i=1}^{n} c_i u_i \tag{2}$$

satisfying the equation exactly. Thus $R[\tilde{u}] \neq 0$ everywhere. The values of the coefficients can be determined by requiring that the approximate solution, $\tilde{u}$, satisfy the differential equation in some integrated sense.

$$\int_D w_i(\underline{x})\ R[\tilde{u}(\underline{x})]\ dv = 0 \quad (i=1, \ldots, n) \tag{3}$$

$R[\tilde{u}]$ is referred to as the residual function. The exact solution, u, would satisfy eq. 3 for any family of weighting functions, $w_i(\underline{x})$. Different choices of the weighting functions in eq. 3 correspond to different methods of weighted residuals, which are summarized in Table 1.

Table 1

Correspondence of Weighting Functions to Different Methods of Weighted Residuals

Weighting Function, $w_i(\underline{x})$	Method
$u_i(\underline{x})$	Galerkin's method
x^i	Method of moments
1 for $x \in D_i$	Subdomain method
$\frac{\partial R[\tilde{u}]}{\partial c_i}$	Method of least-squares
$\delta(\underline{x} - \underline{x}_i)$	Method of collocation

For many types of nonlinearities the expansion coefficients of $\tilde{u}$ appear in a form which precludes their separation from the integrand of eq. 3, for example,

$$\sin\left[\sum_{i=1}^{n} c_i\, u_i(\underline{x})\right] .$$

The method of collocation is particularly effective with this type of nonlinearity because eq. 3 becomes algebraic rather than integral,

$$R\left[\sum_{j=1}^{n} c_j\, u_j(\underline{x}_i)\right] = 0 \ , \ (i=1, \ldots, n). \tag{4}$$

In brief, the method of collocation requires the approximate solution to satisfy the differential equation exactly on a set of n discrete points in D. One of the difficulties until recently was the positioning of the collocation points. As shown by Villadsen (19), an arbitrary positioning of the collocation points can lead to numerical divergence for even the simplest problems. This is also exhibited in the following example.

A relatively simple nonlinear ordinary differential equation was investigated:

$$R[y] \equiv \frac{1}{r^2}\frac{d}{dr}\left(r^2\frac{dy}{dr}\right) - y^2 = 0$$

$$y'(0) = 0$$

$$y(1) = 1 \ .$$

This corresponds to the dimensionless mass balance for a second order, isothermal chemical reaction in a spherical catalyst particle, where the Thiele modulus has been chosen as 1. Two different approximate solutions are studied $\tilde{y}^{(1)}$ and $\tilde{y}^{(2)}$ (see eqs. 7 and 8). Two types of collocation are investigated— (a) ordinary collocation, eq. 5, and (b) least-squares collocation, eq. 6:

$$R[\tilde{y}(r_j)] = 0, \ (j=1, \ldots, m=n) \tag{5}$$

and

$$\frac{\partial}{\partial c_j} \sum_{i=1}^{m} R[\tilde{y}(r_i)]^2 = 0, \ (j=i, \ldots, n)$$

or
$$\sum_{i=1}^{m} R[\tilde{y}(r_i)]^2 = \text{minimum} \qquad (6)$$

where in eq. 6, m is greater than/or equal to n (we have n coefficients and m collocation points). The first approximate solution, $\tilde{y}^{(1)}$, has the form

$$\tilde{y}^{(1)} = 1 + (1 - r^2) \sum_{i=1}^{n} a_i^{(n)} \cos(i-1)\,\pi r \,. \qquad (7)$$

The collocation points are chosen as the zeroes of $\cos(m-1)\pi r$ and r=1. Notice that the approximate solution satisfies the boundary conditions. The second approximate solution, $\tilde{y}^{(2)}$, has the form that would result from assuming the exact solution, y, could be expressed as a power series.

$$\tilde{y}^{(2)} = 1 + \sum_{i=1}^{n} b_i^{(n)} (r^{2i} - 1) \qquad (8)$$

The collocation points for $\tilde{y}^{(2)}$ are chosen as $r_j = j/m$ for $j=1, \ldots, m$. This form of approximate solution also satisfies the boundary conditions exactly. The first few expansion functions for $\tilde{y}^{(1)}$ and $\tilde{y}^{(2)}$ are shown in figures 1 and 2.

Figures 3 and 4 exhibit the approximate solutions for ordinary collocation. Obviously, the cosine series yields inferior results in comparison to the power series. This is mirrored in the behavior of

the residual function (figures 5 and 6). Based on these observations, the power series solution should be judged acceptable. The cosine series solution is of doubtful value. Remember though that the expansion functions and the collocation points have been chosen separately. The behavior of $\tilde{y}^{(1)}$ can be a result of the choice of the collocation points.

Figures 7 through 10 provide the same information for the least-squares collocation method. It appears that $\tilde{y}^{(1)}$ may be acceptable, but notice the order of magnitude difference in the residual function compared to that for $\tilde{y}^{(2)}$. Auxilliary calculations show that the behavior of the solutions, $\tilde{y}^{(1)}$ and $\tilde{y}^{(2)}$, is also mirrored in the following quantities:

(a) the expansion coefficients

(b) the mean-square integral of the residual function

(c) the maximum absolute value of the residual function

Equation 6 is a crude approximation to the method of least-squares (table 1)—particularly so when using equally spaced collocation points. As illustrated in figure 11, the mean-square integral of the residual converges to a limiting value as m, the number of collocation points, increases. Even more important is the fact that the mean-square error bound is proportional to the mean square residual:

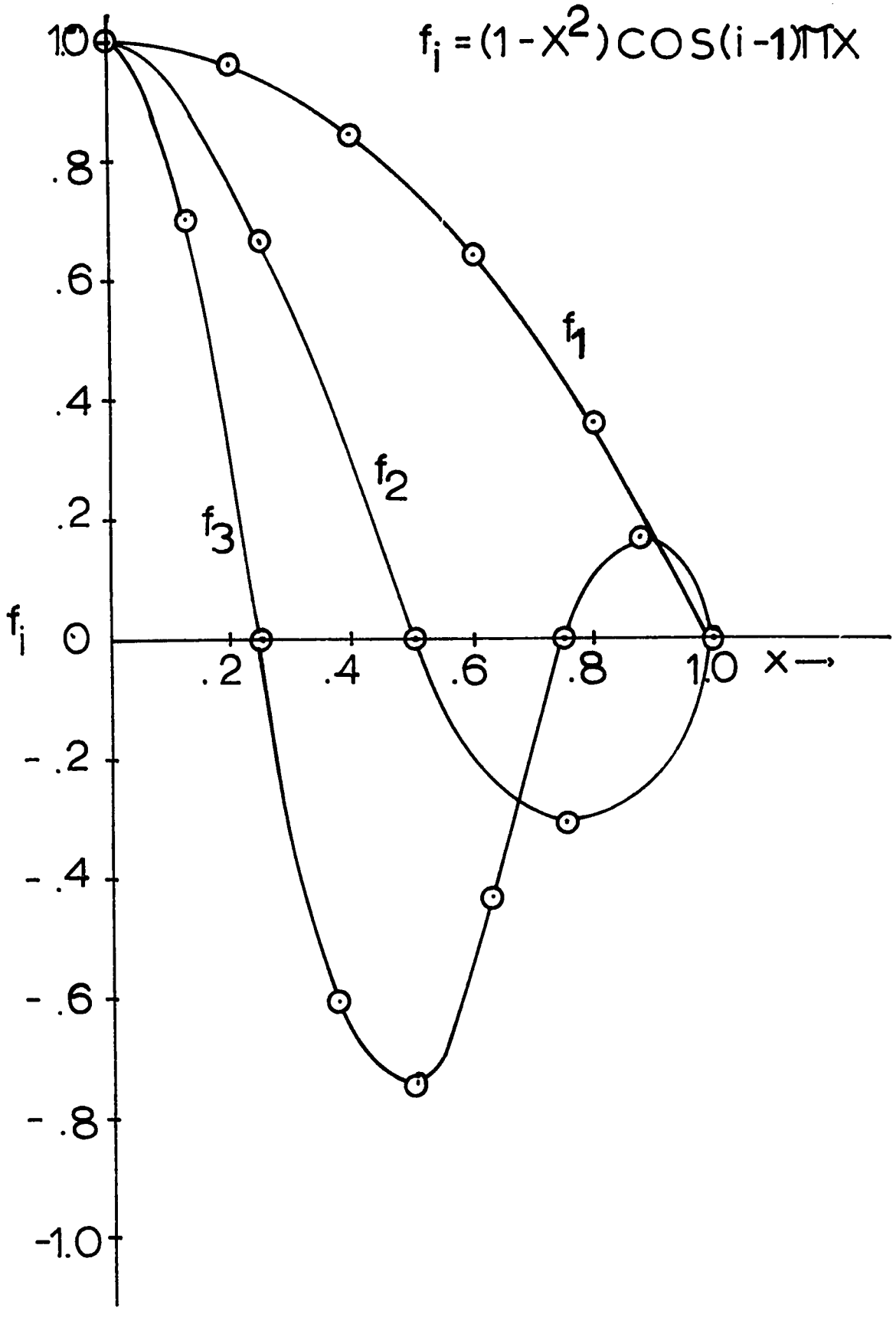

Figure 1. Cosine expansion functions versus x.

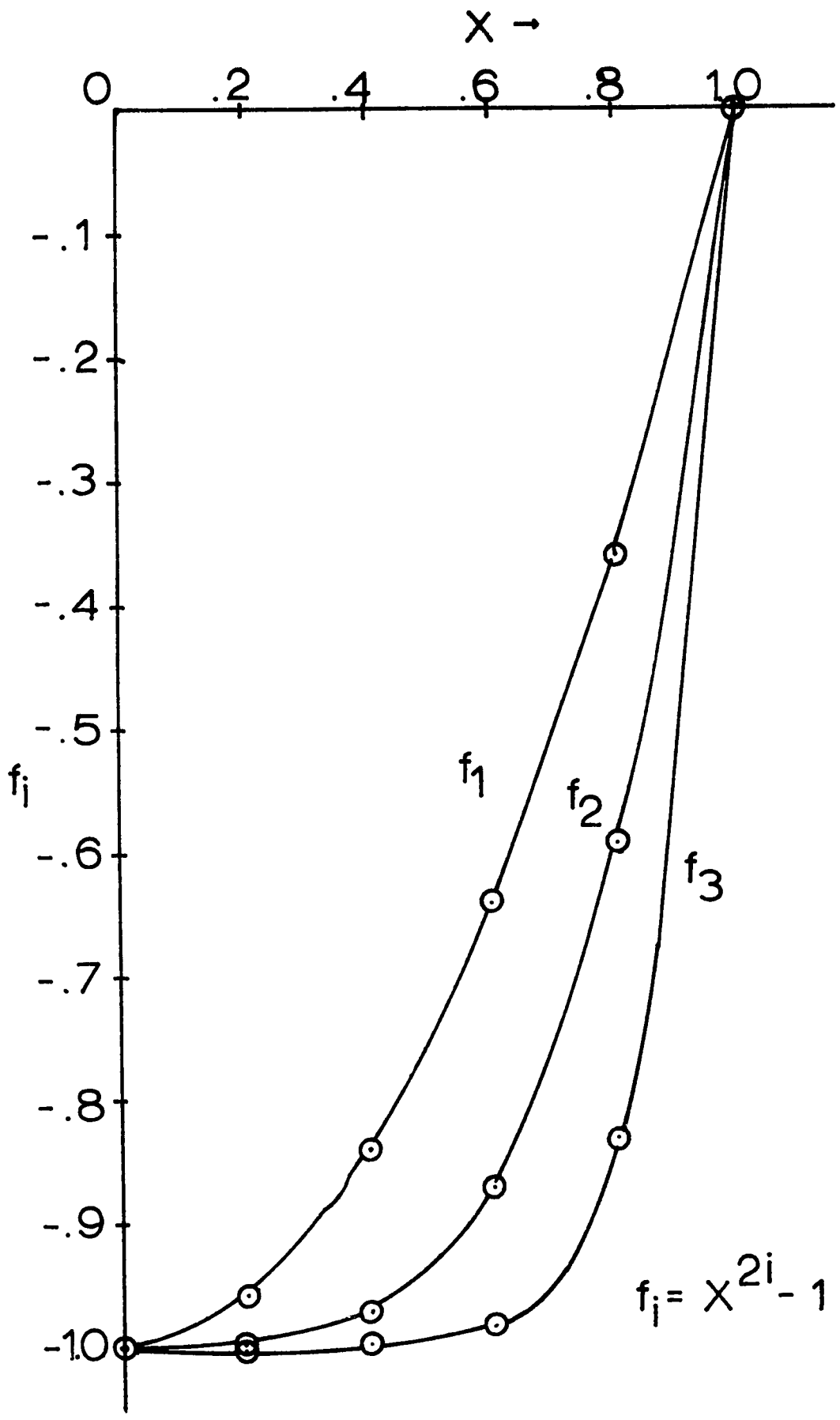

Figure 2. Power series expansion functions versus x.

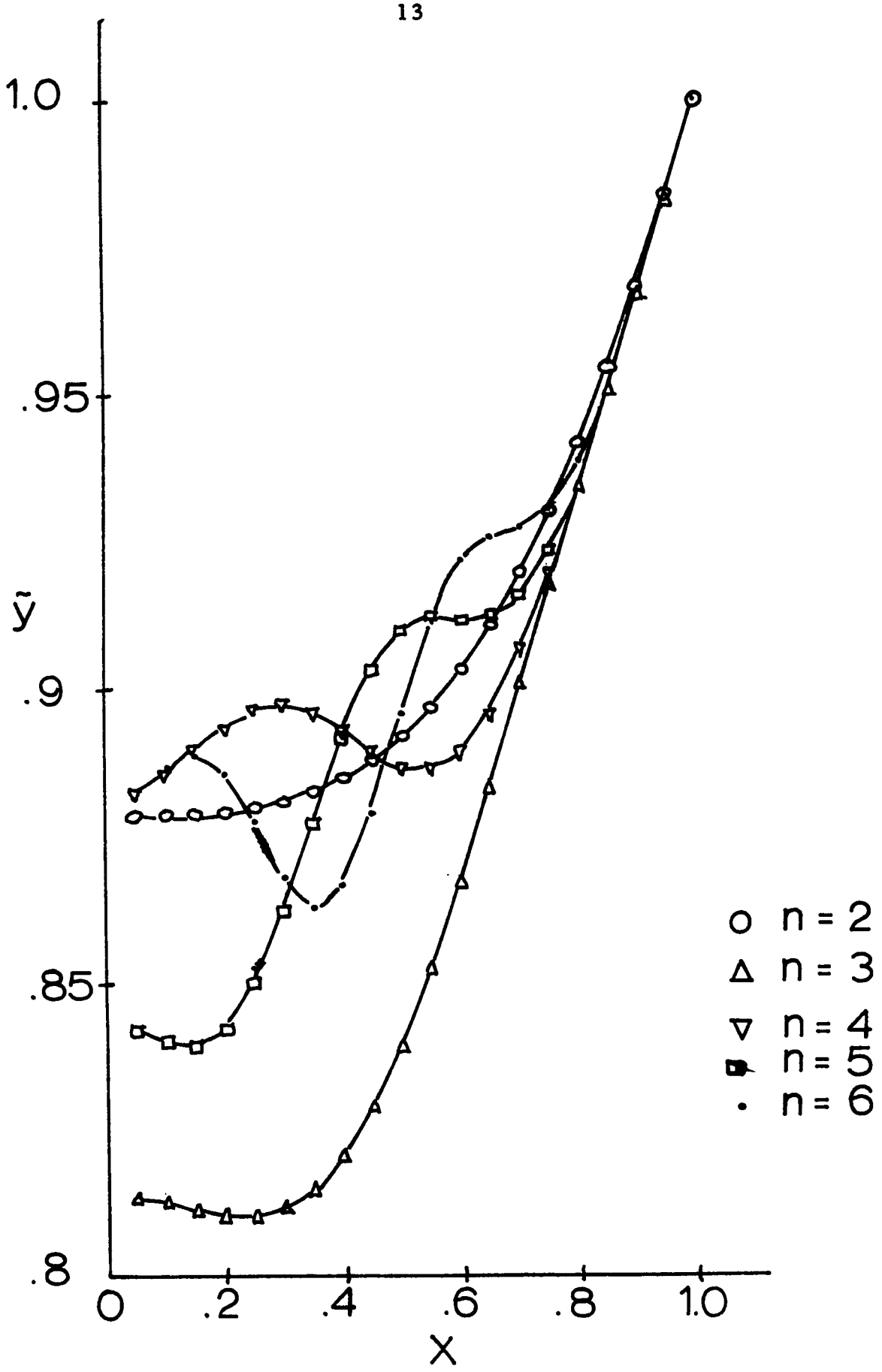

Figure 3. Ordinary collocation solution versus x. (Using the cosine expansion functions).

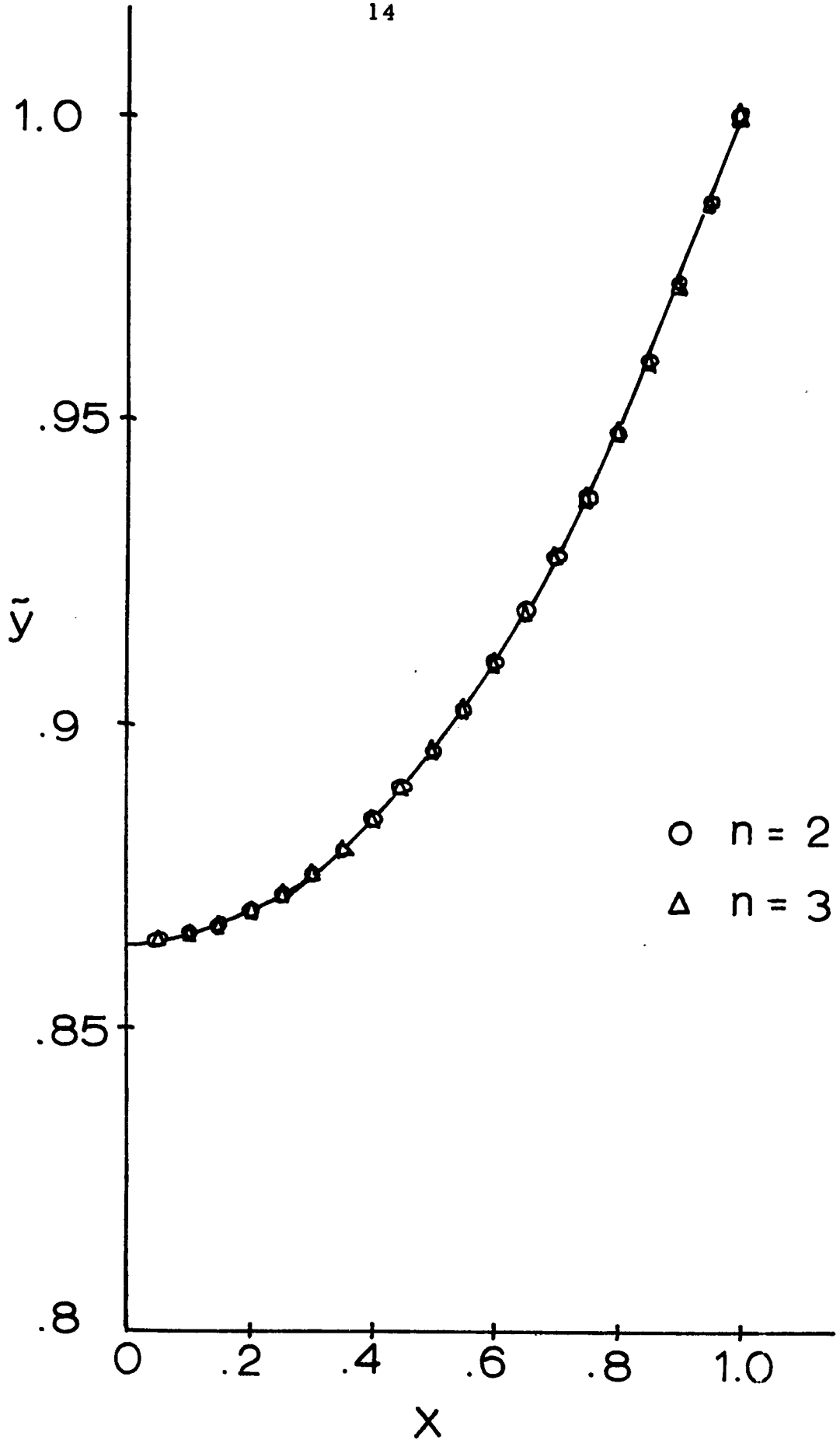

Figure 4. Ordinary collocation solution versus x. (Using the power series expansion functions).

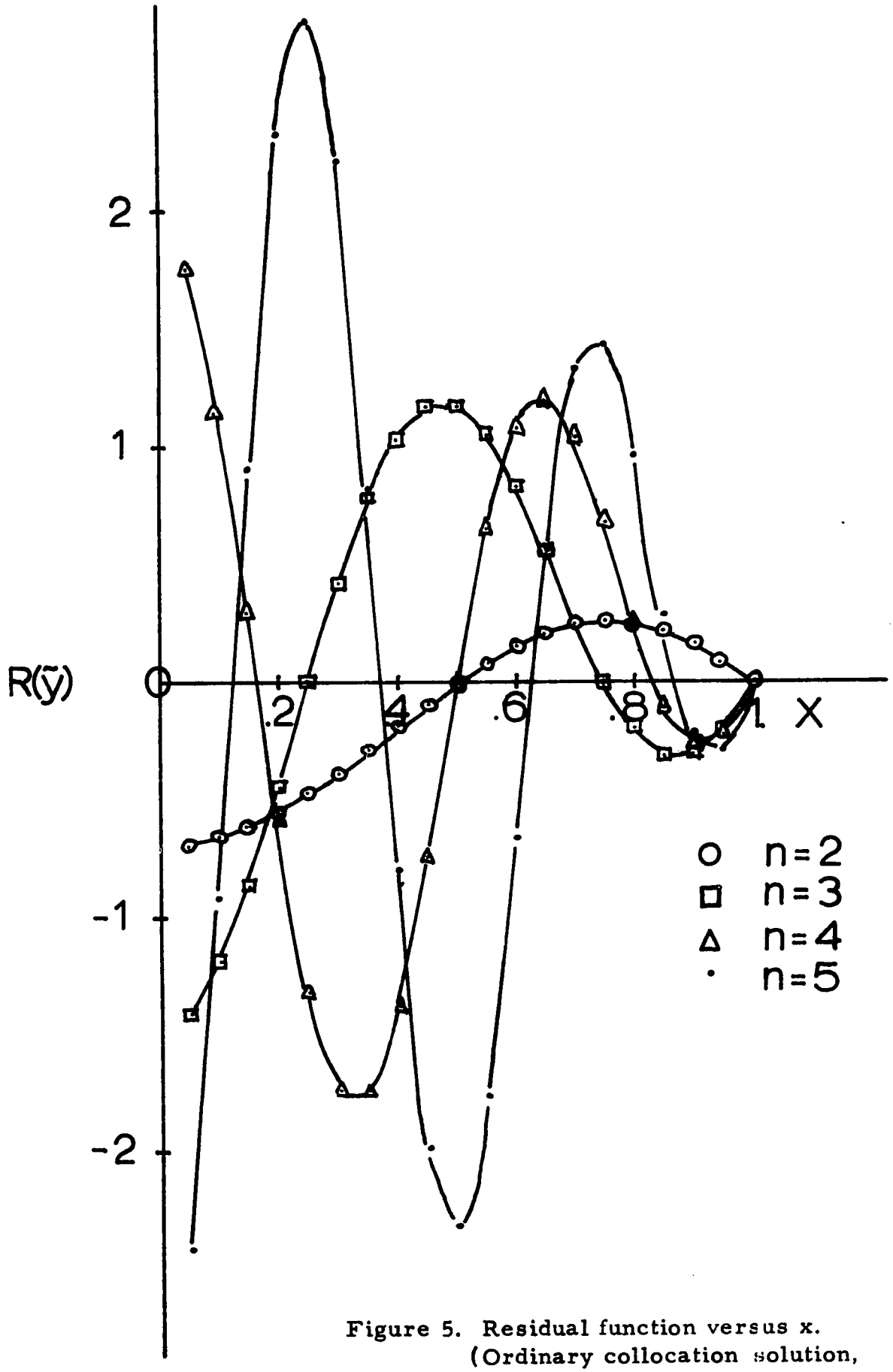

Figure 5. Residual function versus x.
(Ordinary collocation solution,
using the cosine expansion functions).

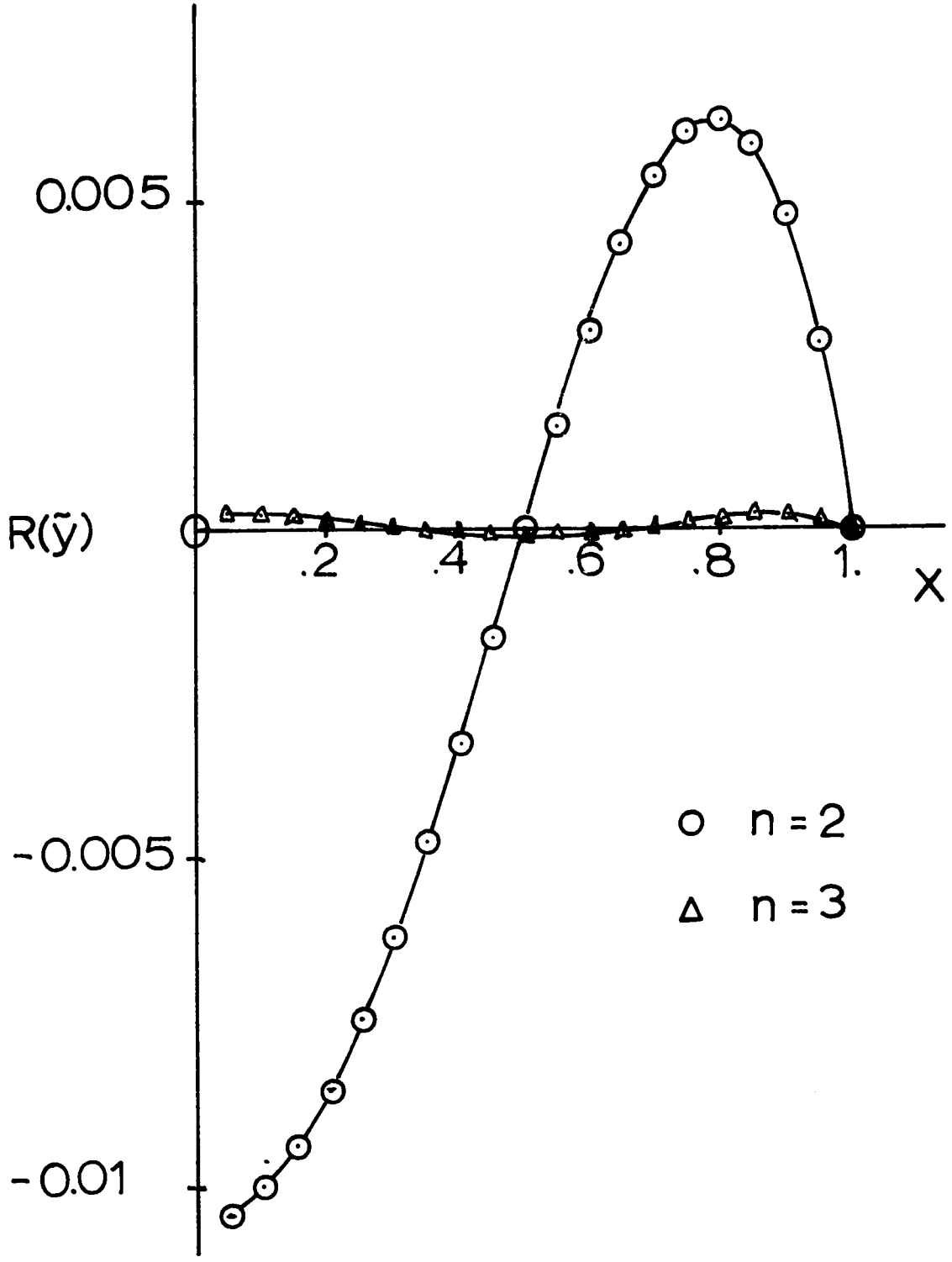

Figure 6. Residual function versus x. (Ordinary collocation solution, using the power series expansion functions).

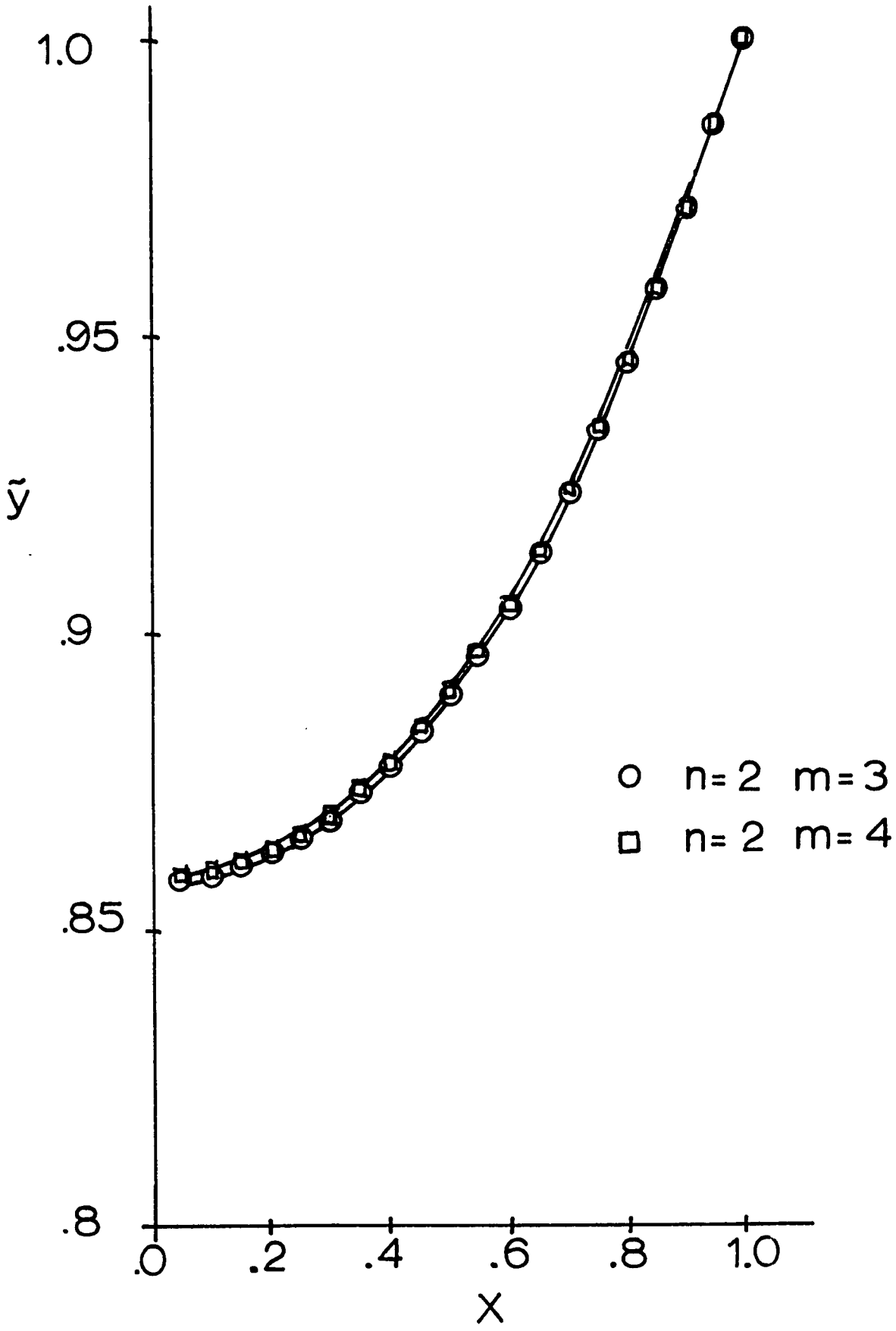

Figure 7. Least squares collocation solution versus x. (Using the cosine expansion functions).

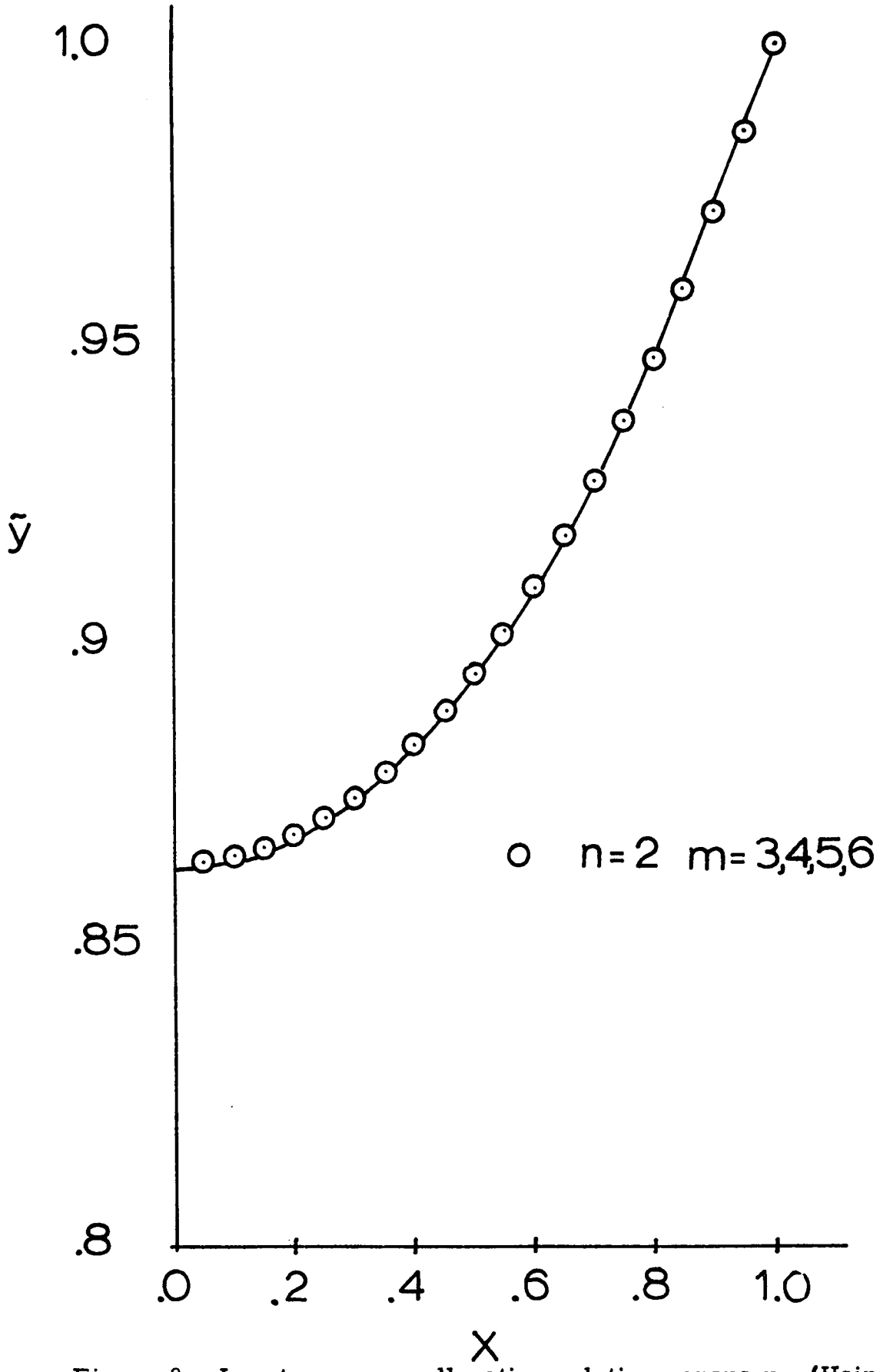

Figure 8. Least squares collocation solution versus x. (Using the power series expansion functions).

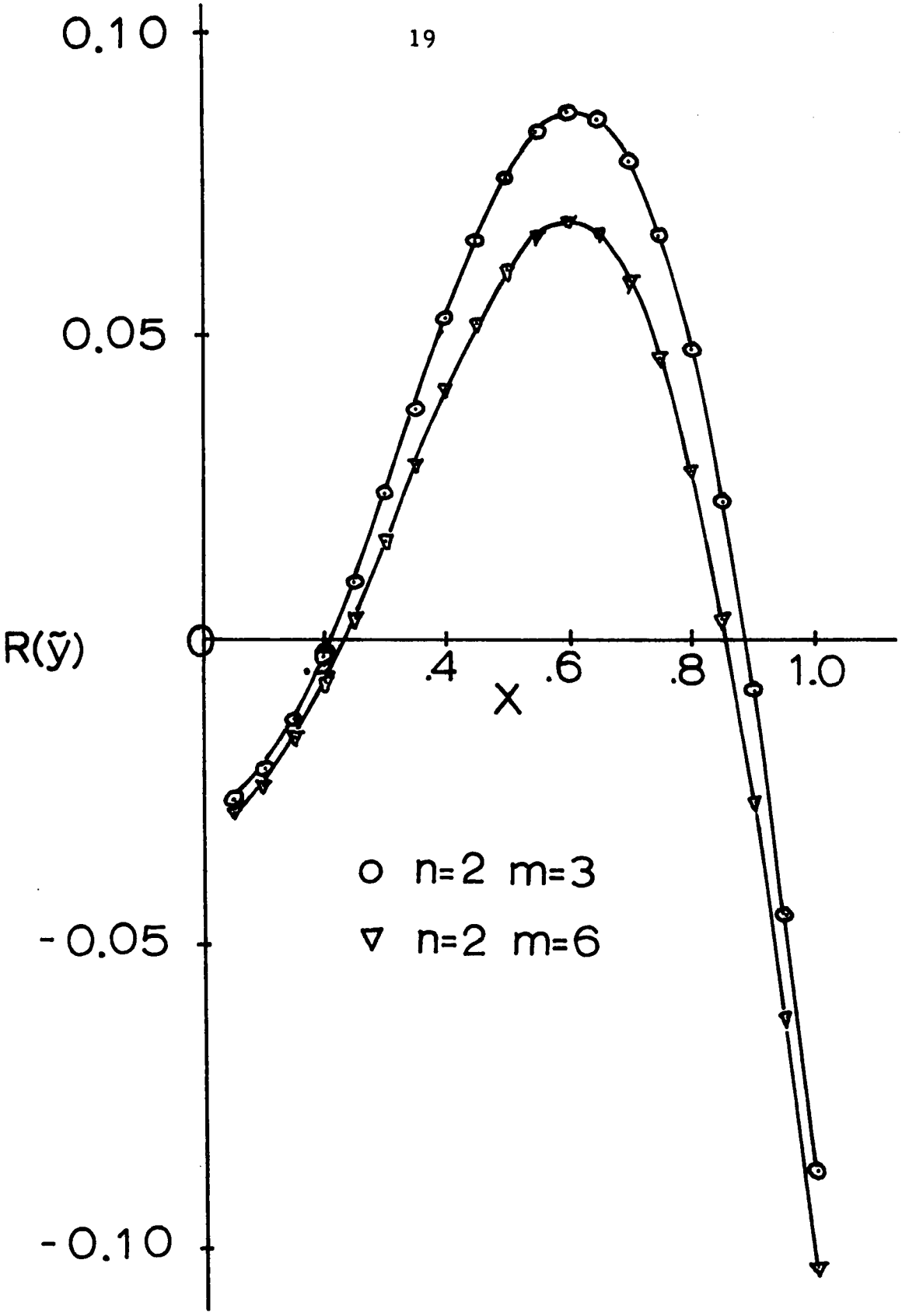

Figure 9. Residual function versus x. (Least squares collocation solution, using the cosine expansion functions).

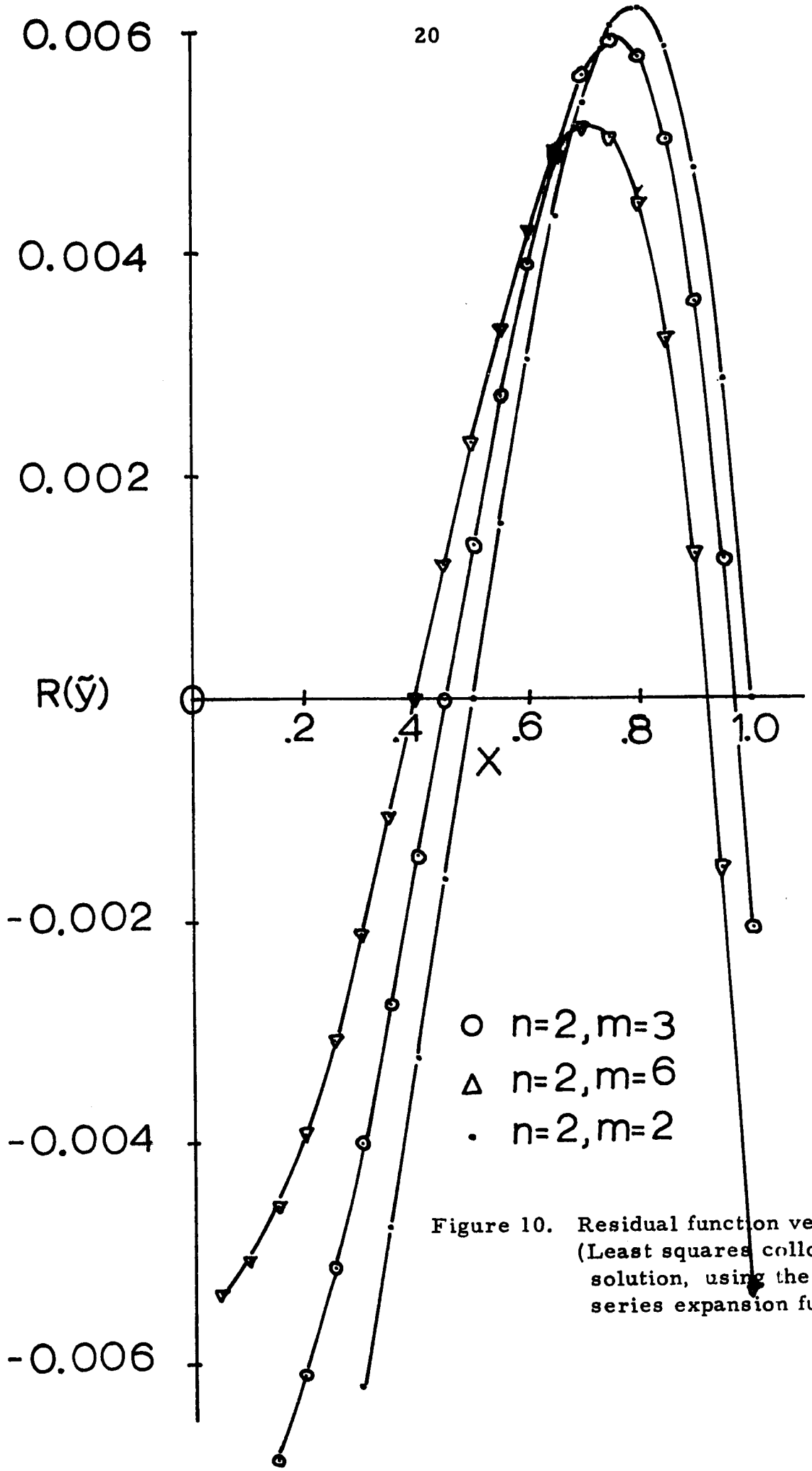

Figure 10. Residual function versus x. (Least squares collocation solution, using the power series expansion functions).

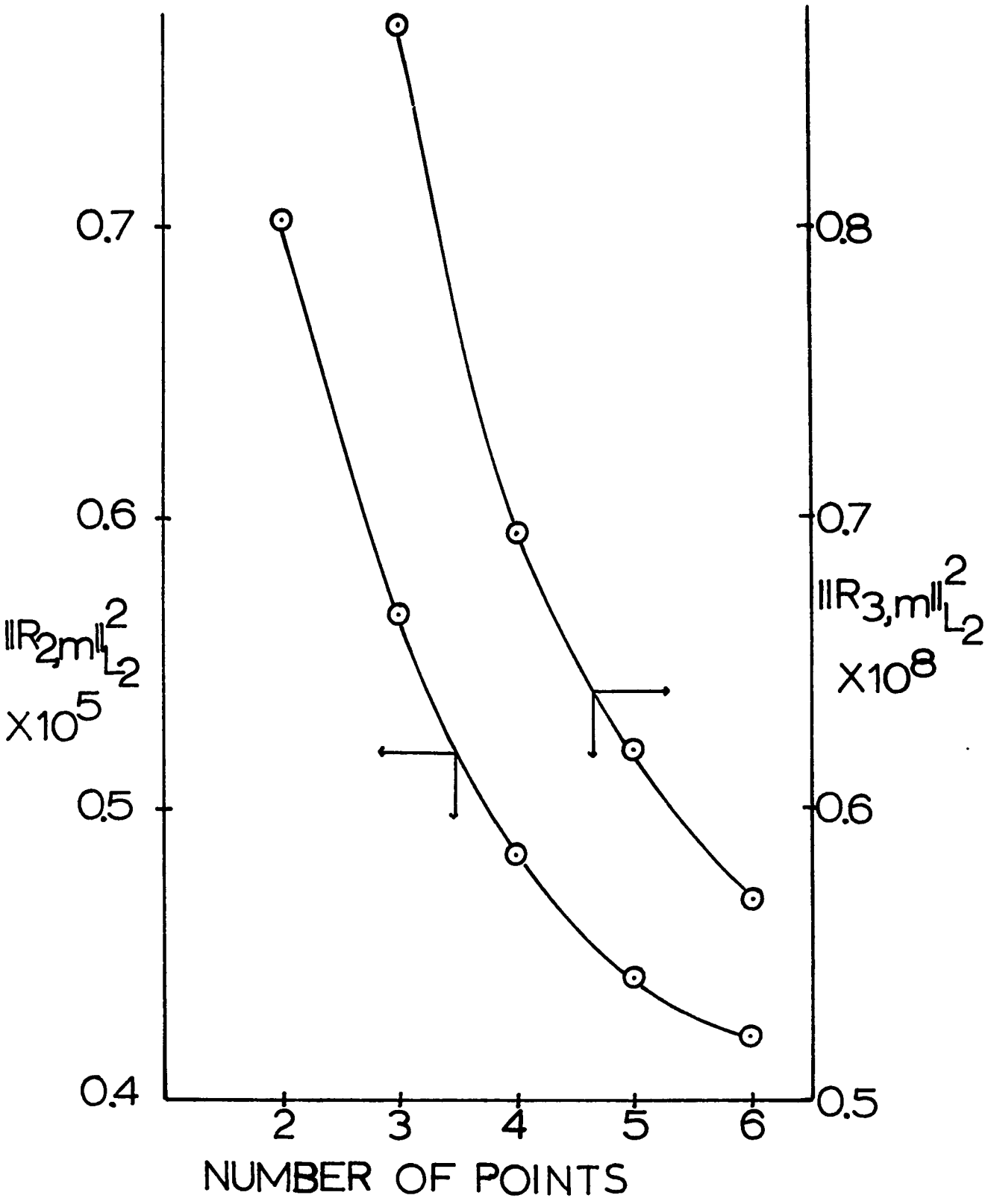

Figure 11. Integral of the square of the residual function versus n. (Least squares collocation solution, power series expansion functions).

NOTE: $\| R_{i,M} \|_{L_2}^2 = \int_o^1 R\,[\tilde{y}^{(2)}(n=i,\ m=M)]^2\,dx$

Table 2

Mean Square Error Bound for Least-Square Collocation

(Power Series Solution)

Number of Expansion Functions	Number of Collocation Points	Mean-Square Error Bound
2	2	3.542×10^{-4}
	3	3.181×10^{-4}
	4	2.940×10^{-4}
	5	2.811×10^{-4}
	6	2.747×10^{-4}
3	3	1.245×10^{-5}
	4	1.114×10^{-5}
	5	1.052×10^{-5}
	6	1.008×10^{-5}
4	4	4.514×10^{-7}
	5	3.524×10^{-7}
	6	$\sim 3 \times 10^{-7}$
5	5	1.015×10^{-7}
	6	$\sim 9 \times 10^{-8}$

$$\left[\int_0^1 (\tilde{y} - y)^2 \, r^2 dr\right]^{\frac{1}{2}} < k\left[\int_0^1 R[\tilde{y}]^2 \, r^2 dr\right]^{\frac{1}{2}}$$

(Refer to Chapter B). One can conclude that the least-square collocation solution is better than the ordinary collocation solution for this problem and that the improvement is limited by the accuracy of the least-squares method of Table 1. For the data of Table 2, the improvement is roughly 25%.

For this particular problem, the power series solution is superior to the cosine series solution. However, if the choice of the expansion functions is a poor one, e.g., cosine series, then the least squares collocation helps improve the results obtained with ordinary collocation. In addition, error bounds are derived in Chapter B and the error is proportional to the mean square residual. Consequently the least squares collocation minimizes the error bound since it minimizes the mean square residual. These advantages of least squares collocation are overruled, however, by one overriding constraint: ease of computation. Ordinary collocation is easier to use, and the method of orthogonal collocation is even easier and is described below.

2. Orthogonal Collocation for Ordinary Differential Equations

After learning of the difficulties that can occur with an unfortunate choice for the expansion functions or the collocation points, one should appreciate the importance of the advance recently made by Villadsen and Stewart (21). These authors show that a particular set of

orthogonal polynomials, which satisfy the boundary conditions, can be associated with each particular problem and that the roots of the $(n+1)^{th}$ polynomial of this set should be used as the collocation points for an n-term expansion. Until this time (1967) there had been no way of systematically increasing the number of collocation points while accounting for the boundary conditions. Further, Villadsen and Stewart show that the values of the approximate solution at the collocation points can be evaluated without calculating the expansion coefficients explicitly. Their method, referred to as orthogonal collocation, is a discretized form of Galerkin's method. Recent applications include the work of Stewart and Villadsen (17) to predict the occurrence of multiple steady-state solutions to the mass and energy balances in a catalyst particle, Livbjers, et al. (13) to study the catalytic oxidation of SO_2, McGowin and Perlmutter (15) to delineate regions of asymptotic stability for problems with multiple solutions, Ferguson and Finlayson (5) to study the transient behavior of the coupled heat and mass balances for a first order chemical reaction, and Finlayson (6a) to analyze the radial dispersion model of a packed-bed reactor for a highly exothermic chemical reaction. Villadsen and Sorenson (20) extended the method of orthogonal collocation by advocating collocation in both the spatial and time variables. This last modification allows the use of large time steps while maintaining high accuracy.

As an example of the use of orthogonal collocation, let us examine a particular differential equation with the following boundary conditions:

$$\frac{1}{x^{a-1}} \frac{d}{dx} \left(x^{a-1} \frac{dy}{dx} \right) = f(x, y) \tag{9}$$

$$\frac{dy(0)}{dx} = 0$$

$$y(1) = 1 \quad .$$

An expansion which satisfies the boundary conditions exactly is

$$\tilde{y}(x^2) = y(1) + (1 - x^2) \sum_{i=1}^{n} a_i P_{i-1}(x^2) \quad . \tag{10}$$

The factor $(1 - x^2)$ enters into $\tilde{y}$ in satisfying the boundary conditions, and Villadsen and Stewart chose to define the P_i as the polynomials satisfying the condition

$$\int_0^1 (1 - x^2) P_i (x^2) P_j(x^2) (x^{a-1} dx) = \delta_{ij} \quad (i, j = 0, 1, \ldots). \tag{11}$$

P_i is an i-th order polynomial in x^2. A property of the orthogonal polynomial, $P_i(x^2)$, is that there are (i) roots on the interval (0, 1) for the i^{th} polynomial. The approximate solution, $\tilde{y}$, involves n coefficients so that we need n conditions in order to specify the function. In ordinary collocation one would simply choose some n collocation points For

orthogonal collocation the collocation points are the roots of $P_n(x^2) = 0$: $x_1^2, \ldots, x_n^2$. Although the polynomials are defined as in eq. 11, all one really needs computationally are the roots, x_j^2. These have been compiled for many polynomials by Stroud and Secrest (18). $\tilde{y}(x^2)$ can be written equivalently as

$$\tilde{y}(x^2) = \sum_{i=1}^{n+1} b_i (x^2)^{i-1}$$

such that $$\tilde{y}(x_j^2) = \sum_{i=1}^{n+1} b_i (x_j^2)^{i-1} = \sum_{i=1}^{n+1} Q_{ji}\, b_i \quad \text{or} \quad \langle \tilde{y} \rangle = [Q] \langle b \rangle$$

If one is solving an ODE which involves first derivatives then

$$\left.\frac{d\tilde{y}}{dx}\right|_{x^2=x_j^2} = \sum_{i=1}^{n+1} b_i \left.\frac{d}{dx}(x^{2i-2})\right|_{x=x_j} = \sum_{i=1}^{n+1} C_{ji}\, b_i \qquad (12)$$

or $$\langle \frac{d\tilde{y}}{dx} \rangle = [C] \langle b \rangle$$

and in the case of the one-dimensional Laplacian operator,

$$\left.\frac{1}{x^{a-1}} \frac{d}{dx}\left(x^{a-1} \frac{d\tilde{y}}{dx}\right)\right|_{x=x_j} = \left.\sum_{i=1}^{n+1} b_i \frac{1}{x^{a-1}} \frac{d}{dx}\left(x^{a-1} \frac{dx^{2i-2}}{dx}\right)\right|_{x=x_j} \qquad (13)$$

$$= \sum_{i=1}^{n+1} D_{ji}\, b_i$$

or $$\langle \nabla^2 \tilde{y} \rangle = [D] \quad \langle b \rangle .$$

But $\langle b \rangle = [Q]^{-1} \quad \langle \tilde{y} \rangle$ such that

$$\langle \tilde{y}' \rangle = [C] [Q]^{-1} \langle \tilde{y} \rangle \equiv [A] \quad \langle \tilde{y} \rangle \tag{14}$$

$$\langle \nabla^2 \tilde{y} \rangle = [D] [Q]^{-1} \langle \tilde{y} \rangle \equiv [B] \quad \langle \tilde{y} \rangle . \tag{15}$$

The net result is the reduction of the example problem to

$$[B] \langle \tilde{y} \rangle - \langle f(\tilde{y}) \rangle = 0$$

which is an algebraic system of (n) nonlinear equations with $\tilde{y}_{n+1} \equiv y(1) = 1$. Notice that the problem has been reduced to that of solving for the values of $\tilde{y}$ at the collocation points rather than for the values of the expansion coefficients, a_i.

The matrix elements of [A] and [B] can be determined explicitly in terms of the collocation points. This is a new result and has one immediate application. In studying a particular problem for which the [A] and [B] matrices have not been tabulated, the explicit expressions for A_{ij} and B_{ij} could be evaluated at a desk calculator where otherwise one would have to use a matrix inversion subroutine and a digital computer—particularly for values of n greater than 2. Further application of the expressions depends on their accuracy and ease of use. To derive the explicit expressions consider the following equivalent Lagrange

interpolation polynomial for the approximate solution, $\tilde{y}(x^2)$:

$$\tilde{y}(x^2) = \sum_{i=1}^{n+1} L_i(x^2)\, \tilde{y}(x_i^2)$$

where the L_i are the Lagrange interpolation functions,

$$L_i(x^2) = \prod_{k \neq i} \frac{(x^2 - x_k^2)}{(x_i^2 - x_k^2)} .$$

If one is then interested in the first derivative of $\tilde{y}(x^2)$ (at any point in the interval of definition), one can differentiate the Lagrange interpolation polynomial for $\tilde{y}(x^2)$. First, consider the individual function, $L_i(x^2)$. By using the definition of the natural logarithm function,

$$\ln(L_i(x^2)) = \sum_{k \neq i} \ln(x^2 - x_k^2) - \sum_{k \neq i} \ln(x_i^2 - x_i^2)$$

one obtains dL_i/dx quite easily,

$$\frac{L'_i}{L_i} = \cdot \sum_{k \neq i} \frac{2x}{(x^2 - x_k^2)}$$

or

$$\frac{dL}{dx^i}(x^2) = \prod_{k \neq i} \frac{(x^2 - x_k^2)}{(x_i^2 - x_k^2)} \cdot \sum_{k \neq i} \frac{2x}{(x^2 - x_k^2)} .$$

By comparing the first derivative of $\tilde{y}(x^2)$ as defined by eq. 14 and the

first derivative of the Lagrange interpolation polynomial for $\tilde{y}(x^2)$, one finds that

$$A_{ij} = \frac{dL_i}{dx}(x_j^2)$$

$$= \frac{\prod_{k\pm i}(x_j^2 - x_k^2)}{\prod_{k\pm i}(x_i^2 - x_k^2)} \cdot \sum_{k\pm i} \frac{2x_j}{(x_j^2 - x_k^2)} \qquad (16)$$

where the first quotient of A_{ij} has the value 1 for i=j. Similarly, one is able to show that B_{ij} is given by

$$B_{ij} = \nabla^2 L_i \Big|_{x=x_j}$$

$$= \frac{\prod_{k\pm i}(x_j^2 - x_k^2)}{\prod_{k\pm i}(x_i^2 - x_k^2)} \left[\left(\sum_{k\pm i} \frac{2x_j}{(x_j^2 - x_k^2)} \right)^2 + 2 \sum_{k\pm i} \frac{1}{(x_j^2 - x_k^2)} - \right.$$

$$\left. \sum_{k\pm i} \left(\frac{2x_j}{(x_j^2 - x_k^2)} \right)^2 + \frac{a-1}{x_j} \sum_{k\pm i} \frac{2x_j}{(x_j^2 - x_k^2)} \right]. \qquad (17)$$

Similar expressions can be obtained for $\tilde{y}(x)$ (where $\tilde{y}$ is <u>not</u> an even function).

Now consider a boundary condition of the third kind at x = 1:

$$\frac{2}{K_1} \frac{dy(1)}{dx} + y(1) = k_2 \quad . \qquad (18)$$

For heat transfer to a catalyst particle, y(1) would be the dimensionless temperature at the surface, k_1 would be a Nussalt number (in the heat transfer literature, this usually referred to as a Biot number),

$$Nu = h_t \, d_p / \, k_s^e \quad ,$$

and k_2 would be the bulk fluid temperature. With this type of boundary condition, y(1) is now an unknown quantity and the approximate solution can be represented as,

$$\tilde{y}(x^2) = \tilde{y}(1) + (1 - x^2) \sum_{i=1}^{n} a_i P_{i-1}(x^2) \quad . \tag{19}$$

Replacing eq. 18 (using eq. 14 for $x_{n+1} = 1$) as

$$\frac{2}{k_1} \sum_{j=1}^{n+1} A_{n+1,\,j} \tilde{y}_j + \tilde{y}_{n+1} = k_2 \quad , \tag{20}$$

one has a system of (n) nonlinear equations (eq. 21) and one linear equation (eq. 20) to solve for the (n+1) unknowns:

$$\sum_{j=1}^{n+1} B_{ij} \, \tilde{y}_j \; - \; f(\tilde{y}_j) \; = \; 0 \; , \; (i=1, \ldots, n) \tag{21}$$

Define the polynomials of eq. 19 as,

$$\int_o^1 P_i(x^2) \, P_j(x^2) \, (x^{a-1} dx) \; = \delta_{ij} \quad . \tag{22}$$

As discussed by Villadsen and Stewart (21), if one is able to know the exact value of y at x=1, then one should use orthogonal polynomials which have a weight function which vanishes at x=1. On the other hand, here we do not know the exact value of y at x=1. This value has to be approximated and because of this, a weighting function which does not vanish at x=1 has been chosen. The polynomials defined by eq. 22 are referred to here as Legendre polynomials.

To each set of orthogonal polynomials, defined similarly to eq. 22, there is associated a Gaussian-like quadrature scheme. These schemes depend on the proper placement of the quadrature points for their great accuracy. More specifically, the quadrature points are the roots of the defined polynomials. Assume that one has the following orthogonal collocation equations:

$$R\left[\tilde{y}(x_j^2)\right] = 0 , \quad (j=1,\ldots,n+1) .$$

Then by multiplying each be $W_j^{(n+1)} \cdot w_i(x_j)$, where $W_j^{(n+1)}$ is the jth quadrature weight coefficient for the (n+1)th order quadrature scheme, and by summing over j, one obtains

$$\sum_{j=1}^{n+1} W_j^{(n+1)} \, w_i(x_j) \, R\left[\tilde{y}(x_j^2)\right] = 0 , \quad i=1,\ldots,n+1$$

which is identical to the equations for Galerkin's method (up to the error term of the quadrature method):

$$\int_0^1 w_i(x)\, R\,[\tilde{y}(x^2)]\;\; (x^{a-1}dx) \;=\; \sum_{j=1}^{n+1} W_j^{(n+1)}\, w_i(x_j)\, R[\tilde{y}(x_j^2)] \;+\; E^{(n+1)} = 0.$$

This explains why the method of orthogonal collocation is referred to as a discretized Galerkin method.

3. Application of Orthogonal Collocation—Boundary Value Problem

An area of study which is particularly amenable to the use of orthogonal collocation is chemical reactor analysis. This is because of the typical types of rate expressions encountered, viz.,

$$\text{rate} = k\, c$$

$$\text{rate} = \frac{-\,k\, K_A\, K_B\, P_A\, P_B}{(1 + K_A\, P_A + K_B P_B)^2}$$

where $k = A \exp(-E/(R_g T))$ and $K_i = (\text{constant}) \times \exp(\pm \Delta H_i^s/(R_g T))$ (k is the rate constant while K_i is an adsorption equilibrium constant). If a chemical reactor is operated isothermally, the rate depends only on the concentration, C, or the partial pressures, P_A and P_B. However, if the reactor is operated in a nonisothermal fashion, the rate of reaction depends on the local temperature. The temperature dependence of the rate expression is shown above as being of exponential nature. The exponential function has the ability to increase by an order of magnitude or more for a much smaller change in the dependent variable—temperature. The exponential temperature dependence on the rate expressions

makes the analysis of a nonisothermal reactor more difficult than that of an isothermal reactor. Additionally, one finds that accurate solutions to the problem of the nonisothermal reactor can require considerable effort and sometimes ingenuity.

As an example, consider the following problem. A first order irreversible chemical reaction is occurring in a nonisothermal, spherical catalyst particle. Consequently, one must consider both the heat balance and the mass balance. One finds that the rate expression describes the rate of heat generation in the heat balance and the rate of disappearance of the reactant in the mass balance. It is the rate expression which 'couples' the two conservation equations—the rate expression depends, itself, on both the temperature and the reactant concentration. A physical example of such a problem is the oxyhalogenation of saturated hydrocarbons.

For such a problem with a boundary condition of the first kind, it is known that the system can be described by the following equations:

$$\frac{1}{r^2}\frac{d}{dr}\left(r^2\frac{dT}{dr}\right) - \phi^2\left[T - (1+\beta)\right]\exp\left(-\gamma\left(1/|T| - 1\right)\right) = 0 \qquad (23)$$

$$T'(0) = 0$$

$$T(1) = 1$$

$$c(r) = c(1) - \frac{1}{\beta}\left[T(r) - T(1)\right] .$$

If we know T(r), we know c(r); consequently, we only need to solve the differential equation for T(r). The square of the Thiele modulus, ϕ^2, is the ratio of the rate of reaction at the surface conditions to the rate of diffusion into the particle. β is the dimensionless heat of reaction—positive for exothermic reactions. For this problem, $1 + \beta$ is the maximum temperature which the reaction will support. γ is the dimensionless activation energy. Mathematically, the analysis of this problem follows the format developed in eqs. 9-15. It is known (16) that this problem has three mathematical solutions for the following choice of parameters:

$$\phi^2 = R_p^2 \frac{k(T_{ref})}{D_s^e} = .25$$

$$\beta = \frac{D_s^e \Delta H_{rxn} c_{ref}}{k_s^e T_{ref}} = .6$$

$$\gamma = E/(R_g T_{ref}) = 20.$$

The solutions to this problem are qualitatively represented in the following sketch:

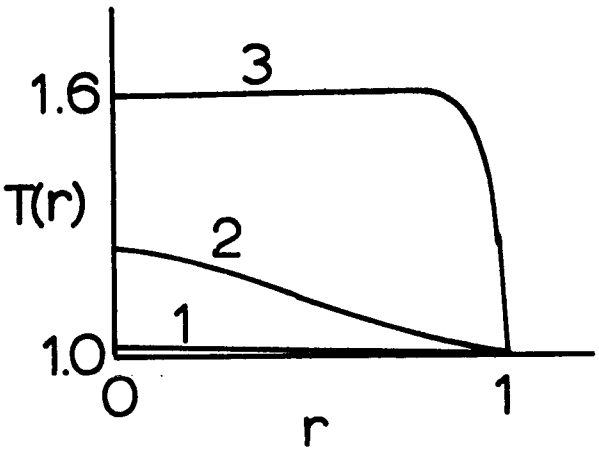

As might be expected, the solutions become progressively more difficult to approximate going from 1 to 3. The engineer is interested in two properties of this problem: (1) the maximum temperatures which occur in the center of the particle and (2) the effectiveness factor. The effectiveness factor is the ratio of the mean rate of reaction within the particle to the rate which would occur if the surface conditions prevailed throughout the particle. It can be shown that the effectiveness factor, ξ , is given by

$$\xi = \frac{(-3)}{\phi^2 \beta} \left. \frac{dT}{dr} \right|_{r=1}$$

or by integrating eq. 23 over r,

$$\xi = \frac{(-3)}{\phi^2 \beta} \int_0^1 \phi^2 [T - (1 + \beta)] \exp(-\gamma (1/|T| - 1)) (r^2 dr) .$$

The first form for ξ will be referred to as the derivative value and the second as the integrated value. Although the two forms are identical for the exact solution, T, they will not be numerically identical when the approximate solution, $\tilde{T}$, is used to evaluate ξ .

Applying orthogonal collocation to eq. 23 gives

$$\sum_{j=1}^{n+1} B_{ij} \tilde{T}_j - \phi^2 [\tilde{T}_i - (1 + \beta)] \exp(-\gamma (1/|\tilde{T}_i| - 1)) = 0 \qquad (24)$$

$$(i=1, \ldots, n)$$

where $T(1) = \tilde{T}(1) = \tilde{T}_{n+1} = 1$. $[B_{ij}]$ is defined by eq. 15 or 17 and depends only on the collocation points. In this case the collocation points are the roots of the polynomials defined by eq. 11 with a=3 (spherical geometry). Villadsen and Stewart (21) refer to this choice of polynomial as a type of Jacobi polynomial. Eq. 24 represents a set of nonlinear algebraic equations which are solved with the Newton-Raphson technique: the equations are linearized and solved iteratively. To assess the accuracy we can look at the numerical convergence for increasing n. We do that here and also compare to the results obtained by a second method.

The method of quasilinearization (11) is used to obtain a finite difference solution. Quasilinearization refers to the manner in which the nonlinearity is treated:

$$\frac{d^2T_{k+1}}{dr^2} + \frac{a-1}{r}\frac{dT_{k+1}}{dr} - \frac{\partial f}{\partial T}\bigg|_{T=T_k} \cdot T_{k+1} = f(T_k) -$$

$$\frac{\partial f}{\partial T}\bigg|_{T=T_k} \cdot T_k \quad (k=0, 1, 2, \ldots)$$

where $f(T_k) = \phi^2 [T_k - (1 + \beta)] \exp(-\gamma (1/|T_k| - 1))$

$$\frac{\partial f}{\partial T}\bigg|_{T=T_k} = \phi^2 \exp(-\gamma (1/|T_k| - 1)) \left[1 + \frac{T_k - (1 + \beta))\gamma}{T_k^2} \right] .$$

One is solving a succession of linear ordinary differential equations. The initial guess, T_o, was chosen as $\tilde{T}$ with a small value of n(1 or 2). The derivatives are approximated by the following differences:

$$\frac{dT_{k+1}}{dr} = \frac{1}{\Delta r} [T_{k+1}((j+1)\Delta r) - T_{k+1}(j\Delta r)]$$

$$= \frac{1}{\Delta r} [T_{k+1}(j+1) - T_{k+1}(j)]$$

$$\frac{d^2T_{k+1}}{dr^2} = \frac{1}{(\Delta r)^2} [T_{k+1}(j+1) - 2T_{k+1}(j) + T_{k+1}(j-1)]$$

with $j=2, \ldots, n+1$ such that $T_{k+1}(1) = T_{k+1}(r=0)$ and $T_{k+1}(n+2) = T_{k+1}(r=1)$. There are (n-1) interior grid points. Although the Laplacian operator may be singular in cylindrical or spherical geometries, there is no

problem here. We only difference the ODE at interior points. Additionally, the condition of $dT/dr(0) = 0$ guarantees that the Laplacian operator has the form $3(d^2T/dr^2)$ in the limit as r goes to zero.

The resulting set of algebraic equations is, in matrix form, tridiagonal and can be solved by the Thomas method (16): one sequence of elimination followed by one sequence of back-substitution. The values for ξ obtained by the above finite difference scheme are summarized in Table 3.

Table 3

Effectiveness Factors for Nonisothermal Chemical Reaction

(Finite Difference Calculations)

Solution number	$1/\Delta r$	ξ (integrated) (value)	ξ (differentiated) (value)
1	20	1.3105	1.2740
1	50	1.3216	1.3078
1	100	1.3256	1.3195
1	∞*	1.329	1.331
2	20	3.7828	3.9386
2	50	3.6941	3.7582
2	100	3.6671	3.7002
2	∞*	3.642	3.642
3	20	42.701	43.274
3	50	42.323	42.530
3	100	42.183	42.288
3	∞*	42.05	42.05

*linear extrapolation to the value for $\Delta r=0$

The corresponding results for the method of orthogonal collocation are given in Table 4. An interesting comparison can be made by considering the total number of calculations required for the two methods of solution—finite difference and orthogonal collocation. For one of the finite difference solutions the linear differential operator is replaced by a 20x20 matrix ($\Delta r = .05$) which is tri-diagonal: roughly 60 multiplication and addition operations. Additionally, the nonlinear rate expression has to be evaluated 20 times. Now consider the orthogonal collocation solution. The linear differential operator is replaced by a 6x6 matrix ($n = 6$) which is dense (in fact there are no non-zero elements): roughly 36 multiplication and addition operations. The nonlinear rate expression has to be evaluated 6 times. Consequently, the orthogonal collocation solution should be about 2 to 3 times faster (for $n = 6$) than the finite difference solution (for $1/\Delta r = 20$). By inspecting Tables 3 and 4, one sees that the collocation solution ($n = 6$) is also more accurate than the finite difference solution ($1/\Delta r = 20$) (with respect to the extrapolated values of Table 3).

The derivative values of Tables 3 and 4 for ξ are not as accurate as the integrated value. Interestingly, the collocation solution required about 7 seconds of IBM7094 computation time while the quasilinearization-finite difference solution required about 28 seconds. As mentioned previously, the method of orthogonal collocation is, for problems with this type of nonlinearity, the easiest to apply of the methods of weighted

Table 4

Effectiveness Factors for Nonisothermal Chemical Reaction

(Orthogonal Collocation Calculations)

Solution number	n	(integrated value)	(differentiated value)
1	2	1.329	1.313
1	4	1.329	1.329
1	6	1.329	1.329
2	2	4.250	3.616
2	4	3.672	3.573
2	6	3.643	3.628
3	2	33.33	42.06
3	4	45.51	33.59
3	6	41.79	46.73

residuals. For a similar problem having only one mathematical solution, the accuracy obtained was similar but the computation time for collocation was 3 seconds while that for the finite difference solution was 6 seconds. Part of this variation in computation times from one problem to the next will be due to the initial guess for the iterative scheme used to solve the equations. This makes any comparison open to change if the problem is re-worked using a different initial guess.

4. Orthogonal Collocation for Parabolic Partial Differential Equations

The method of orthogonal collocation is developed for nonlinear, parabolic partial differential equations. In principle, the method can

be applied to the following type of problem:

$$\frac{\partial u}{\partial t} = f(\nabla^2 u,\ u_x,\ u,\ x,\ t) \ . \tag{25}$$

Let us assume the following general boundary conditions:

$$\frac{\partial u}{\partial x}(0, t) = k_o\,(h(t) - u(0, t)) \tag{26}$$

$$\frac{\partial u}{\partial x}(1, t) = k_1(g(t) - u(1, t)). \tag{27}$$

For this case the approximate solution, $\tilde{u}(x, t)$, could be assumed to have the following form:

$$\tilde{u}(x, t) = x\,\tilde{u}(1, t) + (1 - x)\,\tilde{u}(0, t) + x(1 - x) \sum_{i=1}^{n} a_i(t)\, P_{i-1}(x) \tag{28}$$

with $P_i(x)$ defined by

$$\int_o^1 P_i(x)\, P_j(x)\ (x^{a-1} dx) = \delta_{ij} \ . \tag{29}$$

The definition of $P_i(x)$ is also an assumption. We want to select the family of polynomials with the weight function which most accurately describes the information we have about the exact solution on the boundary. For the general boundary conditions, $\tilde{u}(0, t)$ and $\tilde{u}(1, t)$ are both unkown functions of time. Consequently, we choose the family of polynomials with the unit weight function. The factor $(x^{a-1} dx)$ represents

the geometry associated with the physical problem and is not part of the weight function normally associated with a given family of polynomials.

As a variation, consider the boundary conditions with k_o, $k_1 \to \infty$. Then we know that

$$u(0, t) = h(t)$$

$$u(1, t) = g(t)$$

and we have

$$\tilde{u}(x, t) = x\, u(1, t) + (1 - x)\, u(0, t) + x(1 - x) \sum_{i=1}^{n} a_i(t)\, P_{i-1}(x) \qquad (30)$$

with a different set of orthogonal polynomials:

$$\int_o^1 x(1 - x)\, P_i(x)\, P_j(x)\, (x^{a-1} dx) = \delta_{ij} . \qquad (31)$$

Additionally, consider the boundary conditions with $k_o \to 0$ and $k_1 \to \infty$. Then we have

$$\frac{\partial u}{\partial x}\,(0, t) = 0$$

$$u\,(1, t) = g(t) .$$

If we know that u(x, t) is an even function (which would satisfy the first boundary condition),

$$\tilde{u}(x, t) = (1, t) + (1 - x^2) \sum_{i=1}^{n} a_i (t) P_{i=1} (x^2) . \tag{32}$$

The use of even functions seems particularly well suited for problems in cylindrical or spherical geometries where the single independent spatial variable is the radial coordinate. The orthogonal polynomials would then be defined as

$$\int_o^1 (1 - x^2) P_i (x^2) P_j (x^2) (x^{a-1} dx) = \delta_{ij}. \tag{33}$$

We refer to these polynomials as the Jacobi polynomials. The polynomials defined by eq. 33 represent only one member of the family of Jacobi polynomials (2).

Lastly, consider the boundary conditions with $k_o \to 0$. Then we have

$$\frac{\partial u}{\partial x} (0, t) = 0$$

$$\frac{\partial u}{\partial x} (1, t) = k_1 (g(t) - u(1, t))$$

and would choose the following form for $\tilde{u}$ (x, t),

$$\tilde{u} (x, t) = \tilde{u} (1, t) + (1 = x^2) \sum_{i=1}^{n} a_i (t) P_{i-1} (x^2) \tag{34}$$

with $P_i (x^2)$ defined by

$$\int_0^1 P_i(x^2)\, P_j(x^2)\, (x^{a-1}dx) = \delta_{ij} \qquad (35)$$

These polynomials are referred to as the Legendre polynomials. In the classical sense the integration was always on the line: dx rather than $x^{a-1}dx$. The roots tend to be grouped closer to right-hand end of the interval (0, 1) as "a" increases from 1 to 2 to 3.

In all cases where $\tilde{u}(0, t)$ and/or $\tilde{u}(1, t)$ is an unknown function, we need to specify how that function is to be obtained. First though, let us consider an alternative to the assumed forms for $\tilde{u}(x, t)$. Equations 28 and 30 can be written equivalently as (with different b_i)

$$\tilde{u}(x, t) = \sum_{i=1}^{n+2} b_i(t)\, x^{i-1} \qquad (36)$$

such that

$$\tilde{u}_j = \tilde{u}(x_j, t) = \sum_{i=1}^{n+2} b_i(t)\, x_j^{i-1} \qquad (j=1, \ldots, n+2)$$

or $$\langle \tilde{u} \rangle = [Q] \langle b \rangle$$

such that $$\langle b \rangle = [Q]^{-1} \langle \tilde{u} \rangle \quad .$$

The particular x_j's of interest are $x_1 = 0$, $x_{n+2} = 1$ and the (n) roots of $P_n(x)$ defined either by eq. 29 or eq. 31. Any differential operators in the variable x can be evaluated at the collocation points be using eq. 36:

$$\frac{\partial \tilde{u}}{\partial x}(x, t)\Big|_{x=x_j} = \sum_{i=1}^{n+2} b_i(t) \left.\frac{\partial x^{i-1}}{\partial x}\right|_{x=x_j}$$

or $$\left\langle \frac{\partial \tilde{u}}{\partial x} \right\rangle = [X_1] \langle b \rangle = [X_1][Q]^{-1} \langle \tilde{u} \rangle \equiv [A] \langle \tilde{u} \rangle \quad (37)$$

such that $\left.\frac{\partial \tilde{u}}{\partial x}\right|_{x=x_j}$ can be written in terms of the unknown solution at the collocation points. Similarly, for $\nabla^2 \tilde{u}$:

$$\nabla^2 \tilde{u}(x, t)\Big|_{x=x_j} = \sum_{i=1}^{n+2} b_i(t) \left[\nabla^2 x^{i-1}\right]\Big|_{x=x_j}$$

or $$\langle \nabla^2 \tilde{u} \rangle = [X_2][Q]^{-1} \langle \tilde{u} \rangle \equiv [B] \langle \tilde{u} \rangle . \quad (38)$$

There are similar matrices ([A] and [B]) for u(x, t) defined by eqs. 32 and 34.

The reason for utilizing eq. 36 is two-fold: (1) numerically, problems are easier to solve in terms of the values of the solution at the collocation points rather than in terms of the expansion coefficients, and (2) only the roots of the polynomials are required. If, as example, eq. 28 were used rather than eq. 36,

$$\frac{\partial \tilde{u}}{\partial x}(x, t)\Big|_{x=x_j} = \tilde{u}(1, t) - \tilde{u}(0, t) + (1-2x_j) \sum_{i=1}^{n} a_i(t) P_{i-1}(x_j)$$

$$+ x_j (1 - x_j) \sum_{i=1}^{n} a_i (t) (P_{i-1}') \Big|_{x=x_j}$$

the evaluation of the derivatives would require not only the roots, but also the explicit form of the polynomials. This calculation can become quite tedious in practice.

With $\tilde{u}$ (0, t) and/or $\tilde{u}$ (1, t) unknown, one simply utilizes the original boundary condition and the elements of the matrix operator $[A_{ij}]$:

$$\sum_{j=1}^{n+2} A_{1,j} \tilde{u}_j = k_o (h (t) - \tilde{u}_1)$$

or

$$\sum_{j=1}^{n+2} A_{n+2,j} \tilde{u}_j = k_1 (g (t) - \tilde{u}_{n+2})$$

with the linear boundary conditions. This does not imply that the boundary conditions need to be linear. Consider the dimensionless equations governing the laminar flow of a fluid through a pipe in which a chemical reaction is occurring at the wall:

$$(1 - r^2) \frac{\partial c}{\partial z} = \frac{1}{Pe} \frac{(4L)}{D_t} \frac{1}{r} \frac{\partial}{\partial r} \left(r \frac{\partial c}{\partial r}\right)$$

$$c(r, 0) = \phi (r)$$

$$-\frac{2}{Pe}\ \frac{\partial c}{\partial r}\ (1, z) = \frac{\alpha_1\ c\ (1, z)}{\alpha_2 + c\ (1, z)} \quad .$$

We could let

$$\tilde{c}\ (r, z) = \tilde{c}\ (1, z) + (1 - r^2)\ \sum_{i=1}^{n+1}\ a_i\ (z)\ P_{i-I}\ (r^2)$$

with $P_i\ (r^2)$ defined by

$$\int_o^1\ P_i\ (r^2)\ P_j\ (r^2)\ (rdr)\ = \delta_{ij}$$

such that the nonlinear boundary condition is given by,

$$-\frac{2}{Pe}\ \sum_{i=1}^{n+1}\ A_{n+1,\,i}\ \tilde{c}_i = \frac{\alpha_1\ \tilde{c}_{n+1}}{\alpha_2 + \tilde{c}_{n+1}}$$

where $Pe = v_{z,\,max}\ D_t/D$, $\alpha_1 = k/\ (v_{z,\,max}\ c_{ref})$, and $\alpha_2 = K/c_{ref}$.

Orthogonal collocation would apply to this simple parabolic partial differential equation, and the nonlinear boundary condition would present no difficulty.

Be definition of partial differentiation, we know that

$$\frac{\partial \tilde{u}\ (x, t)}{\partial t}\Bigg|_{x=xj} = \frac{d\tilde{u}}{dt}\ (x_j, t) \equiv \frac{d\tilde{u}_j}{dt} \qquad (39)$$

such that our original nonlinear parabolic PDE can be written as

$$\frac{d}{dt}\langle \underline{\tilde{u}} \rangle = \langle f\left(\sum_{j=1}^{n+2} B_{ij}\,\tilde{u}_j,\ \sum_{j=1}^{n+2} A_{ij}\,\tilde{u}_j,\ \tilde{u}_i,\ x_i,\ t\right) \rangle \qquad (40)$$

(in vector notation) where the initial conditions are obtained from

$$u(x, 0) = \phi(x)$$

as $$\tilde{u}(x_j, 0) = \tilde{u}_j(0) = \phi(x_j) \ .$$

The important questions surrounding the method of orthogonal collocation are the following:

(1) convergence of $\tilde{u}_j(t) \rightarrow u(x_j, t)$
and $\tilde{u}(x, t) \rightarrow u(x, t)$,

(2) bounding the error between $\tilde{u}(x, t)$ and $u(x, t)$ for a particular number of collocation points,

and (3) numerical stability in integrating eq. 40 numerically.

Error bounds are discussed at some length in Chapter B, and the question of numerical stability is investigated for a particular class of problems in the following presentation of illustrative applications.

We can show quite easily that the question of convergence of the orthogonal collocation solution is closely related to the question of the convergence of the solution obtained by Galerkin's method. The relation depends on the connection between orthogonal collocation and the general class of Gaussian-like quadrature schemes. The particular quadrature

weights are positive and can be calculated knowing only the collocation points (21):

$$\int_0^1 w(x)\, f(x)\, (x^{a-1}\, dx) \approx \sum_{i=1}^{n+k} W_i^{(n+k)}\, f(x_i) \quad .$$

The calculation of the quadrature weights, $W_i^{(n+k)}$, depends on the fact that the above approximation is exact for all f (x) which are polynomials of degree less than or equal to 2n+2k (for a quadrature scheme which uses n interior points and k of the end-points of the interval—03 1, or 2):

$$\langle \int_0^1 w(x)\, x^{i-1}\, (x^{a-1} dx) \rangle = \langle W_i^{(n+k)} \rangle \; [x_j^{i-1}]$$

such that

$$\langle W_i^{(n+k)} \rangle = [Q]^{-1} \langle \int_0^1 w(x)\, x^{i-1}\, (x^{a-1} dx) \rangle \quad .$$

The above feature implies that orthogonal collocation is, for fixed n, a highly accurate approximation to Galerkin's method.

$$\int_0^1 w(x)\, P_i(x)\, R[\tilde{u}(x,t)]\, (x^{a-1} dx) = \sum_{j=1}^{n+k} W_j^{(n+k)}\, P_i(x_j)\, R[\tilde{u}(x_j,t)] + E^{(n)}$$

In proving convergence of the solution obtained by Galerkin's method, one requires that

$$\int_0^1 w(x)\, P_i(x)\, R[\tilde{u}(x,t)]\, (x^{a-1}dx)$$

be identically zero for i=0, 1, . . . , (n-1). In the quadrature, Stieltjes theorem (1) states that the quadrature error, $E^{(n)}$, goes to zero as n goes to infinity (provided the residual function be continuous). Since the matrix $[W_j^{(n+k)} P_i(x_j)]$ is invertible, we find that as n goes to infinity (in applying Galerkin's method) that

$$R[\tilde{u}(x_j, t)] = 0 \quad .$$

That is, if the approximate solution satisfies Galerkin's method, it must also satisfy the orthogonal collocation method. This observation makes available to us all the previous work done on the convergence of Galerkin's method for nonlinear parabolic PDEs. (3, 4, 6b, 9)

A simple illustrative example has been selected to exemplify the role that numerical stability plays with the method of orthogonal collocation. It is important to understand how the method of orthogonal collocation effects the numerical stability of a parabolic partial differential equation. By replacing the spatial differential operator by a matrix operator, one should expect the numerical stability to depend on a property of this matrix. For a particular geometry, the matrix elements will depend on the collocation points or more specifically the orthogonal polynomials themselves.

Consider the following parabolic partial differential equation:

$$\frac{\partial u}{\partial t} = \frac{\partial^2 u}{\partial x^2} + f(x, u)$$

$$\frac{\partial u}{\partial x}(0, t) = 0$$

$$\frac{1}{a}\frac{\partial u}{\partial x}(1, t) + u(1, t) = h(t)$$

$$u(x, 0) = \phi(x) \quad .$$

Orthogonal collocation approximates this problem by,

$$\frac{d\tilde{u}_i}{dt} = \sum_{j=1}^{n+1} B_{ij}\,\tilde{u}_j + f(x_i, \tilde{u}_i)$$

$$\frac{1}{a}\sum_{j=1}^{n+1} A_{n+1,j}\,\tilde{u}_j + \tilde{u}_{n+1} = h(t)$$

$$\tilde{u}_i(0) = \phi(x_i)$$

where $\tilde{u}_i(t)$ approximates $u(x_i, t)$. The 'boundary condition approximate' can be solved explicitly for $\tilde{u}_{n+1}(t)$:

$$\tilde{u}_{n+1}(t) = \frac{a\,h(t) - \sum_{i=1}^{n} A_{n+1,i}\,\tilde{u}_j}{a + A_{n+1,n+1}}$$

such that

$$\frac{d\tilde{u}_i}{dt} = \sum_{j=1}^{n} \left[B_{ij} - \frac{B_{i,n+1}\, A_{n+1,j}}{a + A_{n+1,n+1}} \right] \tilde{u}_j + f(x_i, \tilde{u}_i) + \frac{a\, h(t)}{a + A_{n+1,n+1}} \qquad (41)$$

with $\tilde{u}_i(0) = \phi(x_i)$. We abbreviate the working equations (eq. 41) as,

$$\frac{d\tilde{u}_i}{dt} = \sum_{j=1}^{n} N_{ij}\, \tilde{u}_j + f(x_i, \tilde{u}_i) + g(t) \qquad (42)$$

$$\tilde{u}_i(0) = \phi(x_i) \; .$$

The stability analysis for most nonlinear equations is, by necessity, the result of linearizing the equation(s). Let $\tilde{u}_i$ be the exact solution of eq. 42 and let $(\tilde{u}_i - e_i)$ be the numerically calculated value of the solution. Then

$$\frac{d}{dt}(\tilde{u}_i - e_i) = \sum_{j=1}^{n} N_{ij} (\tilde{u}_j - e_j) + f(x_i, \tilde{u}_i - e_i) + g(t) + 0(\Delta t^p)$$

where p depends on the numerical method used to integrate eq. 42. For small Δt, one has

$$\frac{de_i}{dt} = \sum_{j=1}^{n} N_{ij}\, e_j + [f(x_i, \tilde{u}_i) - f(x_i, \tilde{u}_i - e_i)] \; .$$

By linearizing the nonlinear function (about $\tilde{u}_i$ by using a Taylor's series),

$$\frac{de_i}{dt} = \sum_{j=1}^{n} \left[N_{ij} + \frac{\partial f}{\partial u}\Big|_{u=u_i-e_i} \delta_{ij} \right] e_j = \sum_{j=1}^{n} M_{ij}(t)\, e_j$$

of $\quad \frac{d}{dt} \langle e \rangle = [M] \quad \langle e \rangle \quad .$

N_{ij} depends on the particular orthogonal polynomials chosen, and the stability analysis further depends on the numerical method used to integrate the equations. For simplicity, we investigate the improved Euler method (10) which can be symbolically represented as:

$$\text{Predictor:} \quad y^{(o)}[(n+1)\Delta t] = y^{(o)}_{n+1} = y_n + \Delta t\, y'_n$$

$$\text{Corrector:} \quad y^{(m+1)}_{n+1} = y_n + \frac{\Delta t}{2} [y^{(m)}_{n+1} + y'_n]$$

The method is explicit if the corrector is utilized only once per time step, Δt. Corresponding to the explicit improved Euler method, the errors are governed by the following set of algebraic equations:

$$\langle e_{n+1} \rangle = \langle e_n \rangle + \frac{\Delta t}{2} \left\{ [M_{n+1}] \left([I] + \Delta t\, [M_n] \right) + [M_n] \right\} \langle e_n \rangle$$

where $[M_n]$ is evaluated at $n\Delta t$ and $[M_{n+1}]$ is evaluated at $(n+1)\,\Delta t$ using $y^{(o)}_{n+1}$.

This set of algebraic equations is satisfied by solutions of the form

$$\langle e_n \rangle = \begin{bmatrix} e_1^n \\ e_2^n \\ \cdot \\ \cdot \\ \cdot \end{bmatrix} \qquad \text{with } e_k \neq e_1 \text{ for } k \neq 1$$

and n corresponds to $n\Delta t$

where the e_j's are constants determined from

$$\begin{bmatrix} e_1^{n+1} \\ e_2^{n+1} \\ \cdot \\ \cdot \\ \cdot \end{bmatrix} = \begin{bmatrix} e_1^n \\ e_2^n \\ \cdot \\ \cdot \\ \cdot \end{bmatrix} + \frac{\Delta t}{2} \left\{ [M_{n+1}] + \Delta t\, [M_{n+1}]\,[M_n] + [M_n] \right\} \begin{bmatrix} e_1^n \\ e_2^n \\ \cdot \\ \cdot \\ \cdot \end{bmatrix}$$

but

$$\begin{bmatrix} e_1^{n+1} \\ e_2^{n+1} \\ \cdot \\ \cdot \\ \cdot \end{bmatrix} = \begin{bmatrix} e_1 & & & \\ & e_2 & O & \\ & & \cdot & \\ O & & & \cdot \end{bmatrix} \begin{bmatrix} e_1^n \\ e_2^n \\ \cdot \\ \cdot \\ \cdot \end{bmatrix} \equiv [e]\ \langle e^n \rangle$$

As a simplifying assumption, we take

$$[M_{n+1}] = [M_n] + \Delta t\ \frac{d}{dt}[M_n] + 0(\Delta t^2) \tag{43}$$

and then use eq. 43 for M_{n+1} in the equations for $\langle e^n \rangle$ such that

$$[e]\ \langle e^n \rangle = \langle e^n \rangle + \frac{\Delta t}{2} \left\{ 2[M_n] + \Delta t \left(\frac{d}{dt}[M_n] + [M_n]\ [M_n] \right) + (\Delta t)^2 \left(\frac{d}{dt}[M_n] \right) [M_n] \right\} \langle e^n \rangle$$

For problems where the solution changes slowly over the time imterval $[t,\ t + \Delta t]$ one could neglect the effect of $\frac{d}{dt}\ [M_n]$,

$$[e]\ \langle e^n \rangle = \langle e^n \rangle + \frac{\Delta t}{2} \left\{ 2\,[I] + \Delta t\,[M_n] \right\} [M_n]\ \langle e^n \rangle$$

or $$\Delta t \left\{ [M_n] + \frac{\Delta t}{2}\,[M_n]^2 \right\} \langle e^n \rangle = \left\{ [e] - [I] \right\} \langle e^n \rangle .$$

Using the folowing vector norm

$$|| \langle v \rangle ||_\infty \equiv \max_i |\ v_i\ |$$

then,

$$\Delta t\ || \left\{ [M_n] + \frac{\Delta t}{2}\,[M_n]^2 \right\} \langle e^n \rangle ||_\infty = || \left\{ [e] - [I] \right\} \langle e^n \rangle ||_\infty .$$

The definition of the corresponding natural matrix norm is (8);

$$|| [C] ||_\infty \equiv \sup_{\substack{\langle x \rangle \\ \langle x \rangle \neq 0}} \frac{|| [C] \langle x \rangle ||_\infty}{|| \langle x \rangle ||_\infty} = \max_i \sum_{j=1}^{n} |\ C_{ij}\ |$$

such that

$$\Delta t\ || \left\{ [M_n] + \frac{\Delta t}{2}\,[M_n]^2 \right\} \langle e^n \rangle ||_\infty = \frac{|| \left\{ [e] - [I] \right\} \langle e^n \rangle ||_\infty}{|| \langle e^n \rangle ||_\infty} \cdot$$

$$|| \langle e^n \rangle ||_\infty$$

$$\leq || [e] - [I] ||_\infty || \langle e^n \rangle ||_\infty .$$

As discussed by Hildebrand (7), if one is to have numerical stability $|e_j| \leq 1$ $(j=1, \ldots, n)$ is required.

$$|| [e] - [I] ||_\infty = \max_i | e_i - 1 | \leq \max_i | e_i | + 1 < 2$$

such that $$\frac{\Delta t \; || \left\{ [M_n] + \frac{\Delta t}{2} [M_n]^2 \right\} \langle e^n \rangle ||_\infty}{|| \langle e^n \rangle ||_\infty} \leq 2 \; .$$

With

$$\frac{|| \left\{ [M_n] + \frac{\Delta t}{2} [M_n]^2 \right\} \langle e^n \rangle ||_\infty}{|| \langle e^n \rangle ||_\infty} \leq || [M_n] + \frac{\Delta t}{2} [M_n]^2 ||_\infty$$

if $[M_n]$ is bounded, there will always be a value of Δt small enough to guarantee that

$$\Delta t \; || [M_n] + \frac{\Delta t}{2} [M_n]^2 ||_\infty < 2 \; . \tag{44}$$

The stability criteria of eq. 44 can be related to the eigenvalues of the matrix $[M_n] + \frac{\Delta t}{2} [M_n]^2$. A corollary of Geishgorn's theorem (7) states that,

$$\mu \left([M_n] + \frac{\Delta t}{2} [M_n]^2 \right) \leq || [M_n] + \frac{\Delta t}{2} [M_n]^2 ||_\infty$$

where the spectral radius, μ, is defined by

$$\mu \left([M_n] + \frac{\Delta t}{2} [M_n]^2 \right) = \max_i | \lambda_i \left([M_n] + \frac{\Delta t}{2} [M_n]^2 \right) | \; .$$

The values λ_i are the eigenvalues of the matrix, $[M_n] + \frac{\Delta t}{2}[M_n]^2$, and may be complex valued—that is why we measure the modulus of the λ_i. Eq. 44 can then be augmented to utilize the spectral radius,

$$\Delta t \left[\max_i | \lambda_i |\right] \leq \Delta t \, || \, [M_n] + \frac{\Delta t}{2}[M_n]^2 \, ||_\infty \leq 2 \quad .$$

The stability criteria involving the spectral radius has been presented previously as a necessary condition (14) and indicates that larger values of Δt are stable for integration (than indicated by the matrix norm). Although the matrix norm gives a more conservative criteria (and this is due to the particular analysis involved) it would require much less computation time to use than would the calculation of the modulus of the maximum eigenvalue. This is an important consideration.

In the stability criteria just discussed the numerical factor of 2 is particular to the method of numerical integration that was investigated. For Hamming's predictor-modifier-corrector method (10), the factor would be roughly .85.

We stated initially that the stability criteria should encompass some characteristic of the orthogonal polynomials. It has been shown that this characteristic is the maximum eigenvalue for the matrix operator (or an approximation to the maximum eigenvalue). Consider the simple example of

$$\Delta t \left[\max_i | \lambda_i ([N])] \leq \Delta t \, || \, [N] \, ||_\infty \leq 2$$

and the polynomials defined by

$$\int_0^1 (1 - r^2)\, P_i(r^2)\, P_j(r^2)\, (r^2 dr) = \delta_{ij}$$

with a = 27.65 and ∞ (eq. 41). The following results have been obtained (for n = 6):

a	$\max_i \lvert \lambda_i([N]) \rvert$	$\lVert [N] \rVert_\infty$
∞	1150	1482
27.65	570	677

By neglecting the nonlinear term, these results are applicable to a simple parabolic partial differential equation that appears in the next subsection. For this example the use of the simplier expression

$$\Delta t \, \lVert [N] \rVert_\infty \leqslant 2 \tag{45}$$

gives conservative estimates of Δt_{max}, but they are very close to the actual Δt_{max}.

Values of the norm, $\lVert [N] \rVert_\infty$, are shown in fig. 12 for several different polynomials. For all polynomials studied, as n increases, the value of the norm increases. That is, as n increases, one finds that the stability requirement becomes more stringent: Δt has to be decreased. One also finds that the stability requirement is far more stringent for the Lengendre polynomials than for the Jacobi polynomials. It is interesting to note the stabilizing effect of a finite film coefficient at the

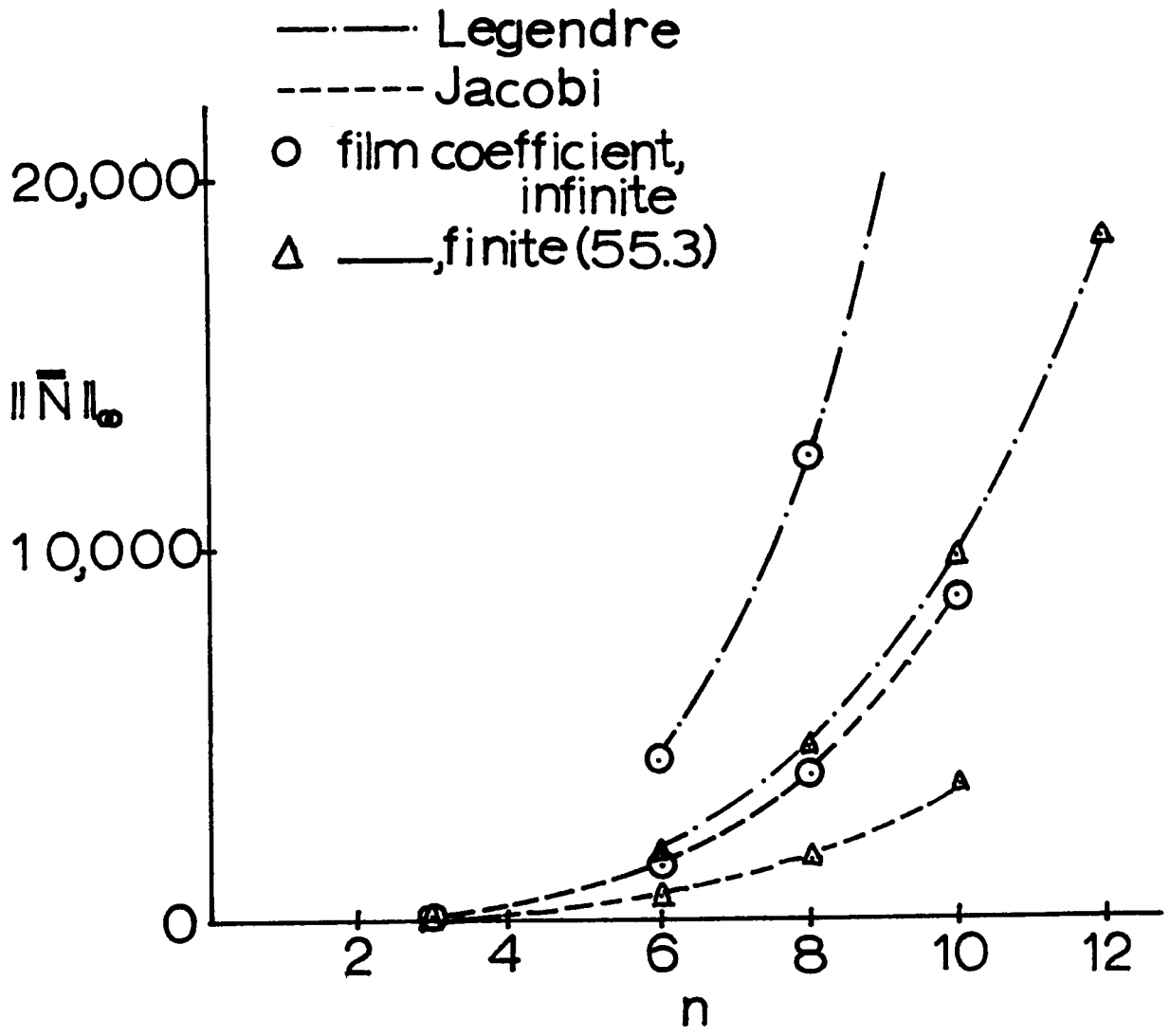

Figure 12. Matrix norm of eq. 45 versus n (spherical geometry).

boundary.

With the nonlinear function, f(x, u), present, it is difficult to predict how the stability requirement can be met: $[M_{ij}]$ depends on the solution itself. It is possible to control Δt and assure stability by utilizing eq. 44 as part of the numerical solution. For the applications (nonlinear) discussed in the following subsection, we have used a Lewis number of .85 and have predicted the stable value of Δt from equation 45. With smaller Lewis numbers, the temperature function and the rate expression (highly nonlinear) will dominate the stability criteria in a manner which would have to be periodically checked.

5. Applications of Orthogonal Collocation—Parabolic Equations

To illustrate the method of orthogonal collocation for nonlinear parabolic partial differential equations we study the unsteady diffusion of mass and energy within a catalyst particle. Due to the nonlinear dependence of reaction rate on temperature, the coupling between mass and energy transport can yield unusual behavior: for example, the maximum temperature achieved during a transient can exceed the maximum steady-state temperature and cause catalyst damage. These equations arise in some models of chemical reactors (16):

$$\frac{N_1}{4}\frac{\partial T}{\partial t} = \frac{1}{r^2}\frac{\partial}{\partial r}\left(r^2 \frac{\partial T}{\partial r}\right) + \phi^2 \beta c \exp(-\gamma(1/|T| - 1)) \qquad (46)$$

$$\epsilon_p \frac{N_2}{4}\frac{\partial c}{\partial t} = \frac{1}{r^2}\frac{\partial}{\partial r}\left(r^2 \frac{\partial c}{\partial r}\right) - \phi^2 c \exp(-\gamma(1/|T| - 1)) \qquad (47)$$

with $$T(r, 0) = \phi(r) \; ; \qquad \frac{\partial T}{\partial r}(0, t) = 0$$

$$c(r, 0) = \psi(r) \qquad \frac{\partial c}{\partial r}(0, t) = 0 \tag{48}$$

and $$-\frac{\partial T}{\partial r}(1, t) = \frac{Nu}{2}\,(T(1, t) - g(t)) \tag{49}$$

$$-\frac{\partial c}{\partial r}(1, t) = \frac{Sh}{2}\,(c(1, t) - h(t)) \tag{50}$$

$$\epsilon = .65 , \quad N_1 = 705 , \quad N_2 = 1225 .$$

In practice, the quantity of interest is the flux of mass and energy to and from the catalyst. Consequently, we compare the accuracy of different calculation methods by comparing the flux. We also compare the computation times for the various methods. Even a small reactor may have 75 catalyst particles (16) and this makes the time savings discussed below for a single particle quite significant.

Because of the conditions placed on $T(r, t)$ and $c(r, t)$ in eqs. 48-50, one might assume the following form for $\tilde{T}(r, t)$:

$$\tilde{T}(r, t) = \hat{T}(1, t) + (1 - r^2) \sum_{i=1}^{n} a_i(t)\, P_{i-1}(r^2) \; .$$

We investigate the use of the polynomials defined by eqs. 33 and 35 (a=3). The approximate solution, $\tilde{T}_i$, is governed by a system of equations similar to eq. 40,

$$\frac{N_1}{4}\frac{d\tilde{T}_i}{dt} = \sum_{j=1}^{n+1} B_{ij}\,\tilde{T}_j + \phi^2\beta\,\tilde{c}_i \exp(-\gamma(1/|\tilde{T}_i| - 1)) \quad (i=1,\ldots,n) \quad (51)$$

$$\epsilon_P \frac{N_2}{4}\frac{d\tilde{c}_i}{dt} = \sum_{j=1}^{n+1} B_{ij}\,\tilde{c}_j - \phi^2\,\tilde{c}_i \exp(-\gamma(1/|\tilde{T}_i| - 1)) \quad (i=1,\ldots,n) \quad (52)$$

Like eq. 15, $[B_{ij}]$ is a square (n+1)-element matrix. $\tilde{T}_{n+1}$ is governed by the boundary condition. For a boundary condition of the first kind,

$$\tilde{T}_{n+1} \equiv \tilde{T}(1,t) = T(1,t) .$$

With a boundary condition of the third kind, eq. 49, we have

$$-\sum_{j=1}^{n+1} A_{n+1,j}\,\tilde{T}_j = \frac{Nu}{2}\,(\tilde{T}_{n+1} - g(t)) \quad (53)$$

and $\tilde{T}_{n+1}$ is an unknown function of time.

The system of first order ordinary differential equations, eqs. 51 and 52, can be integrated numerically using any standard method of integration. A simple explicit forward difference would replace eq. 51 by

$$\frac{N_1}{4}\,\frac{\tilde{T}_{i,m+1} - \tilde{T}_{i,m}}{\Delta t} = \sum_{j=1}^{n+1} B_{ij}\,\tilde{T}_{j,m} + \phi^2\beta\,\tilde{c}_{i,m}\exp(-\gamma(1/|\tilde{T}_{i,m}|)-1)) \quad (54)$$

Finite difference methods will lead to similar equations except that the matrix B will be sparse (and usually of a definite structure such as

tri-diagonal). In the orthogonal collocation method each element of B is non-zero. This difference in the B matrix (and the A matrix as well) arises because finite difference schemes are local methods while orthogonal collocation is a global method:

$$\text{Finite difference: } \left.\frac{\partial^2 u}{\partial x^2}\right|_{x_j,\, t_k} = \frac{1}{\Delta x^2}\left[u_{j+1,\,k}\right] - \frac{2}{\Delta x^2}\left[u_{j,\,k}\right] + \frac{1}{\Delta x^2}\left[u_{j-1,\,k}\right]$$

$$\text{Orthogonal collocation: } \left.\frac{\partial^2 u}{\partial x^2}\right|_{x_j,\, t_k} = \sum_{i=1}^{n+1} B_{ji}\, u_{i,\,k} \quad .$$

Equivalently, with orthogonal collocation the derivatives at x_j depend on the values of the solution at <u>every</u> collocation point, not just three as in the above finite difference example. As a consequence of this very important difference, one usually finds that a small number of collocation points will give very good solutions to most differential equations.

Of the many methods for integrating eqs. 51 and 52, we have chosen Hammings predictor-modifier-corrector method, $0(\Delta t)^5$, and the improved Euler method, $0(\Delta t)^2$. Because of the exponential nonlinearity in eqs. 51 and 52, it is desireable to evaluate the right-hand side as few a number of times per Δt as possible. This requirement excludes the 4-th order Runge-Kutta methods (which use four evaluations per Δt). Both of the methods used require only two evaluations of the nonlinearity per time step.

a. linear diffusion

We first apply orthogonal collocation to the unsteady-state diffusion in a slab. Liu (12) has previously compared finite difference methods for this problem.

$$\frac{\partial u}{\partial t} = \frac{\partial^2 u}{\partial x^2}$$

$$\frac{\partial u}{\partial x}(0, t) = 0, \quad u(1, t) = 1 , \quad u(x, 0) = 0$$

The Jacobi polynomials and Hamming's predictor-modifier-corrector method (10) are used.

The value of the solution at the collocation point was compared to the exact value given by an infinite series and the errors are shown in Table 5. A three-term expansion is accurate within 0.02% and a six-term expansion gives six digit accuracy. For smaller times than those shown some error occurs due to the discontinuous initial conditions, as in finite difference methods. The computation times can be reduced by using another method of integrating ODEs. It was also found that one can use a step size relatively close to that predicted by an equation similar to eq. 45, applicable to Hamming's method.

It is clear from Table 5 that the orthogonal collocation method can give accurate results. Comparison with the calculations reported by Liu (12) shows that the collocation solution is more accurate than finite difference solutions which use three to twelve times as many spatial grid points.

Table 5

Pointwise Error for Linear Diffusion Problem

n	Computation time (Sec. on IBM 7094)	Δt	$\frac{1}{n}\sum_{i=1}^{n} \lvert \tilde{u}(x_i, t) - u(x_i, t) \rvert$	
			t = 0.1	t = 0.5
3	0.237	0.005	.000133	.000000
6	4.097	0.0005	.000000	.000000

b. boundary condition of the first kind

We consider next the diffusion of mass and energy in a spherical catalyst pellet with an exothermic first order irreversible reaction. The equations are given as eqs. 46-50 with

$$T(r, 0) = 1.05, \quad c(r, 0) = 1.00, \quad T(1, t) = c(1, t) = 1.00$$

and $\phi^2 = .25$, $\beta = .6$, and $\gamma = 20$. The collocation equations are given by eqs. 51 and 52. This problem represents the response to a step change in temperature and the solution approaches the first steady-state solution as discussed in subsection 3. Calculations are made using orthogonal collocation and finite difference methods. For a reactor model the flux at the surface of the individual particles is the most important quantity and is expected to be less accurate than the temperature and concentration values themselves. For the collocation solution the flux

is given by

$$\frac{\partial \tilde{T}}{\partial r}\Big|_{r=1} = \sum_{j=1}^{n+1} A_{n+1,j}\,\tilde{T}_j \tag{54}$$

For the finite difference solutions the flux was initially evaluated by a two-point difference. This proved to be so inaccurate, however, that another means was devised. If eq. 46 is integrated over r one obtains:

$$\frac{\partial T}{\partial r}\Big|_{r=1} = \int_0^1 \left[\frac{N_1}{4}\,\frac{\partial T}{\partial t} - \phi^2 \beta\, c\, \exp(-\gamma(1/|T| - 1))\right](r^2 dr). \tag{55}$$

Simpson's rule was used to calculate the integral, and this gives a more accurate representation of the flux for coarse grid spacings. The collocation solution gave nearly identical results using either eq. 54 or 55. Finite difference solutions are identified by the grid spacings (Δr, Δt) and collocation solutions by the number of collocation points and step size (n, Δt).

The collocation solution was calculated using Jacobi polynomials and the equations were integrated to t=5 using Hamming's method. The finite difference scheme used on this problem was Liu's method (see Appendix 1) which is an accurate, stable explicit scheme (12). Calculations for this problem were made on an IBM 7094 computer.

Exploratory calculations, Fig. 13, indicated that the development of the solution in time was relatively smooth except for small times. The large oscillations in the approximate initial condition arise because

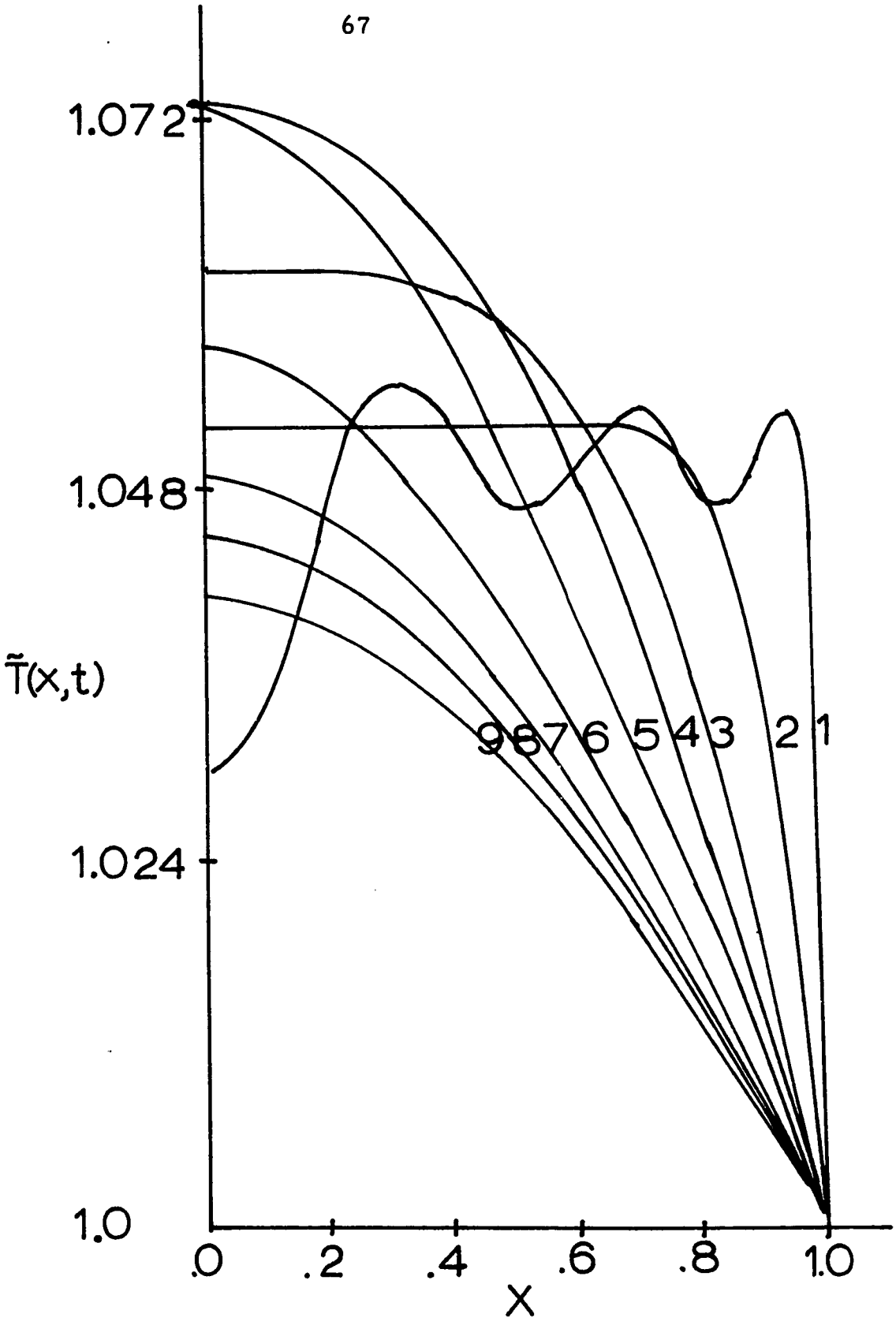

Figure 13. Temperature profiles for various times. (Using Jacobi polynomials, n=6, Hamming's method, $\Delta t = 0.05$) 1 to 9 correspond to t = 0, 1, 5, 10, 25, 50, 75, 100, and ∞.

one is trying to approximate a step function with a low order polynomial. These oscillations die out rapidly ($t < 1$) and have little effect on the solution for $t > 1$. At the collocation points the temperature equals the initial condition value as would the temperature function in a finite difference solution. With a finite difference solution, one merely draws a curve through the solution; while with orthogonal collocation the 'curve' is already specified. To approximate temperature functions with steep gradients more terms are needed, as is shown below. Because of the smoothness of the solution for $t > 5$, and the fact that the steady-state had a dimensionless time of the order of 100, it was decided to limit all further computations to $t < 5$.

A comparison of the collocation solution (6, 0.05) to the best finite difference solution (0.01, 0.005) showed that they agree to within four or five digits. As n increases to eight and ten, the agreement increases to five or six digits. The behavior of the surface flux under different conditions is shown in Tables 6 and 7. The collocation method ($n = 6$) gives the surface flux within one-half per cent whereas the finite difference solution ($\Delta r = 0.05$) is in error by 3%. At $t = 1$, the collocation solution with $n = 10$ gives better results than the finite difference solution with $1/\Delta r = 100$, demonstrating that the number of collocation points can be about ten times less than the number of finite difference grid points for equivalent accuracy. For the same Δt the collocation method with $n = 8$ uses about the same computation time as the finite difference

Table 6

Collocation Surface Derivatives

		Surface Heat Flux		Computation Time (Sec on IBM 7094)
n	Δt	t = 1	t = 5	
6	.05	0.3419	0.1570	4.8
8	.01	0.3430	0.1570	27.7
10	.01	0.3431	0.1570	39.2

Table 7

Finite Difference Surface Derivatives

		Surface Heat Flux		Computation Time (Sec on IBM 7094)
Δr	Δt	t = 1	t = 5	
.05	.01	0.3537	0.1579	25.7
.025	.005	0.3465	0.1575	101.3
.01	.005	0.3449	0.1574	251.2

method with $1/\Delta r = 20$. This provides a quantitative comparison of computation time when the matrix B in eq. 54 is tri-diagonal or complete. In this case the collocation method would be preferred because it is more accurate.

Figure 14 shows the error in the surface flux as a function of computation time. The values are compared to the average of the best

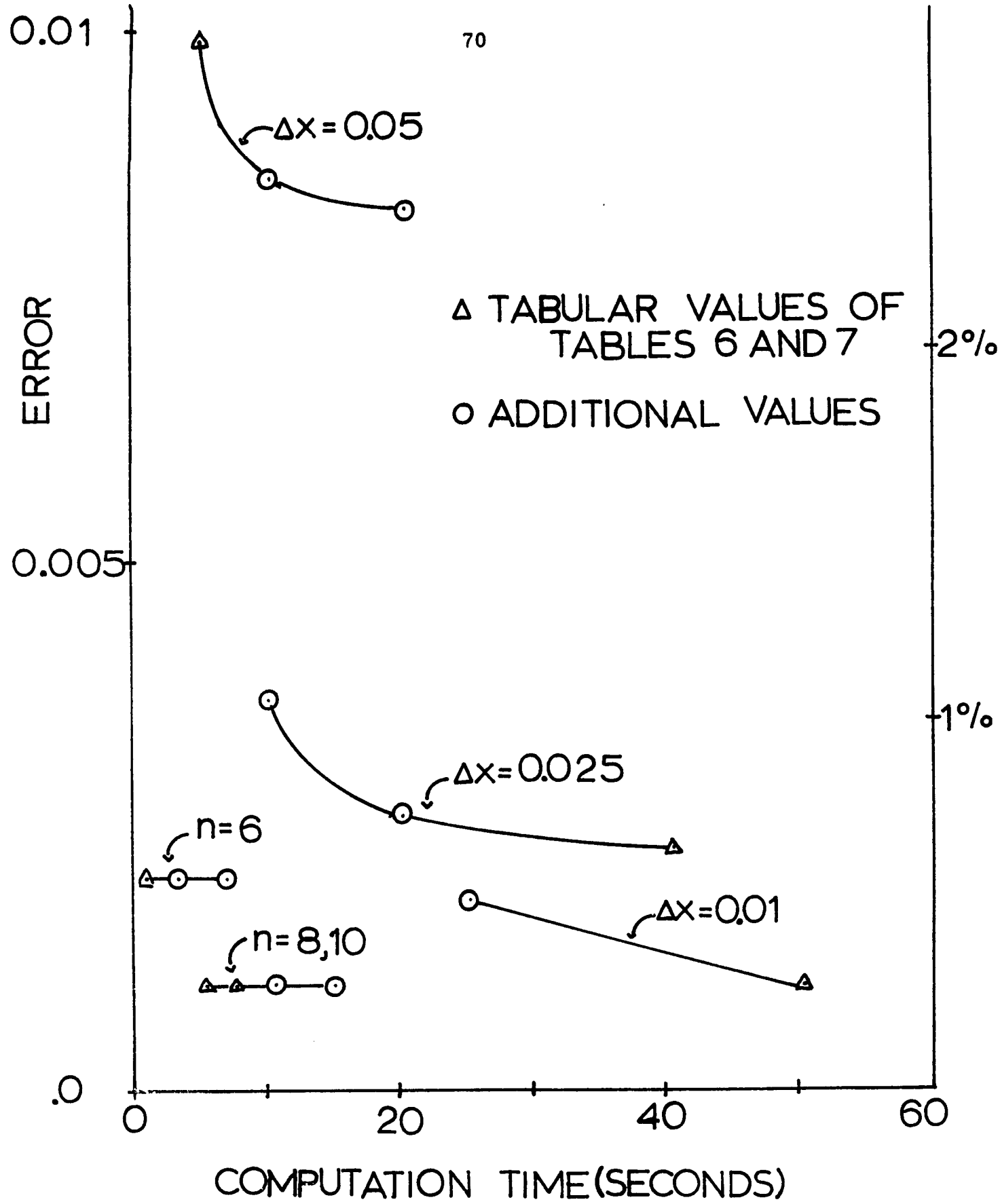

Figure 14. Estimated error in the temperature surface flux versus computation time (t = 1.0).

finite difference and best collocation solutions (they differed by about $\frac{1}{2}$%). The triangle symbols represent the values in Tables 6 and 7. For the collocation method the optimum Δt was just below the value of Δt for which the problem became numerically unstable. Further decreases in Δt, or increases in computation time, caused little if any change.

It is clear from Fig. 14 that the collocation solution is much faster than a finite difference solution of comparable accuracy. If the various solutions are compared to the best solution obtained using the same method, the collocation solution (6, 0.05) is about twenty times as fast as a finite difference solution (0.025, 0.005) of about the same accuracy. In this case the speed advantage is due to the ability to take larger time steps in the collocation method, and this is made possible due to the smaller number of terms necessary to obtain the solutions.

c. boundary condition of the third kind

For this case we have boundary conditions given by eqs. 49 and 50.

$$g(t) = 1.1, \quad h(t) = 1.0, \quad Nu = 55.3, \quad Sh = 66.5 \tag{56}$$

The boundary condition, eqs. 49, 50 and 56, are satisfied by eq. 53 with a similar equation for concentration. The initial conditions are taken as the two-term approximation to the intermediate steady-state solution for the problem with infinite Nu and Sh. The 10% temperature perturbation on the boundary is sufficient to drive the solution to the third steady-state.

Collocation solutions are derived using Jacobi, Legendre, or Chebycheff ($w(x) = 1/(1 - x^2)^{\frac{1}{2}}$) polynomials and either the improved Euler or Hamming's method of integration. Calculations are continued until $t = 35$. Finite difference solutions are obtained using Liu's method and the implicit method. In the implicit method the boundary conditions are handled using a false boundary to retain the second-order truncation error and the reaction rate term was evaluated at the previous time, as was done by McGuire and Lapidus (16). Calculations were done on a CDC 6400 computer, which proved to be about twice as fast as the IBM 7094 for these problems.

Exploratory calculations, Fig. 15, indicated the solution had large spatial and time derivatives. Consequently, we expect that more terms are needed to approximate the solution. Experience showed, too, that even though the temperature was approximated within two to three digits using 6 to 10 terms and the Jacobi polynomials, the convergence with n was rather slow (see Table 8). If Legendre polynomials are used instead the convergence was much faster. This is probably due to the fact that the Jacobi polynomials weight more heavily the region away from the boundary due to the factor $(1 - r^2)$, whereas the Legendre polynomials give equal weight to all regions (except for the skewness introduced by the spherical geometry). In boundary conditions of the third kind, the temperature at the boundary is not known, so that better results for the flux at the boundary are expected if the region near the boundary is emphasized, or at least not de-emphasized.

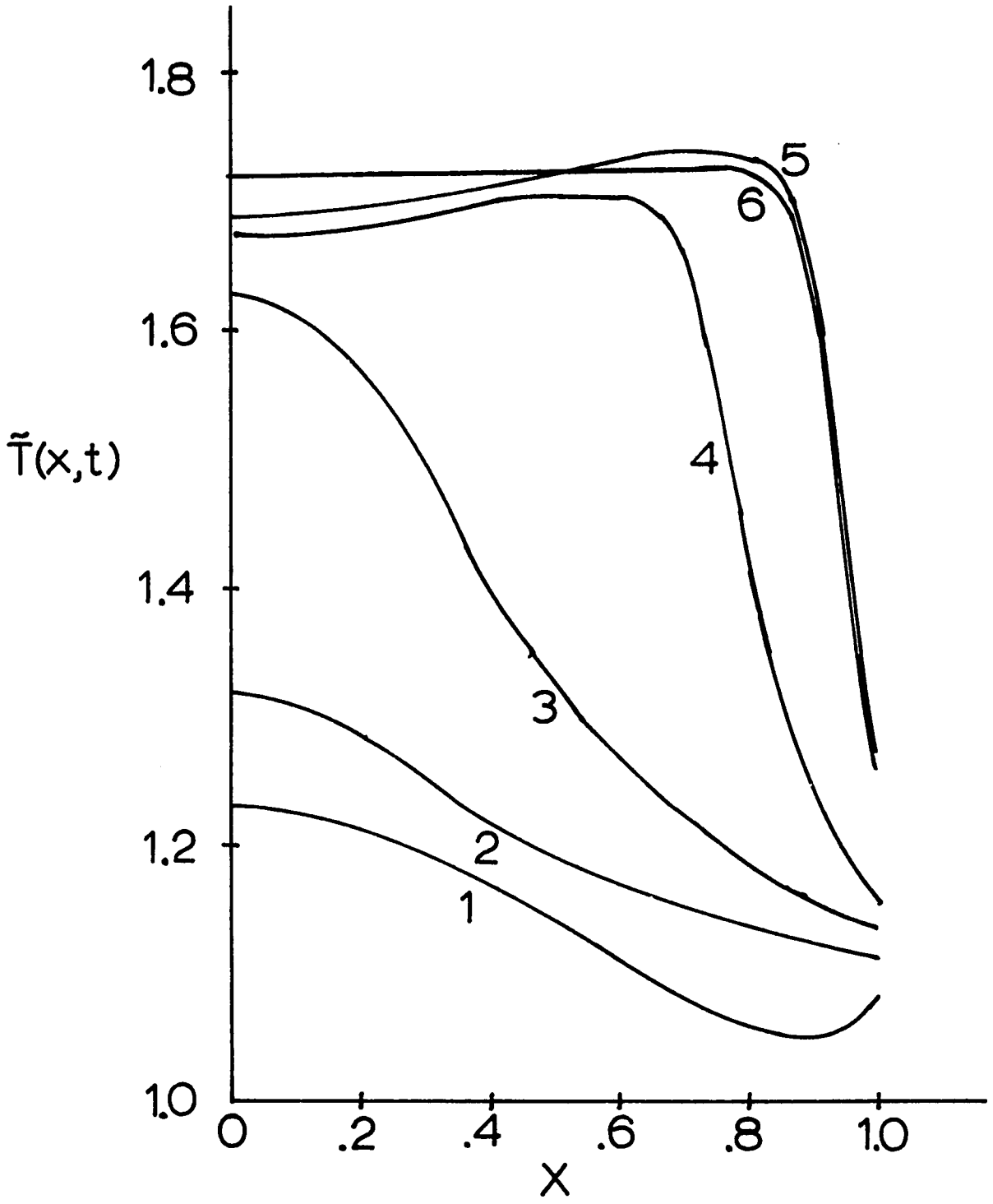

Figure 15. Temperature profiles for various times. (Using Jacobi polynomials, n = 6, Hamming's method, $\Delta t = 0.05$) 1 to 6 correspond to t = 1, 10, 15, 20, 25, and 30.

It was found that Euler's improved method of integration gave accuracy comparable to Hamming's method, took about the same computation time for the same Δt, but allowed time steps about twice as large. Consequently, Euler's improved method is preferred for these problems.

If one looks at the difference between the surface derivative for a collocation solution and the best finite difference solution as a function of time, one finds the type of behavior exhibited in Fig. 16. The spike at $t = 5$ should be ignored since it is in this region that the surface derivative passes through zero. Three characteristic values can be associated with Fig. 16:

$$\begin{aligned} &\text{(i)} \quad \text{let } E_1 = \text{typical error for } 0 < t < 15 \\ &\text{(ii)} \quad \text{let } E_2 = \text{maximum error for } 15 < t < 25 \\ &\text{(iii)} \quad \text{let } E_3 = \text{typical error for } 25 < t \end{aligned} \tag{57}$$

Comparison of Figs. 15 and 16 shows that the error E_2 arises when the temperature increases rapidly in the particle. Using these values one can summarize the effects of the integration scheme, the expansion functions, and the step size as done in Tables 9 and 10.

Based on the results for the problem with boundary condition of the first kind, it was felt that the following choices of grid spacings should give representative results for the finite difference computations; (0.05, 0.05), (0.025, 0.0025), and (0.01, 0.005). Additional values were not examined because of the excessive computation time necessary to use the finite difference methods.

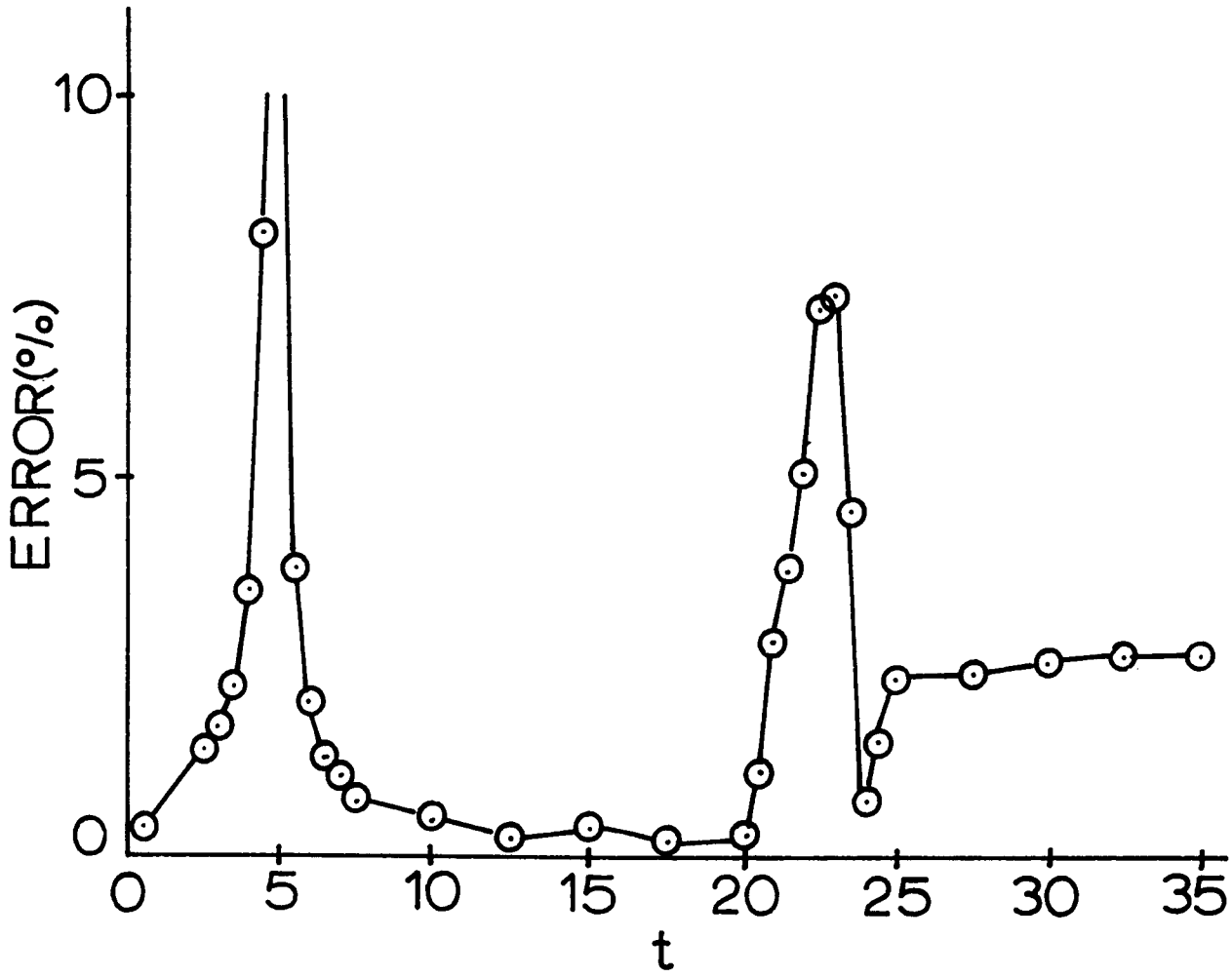

Figure 16. Estimated error in the surface flux as a function of time. (Using Legendre polynomials, n = 6, Hamming's method, $\Delta t = 0.05$).

Table 8

Heat Flux from Catalyst

Polynomial	n	Δt	Flux t = 22	Flux t = 35
Jacobi*	6	0.05	2.348	4.241
Jacobi*	8	0.025	2.857	4.594
Jacobi*	10	0.025	2.489	5.078
Legendre†	6	0.10	2.477	5.159
Legendre†	8	0.05	2.539	4.956
Legendre†	10	0.04	2.572	5.042
Legendre†	12	0.025	2.584	5.024

*Jacobi results using Hamming's method

†Legendre results using Euler's modified method

The comparative errors for the classical implicit method (Table 10) are indicative of the unacceptable pointwise errors. Based on Liu's comparison of his own method to the implicit scheme (12), and the errors found in Table 10, it was decided not to use the implicit method further.

Based on the data in Tables 8 and 9 the improved Euler method is recommended over Hamming's method for integration of the ODE. For boundary conditions of the third kind Legendre polynomials are recommended over Jacobi polynomials. Comparison of the collocation

solution, entries 10 and 11 in Table 9, with a finite difference solution of comparable accuracy, entry 3 of Table 10 reveals that the collocation solution is from twenty to forty times faster. This advantage is due to the larger time step and the smaller number of terms in the collocation method (10-12 rather than 40-100). It is also clear from this problem and the previous one that large computation times are necessary to model nonisothermal diffusion with reactions of this type, and that the savings made possible by the collocation method is especially welcome when several of these problems must be solved as in the case in the reactor model.

Table 9

Representative Error Estimates for Collocation Surface Derivatives

Entry	n	Δt	Integration	Functions	E_1	E_2	E_3	Computation Time (Seconds)
1	6	.05	Hamming	Jacobi	1.5%	19.6%	15.5%	11.9
2	8	.025	"	"	1.0	15.6	8.6	30.6
3	10	.025	"	"	< 1	12.0	1.0	41.1
4	10	.01	"	"	< 1	12.0	1.0	98.0
5	6	.05	"	Chebycheff	< 1	7.1	9.8	11.9
6	6	.05	"	Legendre	< 1	7.2	2.7	11.9
7	8	.025	"	Legendre	< 1	2.4	1.4	30.6
8	6	.10	Euler	Legendre	< 1	8.0	2.7	5.1
9	8	.05	"	"	< 1	2.4	1.4	13.3
10	10	.04	"	"	< 1	1.8	.34	21.8
11	12	.025	"	"	< 1	1.4	.02	45.6

Table 10

Representative Error Estimates for Finite Difference Surface Derivatives

Entry	Δr	Δt	Method of Integration	E_1	E_2	E_3	Computation Time (Seconds)
1	0.05	0.05	Implicit	6%	15%	20%	11
2	0.05	0.05	Liu's	2	7.4	1.5	21
3	0.025	0.0025	"	< 1	2.8	.1	830
4	0.01	0.005	"	–	–	–	1050

6. Summary

In examining the dimensionless mass balance for an isothermal, second-order chemical reaction (using the method of collocation) we succeeded in illustrating the characteristics of a good approximate solution (the power series expansion): the solution exhibits numerical convergence and the residual function approaches zero as we increase the number of collocation points. We also see that a poor approximate solution does not possess these characteristics.

We then discussed Villadsen and Stewart's method of orthogonal collocation. The method of orthogonal collocation reduces an ordinary differential equation to a coupled system of algebraic equations. The differential operators are transformed into matrix operators. We derive an explicit expression for the matrix elements (as compared to the use of matrix inversion by Villadsen and Stewart). For boundary conditions of the third kind we propose the use of a type of Legendre polynomial as the expansion function in the approximate solution. With boundary conditions of the first kind the Jacobi polynomials should be used. We then applied the method of orthogonal collocation to a non-linear ordinary differential equation, eq. 23. The approximate solution of the surface flux is compared to the surface flux as obtained by a finite-difference solution. The method of orthogonal collocation requires $\frac{1}{4}$ to $\frac{1}{2}$ the computation time of the finite-difference method and is more accurate.

The method of orthogonal collocation was then developed for nonlinear parabolic partial differential equations. We suggested the use of different orthogonal polynomials for different combinations of boundary conditions at $x = 0$ and $x = 1$. The method of orthogonal collocation transforms a nonlinear parabolic partial differential equation into a system of first-order ordinary differential equations. We show that the convergence of the approximate solution obtained by Galerkin's method is a sufficient condition for the convergence of the approximate solution obtained by the method of orthogonal collocation. The system of first-order ordinary differential equations can be integrated by any appropriate technique. We investigated the relation between numerical stability as the equations are integrated in time and the step size, Δt, for the system of equations resulting from a simple semi-linear parabolic partial differential equation. For the integration scheme referred to as the improved Euler method we derived a stability criteria, eq. 44. For the linear diffusion problem we show that the use of the Legendre polynomials and the improved Euler method requires a more stringent step size than does the use of the Jacobi polynomials and the improved Euler method.

The method of orthogonal collocation is applied to the coupled, transient mass and energy balances for a nonisothermal, first-order chemical reaction in a spherical catalyst particle. We calculate the approximate values for the surface flux (heat) and compared these values

with those obtained by Liu's finite-difference scheme. The method of orthogonal collocation is from 4 to 40 times as fast as the finite-difference scheme for comparable accuracy. Although we illustrate the method on specific differential equations, the results seem to be consistent: the method is fast with respect to computation time and very accurate (as determined either by an error estimate or error bound).

7. Bibliography

1) Cheney, E. W., Introduction to Approximation Theory, McGraw-Hill, 1966.

2) Courant, R., and Hilbert, D., Methods of Mathematical Physics, Interscience Publishers, Inc., 1966.

3) Douglas, J., Jr., and Dupont, T., Galerkin methods for parabolic equations, Journal of S. I. A. M. Numer. Anal., 7 (1970) pp. 575-626.

4) Dubinskii, J. A., Weak convergence in nonlinear elliptic and parabolic equations, Amer. Math. Soc. Transl. (2) 67 (1968) pp. 226-258.

5) Ferguson, W. B., and Finlayson, B. A., Transient chemical reaction analysis by orthogonal collocation, Chem. Engng. Journal, 1 (1970) pp. 327-336.

6a) Finlayson, B. A., to appear in Chem. Eng. Sci. 26 (1971).

6b) Finlayson, B. A., Convergence of the Galerkin's method for nonlinear problems involving chemical reaction, to appear in S. I. A. M. Journal of Numer. Anal.

7) Hildebrand, F. B., Introduction to Numerical Analysis, McGraw-Hill, 1956.

8) John, F., Lectures on Advanced Numerical Analysis, Gordon and Breach, 1967.

9) Ladyzenskaja, O. A., Solonnikov, V. A., and Ural'ceva, N. N., Linear and Quasilinear Equations of Parabolic Type, American Mathematical Society, 1968.

10) Lapidus, L., and Seinfeld, J. H., Numerical Solution of Ordinary Differential Equations, Academic Press, 1971.

11) Lee, E. S., Quasilinearization, difference approximation, and non-linear boundary value problems, A. I. Ch. E. Journal, 14 (1968) pp.490-496.

12) Liu, S. L., Stable explicit difference approximations to parabolic partial differential equations, A. I. Ch. E. Journal, 15 (1969) pp. 334-338.

13) Livbjerg, H., Antonsen, P., and Villadsen, J., 3rd CHISA Congress, Marianske Lazne, 1969, paper A4.7.

14) Lomax, H., An operational unification of finite difference methods for the numerical integration of ordinary differential equations, N.A.S.A. Technical Report, R-262 (May, 1967).

15) McGowin, C.R., and Perlmutter, D.D., Regions of asymptotic stability for distributed parameter systems, Chem. Eng. Sci., 26 (1971) pp. 275-286.

16) McGuire, M.L., and Lapidus, L., On the stability of a detailed packed-bed reactor, A.I.. Ch. E. Journal, 11 (1965) pp. 85-95.

17) Stewart, W.E., and Villadsen, J.V., Graphical calculation of multiple steady states and effectiveness factors for porous catalysts, A. I. Ch. E. Journal, 15 (1969) pp. 28-34.

18) Stroud, A.H., and Secrest, D., Gaussian Quadrature Formulas, Prentice-Hall, 1966.

19) Villadsen, J., Nord DATA, Vol. 1, pp. 138-175. Helsinki, 1968.

20) Villadsen, J., and Sorenson, J.P., Solution of parabolic partial differential equations by a double collocation method, Chem. Eng. Sci., 24 (1969) pp. 1337-1349.

21) Villadsen, J.V., and Stewart, W.E., Solution of boundary-value problems by orthogonal collocation, Chem. Eng. Sci., 22 (1967) pp. 1483-1501.

CHAPTER B

Error Bounds for Approximate Solutions

While approximate methods are used quite frequently in solving differential equations, there has been too little progress made in the error analysis of such methods. An error analysis provides some rigorous measure of the discrepancy between the approximate solution and the exact solution. We refer to such a measure as an error bound. We are interested only in those bounds which do not require the exact solution to be known since in most engineering applications the exact solution is not known. With these types of bounds one simply solves for the approximate solution and calculates the error bound. Bounds are inherently conservative in that they are usually larger than the true error. While the exact solution satisfies the differential equation exactly, the approximate solution may only satisfy the differential equation at a few points in the domain of the independent variables. The approximate solution only fits the differential equation roughly and this non-zero fit is referred to as the residual function. The residual function is one of the most natural concepts associated with the approximate solution, and we show that it can be an important part of an error bound.

In reviewing the literature one finds that a small residual is recognized as characterizing an accurate approximate solution but that few authors have attempted to establish rigorous error bounds which incorporate this function. Because of the inherent simplicity of the

residual function, both in form and concept, we chose to direct our attention to deriving new error bounds which would utilize the information contained in the residual function. We have considered two classes of differential equation: (1) systems of second-order nonlinear ordinary differential equations in which only the dependent variables occur non-linearily (not the derivatives of the dependent variables) and (2) systems of semi-linear parabolic partial differential equations. The first class of equation corresponds to the type of problem involved in distributed parameter systems while the second class corresponds to the transient transport equations. We derive both a pointwise error bound and a mean square error bound for the problems of class (1) but only a mean square error bound for the problems of class (2). The error bounds for the ordinary differential equations are very good for the applications which we have considered (0.01% to 0.0001% error using three collocation points in the method of orthogonal collocation). We outline the application of the error bound for problems of class (2) by considering the coupled, transient heat and mass balances for a nonisothermal, first order chemical reaction in a spherical catalyst particle. These new error bounds provide an unequivocal means of comparing different approximate solutions to an equation, for example using different expansion functions. Being able to obtain an approximate solution and to know its accuracy represents a significant advance in the field of approximate methods of solution.

I. Background

In obtaining approximate solutions to differential equations, one needs to consider the amount of error associated with the approximation method and its solution. There has been much published in the last five years on the subject of bounding the error between the approximate solution, $\tilde{y}(\underline{x})$, and the exact solution, $y(\underline{x})$, of a differential equation. These reports have dealt primarily with the pointwise error bound, eq. 1, and the weighted, mean-square error bound, eq. 2.

$$\max_{x \in \Omega} | \tilde{y}(\underline{x}) - y(\underline{x}) | \tag{1}$$

$$\left(\int_{\Omega} (\tilde{y}(\underline{x}) - y(\underline{x}))^2 \, w(\underline{x}) \, d\underline{x} \right)^{\frac{1}{2}} \tag{2}$$

Before considering the extent of the available results, let us consider a concept that is often presented as an error bound.

In many numerical studies the error associated with a solution is estimated. A simple example of an error estimate is provided by the following: having replaced the heat equation by a difference equation, one solves the resulting algebraic equations for several different mesh spacings, (Δx, Δt). The solutions are then compared. If the solutions differ in only the fourth decimal place, we can estimate the error to be $0(10^{-4})$ for a solution of $0(1)$. This is called an error estimate, not an error bound, because there is no theoretical reason the error is actually less than or equal to $0(10^{-4})$. This comparison only serves to characterize a convergent numerical scheme.

To derive an error bound, various features of the problem must be considered: the type of equation, the degree of generality associated with the equation (viz., variable coefficients versus constant coefficients), the nature of the auxiliary data (viz., boundary conditions), the method used to approximate the solution, and the degree of differentiability . . required of the exact solution.

The following presentation of error bounds serves two purposes: (1) to support the contention that many numerical problems could be accompanied by an error analysis and (2) to indicate the different types of error bounds. Error bounds have been obtained for various types of problems using various methods. Linear ordinary differential equations with variable coefficients were investigated by Vainikko (34) while Karpilovskaya (20) investigated a particular linear elliptic partial differential equation. Both authors obtained asymptotic error bounds (similar to eq. 3) for the approximation method referred to as collocation.

$$\max_{\underline{x} \in \Omega} \left| \tilde{y}(\underline{x}) - y(\underline{x}) \right| = 0(n^{-r-\alpha}), \quad (n, r, \alpha > 0) \tag{3}$$

In eq. 3, n is the number of collocation points, r is the degree of continuous differentiability of the exact solution, and α is the exponent for a Lipschitz condition on the r-th derivative of the exact solution. These results were obtained by combining the existance of certain Green's functions with the theory of approximation. This type of bound, eq. 3, assures convergence of the approximate solution to the exact solution and indicates how fast the error decreases as n, the number of collocation

points, increases. For both studies the collocation points are roots of an $(n + 1)$-th orthogonal polynomial of an appropriate set. Notice that for fixed values of r and α eq. 3 indicates that all selections of n collocation points are asymptotically equivalent with respect to the error generated. As a result, this type of error bound does not allow the comparison of errors with different collocation points for small values of n. Numerically, we are usually interested in using as few collocation points as possible while obtaining the desired accuracy.

Another error bound measures the error in terms of how close the boundary data is approximated and how close the residual function is to zero. This type of bound is derived using both standard integral inequalities and Green's identities. This method of bounding the error has been used on fairly general elliptic and parabolic partial differential equations (1, 2, 6, 7, 24, 25, 30, 31, 32, 33), but does require that the approximate solution possess at least first order piecewise continuous derivatives. Sigillito investigated error bounds for parabolic partial differential equations in which the solution, $u(\underline{x}, t)$, appears nonlinearily (30, 31, 33). Bellar(1, 2) investigated equations in which the solution and the gradient of the solution, $u(\underline{x}, t)$ and $\nabla u(\underline{x}, t)$, appear nonlinearily. Much of the work in this area has been done by Bramble, Payne, and Weinberger.

Recently there has been considerable interest in the application of Galerkin's method and the derivation of associated error bounds (15, 18, 26, 28, 29, 36). Denote by H_n the subspace spanned by the expansion functions occurring in the expression for the approximate solution. The

associated error bounds are then usually expressed in a manner similar to eq. 4,

$$\| \tilde{y} - y \| \leq \inf_{v \in H_n} \| y - v \| \tag{4}$$

which involves the 'minimum distance' between the exact solution and the subspace H_n as measured by a particular norm. The ability to derive a bound for the right-hand side of eq. 4 from approximation theory depends on the properties that the exact solution is assumed to possess. The right-hand side of eq. 3 is such a result and the exact solution has been assumed to possess r-th continuous derivatives. Many such results are available for the approximation of a function of one variable by polynomials.

Several other methods have also been studied and offer equally good results: the Newton-Kantorovich method(3, 4, 23), fixed-point theorems (21), the use of interpolation spline functions(5, 9, 10, 11, 12, 13, 22, 25), and the maximum principle(17). Whether a particular method applies depends on the equation, but if the method applies, one can use the results for any approximate solution.

All further discussion pertains to the error bounds which measure the error in terms of the 'fit' of the boundary data and closeness of the residual function to zero. For approximation methods in which one uses only a small number of adjustable parameters the residual function may become quite small for one, two, or more parameters. If this happens, do we have an equally small error ? This potential has been validated for the following two particular classes of nonlinear problems and is developed

further in the sections on new error bounds. Again, we are interested in showing that for many problems, the error can be bounded by some characteristic of the residual function. Several authors(16, 19, 21) have referred to the mean-square integral of the residual as characterizing the error of the approximate solution. What is shown here is that many problems have some multiple of the mean-square integral of the residual as a rigorour error bound, hence increasing its practical value significantly.

The first class of nonlinear problem is

$$\frac{1}{x^{a-1}} \frac{d}{dx} \left(x^{a-1} \frac{du}{dx}\right) - f(x, u) = 0 \tag{5}$$

with the following linear boundary conditions:

$$\frac{2}{k_1} \frac{du}{dx} (1) + u(1) = k_2 \tag{6}$$

$$\frac{du}{dx}(0) = 0$$

If the approximate solution satisfies the boundary conditions exactly, it follows (as a straightforward simplification) from the work of Sigillito (30) that the error is bounded by a constant times the mean-square integral of the residual:

$$\left[\int_0^1 [\tilde{u}(x)-u(x)]^2 x^{a-1} dx\right]^{\frac{1}{2}} \leq \frac{1}{\lambda_1 - M} \left[\int_0^1 R[\tilde{u}(x)]^2 x^{a-1} dx\right]^{\frac{1}{2}} \tag{7}$$

where λ_1 is the minimum eigenvalue of eq. 8,

$$\frac{1}{x^{a-1}} \frac{d}{dx}\left(x^{a-1} \frac{dv}{dx}\right) + \lambda v = 0 \qquad (8)$$

where $v(x)$ satisfies homogeneous boundary conditions analogous to eq. 6 and M is the Lipschitz constant for $f(x, u)$ defined by eq. 9.

$$|f(x, v_1) - f(x, v_2)| \leq M|v_1 - v_2|, \quad x \in (0, 1) \qquad (9)$$

The inequality of eq. 9 treats $f(x, u)$ as an algebraic function of the real variable u and must be valid for all u of interest. If nothing is known about the solution, then $-\infty < v_1, v_2 < +\infty$. On the other hand, if we know that $0 \leq u \leq 1$, then eq. 9 need only be valid for this range of values. The error bound is <u>only valid</u> for $\lambda_1 > M$. If $f(x, u)$ is continuously differentiable in the second argument, the condition for the validity of the error bound is sufficient to guarantee the uniqueness of the solution to eq. 5. To see this, assume the existance of two distinct solutions, u_1 and u_2, both of which satisfy eq. 5 and the boundary conditions, eq. 6. Subtract the differential equation for u_1 from that for u_2 (similarly for the boundary conditions):

$$\frac{1}{x^{a-1}} \frac{d}{dx}\left(x^{a-1} \frac{d}{dx}(u_2 - u_1)\right) - (f(x, u_2) - f(x, u_1)) = 0 \qquad (10)$$

$$\frac{d}{dx}(u_2 - u_1)(0) = 0$$

$$\frac{2}{k_1} \frac{d}{dx}(u_2 - u_1) + (u_2 - u_1) = 0 \quad , \quad \text{for } x = 1.0$$

By the mean-value theorem for functions of a real variable, eq. 10 is equivalent to eq. 11 (using the fact that f is continuously differentiable),

$$\frac{1}{x^{a-1}} \frac{d}{dx} \left(x^{a-1} \frac{d}{dx} (u_2 - u_1)\right) - \left[\frac{\partial f}{\partial u} \Big|_{u=u^*}\right](u_2 - u_1) = 0 \qquad (11)$$

where u^* is a function whose values are, pointwise in x, between u_2 and u_1. We do not need to know u^* explicitly, but only the fact that it exists. We do know that

$$-M \leq \left[\frac{\partial f}{\partial u} \Big|_{u=u^*}\right] \leq +M$$

such that, by a theorem from Courant and Hilbert(14, page 411), we conclude that the null solution is the only solution for eq. 11 if $\lambda_1 > M$. If the null solution is the only solution, then u_2 is identical to u_1 and we have uniqueness for eq. 5.

The second class of problems is

$$\sum_{i,j} (a^{ij} u_{,i})_{,j} - \frac{\partial u}{\partial t} - f(\underline{x}, t, u) = 0 \qquad (12)$$

Sigillito has done studies on eq. 12 for both the first and second initial-boundary value problems (30, 31). These studies show that, if the approximate solution satisfies the boundary conditions and initial condition exactly, the error is bounded by a constant times the mean-square integral of the residual function:

$$\left[\int_0^T \int_\Omega (u - u)^2 \, d\underline{x} \, dt\right]^{\frac{1}{2}} \leq \frac{1}{b + a_o \lambda_1 - M} \left[\int_0^T \int_\Omega R^2(\tilde{u}) \, e^{2b(T-t)} d\underline{x} \, dt\right]^{\frac{1}{2}} \qquad (13)$$

where a_o is positive and defined by

$$\sum_{i,j} a^{ij} v_i v_j \geq a_o \sum_i v_i^2 > 0, \quad \text{(for all real } v_k\text{)}$$

a_o is referred to as the uniform ellipticity constant for $[a^{ij}]$. λ_1 is the minimum eigenvalue for the following equation

$$\sum_{i,j} (a^{ij} w_{,i})_{,j} + \lambda w = 0$$

with homogeneous boundary conditions and "b" is an adjustable parameter chosen such that the expression

$$b + a_o \lambda_1 - M$$

is positive (b may be zero). M is a Lipschitz constant for the nonlinear function in eq. 12 such that

$$|f(\underline{x}, t, v_2) - f(\underline{x}, t, v_1)| \leq M |v_2 - v_1|$$

If we have $f(\underline{x}, t)$ independent of u, M is zero.

In the approximation of solutions to differential equations one often utilizes linear combinations of known functions with unknown expansion coefficients which may be functions themselves. In this approach one would like to be able to say how the accuracy changes as the number of terms increases, as different expansion functions are used, or as different methods are used to determine the expansion coefficients. The availability of an error bound serves to answer these types of questions. It is recognized that in lieu of an error bound, one can estimate the error by

comparing the results to another solution (viz., finite-difference solution). Additionally, the error bound could be used to compare entirely different solutions to the same problem or for finite difference calculations (if one provides the necessary interpolation polynomial).

2. New Error Bounds for Ordinary Differential Equations

In chemical reaction engineering, one is often presented with coupled chemical reactions that can be described in the following form:

$$\frac{1}{x^{a-1}} \frac{d}{dx} \left(x^{a-1} \frac{dc_j}{dx}\right) - f_j(c_1, \ldots, c_j, \ldots, c_n) = 0 \qquad (14)$$

$$(j = 1, \ldots n; \quad a = 1, 2, 3)$$

with boundary conditions such as

$$\frac{dc_j}{dx} (0) = 0 \qquad (15)$$

$$\frac{2}{Sh} \frac{dc_j}{dx} (1) + c_j(1) = g_j, \quad (j=1, \ldots, n) \qquad (16)$$

With eqs. 15 and 16, one can study an equivalent system of integral equations rather than eq. 14,

$$c_j(x) = g_j - \int_0^1 G(x, t, Sh)\, f_j(\underline{c}(t))\, (t^{a-1} dt) \quad (j=1, \ldots, n) \qquad (17)$$

where $G(x, t, Sh)$ is the appropriate Green's function. If eq. 14 is solved approximately, one obtains

$$\frac{1}{x^{a-1}} \frac{d}{dx} \left(x^{a-1} \frac{d\tilde{c}_j}{dx}\right) - f_j(\tilde{c}_1, \ldots, \tilde{c}_n) \equiv R_j(\underline{\tilde{c}})$$

where $R_j(\underline{\tilde{c}})$ will be small but not identically zero as in eq. 14.

Similarly,

$$\tilde{c}_j(x) = g_j - \int_o^1 G(x, t, Sh) \left[f_j(\underline{\tilde{c}}(t)) + R_j(\underline{\tilde{c}})\right] (t^{a-1}\, dt) \tag{18}$$

Assume that $f_j(y_1, \ldots, y_n)$ satisfies a Lipschitz condition of order one in the y_k,

$$|f_j(\underline{y}) - f_j(\underline{v})| \leq \sum_{i=1}^{n} M_{ji} \, | y_i - v_i| \tag{19}$$

Then we prove the following theorem:

Note: while this bounds the mean-square error, we later consider the pointwise error and an appropriate error bound

Theorem Assume the existence of a solution to eqs. 14-16 and require $f_j(y_1, \ldots, y_n)$ to satisfy the Lipschitz condition (19). Then the error for an approximate solution is bounded by

$$\{\int_o^1 [\tilde{c}_j - c_j]^2 (x^{a-1} dx)\}^{\frac{1}{2}} \leq k_o\left(\int_o^1 R_j^2(\underline{\tilde{c}})\, x^{a-1}\, dx\right) + k_o k_j \left(\sum_{i=1}^{n} \int_o^1 R_i^2(\underline{\tilde{c}}) x^{a-1} dx\right)^{\frac{1}{2}} \tag{20}$$

Proof: Eqs. 17 and 18 can be combined,

$$(\tilde{c}_j(x) - c_j(x))^2 = \left(\int_o^1 G(x, t, Sh)\, (R_j + (f_j(\underline{\tilde{c}}) - f_j(\underline{c})))\, (t^{a-1}\, dt)\right)^2$$

and applying Schwartz's inequality, then

$$(\tilde{c}_j(x) - c_j(x))^2 \leq \int_o^1 G^2(x, t, Sh)(t^{a-1} dt) \int_o^1 (R_j + (f_j(\underline{c}) - f_j(\underline{c})))^2 (t^{a-1} dt)$$

such that

$$\|\epsilon_j\|_2 \equiv \left(\int_o^1 (\bar{c}_j - c_j)^2 t^{a-1} dt\right)^{\frac{1}{2}} \leq \left(\int_o^1 \int_o^1 G^2(x, t, Sh)\, t^{a-1} dt\, x^{a-1} dx\right)^{\frac{1}{2}} .$$

$$\left(\int_o^1 (R_j + (f_j(\underline{\bar{c}}) - f_j(\underline{c})))^2 t^{a-1} dt\right)^{\frac{1}{2}}$$

If we then apply Minkowski's inequality to the last integral of the above inequality,

$$\|\epsilon_j\|_2 \leq \|G(a; Sh)\|_2 \left(\left(\int_o^1 R_j^2(\underline{c})\, t^{a-1} dt\right)^{\frac{1}{2}} + \left(\int_o^1 (f_j(\underline{\bar{c}}) - f_j(\underline{c}))^2 t^{a-1} dt\right)^{\frac{1}{2}}\right)$$

Since f_j satisfies a Lipschitz condition, eq. 19, the last integral of the above inequality can be bounded in terms of the errors,

$$\|\epsilon_j\|_2 \leq \|G\|_2 \left[\left(\|R_j\|_2 + \left(\sum_{i=1}^n M_{ji}^2\right)^{\frac{1}{2}} \left(\sum_{i=1}^n \int_o^1 \epsilon_i^2\, t^{a-1}\, dt\right)^{\frac{1}{2}}\right]\right.$$

or

$$\|\epsilon_j\|_2 \leq \|G\|_2 \left[\|R_j\|_2 + \left(\sum_{i=1}^n M_{ji}^2\right)^{\frac{1}{2}} \left(\sum_{i=1}^n \|\epsilon_i\|_2^2\right)^{\frac{1}{2}}\right] \qquad (21)$$

Abbreviate $\left(\sum_{i=1}^n M_{ji}^2\right)$ by N_j, then the result of squaring both sides of eq. 21, adding over the subscript j, and taking the square-root of both sides of the resulting expression is

$$\left(\sum_{j=1}^n \|\epsilon_j\|_2^2\right)^{\frac{1}{2}} \leq \|G\|_2 \left[\sum_{i=1}^n \left(\|R_j\|_2 + N_j^{\frac{1}{2}} \left(\sum_{i=1}^n \|\epsilon_i\|_2^2\right)^{\frac{1}{2}}\right)^2\right]^{\frac{1}{2}}$$

$$\leq \|G\|_2 \left[\left(\sum_{j=1}^n \|R_j\|_2^2\right)^{\frac{1}{2}} + \left(\sum_{i=1}^n \|\epsilon_i\|_2^2\right)^{\frac{1}{2}} \left(\sum_{j=1}^n N_j\right)^{\frac{1}{2}}\right] .$$

By solving for $(\sum^{n} \|\epsilon_j\|_2^2)^{\frac{1}{2}}$, one can reduce eq. 21 to the final result:

$$\|\epsilon_j\|_2 \leq \|G\|_2 \left(\|R_j\|_2 + \frac{N_j^{\frac{1}{2}} \|G\|_2 \left(\sum_{i=1}^{n} \|R_i\|_2^2\right)^{\frac{1}{2}}}{1 - \|G\|_2 \left(\sum_{i=1}^{n} N_i\right)^{\frac{1}{2}}}\right) \tag{22}$$

with $\left(1 - \|G\|_2 \left(\sum_{i=1}^{n} N_i\right)^{\frac{1}{2}}\right) > 0$. A somewhat better bound can be obtained by forming a quadratic inequality in $(\sum \|\epsilon_j\|_2^2)^{\frac{1}{2}}$ and solving for the upper bound of $(\sum \|\epsilon_j\|_2^2)^{\frac{1}{2}}$ —but for small residuals, the improvement is generally negligible

For systems of equations with different Sherwood numbers (Sh), the Green's function would be different for each equation. For this case the error bound is derived in the same manner as eq. 22, and the result is

$$\|\epsilon_j\|_2 \leq \|G_j\|_2 \left\{\|R_j\|_2 + \frac{N_j^{\frac{1}{2}} \left(\sum_{j=1}^{n} \|R_j\|_2^2 \, \|G_j\|_2^2\right)^{\frac{1}{2}}}{1 - \left(\sum_{j=1}^{n} \|G_j\|_2^2 \, N_j\right)^{\frac{1}{2}}}\right. \tag{23}$$

If one of the equations of the system (eq. 14) is linear and uncoupled, that c_j can be obtained exactly. Then $\|\epsilon_j\| \equiv 0$ and $N_j \equiv 0$.

Eq. 22 is also valid for a single nonlinear equation,

$$\|\epsilon\|_2 \leq \frac{\|G\|_2 \, \|R\|_2}{1 - M\|G\|_2} \tag{24}$$

where M is again the Lipschitz constant. A result similar to eq. 24 can be obtained with

$$\bar{M} = \sup_{0 \leq t \leq 1} \left(\int_0^1 \left(\frac{\partial f}{\partial u} \Big|_{u=c + t(\bar{c} - c)} \right)^2 x^{a-1} dx \right)^{\frac{1}{2}} \tag{25}$$

because

$$f(\tilde{u}) - f(u) \equiv \int_0^1 \frac{\partial f(x, v)}{\partial v} \frac{\partial v}{\partial t} \, dt, \quad \text{where} \quad v = u + t(\tilde{u} - u). \tag{26}$$

Eq. 25 allows sharper bounds to be obtained—compared to f being Lipschitz continuous. A similar approach could be applied to systems of equations as there is a multi-dimensional generalization to eq. 26.

There is a very interesting corollary to the results of eqs. 22, 23, and 24.

Corollary: The error bounds of eqs. 22-24 imply that the solution to the appropriate differential equation(s) is unique.

This is quite easy to prove. If there are two solutions, called $u_j^{(1)}$ and $u_j^{(2)}$, let $\epsilon_j = u_j^{(2)} - u_j^{(1)}$. However $\|R_j\|_2 \equiv 0$, so that, $\|\epsilon_j\|_2 = 0$.

For later applications, we require the Green's function in spherical geometry (a = 3) for the homogeneous boundary conditions similar to eqs. 15 and 16:

$$G(x, t, Sh) = \begin{cases} \frac{2}{Sh} + \frac{1}{x} - 1 & , t \leq x \\ \frac{2}{Sh} + \frac{1}{t} - 1 & , t \geq x \end{cases}$$

such that

$$\|G\|_2^2 = \frac{1}{90} + \frac{2}{Sh}\left(\frac{1}{9}\left(\frac{2}{Sh}\right) + \frac{2}{45}\right) \tag{26}$$

A good introduction to Green's functions is provided by Courant and Hilbert (14). For boundary conditions of the first kind, the Green's function is

$$G(x, t) = \begin{cases} \frac{1}{x} - 1, & t \leq x \\ \frac{1}{t} - 1, & t \geq x \text{ (spherical, } a = 3) \end{cases} \tag{27}$$

We will use two integral evaluations of eq. 27:

$$K_1 = \max_{0 \leq x \leq 1} \int_0^1 G(x, t)\, t^2 dt = \frac{1}{6} \tag{28}$$

$$K_2^2 = \max_{0 \leq x \leq 1} \int_0^1 G^2(x, t) t^2 dt = \frac{1}{3}$$

These last two constants, K_1 and K_2, are introduced in the derivation of pointwise error bounds for eq. 14-16, which we now derive.

Theorem If $f(\underline{c})$ of eq. 14 satisfies a Lipschitz condition, eq. 19, and a Green's function exists for eqs. 14-16,

$$\|\tilde{c}_j - c_j\|_\infty \equiv \max_{0 \leq x \leq 1} |\tilde{c}_j(x) - c_j(x)| \leq a \|R_j\|_2 + b_j \sum_{i=1}^{n} \|R_i\|_2$$

Proof: Let $M_j = \max_i [M_{ji}]$. From eqs. 17 and 18,

$$|\tilde{c}_j(x) - c_j(x)| = \left| \int_o^1 G(x, t, Sh) \ (f_j(\underline{\tilde{c}}) - f_j(\underline{c}) + R_j) \ t^{a-1} dt \right|$$

$$\leq \int_o^1 G(x, t, Sh) \left(|f_j(\tilde{c}) - f_j(c)| + |R_j|\right) t^{a-1} \, dt$$

$$\leq \int_o^1 G(x, t, Sh) \ \left(M_j \sum_{i=1}^{n} |\tilde{c}_i(t) - c_i(t)| + |R_j|\right) t^{a-1} \, dt$$

$$= M_j \int_o^1 G(x, t, Sh) \sum_{i=1}^{n} |\tilde{c}_i(t) - c_i(t)| t^{a-1} dt + \int_o^1 G(x, t, Sh) |R_j| t^{a-1} dt$$

where we have used the fact that the Green's function is non-negative.

Rearranging slightly, and using Schwartz's inequality,

$$|\tilde{c}_j(x) - c_j(x)| \leq M_j \sum_{i=1}^{n} \int_o^1 G(x, t, Sh) |\tilde{c}_i - c_i| t^{a-1} dt + K_2 \|R_j\|_2$$

$$\leq M_j \sum_{i=1}^{n} \max_{0 \leq t \leq 1} |\tilde{c}_i(t) - c_i(t)| \int_o^1 G(x, t, Sh) \ t^{a-1} dt + K_2 \|R_j\|_2$$

let

$$K_1 = \max_{0 \leq x \leq 1} \int_o^1 G(x, t, Sh) \ t^{a-1} \, dt$$

$$K_2^2 = \max_{0 \leq x \leq 1} \int_o^1 G^2(x, t, Sh) \ t^{a-1} \, dt$$

then

$$\|\epsilon_j\|_\infty \leq K_1 M_j \sum_{i=1}^{n} \|\epsilon_i\|_\infty + K_2 \|R_j\|_2$$

We need to bound $\sum_{i=1}^{n} \|\epsilon_i\|_\infty$. This can be done by summing this inequality over the subscript j and solving the inequality for $\sum_{i=1}^{n} \|\epsilon_i\|_\infty$. The result of this is,

$$\sum_{i=1}^{n} \|\epsilon_i\|_\infty \leq \frac{K_2 \sum_{j=1}^{n} \|R_j\|_2}{1 - K_1 \sum_{j=1}^{n} M_j} \quad \left(\text{with } 1 - K_1 \sum_{j=1}^{n} M_j > 0\right)$$

such that we obtain the final result.

$$\max_{0 \leq x \leq 1} |\tilde{c}_j(x) - c_j(x)| \leq K_2 \left\{ \|R_j\|_2 + \frac{K_1 M_j}{1 - K_1 \sum_{i=1}^{n} M_i} \sum_{i=1}^{n} \|R_i\|_2 \right\} \tag{29}$$

The following two bounds can be obtained by slight modifications of the above proof:

$$\max_{0 \leq x \leq 1} |\tilde{c}_j(x) - c_j(x)| \leq K_1 \left\{ \|R_j\|_\infty + \frac{K_1 M_j}{1 - K_1 \sum_{i} M_i} \sum_{i=1}^{n} \|R_i\|_\infty \right\} \tag{30}$$

$$\max_{0 \leq x \leq 1} |\tilde{c}_j(x) - c_j(x)| \leq K_2 \left\{ \sum_{i=1}^{n} M_{ji} \|\epsilon_i\|_2 + \|R_j\|_2 \right\} \tag{31}$$

Eq. 30 is the result of considering the maximum, absolute value of the residual function rather than the integral of the square residual. The

proof is identical to that shown. Eq. 31 results from the use of Schwartz's inequality for the integrals appearing in the first part of the proof.

3. Application of Error Bounds—Ordinary Differential Equations

The error bounds for the ordinary differential equations given by eq. 14 are quite easy to apply. This is demonstrated on the following problems: (1) isothermal chemical reactions with different types of rate expressions, (2) nonisothermal first order chemical reaction, and (3) an isothermal chemical reaction system. All of these problems are considered in a spherical catalyst particle.

For the first problem, assume the boundary conditions are the following:

$$\frac{dc}{dx}(0) = 0 \; ; \quad c(1) = 1 \tag{32}$$

If we have the following dimensionless mass balance

$$\frac{1}{x^2}\frac{d}{dx}\left(x^2 \frac{dc}{dx}\right) = \phi^2 c^{2n+1} \quad , (n \text{ is a positive integer}),$$

we can shown by the maximum principle (26a) that $0 \leq c(x) \leq 1$. Then from eq. 25

$$\bar{M} = \sup_{0 \leq t \leq 1} \left[\int_0^1 \left((2n+1)\, \phi^2\, u^{2n} \right) \Big|_{u=c+t(\tilde{c}-c)}^{3} x^2 dx \right]^{\frac{1}{2}}$$

$$= (2n+1)\, \phi^2 \sup_t \left[\int_0^1 (c + t(\tilde{c} - c))^{4n}\, x^2 dx \right]^{\frac{1}{2}}$$

$$= (2n+1)\, \phi^2 \sup_t \left[\int_0^1 ((1-t)\, c + t\tilde{c})^{4n}\, x^2 dx \right]^{\frac{1}{2}}$$

Without knowing $c(x)$, we cannot calculate $\bar{M}$. But since $c(x) \leq 1$, we can bound $\bar{M}$ from above.

$$\bar{M} \leq (2n + 1) \frac{\phi^2}{\sqrt{3}} \max \{1, \max_{0 \leq x \leq 1} [\tilde{c}(x)]^{2n}\}$$

Using eq. 24, we then have the following error bound:

$$\|\tilde{c} - c\|_2 \leq \frac{1}{\sqrt{90} - \frac{\phi^2}{\sqrt{3}} (2n+1) \max \{ 1, \max_{0 \leq x \leq 1} [\tilde{c}(x)]^{2n}\}} \|R(\tilde{c})\|_2$$

If $\tilde{c}(x) \leq 1$ for all x in $[0, 1]$, then the error bound is valid for

$$\phi \leq \frac{4.05}{(2n+1)}$$

This simple rate expression presents a slight problem when the order is even: c^{2n}, where n is a positive integer. In this case, one must first prove that $0 \leq c(x) \leq 1$, but a different approach is necessary since the maximum principle does not apply. We are assuming the existence of a continuous solution on the interval $[0, 1)$. The inclusion of the left end-point of the interval implies that the solution is bounded at $x = 0$. Let us consider the upper bound for $c(x)$. Assume that $c(x) > 1$ for some $x_1 \in [0, 1)$. Then $c(x)$ has a maximum in $[0, 1)$ for some x_2, or

$$0 > \frac{d^2c}{dx^2} = \phi^2 c^{2n} \text{ at } x_2, \text{ but this is impossible.}$$

Such a maximum cannot occur at $x = 0$ either:

$$0 > \left\{\frac{d^2c}{dx^2} + \frac{2}{x}\frac{dc}{dx}\right\}_{x=0} = 3\frac{d^2c}{dx^2} = \phi^2 c^{2n}$$

(using l'Hospital's rule), which is also impossible. Consequently, $c(x) \leq 1$ for all x in the interval $[0, 1]$. To show that $c(x)$ is positive, utilize the equivalent integral equation (of the differential equation),

$$c(x) = 1 - \int_0^1 G(x, t)\, \phi^2\, c^{2n}(t)\, t^2\, dt$$

such that

$$\frac{dc}{dx}(x) = -\int_0^1 G_x(x, t)\, \phi^2\, c^{2n}(t)\, t^2\, dt$$

where, from eq. 27, we find that G_x has the following form,

$$G_x = \begin{cases} -\dfrac{1}{x^2}, & t \leq x \\ 0 & t \geq x \end{cases}$$

such that

$$\frac{dc}{dx}(x) = \int_0^x \frac{1}{x^2}\, \phi^2\, c^{2n}\, t^2\, dt$$

from which it follows that the first derivative is non-negative. Having established that the first derivative is positive, <u>assume</u> the existance of some x_1 such that $c(x_1) = 0$. Qualitatively, we have the situation depicted in the following sketch,

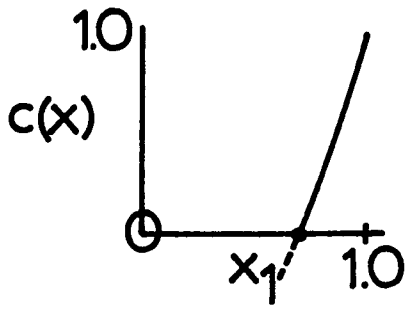

then $c(x) \leq 0$ for all $x \in [0, x_1]$ because of the restriction on the first derivative. But for $x \in [0, x_1]$, $c(x)$ is governed by the following integral equation:

$$c(x) = \int_0^{x_1} G(x, x_1, t)\, \phi^2\, c^{2n}\, t^2 dt \tag{33}$$

where $G(x, x_1, t)$ is

$$G(x, x_1, t) = \begin{cases} \frac{1}{x} - \frac{1}{x_1}, & 0 \leq t \leq x \leq x_1 \\ \frac{1}{t} - \frac{1}{x_1}, & x_1 \geq t \geq x \geq 0 \end{cases}$$

$G(x, x_1, t)$ is a positive function such that the integrand of eq. 33 is positive. This leads to the conclusion that $c(x) \equiv 0$ for $x \in [0, x_1]$ which means that $c(x)$ must be a non-negative function: $0 \leq c(x) \leq 1$. Knowing that $0 \leq c(x) \leq 1$, one can then bound $\bar{M}$ from above,

$$\bar{M} \leq 2n \frac{\phi^2}{\sqrt{3}} \max \{ 1, \max_{0 \leq x \leq 1} [\tilde{c}(x)]^{2n-1} \}$$

such that, using eq. 24 (assuming $0 \leq \tilde{c}(x) \leq 1$, which can be checked when a problem such as this is analyzed numerically),

$$\| \tilde{c} - c \|_2 \leq \frac{\| G \|_2 \, \| R \|_2}{1 - 2n \frac{\phi}{\sqrt{3}} \, \| G \|_2} \tag{34}$$

where, as before, the denominator must be positive for the error bound to be valid.

For the second order chemical reaction investigated in Chapter A, the error bound is given explicitly as (from eq. 34)

$$\| \tilde{c} - c \|_2 \leq \frac{(\frac{1}{\sqrt{90}}) \, \| R \|_2}{1 - \frac{2}{\sqrt{3}} \, (\frac{1}{\sqrt{90}})}$$

Using this expression, the error bound has been calculated for the results obtained with the cosine series and the power series, and these values are summarized in Table 1.

Table 1

Error Bound for the Approximate Solution to the Second Order Chemical Reaction of Chapter A

Number of collocation points (using ordinary collocation)	Mean-square error bound for cosine series	Mean-square error bound for power series solution
2	1.544×10^{-2}	3.542×10^{-4}
4	5.455×10^{-2}	4.514×10^{-7}
6	1.189×10^{-1}	7.930×10^{-8}

The error bound reaffirms our previous contentions that the cosine series solution was diverging and that the power series solution was acceptable. The pointwise error is bounded by the following inequality (see eq. 31):

$$\| \tilde{c} - c \|_\infty \leq K_2 \left(\frac{2}{\sqrt{3}} \| \tilde{c} - c \|_2 + \| R \|_2 \right)$$

where $K_2 = \frac{1}{\sqrt{3}}$. The pointwise error bounds for the same second order chemical reaction of Chapter A are tabulated in Table 2.

Table 2

Error Bound for the Approximate Solution to the Second Order Chemical Reaction of Chapter A

Number of collocation points (using ordinary collocation)	Pointwise error bound for cosine series	Pointwise error bound for power series
2	.0846	.001940
3	.2240	.000068
4	.2988	.000002
6	.6513	.000000

Table 2 indicates that the power series solution is extremely accurate throughout the entire interval [0, 1].

Tor this simple example we have used different properties (some merely being numerical) of the appropriate Green's function. We have summarized these various parameters in Table 3 (for planar, cylindrical, and spherical geometries) for the following Green's functions:

$$-\frac{d}{dx}\left(x^{a-1}\frac{dG}{dx}\right) = \delta(x-t)$$

$$\frac{dG}{dx}(0) = 0 \quad ; \qquad \left(\frac{2}{Sh}\right)\frac{dG}{dx}(1) + G(1) = 0$$

Table 3

Various Numerical Values Associated with the Green's Functions Defined by the One-Dimensional Laplacian Operator with a Radiation Type Boundary Condition

Geometry	Planar	Cylindrical	Spherical
$G(x,t,Sh) =$	$\begin{cases} 1+\frac{2}{Sh}-x, & t\le x \\ 1+\frac{2}{Sh}-t, & t\ge x \end{cases}$	$\begin{cases} \frac{2}{Sh}-\ln(x), & t\le x \\ \frac{2}{Sh}-\ln(t), & t\ge x \end{cases}$	$\begin{cases} \frac{2}{Sh}+\frac{1}{x}-1, & t\le x \\ \frac{2}{Sh}+\frac{1}{t}-1, & t\ge x \end{cases}$
$\|G\|_2^2 =$	$\frac{1}{6}+\frac{2}{Sh}\left[\frac{2}{Sh}+\frac{2}{3}\right]$	$\frac{1}{32}+\frac{2}{Sh}\left[\frac{1}{4}\left(\frac{2}{Sh}\right)+\frac{1}{8}\right]$	$\frac{1}{90}+\frac{2}{Sh}\left[\frac{1}{9}\left(\frac{2}{Sh}\right)+\frac{2}{45}\right]$
$K_1 =$	$\frac{1}{2}+\frac{2}{Sh}$	$\frac{1}{4}+\frac{1}{2}\left(\frac{2}{Sh}\right)$	$\frac{1}{6}+\frac{1}{3}\left(\frac{2}{Sh}\right)$
$K_2^2 =$	$\frac{1}{3}+\left(\frac{2}{Sh}\right)+\left(\frac{2}{Sh}\right)^2$	$\frac{1}{4}+\frac{1}{2}\left(\frac{2}{Sh}\right)+\frac{1}{2}\left(\frac{2}{Sh}\right)^2$	$\frac{1}{3}+\frac{1}{3}\left(\frac{2}{Sh}\right)+\frac{1}{3}\left(\frac{2}{Sh}\right)^2$

With the same boundary conditions as given in eq. 32, we might have a Langmuir-Hinshelwood type rate expression instead of a power-law rate expression:

$$\frac{1}{x^2}\frac{d}{dx}\left(x^2\frac{dc}{dx}\right) = \frac{\phi^2 c}{1+\alpha|c|} \tag{35}$$

with $\alpha > 0$. We assume the existence of a continuous solution to this problem. By utilizing the necessary conditions (for a function of one variable) for the existence of an extremum, it is a straightforward exercise

to show that $0 \leq c(x) \leq 1$. Then from eq. 25,

$$\bar{M} = \sup_{0 \leq t \leq 1} \left[\int_0^1 \left\{ \frac{\phi^2}{(1+\alpha|c+t(T-c)|)^2} \right\}^2 x^2 dx \right] \leq \frac{\phi^2}{\sqrt{3}}$$

such that one has the following mean-squre error bound for an approximate solution to eqs. 32 and 35:

$$\| \tilde{c} - c \|_2 \leq \frac{\sqrt{90}}{1 - \frac{\phi^2}{\sqrt{3}} \left(\frac{1}{\sqrt{90}}\right)} \| R \|_2$$

and is valid for

$$\phi \leq 4.05$$

This result is identical with that for a first order isothermal rate expression.

As a further example, consider a nonisothermal, first order chemical reaction occurring in a spherical catalyst particle. When the boundary conditions specify the temperature and concentration on the surface of the catalyst particle, the problem can be reduced to the study of a single nonlinear ordinary differential equation. We then have the following dimensionless heat balance (we could instead study the dimensionless mass balance):

$$\frac{1}{x^2} \frac{d}{dx} \left(x^2 \frac{dT}{dx} \right) = f(T) \tag{36}$$

where $$f(T) = \phi^2 [T - (1 + \beta)] \exp(-\gamma(1/|T| - 1)) \tag{37}$$

with the boundary conditions as

$$\frac{dT}{dx}(0) = 0 \; ; \quad T(1) = 1 \tag{38}$$

We assume the existence of a continuous solution to the problem described by eqs. 36-38. By utilizing the necessary conditions for a function to possess an extremum (a function of one variable), one can show that $1 \leq T(x) \leq 1 + \beta$. It might be helpful to go through this briefly. First, because of the boundary condition at $x = 0$ (eq. 38), there are no special problems associated with the differential operator of eq. 36 at $x = 0$. By l'Hospital's rule, the Laplacian operator of eq. 36 simply reduces to $3\frac{d^2T}{dx^2}$ at $x = 0$. For simplicity then, we will only discuss eq. 36 as written. Now, assume that $T(x)$ is less than 1.0 for some x_1 in the interval $[0, 1)$. Because of the boundary condition at $x = 1$, our assumption implies that the function T has an interior minimum at some x_2. At the minimum, the first derivative of T vanishes and the second derivative is positive. These are the necessary conditions for a function to possess an extremum. This assumption then implies that, at x_2, the left-hand side of eq. 36 is positive while the right-hand side must be negative. This is clearly a contradiction which invalidates our assumption. Thus $T(x)$ is greater than 1. Now assume that $T(x)$ is greater than $1 + \beta$. This implies that $T(x)$ has an interior maximum. At a maximum, the first derivative of T vanishes and the second derivative is negative. Consequently, the left-hand side of eq. 36 is negative

while the right-hand side must be positive. This is again a contradiction and invalidates our second assumption. This proves our original assertion: $1 \leq T(x) \leq 1 + \beta$. This type of proof does require that we consider $T(x)$ to be a continuous function. Nowhere do we use that $c(x)$ must be within certain limits by physical reasoning.

With these rather crude bounds for the exact solution, $T(x)$, one is able to utilize the mean-square error bound given by eqs. 24 and 25. For the purpose of discussion, we have considered the following set of parameters:

$$\phi^2 = 0.25 \tag{39}$$

$$\beta = 0.0.3 \tag{40}$$

$$\gamma = 18. \tag{41}$$

We can then calculate the necessary value for $\bar{M}$.

$$\bar{M} = \sup_{0 \leq t \leq 1} \left[\int_0^1 \left\{ \frac{\partial f}{\partial T} \Big|_{T = T + t(\tilde{T} - T)} \right\}^2 x^2 dx\right]^{\frac{1}{2}}$$

from which it follows that

$$\bar{M} \leq \frac{1}{\sqrt{3}} \max \left\{ \left|\frac{\partial f}{\partial T}\left(1 + \frac{\beta\gamma - 2(1+\beta)}{\gamma + 2(1+\beta)}\right)\right|, \left|\frac{\partial f}{\partial T}(1+\beta)\right|, \left|\frac{\partial f}{\partial T}(1+\beta+\epsilon)\right| \right\} \tag{42}$$

where ϵ is such that $\tilde{T}(x) - \epsilon \leq 1 + \beta$ for all x. The upper bound for $\bar{M}$ must be such that $\bar{M}_{upper} < \frac{1}{\|G\|_2} = \sqrt{90}$. However $\bar{M}$ derived from eq. 42 is too large ($\bar{M} \leq 14.582$). If we can sharpen the upper bound for the exact solution, $T(x)$, we can accomplish two important

things: (1) the mean-square error bound will be smaller and (2) the mean-square error bound will be valid for a wider range of parameter values. In passing, eq. 24 is also a sufficient condition for the uniqueness of the solution to eqs. 36-38; consequently, a sharper upper bound for $T(x)$ would allow the a priori determination of a wider range of parameters leading to a unique solution of this problem. Let us proceed to show how, in some cases, the a priori upper bound for $T(x)$ can then be sharpened. We start with the crude bounds and the equivalent integral equation (to eqs. 36-38),

$$T(x) = 1 - \int_0^1 G(x,t)\, \phi^2 [T(t) - (1+\beta)] \exp(-\gamma(1/|T| - 1))\, t^2 dt$$

where $G(x,t)$ is a positive function (which can be obtained from Table 3), and $[T - (1 + \beta)]$ is a negative function. Thus we have the following inequalities:

$$T(x) \leq 1 - \phi^2 \min_{1 \leq T \leq 1+\beta} \{[T-(1+\beta)] e^{-\gamma(\frac{1}{|T|}-1)}\} \int_0^1 G(x,t)\, t^2 dt$$

or

$$T(x) \leq 1 - \phi^2 \min_{1 \leq T \leq 1+\beta} \{[T-(1+\beta)] e^{-\gamma(\frac{1}{|T|}-1)}\} [\tfrac{1}{6}(1-x^2)] \qquad (43)$$

Eq. 43 is used to construct an iterative process which does, in some cases, converge to an improved upper bound for $T(x)$. Define T_1 by eq. 44

$$T(x) \leq T_1$$

$$T_1 = 1 + \max \frac{1}{6}\{\phi^2\beta, -\phi^2[u-(1+\beta)]e^{-\gamma(\frac{1}{|u|}-1)}\Big|_{u=\frac{-\gamma+\sqrt{\gamma^2+4\gamma(1+\beta)}}{2}}\} \quad (44)$$

(Eq. 44 follows from eq. 43) T_1 may or may not be less than $1 + \beta$. If $T_1 < 1 + \beta$, we proceed iteratively, as defined by eq. 45, until the successive changes are sufficiently small.

$$T(x) \leq T_i \qquad (i = 1, 2, \ldots)$$

$$T_i = 1 + \frac{1}{6} \max \{\phi^2\beta, - f(T_{i-1})\} \quad (45)$$

Following-up on our example (eq. 39), we find that the improved upper bound on the exact solution is approximately 1.01564. This is considerably different than the previous value of 1.3. If $T(x)$ is bounded by a value that is less than the arguments of $\frac{\partial f}{\partial T}$ in eq. 40, $\bar{M}$ is then bounded by eq. 46.

$$\bar{M} \leq \frac{1}{\sqrt{3}} \left| \frac{\partial f}{\partial T} (T_{\text{upper bound}}) \right| \quad (46)$$

Eq. 46 with the improved upper bound for $T(x)$ leads to the following mean-square error bound for the approximate solution to eqs. 36-38 ($\bar{M} \leq 1.536$):

$$\|\tilde{T} - T\|_2 \leq 0.13 \|R(\tilde{T})\|_2 \quad (47)$$

The improved upper bound for the temperature function, has not, to the author's knowledge, been discussed before. Notice that in using this approach we have validated the error bound and proved uniqueness.

A numerical study is presented for the problem (eqs. 36-38) characterized by the following parameters:

$$\phi^2 = 0.25$$

$$\beta = 0.3$$

$$\gamma = 20.$$

The solution is approximated by the following expansion,

$$\tilde{T}(x) = 1 + (1 - x^2) \sum_{i=1}^{n} a_i P_{i-1}(x^2) \quad . \tag{48}$$

We considered two different sets of polynomials, defined by eq. 49 and eq. 50.

$$\int_0^1 (1 - x^2) P_i(x^2) P_j(x^2) (x^2 dx) = \delta_{ij} \tag{49}$$

$$\int_0^1 P_i(x^2) P_j(x^2) (x^2 dx) = \delta_{ij} \tag{50}$$

Although we have denoted both sets of polynomials by P_i, the two are quite distinct. The method of orthogonal collocation was used to obtain T at the n roots of the n-th order polynomial in (x^2). For the polynomials defined by eq. 49, the results of Table 4 were obtained.

Table 4

Mean-square Residual and Error Bound for Nonisothermal Chemical Reaction

n	$\| R(\tilde{T}) \|_2$	$\| \tilde{T} - T \|_2 \leq$
1	3.4882×10^{-3}	3.8498×10^{-4}
2	1.7535×10^{-4}	1.9353×10^{-5}
3	7.0583×10^{-6}	7.7900×10^{-7}
6	2.0147×10^{-10}	2.2236×10^{-11}
8	7.0953×10^{-14}	7.8308×10^{-15}

For the polynomials defined by eq. 50, the results of Table 5 were obtained.

Table 5

Mean-square Residual and Error Bound for Nonisothermal Chemical Reaction

n	$\| R(\tilde{T}) \|_2$	$\| \tilde{T} - T \|_2 \leq$
1	2.8088×10^{-3}	3.1000×10^{-4}
2	1.2694×10^{-4}	1.4009×10^{-5}
3	4.6037×10^{-6}	5.0809×10^{-7}
6	1.0355×10^{-10}	1.1429×10^{-11}
8	3.1821×10^{-14}	3.5120×10^{-15}

The errors are much smaller than one might expect from viewing the behavior of the expansion coefficients.

The mean-square error bound aids one in the choice of the expansion functions and in the number of expansion functions used. The polynomials defined by eq. 50 consistently give better results for the values of n studied. The error bounds using the functions defined by eq. 50 are from 20 to 55 per cent lower than the error bounds obtained by using the polynomials defined by eq. 49. Similarly, one finds that the errors are sufficiently small to justify the use of as few as three collocation points—the mean-square error is less than 0.0001 %.

In investigating the error bound for this problem, we need to evaluate M (the Lipschitz constant):

$$f(T) = \phi^2[T - (1 + \beta)] \exp(-\gamma(1/|T|-1))$$

$$|f(T_2) - f(T_1)| = \left| \int_0^1 \frac{\partial f}{\partial v} \Big|_{v=T_1+t(T_2-T_1)} (T_2-T_1)\, dt \right|$$

$$|f(T_2) - f(T_1)| \leq \left\{ \max_{1 \leq T \leq T_{upper}} \left| \frac{\partial f}{\partial v} \right| \right\} |T_2-T_1|$$

then $M \leq 1.548$, such that from eq. 31, we obtain

$$\|\tilde{T} - T\|_\infty \leq \frac{1}{\sqrt{3}} (1.548 \|\tilde{T} - T\|_2 + \|R\|_2) \qquad (51)$$

Eq. 51 and the data of Table 4 and 5 provide the pointwise error bounds presented in Table 6.

Table 6

Pointwise Error Bound for Temperature in Nonisothermal Chemical Reaction—Comparison of Jacobi and Legendre Polynomial Expansions

n	Pointwise error bound for Legendre polynomial expansion (eq. 50)	Pointwise error bound for Jacobi polynomial expansion (eq. 49)
1	1.899×10^{-3}	2.358×10^{-3}
2	8.581×10^{-5}	1.185×10^{-4}
3	3.112×10^{-6}	4.771×10^{-6}
6	7.000×10^{-11}	1.362×10^{-10}
8	2.151×10^{-14}	4.796×10^{-14}

The pointwise error bounds are roughly six times as large as the mean-square error bounds for this problem. As with the mean-square error bounds, the Legendre polynomials (eq. 50) provide pointwise error bounds that are 20 to 50% smaller than those obtained using the Jacobi polynomials (eq. 49). For this problem the pointwise error bounds indicate that three expansion functions would be adequate for most calculations—less than 0.001% error. Notice that the one term expansion is accurate to about 0.2%.

As our final application of error bounds, we chose to study numerically a pair of parallel, isothermal chemical reactions. The dimensionless mass balances are,

$$\frac{1}{x^2}\frac{d}{dx}\left(x^2\frac{dc_B}{dx}\right) = \alpha_1 c_B - \alpha_2(1-3(c_B+c_C))^3 \qquad (52)$$

$$\frac{1}{x^2}\frac{d}{dx}\left(x^2\frac{dc_C}{dx}\right) = \alpha_3 c_C - \alpha_4(1-3(c_B+c_C))^3 \tag{53}$$

with

$$\begin{aligned} \alpha_1 &= 0.1 \quad ; \quad \alpha_3 = 0.2 \\ \alpha_2 &= 1.0 \quad ; \quad \alpha_4 = 1.2 \end{aligned} \tag{54}$$

and the following boundary conditions:

$$\frac{dc_B}{dx}(0) = \frac{dc_C}{dx}(0) = 0 \tag{55}$$

$$\frac{2}{Sh}\frac{dc_B}{dx}(1) + c_B(1) = 0.10 \tag{56}$$

$$\frac{2}{Sh}\frac{dc_C}{dx}(1) + c_C(1) = 0.10 \tag{57}$$

These equations correspond to the following chemical reactions which are

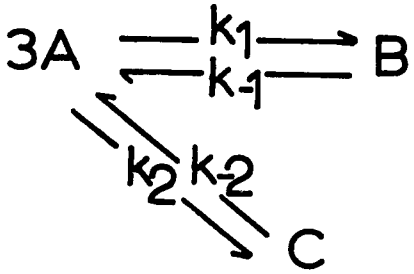

occurring in an isothermal, spherical catalyst particle and experiencing diffusional resistance. Our error bounds (eq. 23) allow for different Sherwood(Sh) numbers but we have assumed that the Sherwood number is identical for the two products, c_B and c_C. The over-all mass balance implies that

$$c_A = 1 - 3(c_B + c_C) \tag{58}$$

If we assume the solutions to eqs. 52-57 are positive, the over-all mass balance implies that $c_A \leq 1$. This bound on c_A can be sharpened by formulating the equivalent integral equations (to eqs. 52-57):

$$c_B(x) = 0.10 + \int_o^1 G(x, t, Sh, \alpha_1)\alpha_2(1-3(c_B+c_C))^3 t^2 dt \tag{59}$$

$$c_C(x) = 0.10 + \int_o^1 G(x, t, Sh, \alpha_3)\alpha_4 (1 - 3(c_B+ c_C))^3 t^2 dt \tag{60}$$

where $G(x, t, Sh, \alpha_i)$, $(i = 1, 3)$ is the Green's function defined by the following problem:

$$-\frac{d}{dx}\left(x^2 \frac{dG}{dx}\right) + \alpha_i x^2 G = \delta(x - t)$$

$$\frac{dG}{dx}(0) = 0$$

$$\frac{2}{Sh}\frac{dG}{dx}(1) + G(1) = 0$$

such that

$$G(x, t, Sh, \alpha_i) = \begin{cases} \dfrac{\sinh \sqrt{\alpha_i}\, t}{\sqrt{\alpha_i}\, x\, t}\left[\dfrac{\sqrt{\alpha_i}\cosh\sqrt{\alpha_i}(1-x)-(1-\frac{Sh}{2})\sinh\sqrt{\alpha_i}(1-x)}{\sqrt{\alpha_i}\cosh\sqrt{\alpha_i}-(1-\frac{Sh}{2})\sinh\sqrt{\alpha_i}}\right], & t \leq x \\ \dfrac{\sinh\sqrt{\alpha_i}\, x}{\sqrt{\alpha_i}\, x\, t}\left[\dfrac{\sqrt{\alpha_i}\cosh\sqrt{\alpha_i}(1-t)-(1-\frac{Sh}{2})\sinh\sqrt{\alpha_i}(1-t)}{\sqrt{\alpha_i}\cosh\sqrt{\alpha_i}-(1-\frac{Sh}{2})\sinh\sqrt{\alpha_i}}\right], & t \geq x \end{cases}$$

$$(i = 1, 3), \tag{61}$$

By inspection, one can see that $G(x, t, Sh, \alpha_i)$ is a positive function for Sherwood numbers greater than 2 (these are the only ones we are interested in anyway). The result of this diversion is that, <u>for positive solution</u> with Sh greater than 2, the c_B and c_C are bounded below by 0.10; consequently, c_A, because of eq. 58, is bounded above by 0.40. We make use of this result in obtaining the Lipschitz constants for the rate expressions (right-hand sides of eqs. 52 and 53).

Notice that we still require the assumption that the unknown solutions are positive. Let us consider the Lipschitz constants for this problem. The functions of interest are

$$f_1(c_B, c_C) = \alpha_1 c_B - \alpha_2 (- 3(c_B+c_C))^3$$

$$f_2(c_B, c_C) = \alpha_3 c_C - \alpha_4 (1 - 3(c_B + c_C))^3,$$

the over-all rate espressions for the products. We are interested in the following identity,

$$f_j(v_2, u_2)-f_j(v_1, u_1) = \int_o^1 \frac{\partial f_j}{\partial v}\Big|_{v= v_1+t(v_2-v_1)} (v_2-v_1)\, dt + \int_o^1 \frac{\partial f_j}{\partial u}\Big|_{u= u_1+t(u_2-u_1)} (u_2-u_1)\, dt \quad (j= 1, 2)$$

such that if we can bound the various partial derivatives of f_j $(j= 1, 2)$ we will have obtained valid Lipschitz constants for an inequality such as eq. 19. In bounding the partial derivatives of f_j we have utilized

the assumption of positive solutions and the resultant fact that c_A is then less than or equal to 0.40.

$$M_{1B} = \alpha_1 + 9\,\alpha_2(1 - 3(c_B + c_C))^2 \leq 1.54$$

$$M_{1C} = 9\,\alpha_2(1 - 3(c_B + c_C))^2 \leq 1.44$$

$$M_{2B} = 9\,\alpha_1(1 - 3(c_B + c_C))^2 \leq 1.728$$

$$M_{2C} = \alpha_3 + 9\,\alpha_1\,(1 - 3(c_B + c_C))^2 \leq 1.928$$

(the numerical bounds are for the parameters of eq. 54)

If one checks to see what values of the Sherwood number will guarantee that the denominator of eq. 22 is positive (such that the error bound is valid), one finds that the Sherwood number is required to be greater than 3.01. Let us now consider several specific choices for the Sherwood number.

Eqs. 52-57 were replaced by a finite system of $2(n + 1)$ algebraic equations generated by the method of orthogonal collocation. The approximate solutions, $\tilde{c}_B$ and $\tilde{c}_C$, satisfied the boundary conditions exactly. Two values of Sh were studied: case I) $Sh \to \infty$ and case II) $Sh = 7.0$. Some of the numerical results are tabulated in Tables 7-16. All of the integrations for the mean-squared integrals were done using Simpson's rule with 101 points (accurate to more digits than shown—checked against 201 points).

In both cases a comparison is made using the roots of the Jacobi polynomials (eq. 49) and the roots of the Legendre polynomials (eq. 50)

Table 7

Mean-squared Error Bounds for Parallel, Chemical Reactions—Using Jacobi Polyno. als (Case I)

n	$\|\tilde{c}_B - c_B\|_2 \leq$	$\|\tilde{c}_C - c_C\|_2 \leq$
1	5.737×10^{-4}	7.050×10^{-4}
2	3.991×10^{-5}	4.890×10^{-5}
3	2.235×10^{-6}	2.723×10^{-6}
6	2.125×10^{-10}	2.577×10^{-10}
8	3.404×10^{-13}	4.125×10^{-13}

Table 8

Mean-squared Residual for Parallel, Chemical Reactions—Using Jacobi Polynomials (Case I)

n	$\|R_B\|_2$	$\|R_C\|_2$
1	3.526×10^{-3}	4.335×10^{-3}
2	2.455×10^{-4}	3.005×10^{-4}
3	1.377×10^{-5}	1.672×10^{-5}
6	1.311×10^{-9}	1.580×10^{-9}
8	2.102×10^{-12}	2.528×10^{-12}

Table 9

Computation Times for Parallel, Chemical Reactions (Case I)

n	Solution time (seconds)	Error bound time (seconds)
1	0.018	0.371
2	0.071	0.437
3	0.194	0.509
6	1.006	0.772
8	2.243	0.974

Table 10

Mean-squared Error Bound for Parallel, Chemical Reactions—Using Legendre Polynomials (Case I)

n	$\|\tilde{c}_B - c_B\|_2 \leq$	$\|\tilde{c}_C - c_C\|_2 \leq$
1	5.058×10^{-4}	6.220×10^{-4}
2	2.915×10^{-5}	3.574×10^{-5}
3	1.431×10^{-6}	1.745×10^{-6}
6	1.054×10^{-10}	1.278×10^{-10}
8	1.501×10^{-13}	1.818×10^{-13}

Table 11

Mean-squared Residual for Parallel, Chemical Reactions—Using Legendre Polynomials (Case I)

n	$\|R_B\|_2$	$\|R_C\|_2$
1	3.108×10^{-3}	3.825×10^{-3}
2	1.793×10^{-4}	2.196×10^{-4}
3	8.819×10^{-6}	1.071×10^{-5}
6	6.505×10^{-10}	7.838×10^{-10}
8	9.266×10^{-13}	1.115×10^{-12}

Table 12

Mean-square Error Bounds for Parallel, Chemical Reactions—Using Jacobi Polynomials (Case II)

n	$\|\tilde{c}_B - c_B\|_2 \leq$	$\|\tilde{c}_C - c_C\|_2 \leq$
1	1.226×10^{-3}	1.506×10^{-3}
2	7.469×10^{-5}	9.169×10^{-5}
3	3.712×10^{-6}	4.540×10^{-6}
6	2.502×10^{-10}	3.050×10^{-10}
8	3.191×10^{-13}	3.887×10^{-13}

Table 13

Mean-squared Residual for Parallel, Chemical Reactions—Using Jacobi Polynomials (Case II)

n	$\|R_B\|_2$	$\|R_C\|_2$
1	2.666×10^{-3}	3.277×10^{-3}
2	1.626×10^{-4}	1.995×10^{-4}
3	8.106×10^{-6}	9.855×10^{-6}
6	5.482×10^{-10}	6.607×10^{-10}
8	6.994×10^{-13}	8.415×10^{-13}

Talbe 14

Mean-squared Error Bound for Parallel, Chemical Reactions—Using Legendre Polynomials (Case II)

n	$\|\tilde{c}_B - c_B\|_2 \leq$	$\|\tilde{c}_C - c_C\|_2 \leq$
1	1.061×10^{-3}	1.304×10^{-3}
2	5.451×10^{-5}	6.693×10^{-5}
3	2.381×10^{-6}	2.912×10^{-6}
6	1.244×10^{-10}	1.517×10^{-10}
8	1.410×10^{-13}	1.718×10^{-13}

Table 15

Mean-squared Residual for Parallel, Chemical Reactions—Using Legendre Polynomials (Case II)

n	$\|R_B\|_2$	$\|R_C\|_2$
1	2.307×10^{-3}	2.840×10^{-3}
2	1.186×10^{-4}	1.456×10^{-4}
3	5.197×10^{-6}	6.322×10^{-6}
6	2.726×10^{-10}	3.286×10^{-10}
8	3.091×10^{-13}	3.719×10^{-13}

Table 16

Expansion Coefficients for a Power Series Representation of the Approximate Solution, $\tilde{c}_B$, Obtained Using Jacobi Polynomials (Parallel, Chemical Reactions—Case I)

$$\tilde{c}_B = \sum_{i=1}^{n+1} d_i \, x^{2i-2}$$

n →	1	2	3	6	8
i ↓					
1	1.0710×10^{-1}	1.0674×10^{-1}	1.0677×10^{-1}	1.0676×10^{-1}	1.0676×10^{-1}
2	-7.0978×10^{-3}	-5.8690×10^{-3}	-5.9736×10^{-3}	-5.9672×10^{-3}	-5.9672×10^{-3}
3		-8.8187×10^{-4}	-6.9001×10^{-4}	-7.1081×10^{-4}	-7.1080×10^{-4}
4			-1.0176×10^{-4}	-7.7244×10^{-5}	-7.7281×10^{-5}
5				-8.5793×10^{-6}	-8.4958×10^{-6}
6				-8.4253×10^{-7}	-9.4242×10^{-7}
7				-1.6512×10^{-7}	-1.0777×10^{-7}
8					-9.4264×10^{-9}
9					-2.2959×10^{-9}

(in spherical geometry). With $Sh \to \infty$, the integrated mean-square error bound (Tables 7 and 10) is 12 to 56 percent smaller using the Legendre roots (as n increases from 1 to 8). This behavior is mirrored in the integrated mean-squared residual (Tables 8 and 11). The error bound requires 43% of the computation time for $n = 6$ and 30% of the time for $n = 8$ (Table 9). It is noteworthy that the integrated mean-square error bound decreases roughly as $0(10^{-(n+2)})$.

For $Sh = 7.0$, the integrated mean-square error bound (Tables 12 and 14) is 13 to 56% smaller using the Legendre roots (eq. 50), with the difference most pronounced with n equal to 8(56%). The residual is consistently smaller than for $Sh \to \infty$, but the error bound is not: this observation is related to the coefficients which occur in the bound.

The coefficients for a power series expansion of the approximate solution of c_B for n from 1 to 8 ($Sh \to \infty$) are given in Table 16. This shows that for this problem the convergence of the solution is indicated in the convergence of the coefficients. The convergence of the coefficients is even more pronounced when the solution is represented in a sum of the corresponding orthogonal polynomials rather than in a power series.

Similarly, we investigated the pointwise error bounds for this problem. Using the bound given by eq. 31 seems to give results which are superior to eqs. 29 and 30. As an example, the bound for c_B is

$$\|\tilde{c}_B - c_B\|_\infty \leq K_2 \left[\sum_{j=B,C} M_{1j} \|\tilde{c}_j - c_j\|_2 + \|R_B\|_2 \right]$$

It is worth note that for the polynomials defined by eq. 49, the $\max_{0 \leq x \leq 1} |R_j(x)|$ for the two components occurred always at $x = 1.0$ and for the polynomials defined by eq. 50 at $x = 0$. This corresponds to the point where the weight function in the respective definitions (eqs. 49 and 50) is zero.

For case I), we have the following explicit expressions for the pointwise error bounds:

$$\|\tilde{c}_B - c_B\|_\infty \leq \frac{1}{\sqrt{3}} \left[1.54 \|\tilde{c}_B - c_B\|_2 + 1.44 \|\tilde{c}_C - c_C\|_2 + \|R_B\|_2 \right]$$

$$\|\tilde{c}_C - c_C\|_\infty \leq \frac{1}{\sqrt{3}} \left[1.728 \|\tilde{c}_B - c_B\|_2 + 1.928 \|\tilde{c}_C - c_C\|_2 + \|R_C\|_2 \right]$$

The numerical results, Table 17, show that the error is dominated by the value of the mean-square residual rather than the individual mean-square error bounds for $\tilde{c}_B$ and $\tilde{c}_C$. Again, the Legendre polynomials (eq. 50) provide a better error bound. This is, of course, related to the smallness of the integral of the mean-squared residual. One need only use three expansion functions to obtain an accuracy (pointwise) of 0.01%. This is usually an acceptable accuracy for engineering calculations of this kind.

Table 17

Pointwise Error Bounds for Parallel Chemical Reactions (Case I)

	Legendre polynomials		Jacobi polynomials	
n	$\|\tilde{c}_B - c_B\|_\infty \leq$;	$\|\tilde{c}_C - c_C\|_\infty \leq$	$\|\tilde{c}_B - c_B\|_\infty \leq$;	$\|\tilde{c}_C - c_C\|_\infty \leq$
1	2.761×10^{-3}	3.405×10^{-3}	3.132×10^{-3}	3.860×10^{-6}
2	1.592×10^{-4}	1.957×10^{-4}	2.179×10^{-4}	2.677×10^{-4}
3	7.815×10^{-6}	9.554×10^{-6}	1.220×10^{-5}	1.491×10^{-5}
6	5.756×10^{-10}	6.999×10^{-10}	1.160×10^{-9}	1.411×10^{-9}
8	8.196×10^{-13}	9.956×10^{-13}	1.859×10^{-12}	2.258×10^{-12}

4. Summary—Error Bounds for Ordinary Differential Equations

We have derived mean-square and pointwise error bounds for approximate solutions of the following type of equation:

$$\frac{1}{x^{a-1}} \frac{d}{dx}\left(x^{a-1} \frac{dy_j}{dx}\right) - f_j(y, \ldots, y_n) = 0 \qquad (j=1, \ldots, n)$$

with boundary conditions such as

$$\frac{dy_j}{dx}(0) = 0$$

$$\frac{2}{Sh} \frac{dy_j}{dx}(1) + y_j(1) = g_j \qquad (j = 1, \ldots, n)$$

The error bounds were derived using the equivalent integral formulation of the above problem. Other boundary conditions could be studied—the important thing is that the boundary conditions be linear and that there

exist the appropriate Green's function for the differential operator. The nonlinear function, f_j, is required to satisfy a Lipschitz condition in the y_j's. The error between the approximate solution and the exact solution is bounded under these circumstances by the root mean square integral of the residual function. This type of error bound implies the uniqueness of the solution to the original differential equation. For those problems where such a bound does not exist, the root mean square integral of the residual provide a convenient error estimate.

The use of a pointwise or mean square error bound is illustrated by problems particular to chemical reaction analysis. In the applications, the approximate solutions are obtained by the method of collocation. The use of the mean square error bound is first discussed for several simple chemical rate expressions (different f(y)):

$$f(c) = \phi^2 c^n \qquad \text{(n is a positive integer)}$$
$$f(c) = \frac{\phi^2 c}{1 + \alpha|c|} \tag{62}$$

In all of the numerical applications the approximate solution is required to satisfy the boundary conditions exactly. The first numerical application involves eq. 62 with $n = 2$ and $\phi^2 = 1$. One type of expansion solution (cosine series) experienced error bounds that increased as the number of terms increased. A second type of expansion solution (power series) experienced error bounds that decreased (numerically) roughly as $0(10^{-(n+2)})$. The error bounds allow us to conclude that the cosine series

solution diverges while the power series solution converges (numerically). The second numerical application involved a nonisothermal, first order chemical reaction. The error bounds were used to compare the Jacobi and Legendre polynomials. Legendre polynomials provided approximate solutions that had consistently smaller error bounds—by 20 to 50%—than Jacobi polynomials. Both polynomials provided approximate solutions with error bounds of roughly 0.05% for one term solutions and 0.0001% for three term solutions. The final application involved a pair of parallel, reversible chemical reactions. The error bounds for the approximate solution obtained using the Legendre polynomials were consistently smaller than those for the Jacobi polynomials. Both polynomials provided approximate solutions with error bounds of roughly 1.0% for one term solutions and 0.005% for three term solutions.

All of the derived error bounds are easy to apply and allow the comparison of different approximate solutions. In comparing different approximate solutions, we have considered different methods of solution, different expansion functions, and different numbers of expansion functions. For the problems studied, three term solutions consistently yielded error bounds of about 0.005%.

5. New Error Bounds for Coupled, Semi-linear Parabolic Partial Differential Equations

Another type of problem common to chemical reaction engineering is the following system of semi-linear parabolic partial differential equations:

$$\alpha_j \frac{\partial u_j}{\partial t} + \underline{v} \cdot \nabla u_j = \nabla^2 u_j + f_j(u_1, \ldots, u_n) \quad (j=1, \ldots, n) \qquad (63)$$

where $\alpha_j > 0$ and $\underline{v}$ is a given vector function of the spatial coordinates, $\underline{x}$. Eq. 63 includes the effects of accumulation, convective transport, diffusion, and any coupling terms in $\underline{u}(\underline{x}, t) = (u_1(\underline{x}, t), \ldots, u_n(\underline{x}, t))$. Such a system of equations would describe the transient response of the reactant concentrations upon start-up for an isothermal, tubular reactor. If eq. 63 is made nondimensional and the length standard, x_s, is chosen appropriately, one obtains an identical equation (to eq. 63) but with one significant difference: the maximum modulus of the vector function $\underline{v}$ (nondimensionalized) is unity. This fact is required below.

We derive a mean square error bound for approximate solutions of eq. 63 when the spatial domain is bounded and denoted by Ω. The result is stated as follows:

Theorem Let $u_j(\underline{x}, t)$ and $\tilde{u}_j(\underline{x}, t)$ be functions defined in $(\Omega \times (0, T])$ with piecewise continuous first derivatives with respect to t. Assume $u_j(\underline{x}, t)$ satisfies eq. 63 and that f_j satisfies a Lipschitz condition in $\underline{u}$. Let $\epsilon_j(\underline{x}, t) \equiv u_j(\underline{x}, t) - \tilde{u}_j(\underline{x}, t)$. Assume $\tilde{u}_j(\underline{x}, t) = u_j(\underline{x}, t)$ on the spatial boundary: $\partial\Omega$. Then

$$\int_0^T \int_\Omega \epsilon_j^2 \, d\underline{x}\, dt \leq \delta_j \int_\Omega \epsilon_j^2(\underline{x}, 0) \, d\underline{x} + \beta_j \int_0^T \int_\Omega R_j^2 [\tilde{\underline{u}}] \, d\underline{x}\, dt$$

$$+ \gamma_j \sum_{i=1}^{n} \left[\delta_i \int_\Omega \epsilon_i^2(\underline{x}, 0) \, d\underline{x} + \beta_i \int_0^T \int_\Omega R_i^2 [\tilde{\underline{u}}] \, d\underline{x}\, dt\right] \quad (j=1, \ldots, n) \qquad (64)$$

and $$R_i[\tilde{\underline{u}}(\underline{x},t)] = f_i(\tilde{u}_1,\ldots,\tilde{u}_n) - [\nabla^2 \tilde{u}_i - \underline{v}\cdot\nabla\tilde{u}_i - \alpha_i \frac{\partial \tilde{u}_i}{\partial t}] \qquad (65)$$

Proof: Denote the differential operator by $K_i[\tilde{u}_i]$:

$$K_i[\tilde{u}_i] = \nabla^2\tilde{u}_i - \underline{v}\cdot\nabla\tilde{u}_i - \alpha_i \frac{\partial \tilde{u}_i}{\partial t}\ , \quad \text{then}$$

$$K_i[u_i-\tilde{u}_i] = f_i(\underline{u}) - f_i(\tilde{\underline{u}}) + R_i\ , \qquad \text{such that}$$

$$|K_i[\epsilon_i]| \le \sum_{j=1}^{n} M_{ij}\,|\epsilon_j| + |R_i|.$$

Introduce the following change of variables,

$v_i = \epsilon_i \exp(b(T-t))$, where b is an arbitrary, non-negative constant, then

$$K_i[\epsilon_i] = \{K_i[v_i] - \alpha_i v_i\, b\}\ \exp(-b(T-t))$$

Our method of proof follows that presented by Sigillito(30), but our goal is different in two ways: (1) treating systems of equations and (2) including the convective transport term $(\underline{v}\cdot\nabla u_i)$. We now introduce the adjoint operator of K_i which is defined by the following integral:

$$\int_0^T \int_\Omega \{u\,K[v] - v\,K^*[u]\}\ d\underline{x}\,dt = 0$$

In determining the adjoint operator, K^*, one starts with the integral of $u \cdot K[v]$ and, by integration by parts, proceeds to remove all

differentiations from the function v. In doing so, one obtains a new operator involving only differentiations of the function u. This new operator is referred to as the adjoint operator. In obtaining K^*, one normally introduces various boundary integrals. The definition of the operator requires that the boundary integrals vanish. This requirement is met by utilizing the boundary and initial conditions associated with the original problem and by setting boundary and initial conditions on the adjoint function, u. The adjoint operator of K_i is,

$$K_i^*[\,] = \nabla^2[\,] + \nabla \cdot (\underline{v}\,[\,]) + \alpha_i \frac{\partial}{\partial t}[\,]$$

and the associated boundary and initial conditions for K_i^* are that the function vanish on the spatial boundary and at the "initial time" T. While the original problem has an initial condition at $t = 0$, the adjoint problem has an initial condition at $t = T$. In obtaining the adjoint operator, one must pay particular attention to the boundary and initial conditions that result.

We then introduce an auxiliary function, θ_i, which is the solution to the following problem:

$$K_i^*[\theta_i] - \alpha_i b\theta_i = v_i \quad \text{in} \quad \Omega \; x(0, T]$$

with $$\theta_i = 0 \quad \text{on} \quad \partial\Omega$$

and $$\theta_i(\underline{x}, T) = 0.$$

In general, v_i is non-zero. For such a problem a solution exists if θ_i can be bounded. We later show that θ_i is bounded by an integral of v_i.

Since

$$v_i^2 = v_i \left(K_i^* [\theta_i] - \alpha_i b \theta_i\right)$$

it follows that

$$\int_o^T \int_\Omega v_i^2 \, d\underline{x}dt = \int_o^T \int_\Omega \theta_i \{K_i[v_i] - \alpha_i b v_i\} \, d\underline{x}dt + \int_o^T \int_{\partial\Omega} v_i \frac{\partial \theta_i}{\partial n} \, d\underline{\sigma}$$

$$- \int_\Omega \alpha_i \theta_i (\underline{x}, 0) \, v_i (\underline{x}, 0) \, d\underline{x}$$

but we have hypothesized that v_i vanishes on the spatial boundary such that the boundary integral vanishes:

$$\int_o^T \int_\Omega v_i^2 \, d\underline{x}dt = \int_o^T \int_\Omega \theta_i \{K_i [v_i] - \alpha_i b v_i\} \, d\underline{x}dt - \int_\Omega \alpha_i \theta_i (\underline{x}, 0) \, v_i (\underline{x}, 0) d\underline{x} \tag{66}$$

As Sigillito(30) demonstrates, the assumption that v_i vanish on the spatial boundary can be removed entirely. Using the algebraic inequality,

$$| a + b | \leq (2a^2 + 2b^2)^{\frac{1}{2}}$$

eq. 66 reduces to,

$$\| v_i \|_{2,1}^2 \equiv \int_o^T \int_\Omega v_i^2 \, d\underline{x}dt \leq [2(\int_o^T \int_\Omega \theta_i [K_i [v_i] - \alpha_i b v_i] \, d\underline{x}dt)^2$$

$$+ 2 \alpha_i^2 \, (\int_\Omega \theta_i (\underline{x}, 0) \, v_i (\underline{x}, 0) \, d\underline{x})^2]^{\frac{1}{2}} \tag{67}$$

Each integral on the right-hand side of eq. 67 is bounded via Schwartz's integral inequality,

$$\| v_i \|^2_{2,1} \leq [2 \int_o^T \int_\Omega \theta_i^2 \, d\underline{x}dt \int_o^T \int_\Omega [K_i(v_i) - \alpha_i b v_i]^2 \, d\underline{x}dt$$

$$+ 2\alpha_i^2 \int_\Omega \theta_i^2 \, (\underline{x}, 0) \, d\underline{x} \int_\Omega v_i^2 \, (\underline{x}, 0) \, d\underline{x} \,]^{\frac{1}{2}}$$

$$\leq \sqrt{2} \, [\frac{1}{c_1} \int_\Omega \theta_i^2 \, (\underline{x}, 0) \, d\underline{x} + \frac{1}{c_2} \int_o^T \int_\Omega \theta_i^2 \, d\underline{x} \, dt]^{\frac{1}{2}} .$$

$$[c_1 \, \alpha_i^2 \int_\Omega v_i^2 \, (\underline{x}, 0) \, d\underline{x} + c_2 \int_o^T \int_\Omega [K_i[v_i] - \alpha_i \, b \, v_i]^2 \, d\underline{x} \, dt]^{\frac{1}{2}} \quad (68)$$

(for any c_1, c_2 positive) we chose the following values for c_1 and c_2:

$$c_1 = 1 \quad ; \quad c_2 = \frac{\alpha_i}{2(\alpha_i \, b + \lambda_1)}$$

where λ_1 is the minimum eigenvalue for the following differential equation:

$$\nabla^2 y + \lambda \, y = 0 \qquad \underline{x} \in \Omega$$

$$y = 0 \qquad \underline{x} \in \partial\Omega$$

In a manner similar to Sigillito(30), one can show that

$$\int_\Omega \theta_i^2 \, (\underline{x}, 0) \, d\underline{x} + \frac{2}{\alpha_i} \, (\alpha_i \, b + \lambda_1) \int_o^T \int_\Omega \theta_i^2 \, d\underline{x}dt \leq \frac{2}{\alpha_i} \, \frac{1}{(\lambda_1^{\frac{1}{2}} - N)^2} \, \| v_i \|^2_{2,1} \quad (69)$$

$$\text{where } N^2 = \max_{\underline{x}} \underline{v} \cdot \underline{v}$$

It is helpful to outline the approach used to obtain eq. 69. Consider the following simple identity:

$$- \int_\Omega \theta_i^2 \, d\underline{x} = \int_o^T \int_\Omega \frac{\partial(\theta_i^2)}{\partial t} \, d\underline{x}dt$$

$$= 2 \int_o^T \int_\Omega \theta_i \frac{\partial \theta_i}{\partial t} \, d\underline{x}\,dt$$

$$= \frac{2}{\alpha_i} \int_o^T \int_\Omega \theta_i \left[K_i^*[\theta_i] - \nabla^2 \theta_i - \nabla \cdot (\underline{v}\,\theta_i)\right] d\underline{x}dt$$

such that by integration by parts for the second term of the right-hand integral, one obtains eq. 70.

$$\int_\Omega \theta_i^2 \, d\underline{x} + \frac{2}{\alpha_i} \int_o^T \int_\Omega \nabla \theta_i \cdot \nabla \theta_i \, d\underline{x}dt = - \frac{2}{\alpha_i} \int_o^T \int_\Omega \theta_i [K_i^*[\theta_i] + \underline{v} \cdot \nabla \theta_i] \, d\underline{x}dt \quad (70)$$

Eq. 70 is the key equation for deriving the following inequality, eq. 71,

$$\| \nabla \theta_i \|_{2,1} \leq \frac{1}{\lambda_1^{\frac{1}{2}} - N} \| v_i \|_{2,1} \quad (71)$$

By adding a particular integral to the right and left-hands sides of eq. 70, one obtains,

$$\int_{\Omega} \theta_i^2 \, d\underline{x} + \frac{2}{\alpha_i} \left[\int_o^T \int_{\Omega} \{ \nabla \theta_i \cdot \nabla \theta_i + \alpha_i \, b \theta_i^2 \} \, d\underline{x} dt \right]$$

$$= - \frac{2}{\alpha_i} \int_o^T \int_{\Omega} \theta_i \left[K_i^*[\theta_i] - \alpha_i \, b \, \theta_i + \underline{v} \cdot \nabla \theta_i \right] d\underline{x} \, dt \qquad (72)$$

Sigillito shows that, for this type of problem, the following inequality is valid for the auxiliary functions,

$$\int_o^T \int_{\Omega} \theta_i^2 \, d\underline{x} \, dt \leq \frac{1}{\lambda_1} \int_o^T \int_{\Omega} \nabla \theta_i \cdot \nabla \theta_i \, d\underline{x} dt \qquad (73)$$

where λ_1 is the previously mentioned "minimum eigenvalue." Using eq. 71 to bound the root mean square integral of grad(θ_i) and eq. 73, eq. 72 allows one to obtain eq. 69.

From the introductory remarks to this section we know that N is less than or equal to unity. Eq. 71 requires that N is less than the square root of the minimum eigenvalue of the equation prior to eq. 69. For axial flow the minimum eigenvalue is π^2 and this would clearly satisfy the requirement.

For our choice of c_1 and c_2 we combine eqs. 68 and 69 to obtain the inequality of eq. 74,

$$\| v_i \|_{2,1} \leq \frac{2}{\sqrt{\alpha_i}} \frac{1}{(N\lambda_1 - N)} \{ \alpha_i^2 \int_{\Omega} v_i^2 (\underline{x}, 0) d\underline{x} + \frac{\alpha_i}{2(\alpha_i b + \lambda_1)} \int_o^T \int_{\Omega} [K_i[v_i] -$$

$$- \alpha_i \, b \, v_i]^2 \, d\underline{x} \, dt \}^{\frac{1}{2}} \qquad (74)$$

The second integral on the right-hand side of eq. 74 is bounded via the Lipschitz condition on the nonlinearity, f_i.

$$\int_0^T \int_\Omega [K_i[v_i] - \alpha_i b v_i]^2 \, d\underline{x}dt \leq 2[\sum_{j=1}^n M_{ij}^2 \sum_{j=1}^n \|v_j\|_{2,1}^2 + \|R_i e^{b(T-t)}\|_{2,1}^2] \quad (75)$$

Let us introduce the following definitions:

$$N_i = \sum_{j=1}^n M_{ij}^2$$

$$k_j = \frac{2}{\sqrt{\alpha_j}} \frac{1}{(\sqrt{\lambda_1} - N)}$$

$$\ell_j = \frac{\alpha_i}{\alpha_j b + \lambda_1} \quad (76)$$

Combining eqs. 74-76, one obtains the following, eq. 77,

$$\|v_i\|_{2,1} \leq k_i [\alpha_i^2 \int_\Omega v_i(\underline{x}, 0)^2 \, d\underline{x} + \ell_i (N_i \sum_{j=1}^n \|v_j\|_{2,1}^2 + \|R_i e^{b(T-t)}\|_{2,1}^2)]^{\frac{1}{2}} \quad (77)$$

Squaring both sides of eq. 77 and summing over the index i, one is able to solve for $[\sum_{j=1}^n \|v_j\|_{2,1}^2]$,

$$\sum_{j=1}^n \|v_j\|_{2,1}^2 \leq \frac{1}{1 - \sum_{j=1}^n k_j^2 \ell_j N_j} [\sum_{j=1}^n k_j^2 \alpha_j^2 \int_\Omega v_j^2(\underline{x}, 0) \, d\underline{x} + \sum_{j=1}^n k_j^2 \ell_j \|R_j e^{b(T-t)}\|_{2,1}^2] \quad (78)$$

Eq. 78, where $(1 - \sum_{i=1}^{n} k_i^2 \ell_i N_i)$ must be positive, allows us to obtain the final desired result:

$$\|\epsilon_i\|_{2,1}^2 \leq \|v_i\|_{2,1}^2 \leq k_i^2 \alpha_i^2 \int_\Omega v_i^2(\underline{x}, 0)\, d\underline{x} + k_i^2 \ell_i \|R_i e^{b(T-t)}\|_{2,1}^2$$

$$+ \frac{k_i^2 \ell_i N_i}{1 - \sum_{j=1}^{n} k_j^2 \ell_j N_j} \left[\sum_{j=1}^{n} k_j^2 \alpha_i \int_\Omega v_j^2(\underline{x}, 0)\, d\underline{x} + \sum_{j=1}^{n} k_j^2 \ell_j \|R_j e^{b(T-t)}\|_{2,1}^2 \right]$$

where $v_i(\underline{x}, 0) = \epsilon_i(\underline{x}, 0)\, e^{bT}$. Then

$$\|\epsilon_i\|_{2,1}^2 \leq \delta_i \|\epsilon_i(0)\|_2^2 + \beta_i \|R_i\|_{2,1}^2 + \gamma_i \left[\sum_{j=1}^{n} \delta_j \|\epsilon_j(0)\|_2^2 + \sum_{j=1}^{n} \beta_j \|R_j\|_{2,1}^2 \right]$$

with $\delta_i \equiv \dfrac{2\alpha_i e^{2bT}}{(\sqrt{\lambda}_1 - N)^2}$; $\beta_i \equiv \dfrac{2e^{2bT}}{(\sqrt{\lambda}_1 - N)^2 (\alpha_i b + \lambda_1)}$

$$\gamma_i \equiv \frac{\beta_i \sum_{j=1}^{n} M_{ij}^2}{1 - \sum_{j=1}^{n} \left[\dfrac{2}{(\sqrt{\lambda}_1 - N)^2 (\alpha_i b + \lambda_1)} \sum_{m=1}^{n} M_{jm}^2 \right]} \tag{79}$$

The denominator of the expression for γ_i must be positive, and this is how a value for the arbitrary parameter, b, is chosen. For those problems where b must be greater than zero, the error bound is not

uniform in time—it permits unbounded growth for large times. But there are cases where b can be selected to be equal to zero. For example, if

$$M_{ij} = 2, \qquad \text{for all } i, j$$

$$\lambda_1 = \pi^2$$

$$N = 1$$

then, the denominator of the expression for γ_i is positive for $b = 0$ if $n \leq 5$. If $M_{ij} = 3$, n must be less than or equal to 2.

This bound, particularly when it is uniform in t, appears to offer a more useful approach to bounding the error than an approach proposed by Carasso(8). Carasso proposes that an asymptotic value of t be obtained for the steady state solution; this in turn provides the information necessary to transform the problem into a boundary value problem in x and t.

One cannot help but notice the similarity between the mean square error bound for the ordinary differential equations, eq. 22, and that for the semi-linear parabolic partial differential equations. It would appear that under the restrictions of the theorem that a Green's function exists and is bounded (in norm) by

$$\sqrt{\frac{2}{(\sqrt{\lambda}_1 - N)^2(\lambda_1)}}$$

for cases where b can be set equal to zero.

The error bound given in eq. 79 can be simplified for

$$\frac{\partial u}{\partial t} + \underline{v} \cdot \nabla u = \nabla^2 u \tag{80}$$

to

$$\|\epsilon\|_{2,1}^2 \leq \frac{2}{(\sqrt{\lambda_1} - N)^2} \left[\int_\Omega \epsilon^2 (\underline{x}, 0)\, d\underline{x} + \frac{1}{\lambda_1} \int_0^T \int_\Omega R^2[\tilde{u}]\, d\underline{x}\, dt \right]$$

6. Application of Error Bound—Parabolic Equations

We discussed the following transient diffusion-reaction problem in Chapter A:

$$\frac{N_1}{4} \frac{\partial T}{\partial t} = \frac{1}{r^2} \frac{\partial}{\partial r} \left(r^2 \frac{\partial T}{\partial r} \right) + \phi^2 \beta c \exp\left(-\gamma(1/|T| - 1)\right)$$

$$\epsilon \frac{N_2}{4} \frac{\partial c}{\partial t} = \frac{1}{r^2} \frac{\partial}{\partial r} \left(r^2 \frac{\partial c}{\partial r} \right) - \phi^2 c \exp\left(-\gamma(1/|T| - 1)\right)$$

$$\frac{\partial T}{\partial r}(0, t) = \frac{\partial c}{\partial r}(0, t) = 0$$

$$T(1, t) = c(1, t) = 1.0$$

$$T(r, 0) = 1.05$$

$$c(r, 0) = 1.0$$

$N_1 = 705$ $\qquad$ $\phi^2 = 0.25$

$N_2 = 1225$ $\qquad$ $\beta = 0.6$

$\epsilon = 0.65$ $\qquad$ $\gamma = 20.$

This type of problem has two characteristics which make it difficult to solve numerically: (1) rather ill-behaved solutions when the reciprocal of the dimensionless thermal diffusivity is much smaller than the reciprocal of the dimensionless mass diffusivity ($N_1 << N_2$) and (2) extremely large Lipschitz constants for the nonlinearity when one knows only that

$$1 \leq T(r,t) \leq +\infty$$

$$0 \leq c(r,t) \leq 1.0$$

The first characteristic actually effects the numerical solution in a rather severe manner leading to extremely small stable step sizes in the time variable. The second characteristic more directly affects any attempt at bounding the error of an approximate solution to the problem. This particular problem experiences the second characteristic. When a problem such as this is known to be a 'bad actor' numerically, one often takes particular measures to assess the accuracy of the approximate solution. Let us then consider how the mean square error bound of eq. 79 might be used for this particular problem.

The Lipschitz constants for the dimensionless rate expression,

$$c \exp(-\gamma(1/|T| - 1))$$

are given by

$$|f(c_2, T_2) - f(c_1, T_1)| \leq \exp(\gamma)\,|c_2 - c_1| + \frac{4}{\gamma}\exp(\gamma - 2)\,|T_2 - T_1|$$

such that for $\gamma = 20.$,

$$\exp(\gamma) = 4.85 \times 10^{8}$$

$$\frac{4}{\gamma} \exp(\gamma-2) = 1.31 \times 10^{7}$$

Consequently, $b = 0(10^{13})$. As a result of the large value of b, the residual function would have to be $0(10^{-10^{13}})$ to obtain a meaningful error bound.

If an a priori upper bound can be specified for $T(r,t)$, one finds that the Lipschitz constants are given as,

$$|f(c_2, T_2) - f(c_1, T_1)| \leq k_1 |c_2-c_1| + k_2 |T_2-T_1|$$

where $k_1 = \exp(-\gamma(1/|m| - 1))$

and

$$k_2 = \max_{1 \leq v \leq m} \left[\frac{\gamma \exp(-\gamma(1/|v|-1))}{v^2} \right]$$

with $T(r,t) \leq m(t)$

Such an upper bound has been obtained (see appendix). It is only useful for $t \leq 15$ for this particular example (which approaches a steady state solution for t roughly 100). For $t \leq 10$, one find that

$$\bar{T}(r,t) \leq 1.0776$$

or $k_1 = 4.2217$

$k_2 = 72.7113$

The Lipschitz constants for the nonlinearities in the partial differential equations are then

$$M_{TT} = \phi^2 \beta k_1 \quad ; \quad M_{TC} = \phi^2 \beta k_2$$

$$M_{CT} = \phi^2 k_1 \quad ; \quad M_{CC} = \phi^2 k_2$$

such that b must be greater than 0.44 for the error bound, eq. 79, to be valid. This is considerably smaller than previously. We have chosen to use a value for b of 1. By obtaining an improved upper bound of the exact solution $T(r,t)$, we are able to demonstrate a useable mean-square error bound for approximate solutions of this problem. Define the following quantities:

$$\alpha_c = \frac{(.65)(1225)}{4} \quad ; \quad \alpha_T = \frac{(705)}{4}$$

$$\lambda_1 = \pi^2 \quad ; \quad b = 1.0$$

such that (see eq. 79)

$$\delta_c \equiv \frac{2\alpha_c e^{2bt'}}{\lambda_1} = 40.338\ e^{2t'} \qquad (t' \leq 10)$$

$$\delta_T \equiv \frac{2\alpha_T e^{2bt'}}{\lambda_1} = 35.716\ e^{2t'}$$

$$\beta_c \equiv \frac{2\, e^{2bt'}}{\lambda_1(\alpha_c b + \lambda_1)} = 0.00096990\ e^{2t'}$$

$$\beta_T \equiv \frac{2\, e^{2bt'}}{\lambda_1(\alpha_T b+\lambda_1)} = 0.0010888\, e^{2t'}$$

$$\gamma_c \equiv \frac{\beta_c \sum_{j=c,T} M_{cj}^2}{1-e^{-2bt'}\,\beta_c \sum_{j=c,T}\left(\sum_{k=c,T} M_{jk}^2\right)} = 0.57151 e^{2t'}$$

$$\gamma_T \equiv \frac{\beta_T \sum_{j=c,T} M_{Tj}^2}{1-e^{-2b'}\,\beta_T \sum_{j=c,T}\left(\sum_{k=c,T} M_{jk}^2\right)} = 0.25529\, e^{2t'}$$

$$F(t') \equiv [\delta_c \|\tilde{c}-c\|_2^2(0) + \beta_c \|R_c\|_{2,1}^2(t')]$$

$$G(t') \equiv [\delta_T \|\tilde{T}-T\|_2^2(0) + \beta_T \|R_T\|_{2,1}^2(t')]$$

such that (see eq. 79)

$$\|\tilde{c}-c\|_{2,1}^2(t') \leq F(t') + \gamma_c [F(t') + G(t')]$$

$$\|\tilde{T}-T\|_{2,1}^2(t') \leq G(t') + \gamma_T [F(t') + G(t')]$$

For clarity,

$$\|R_T\|_{2,1}^2(t') = \int_0^{t'}\int_0^1 e^{-2t}\left\{\frac{N_1}{4}\frac{\partial\tilde{T}}{\partial t} - \frac{1}{r^2}\frac{\partial}{\partial r}\left(r^2\frac{\partial\tilde{T}}{\partial r}\right) - \phi^2\beta\tilde{c}e^{-\gamma\left(\frac{1}{|\tilde{T}|}-1\right)}\right\}^2 r^2\, dr\, dt$$

while

$$\| \tilde{T} - T \|_2^2 (0) = \int_0^1 [\tilde{T}(r, 0) - T(r, 0)]^2 \, r^2 \, dr$$

(similarly for $\tilde{c}$).

If a further improved upper bound were available for the function $T(r, t)$, the coefficients involved in this mean square error bound could be improved. The futility of such a thought is displayed in Fig. 13 of Chapter A. Our approximate solution to this problem indicates that the exact solution does possess a maximum value of roughly 1.073 (near $r = 0$ and between the dimensionless times of 10 and 25). The fact that this error bound is only valid for times of 0(10) is a shortcoming. Even so, it does allow one to compare various approximate solutions with various expansion functions over this interval of time. This certainly is some degree of success, but it is only fair to warn that the nature of the solution to a problem of this complexity can and does change drastically for different parameters and for longer lengths of time.

7. Conclusions

We have demonstrated a rather general method for deriving pointwise and mean square error bounds for systems of nonlinear ordinary differential equations. The error, using this method, is bounded by various characteristics of the residual function. Particular attention is directed to those results which bound the error by the root-mean-square integral of the residual functions. In general, the method requires the existence of an appropriate Green's function for part or all of the linear

portion of the differential operator. We have investigated second-order differential equations but this is not a restriction. The nonlinearity is required to satisfy a Lipschitz condition in the dependent variables, but this can be extended to include nonlinearities in the lower order derivatives. The critical point centers on the Lipschitz constants—these often depend explicitly on the upper and lower bounds of the exact solution. Correspondingly, the inclusion of nonlinearities involving the lower order derivatives would produce Lipschitz constants that depend on the upper and lower bounds of the particular derivative.

A particular class of second-order nonlinear ordinary differential equations was investigated. Different nonlinearities in the dependent variable were studied. The approximate solutions to these problems were obtained using the method of collocation and the method of orthogonal collocation. For problems involving a single differential equation, the mean square error bounds were roughly 0.0001% for a three-term approximate solution while the pointwise error bound was roughly 0.01-0.001%. For a pair of nonlinear ordinary differential equations, the corresponding mean square error were roughly 0.001-0.005% while the pointwise error bounds were roughly 0.01-0.02%. The error bounds are easy to apply and allow one to compare various approximate solutions in order to select the best one of those compared.

We have derived a mean-square error bound for systems of semi-linear parabolic partial differential equations. The method of derivation follows that introduced by Sigillito(30) but we have extended the results to

include the convective transport mechanism for systems of equations. Interestingly, this result is similar to that obtained for systems of ordinary differential equations. We found, by application, that the Lipschitz constants play a similar role— they depended on the upper and lower bounds on the exact solution. For parabolic equations the error bound involves the integral of the residual function with respect to distance and time. Although the error bound for the parabolic equations is more difficult to apply, it does allow one to select among different approximate solutions for that one which is most accurate.

8. Bibliography

1) Bellar, F., Pointwise bounds in elliptic and parabolic partial differential equations, Ph. D. Thesis (1961), University of Maryland (College Park).

2) _____, Pointwise bounds for the second initial-boundary value problem of parabolic type, Pacific J. Math., 19 (1966) pp. 205-219.

3) Bellman, R., Juncosa, M. L. and Kalaba, R., Some numerical experiments using Newton's method for nonlinear parabolic and elliptic boundary-value problems, Comm. of ACM, 4, 4 (1961) pp. 187-191.

4) Bel'tyukov, B. A., Solution of nonlinear integral equations by Newton's method, Diff. Equations, 2, 8 (1966) pp. 555-560.

5) Birkhoff, G., Schultz, M. H. and Varga, R. S., Piecewise Hermite interpolation in one and two variables with applications to partial differential equations, Numer. Math., 11 (1968) pp. 232-256.

6) Bramble, J. H. and Payne, L. E., Bounds in the Neumann problem for second order uniformly elliptic operators, Pacific J. Math., 12 (1962) pp. 823-833.

7) _____, Error bounds in the pointwise approximation of solutions of elastic plate problems, J. Res. Nat. Bur. Stand., 67B (1963) pp. 145-155.

8) Carasso, A., A long-range numerical solution of mildly nonlinear parabolic equations, Numer. Math., 16, 4 (1971) pp. 304-321.

9) Ciarlet, P. G., Schultz, M. H. and Varga, R. S., Numerical methods of high-order accuracy for nonlinear boundary value problems: I One dimensional problems, Numer. Math., 9 (1967) pp. 394-430.

10) _____, Numerical methods of high-order accuracy for nonlinear boundary value problems: II Nonlinear boundary conditions, Numer. Math., 11 (1968) pp. 331-345.

11) _____, Numerical methods of high-order accuracy for nonlinear boundary value problems: III Eigenvalue problems, Numer. Math., 12 (1968) pp. 120-133.

12) Ciarlet, P. G., Schultz, M. H. and Varga, R. S., Numerical methods of high-order accuracy for nonlinear boundary value problems: IV Periodic boundary conditions, Numer. Math., 12 (1968) pp. 266-279.

13) _____, Numerical methods of high-order accuracy for nonlinear boundary value problems: V Monotone operator theory, Numer. Math., 13 (1969) pp. 51-77.

14) Courant, R. and Hilbert, D., Methods of Mathematical Physics, Volume I, Interscience Publishers, Inc. (New York) 1966.

15) Douglas, J., Jr. and Dupont, T., Galerkin methods for parabolic equations, SIAM J. Numer. Anal., 7, 4 (1970) pp. 575-626.

16) Finlayson, B. A., Approximate solutions of equations of change; convective instability by active stress, Ph. D. Thesis (1965), University of Minnesota.

17) Finlayson, B. A. and Scriven, L. E., Upper and lower bounds for solutions to the transport equation, AIChE J., 12, 6 (1966) pp. 1151-1157.

18) Green, J. W., An expansion method for parabolic partial differential equations, J. Res. Nat. Bur. Stand., 51, 3 (1953) pp. 127-132.

19) Hulbert, L. E., The numerical solution of two-dimensional problems of the theory of elasticity, Ph. D. Thesis (1963), Ohio State University.

20) Karpilovskaya, E. B., Convergence of the collocation method for certain boundary value problems of mathematical physics, Sib. Math. Zh., 4, 3 (1963) pp. 632-640.

21) Krasnoselskii, M. A., A posteriori error estimates, Soviet Math. Dokl., 9, 4 (1968) pp. 984-987.

22) Lucas, T. R., A generalization of L-splines, Numer. Math., 15, 5 (1970) pp. 359-370.

23) Moore, R. H., Approximations to nonlinear operator equations and Newton's method, Numer. Math., 12 (1968) pp. 23-34.

24) Payne, L. E., Error bounds based on a priori inequalities, Numerical Solutions of Partial Differential Equations (Ed.: J. H. Bramble), Academic Press (New York–1966) pp. 83-94.

25) Payne, L. E. and Weinberger, H. F., New bounds for solutions of second order elliptic partial differential equations, Pacific J. Math., 8 (1958) pp. 551-573.

26) Price, H. S. and Varga, R. S., Error bounds for semi-discrete Galerkin approximations of parabolic problems with applications to petroleum reservoir mechanics, Numerical Solution of Field Problems in Continuum Physics, AMS (Providence-1970) pp. 74-94.

26a) Protter, M. H., and Weinberger, H. F., Maximum Principles in Differential Equations, Prentice-Hall, Inc., 1967.

27) Rosen, J. B., Approximate solution and error bounds for quasi-linear elliptic boundary value problems, SIAM J. Numer. Anal., 7 (1970) pp. 80-103.

28) Schultz, M. H., Error bounds for the Rayleigh-Ritz-Galerkin method, J. Math. Anal. Appls., 27 (1969) pp. 524-533.

29) _____, The Galerkin method for nonselfadjoint differential equations, J. Math. Anal. Appls., 28 (1969) pp. 647-651.

30) Sigillito, V. G., A priori inequalities and pointwise bounds for solution of certain elliptic and parabolic boundary value problems, Ph. D. Thesis (1965), John Hopkins.

31) _____, Pointwise bounds for solutions of the first initial boundary value problem for parabolic operators, SIAM J. Appl. Math., 14 (1966) pp. 1038-1056.

32) _____, On a continuous method of approximating solutions of the heat equation, J. of ACM, 14, 4 (1967) pp. 732-741.

33) _____, Pointwise bounds for solutions of semi-linear parabolic equations, SIAM Review, 9, 3 (1967) pp. 581-585.

34) Vainikko, G. M., On the stability and convergence of the collocation method, Diff. Equations, 2, 1 (1966) pp. 186-194.

35) Varga, R. S., Hermite interpolation-type Ritz methods for two-point boundary value problems, Numerical Solutions of Partial Differential Equations (Ed.: J. H. Bramble), Academic Press (New York-1966).

36) _____, Accurate numerical methods for nonlinear boundary value problems, Numerical Solution of Field Problems in Continuum Physics, AMS (Providence-1970) pp. 152-167.

CHAPTER C

Analysis of the Removal of NO_x From Automobile Exhaust

The method of orthogonal collocation is utilized in the analysis of a contemporary air pollution problem—the removal of the nitric oxide from automobile exhaust by an axial flow, packed-bed reactor. The reactor is modelled by a series of four mixing cells; in each cell, one must solve a pair of coupled nonlinear ordinary differential equations with nonlinear integral boundary conditions. The physical problem is unlike commercial reactors in that the inlet conditions vary with time (as described by the Federal Test Procedure) over a rather wide range. A model allows the delineation of the significant operating and design variables—in this case, the heat load and the thermal inertia of the solid packing. The variables studied include (1) different levels of the inlet carbon monoxide and nitric oxide concentrations, (2) the solid-density and heat capacity (related to the thermal inertia), and (3) the effective diffusivity in the particle.

1. The Automobile Air Pollution Problem with NO_x

Air pollution commonly refers to the presence of various chemicals and substances in the air which are either proven or potential health hazards. Many air pollutants also cause property damage and present safety hazards. The major air pollutants are carbon monoxide (CO), sulfur dioxide (SO_2), nitric oxide (NO), hydrocarbons (HC), and airborn particles. Of the major pollutants, it is estimated that the internal

combustion engine contributes about 86 million tons/year of a total of 142 million tons/year (1). The primary automotive source is the exhaust gas. There are several recent reviews which summarize the automobile air pollution problems, the suggested solutions, and the current research (12, 28).

The exhaust composition varies with automobile, but Table 1 lists typical time average values for older vehicles (18):

Table 1

Exhaust Composition

component	concentration
CO_2	12 volume %
N_2	74 volume %
H_2O	10 volume %
CO	3 volume %
H_2	.5 volume %
O_2	.4 volume %
total hydrocarbons	5000 ppm by volume
total aldehydes	100 ppm by volume
NO_x	1300 ppm by volume

Notice that the more objectionable components are present in fairly low concentrations. The air pollution problem arises because of the large

number of automobiles in operation. NO_x is symbolic for a mixture of the nitrogen oxides. Kohayakawa (20) reports that NO_x is composed of roughly 95% nitric oxide and 3-4% nitrogen dioxide. There are lesser amounts of other oxides. Newer automobiles emit lesser amounts of CO (about 1 volume %) and hydrocarbons (about 200 ppm by volume) than shown in Table 1. The improved control of these emissions has, to date, been obtained by making relatively minor modifications of the overall engine. Hydrocarbon emissions were greatly reduced when the crank-case emissions were vented back into the intake manifold. The carbon monoxide level has been controlled by operating the engine at higher air-to-fuel (A/F) ratios (lean) and by changing the timing to increase the peak combustion temperature. Unfortunately, both of these modifications for CO-control increase the NO_x emissions. This is qualitatively shown in Fig. 1 for various A/F ratios. As the A/F ratio is increased, the combustion mixture experiences quenching at the cylinder wall (19). The quenching is hypothesized as the reason for the maximum in the NO concentration as shown in Fig. 1.

The initial Federal legislation (13) specified the allowable CO and HC emission levels and indicated allowable test procedures. The procedure for measuring the exhaust emissions is referred to as the Federal Test Procedure (FTP). Briefly, the procedure consists of starting the engine cold and running the engine (on a test-stand, connected to a dynamometer) through seven cycles of varying acceleration.

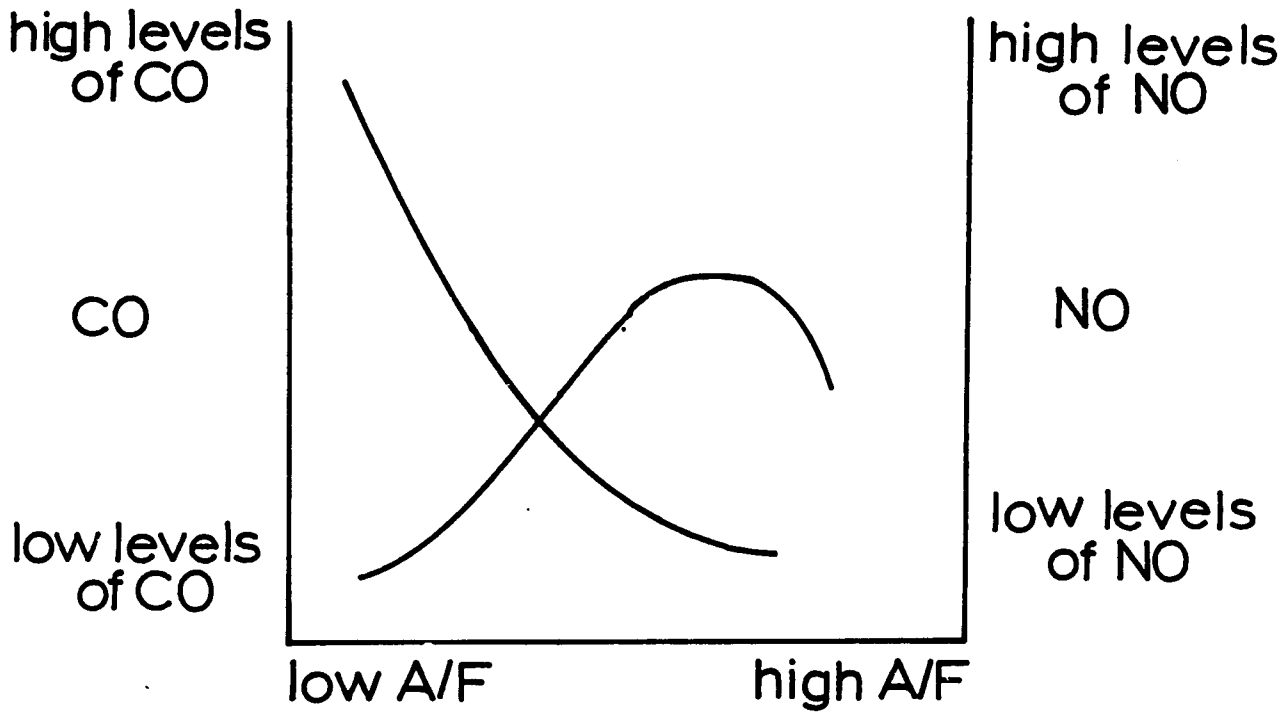

Figure 1. Carbon monoxide and nitric oxide concentrations versus A/F. (Qualitative).

The cold cycles (first four cycles) contribute more CO and less NO than the hot cycles. Recently (14), the procedure for measuring the exhaust emissions was changed. Here we use the older procedure because of the availability of the requisite data as functions of time. While the first controls, which went into effect in 1968, limited the emissions of CO and HC in new automobiles, the proposed controls for 1975 will include NO_x. For 1975 the proposed emission standard for NO_x is 225 ppm by volume, and this standard would be tightened to 100 ppm by 1980 (10). Interest in NO_x control stems from the part which NO may play in smog formation and the fact that NO is oxidized to

NO_2. Nitrogen dioxide is several times more toxic than CO.

A closer look at the level of the NO_x emissions reveals that the absolute values for these gases depend upon the manner in which the automobile is driven (20):

Driving Mode	NO_x (ppm by volume)
idle	130
acceleration	1550
cruise	720
deceleration	220

It also known that the NO_x emission are lower while the engine is warming-up (24). This can be attributed to the rich fuel mixture that an engine burns while warming-up. This behavior of the NO_x concentrations varying with driving mode implies that any analysis has to be a dynamic study.

The nitric oxide found in the exhaust is a result of the reactions between nitrogen, oxygen, and water.

$$N_2 + 0_2 \rightleftharpoons 2NO$$

$$N_2 + 2H_20 \rightleftharpoons 2NO + 2H_2$$

The equilibrium constants for these reactions are such that less than 1 ppm NO could be formed if the combustion temperature were less

than 1200°F (16). Assuming that the internal combustion engine is not replaced and that the combustion process (and associated temperatures) remains the same as it is now, one realizes that any solution for controlling the NO_x emissions must treat the exhaust gases. As pointed out before, minor engine modifications have not been successful in reducing both CO and NO_x.

One of the often-mentioned control devices for automotive exhaust emissions is the catalytic convertor. The Stanford Research Institute recently completed a state-of-the-art study regarding the use of catalytic reactors for controlling the level of the NO_x in the automobile exhaust (39). In this study it is concluded that "for the removal of oxides of nitrogen, the available experimental data are incomplete and meager. A promising approach to catalytic control of oxides of nitrogen appears to be its reaction with carbon monoxide in a two stage catalytic system, although such a system has not been tested to any extent under road-test conditions." Since this study was published, much of the necessary experimental data has become available. It is interesting to note that the two stage system referred to by the Stanford Research Institute was first proposed by Roth and Doerr (25) in 1961. In such a two stage catalytic system, the first convertor reduces nitric oxide to nitrogen, carbon dioxide, and water (using a stoichiometric excess of CO and H_2):

$$NO + CO \rightleftharpoons \tfrac{1}{2}N_2 + CO_2$$

$$NO + H_2 \rightleftharpoons \tfrac{1}{2}N_2 + H_2O$$

The catalyst must be selected with care because some catalysts promote the formation of ammonia (10),

$$NO + \frac{5}{2}\ H_2 \rightleftharpoons H_2O + NH_3$$

The second converter then oxidizes the CO to CO_2 using injected air,

$$CO + \tfrac{1}{2}O_2 \rightleftharpoons CO_2$$

Any ammonia formed in the first conveter is usually oxidized to NO in the second convertor,

$$NH_3 + \frac{5}{4}\ O_2 \rightleftharpoons NO + \frac{3}{2}\ H_2O$$

Such ammonia formation needs to be minimized. This problem has been encountered by Bernstein et al. (10) and is still unresolved.

Although a considerable effort has been made to determine an acceptable catalyst for the nitric oxide convertor, none is currently available. Those that do catalyze the reactions fail to exhibit the necessary mechanical and thermal resistance to deterioration—particularly due to misfiring or sustained high speed driving. Another problem is the poisoning and fouling of catalysts when exposed to the raw automobile exhaust. This may eventually require the use of a low sulfur, lead-free

gasoline. Let us consider some of the experimental work which has been done in the search for an acceptable catalyst.

2. Catalytic Reduction of NO_x

As early as 1961 it was recognized that any nitric oxide in automobile exhaust could be reduced chemically be reacting it with carbon monoxide or hydrogen (both of which are present in the exhaust). The reactions of interest are

$$NO + CO \rightleftharpoons CO_2 + \tfrac{1}{2}N_2 \qquad (1)$$

$$NO + H_2 \rightleftharpoons H_2O + \tfrac{1}{2}N_2 \qquad (2)$$

$$NO + \tfrac{5}{2}H_2 \rightleftharpoons H_2O + NH_3 \qquad (3)$$

The last reaction (eq. 3) is undesirable and its occurrence should be eliminated or at least minimized. For the temperatures of interest (0-800°C) equilibrium thermodynamics predicts that the equilibrium constants will all be in excess of 10^{10}. The equilibrium constants for eqs. 1 and 2 are presented in the appendix. Although the equilibrium constants favor the reduction of NO, one must still determine experimentally the catalyst which has a favorable rate of reaction.

Baker and Doerr (25) demonstrated that various copper chromite catalysts would catalyze the reaction between carbon monoxide and nitric oxide (eq. 1). They found that an excess of the reducing agent (CO) increased the rate of reaction and that oxygen deleteriously

competed with the nitric oxide for the reducing agent. Unfortunately, the space velocities studied (5-10,000hr^{-1}) are considerably lower than those that would occur in typical automobiles. The results cannot safely be extrapolated to more typical conditions. Sourirajan and Blumenthal (35) performed a parametric study of (1) the reductant/oxidant ratio, (2) space velocity, and (3) gas temperature. They investigated the above reactions (eqs. 1-3) and several others involving nitrogen dioxide (NO_2). It was observed that the per cent conversion of NO increased as the excess of reductant (CO, H_2) increased and decreased as the space velocity increased. They also achieved higher conversions for higher temperatures. Both studies (25, 35) concluded that a high conversion is possible at low temperatures (200-300°C), but this is not true at the high space velocities (60,000-100,000hr^{-1}) that actually occur in practice.

Ayen and Peters (4) studied the reactions between NO and H_2 (eqs. 2 and 3) and reported an over-all rate expression for eq. 2. This rate expression was used in the reactor analysis presented in the following subsections. A summary of the rate expression and its parameters is given in the appendix. The catalyst was composed of copper, zinc, and chromia and was chosen because it provided an appreciable quantity of ammonia. Their data indicate that the ammonia reaction (eq. 3) was only $\frac{1}{4}$ to $\frac{1}{2}$ as fast as eq. 2. Consequently, if the CO reaction (eq. 1) is much faster than either of the hydrogen reactions, one can neglect the formation of ammonia.

Baker and Doerr (8) investigated the reaction between NO and CO on a commercial copper chromite catalyst. They reported that the per cent conversion of NO was about 90% for temperature above 270°C and remained at 90% for space velocities as high as 36,000hr^{-1}. They noted the formation of large amounts of nitrous oxide (N_2O) at temperatures below 270°C. Tests were later performed (using this catalyst and a new catalyst) on actual automobile exhaust (7). All catalysts were tested for as long as 350 hours which would correspond to 12,000 miles of driving at 35mph. The temperatures (400-500°C) were higher than before (8) and the space velocity (10,000hr^{-1}) was lower. Hence, the conversion of NO should proceed more easily. It is reported that as the space velocity increases that the conversion decreased.

Ayen and Ng(3) investigated the reaction between NO and CO on a barium promoted copper chromite catalyst. They found that the overall rate expression was well fitted by a Langmuir-Hinshelwood type rate expression (over the temperature range 160-240°C). This rate expression, which is reported in the appendix, has been used in the analysis presented later. Ayen and Yonebayashii (5) investigated the reaction between nitrogen dioxide and carbon monoxide under the same circumstances (3) while Ayen and Amirnazmi studied the reaction between nitrogen dioxide and hydrogen (2).

Ford Motor Company has been responsible for several recent kinetic studies dealing with the problem of removing the nitric oxide

from automobile exhaust. Shelef and Otto have studied the formation of nitrous oxide as an intermediate in the reaction between NO and CO (30). Shelef et al. investigated the interaction of CO, O_2, and NO on various transition metal oxide catalysts (32). An unusual study by Shelef and Otto (31) involved solid carbon as he active site for the three component interaction mentioned above. A survey of the removal of NO by heterogeneous catalytic reactions (29) and of potential catalysts for the decomposition of nitric oxide have also appeared (33). Supported palladium and platinum catalysts have been used to study the interactions between H_2, O_2, NO, and CO (19).

Some of the experimental results regarding the catalytic reactions between NO and (CO, H_2) cannot be realized in practice. A catalyst that works well with laboratory gases and a nitrogen atmosphere need not work well in the corrosive atmosphere of the automobile exhaust. Additionally, in practice the catalyst needs to have superior mechanical strength, to be resistant to damage by excess heating, and to be resistant to lead and sulfur poisoning.

Notwithstanding these shortcomings, our reactor analysis utilizes the overall rate expressions previously mentioned (3, 4). The authors obtained their rate expressions (3, 4) by hypothesizing a reaction mechanism and then testing the data. This is the justification for expecting our results to be realistic.

3. Preliminary convertor study

There are several features of the convertor for the removal of NO from automobile exhaust that are discussed and analyzed for steady-state operating conditions. We have considered the handling capacity, the pressure-drop, and the physical dimensions of such a convertor (assumed to be axial flow). Mass transport limitations within the catalyst particle and heat transfer resistances at the catalyst surface are discussed. By requiring a small pressure-drop, it is found that an axial flow reactor with the desired capacity would have to have a very small length-to-diameter ratio. This small ratio made it necessary to determine the significance of dispersion in the bulk fluid (as distinguished from the particle fluid). The importance of the dispersion was studied using various mathematical models.

The handling capacity of the convertor can be translated quite easily into a minimum required volume of catalyst. Wei (38) states that the exhaust volume ranges from 20 to 125 SCFM. Concentration data (7, 10, 21) indicate that the nitric oxide concentrations range from 200 to 3500 ppm by volume. These figures mean that the convertor must handle as much as 16.6 gms NO/minute (assuming the validity of the ideal gas law, a pressure of 1 atmosphere, and an average molecular weight for the gas stream of 28). This same quantity of NO must be transferred to the catalyst particles,

$$16.6 \text{ gms NO/min.} = k_g^{NO} \rho_f (g_{fluid}^{NO} - g_{surface}^{NO}) S_T \qquad (5)$$

$$\frac{S_T}{v} = \frac{6}{dp} (1-\epsilon)$$

where k_g^{NO}, the mass transfer coefficient, is calculated from Thoenes and Kramers correlation (36),

$$k_g^{NO} = \frac{D_{NO-N_2}}{d_p} (2.42 \, Re^{\frac{1}{3}} \, Sc^{\frac{1}{3}} + .129 \, Re^{.8} \, Sc^{.4} + 1.4 \, Re^{.2}), \qquad (5)$$

S_T is the total external catalyst surface area, ρ_f is the gas density, and $(g_{fluid}^{NO} - g_{surface}^{NO})$ is the mass fraction driving force. As discussed in the appendix, the Schmidt number, Sc, is about .71. Viscosity values are also presented in the appendix, as are diffusivity values. The mass transfer coefficient is found to be 20-100 cm/sec. In all cases we used the following values

$$d_p = .3175$$

$$\epsilon = .35$$

so that the convertor must have a total volume (voids included) of roughly 600 cm^3 (T=800°K, k_g^{NO}=60 cm/sec, g_{fluid}^{NO}=.0016). This calculation assumes the maximum driving force; if the surface concentration is quite close to the bulk fluid concentration, a much larger reactor could be required. We have assumed a reactor volume of 2832cm^3 (or .1ft^3) for further calculations. This value follows the suggestion of Baker and Doerr (7).

Fluid flowing through a packed-bed experiences a pressure-drop which has been correlated by the following expression (Ergun equation):

$$-\frac{\Delta p}{L} = \frac{f G^2 (1-\epsilon)}{\rho_f d_p \epsilon^3} \tag{6}$$

where f, the friction factor, is given by

$$f = 1.75 + \frac{150}{Re} \tag{7}$$

with the Reynolds' number given as,

$$Re = \frac{d_p G}{\mu(1-\epsilon)} \tag{8}$$

The mass flux. G, can be related to the volumetric flux. F(SCFM). We require that the pressure-drop not exceed 0.02-0.03 atmospheres. If $d_p = .3175\text{cm}$ ($\frac{1}{8}$ inch) and $\epsilon = .35$ (as before). then the adverse case introduced in discussing the convertor capacity indicates that the convertor should have the following dimensions (assuming a cylindrical convertor):

$$\text{length} = L = 1.82 \text{ inches}$$

$$\text{radius} = R_t = 5.5 \text{ inches}$$

or L/D = 0.165. Such a small L/D indicates that the operation of such an apparatus can be significantly influenced by dispersion (viz., Chem. Eng. Sci., 17 (1962) pp. 245-264). This point is discussed further following a discussion of several transport mechanisms.

Because the efficiency of the NO convertor is strongly dependent upon any diffusional limitations which the chemical reactions experience, it is important to decide whether such limitations occur. To this end, a study involving the single reaction between NO and CO was done for a single catalyst particle (the rate expression (3) is reported in the appendix). The equations describing such a problem are,

$$k_s^e \frac{1}{r^2} \frac{d}{dr}\left(r^2 \frac{dT}{dr}\right) + \left(-\Delta H_{rxn}\right) \rho_s \left(1-\epsilon_p\right) \left|r_{NO}\right| = 0 \qquad (9)$$

$$\rho_f D_s^e \frac{1}{r^2} \frac{d}{dr}\left(r^2 \frac{dg^{NO}}{dr}\right) - m_{NO} \rho_s \left(1-\epsilon_p\right) \left|r_{NO}\right| = 0 \qquad (10)$$

$$\frac{dT(0)}{dr} = \frac{dg^{NO}(0)}{dr} = 0$$

$$-k_s^e \frac{dT(r)}{dr} = h_t \left(T(r) - T_{bulk}\right), \quad r=r_p$$

$$-\rho_f D_s^e \frac{dg^{NO}(r)}{dr} = \rho_f k_g^{NO} \left(g^{NO}(r) - g_{bulk}^{NO}\right), \quad r=r_p$$

The heat transfer coefficient, h_t, is calculated using a correlation analogous to eq. 5 (with the Sherwood number replaced by the Nussalt number, the Schmidt number replaced by the Prandtl number). The particle diameter is 0.3175cm, the heat of reaction is (-89, 300) cal/gm-mole reactant (see appendix), and the solid effective density, $\rho_s (1-\epsilon_p)$, is assumed to be $0.975 gm/cm^3$.

This study included the bulk fluid conditions listed in Table 2.

Table 2

Typical Bulk Fluid Conditions

case	T_{bulk} (°C)	g^{NO}_{bulk}	F(SCFM)
1	255	.000965	16.9
2	360	.001390	25
3	490	.002040	36.2
4	588	.002790	50

Baker and Doerr report these values as typical exhaust gas conditions(7). The effective thermal conductivity (27) and the mass diffusivity (26) are in the following ranges of values,

$$k^e_s = 10^{-3} \text{ to } 10^{-4} \text{ cal/cm-sec-°C}$$

$$D^e_s = 10^{-1} \text{ to } 10^{-3} \text{ cm}^2/\text{sec}$$

the values used in the calculations were 0.00090 cal/cm-sec-°C and 0.06 cm^2/sec respectively. Numerically, the pair of ordinary differential equations were solved using orthogonal collocation with one, two, or three interior collocation points. The effectiveness factor, a measure of the particle efficiency, was found to be between 0.19 and 0.65 (for the bulk fluid conditions of Table 2). Notice that these low values of the effectiveness factor occur for a relatively high value of

the effective mass diffusicity. If the effective mass diffusicity were lower, the effectiveness factor would be lower. The particle was found to be approximately isothermal with respect to the surface temperature. This was to be expected as the low reactant concentrations (ppm's) provide little exothermic heat. The temperature difference between the bulk fluid and the surface represented 80% of the total difference between the bulk fluid temperature and the center temperature (see appendix). Our dynamic model does retain the finite heat transfer resistance at the surface. As demonstrated by Crider and Foss (15), it is the particle Nussalt number (film resistance) that is responsible for a large portion of the dispersion of heat throughout the reactor during transient operation. This is found to be particularly noticeable when a cold bed is contacted by a hot gas stream. For the above steady-state calculations the total temperature differential (with respect to the particle) was only 2-4°C. In the transient operation it was found to be as much as 10-15°C. These results indicate that the differential mass balance, eq. 10, must be included in our later models while the heat balance can be simplified in ways to be discussed below.

Because of the extremely small L/D ratio required for the axial flow convertor, an examination was made to determine the significance of axial and radial dispersion. The importance of axial dispersion is usually enhanced at low Reynolds' numbers and small (tube length)-to-(particle diameter) ratios (here, L/dp= 15). Similarly, radial dispersion

is usually enhanced at low Reynolds' numbers and small (tube radius)-to-(particle diameter) ratios (here, $R_t/d_p = 88$ is large). The Reynolds' numbers of interest are between 30 and 90.

To examine these effects we considered the following three models.

fluid transport	NO-component balance
bulk flow	$G \frac{dg^{NO}}{dz} = \rho'_s (1 - \epsilon) \lvert r_{NO} \rvert$
bulk flow with axial dispersion	$G \frac{dg^{NO}}{dz} = \rho_f D_z^e \frac{d^2 g^{NO}}{dz^2} + \rho'_s (1 - \epsilon) \lvert r_{NO} \rvert$
bulk flow with radial dispersion	$G \frac{\partial g^{NO}}{\partial z} = \rho_f D_r^e \frac{1}{r} \frac{\partial}{\partial r} \left(r \frac{\partial g^{NO}}{\partial r}\right) + \rho'_s (1-\epsilon) \lvert r_{NO} \rvert$

ρ'_s is the solid effective density. We have assumed that the chemical reaction between NO and CO occurs homogeneously in the bulk fluid This is tantamount to assuming that the effectiveness factor is unity and that the mass transfer resistance is negligible. When these equations are non-dimensionalized (along with the respective heat balance), one finds that the coefficients for the dispersion terms depend on the Peclet numbers. We have studied these models using the data of Table 2 as the inlet conditions to the convertor (with radial and axial Peclet numbers of 10.0 and 2.0 unless specified otherwise). We have assumed a linearly decreasing wall temperature where the wall temperature at $z = 0.0$ matches the inlet bulk fluid temperature and has a slope of

of (-3.5°C/inch). This particular dependence of the wall temperature was extracted from the data reported by Baker and Doerr (7). In the 'bulk flow' and 'bulk flow with axial dispersion' models, the differential heat balance then includes a volumetric heat-loss term defined using an overall heat transfer coefficient.

$$\text{heat-loss per unit volume} = \frac{h_{ot}}{R_t/2} (T_{wall} - T)$$

An overall heat transfer coefficient includes the effects of the effective thermal conductivity in the core of the convertor and the film coefficient at the wall. The film coefficient, h_t, is calculated from a correlation (see appendix). The overall coefficient, h_{ot}, is calculated from the following approximation (see appendix):

$$\frac{1}{h_{ot}} = \frac{1}{h_t} + \frac{R_t}{4k_r^e}$$

See the appendix for values of k_r^e, the effective radial thermal conductivity, and how they may be estimated. The radial dispersion model has a heat-flux boundary condition at the wall which involves the film coefficient, h_t.

These models are studied numerically for identical operating conditions (see Table 2). For the nitric oxide concentrations of interest (900-2600 ppm), the temperature profiles are of minimal interest. The axial temperature differential was between 20°C and 45°C while radially it was between 6°C and 18°C. These radial temperature variations

cause less than a 3% difference in g^{NO} between the wall and the center of the tube. By considering figs. 2 and 3, one then concludes that radial dispersion has an insignificant influence on the conversion of nitric oxide. The radial temperature variations are just not large enough to greatly influence the rate of reaction, and this is what couples the temperature and concentration functions. Figs. 2 and 3 do exhibit "mixing losses" (23) in the first 20% of the reactor, but even this effect is small. Tentatively, it would appear that the axial dispersion has a negligible influence. This is verified by the following additional calculations.

Additional calculations were performed with various axial mass Peclet numbers and catalyst densities, $\rho'_s (1 - \epsilon)$. As the axial mass Peclet number increases from 1.0 to 3.0, the exit conversion improves, also see fig. 4,

Pe_z^m	g^{NO} (z = 1.0)
1.0	.000085
2.0	.000059
3.0	.000050

The inlet mass faction for this example is .00434. Since the improved conversion involves the last 1-2% of the total nitric oxide it is insignificant. The point to recognize is that the resultant conversion is little different than that obtained with the bulk flow model. By increasing the catalyst density, we found that the volumetric rate of reaction

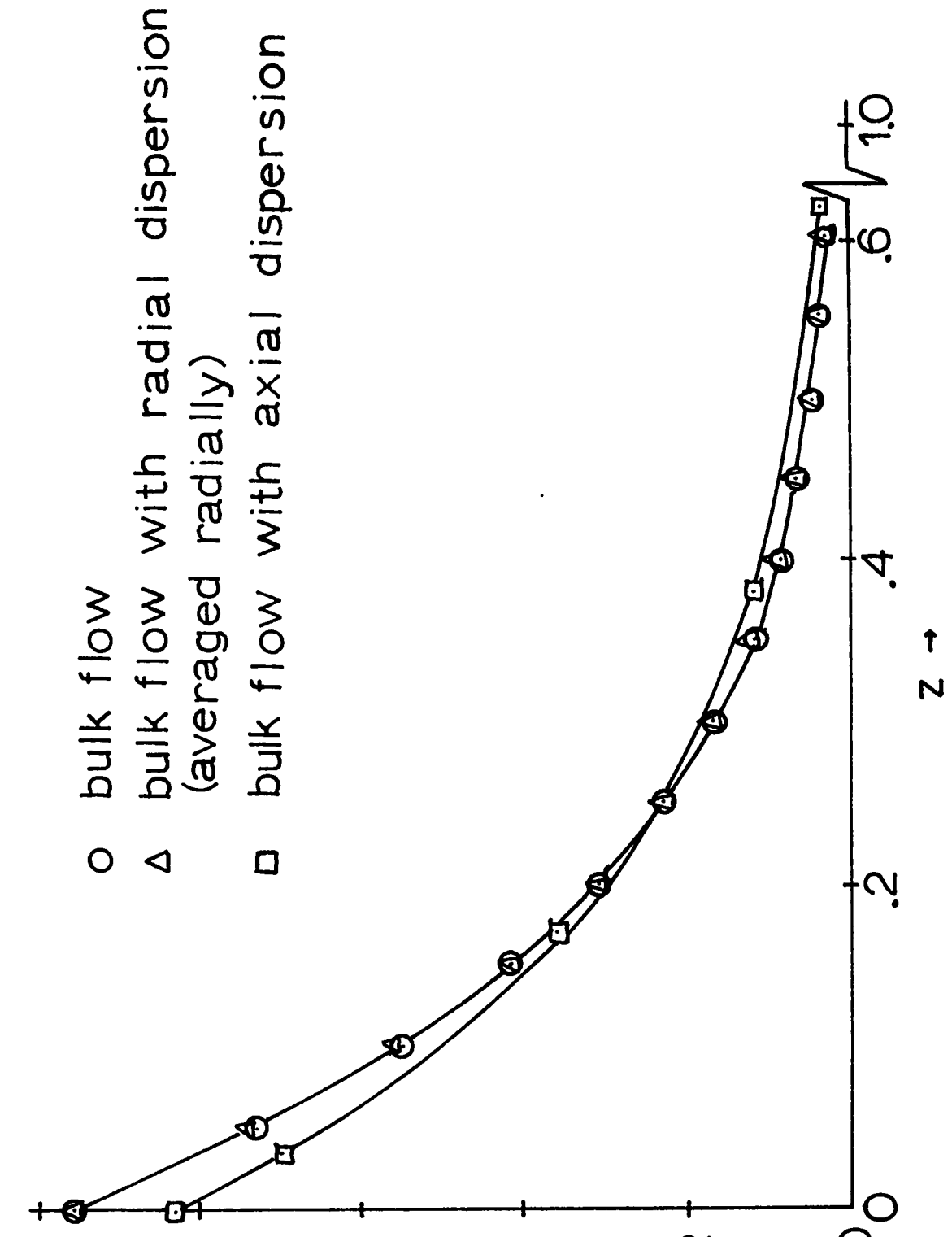

Figure 2. Mass fraction (NO) vs. axial position (Case 1 of Table 2) - Re=31.

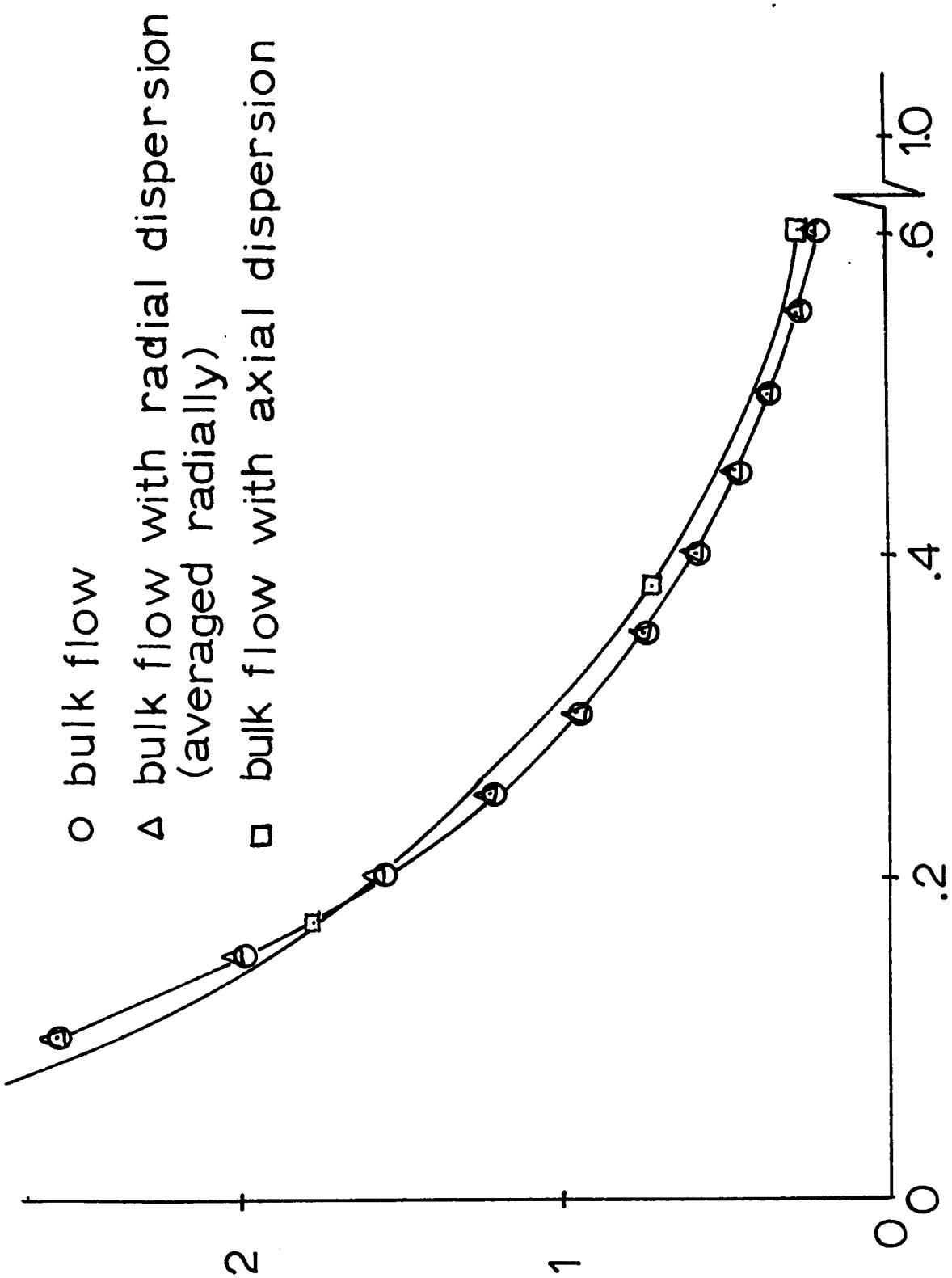

Figure 3. Mass fraction (NO) vs. axial position (case 4 of Table 2) - Re = 87.

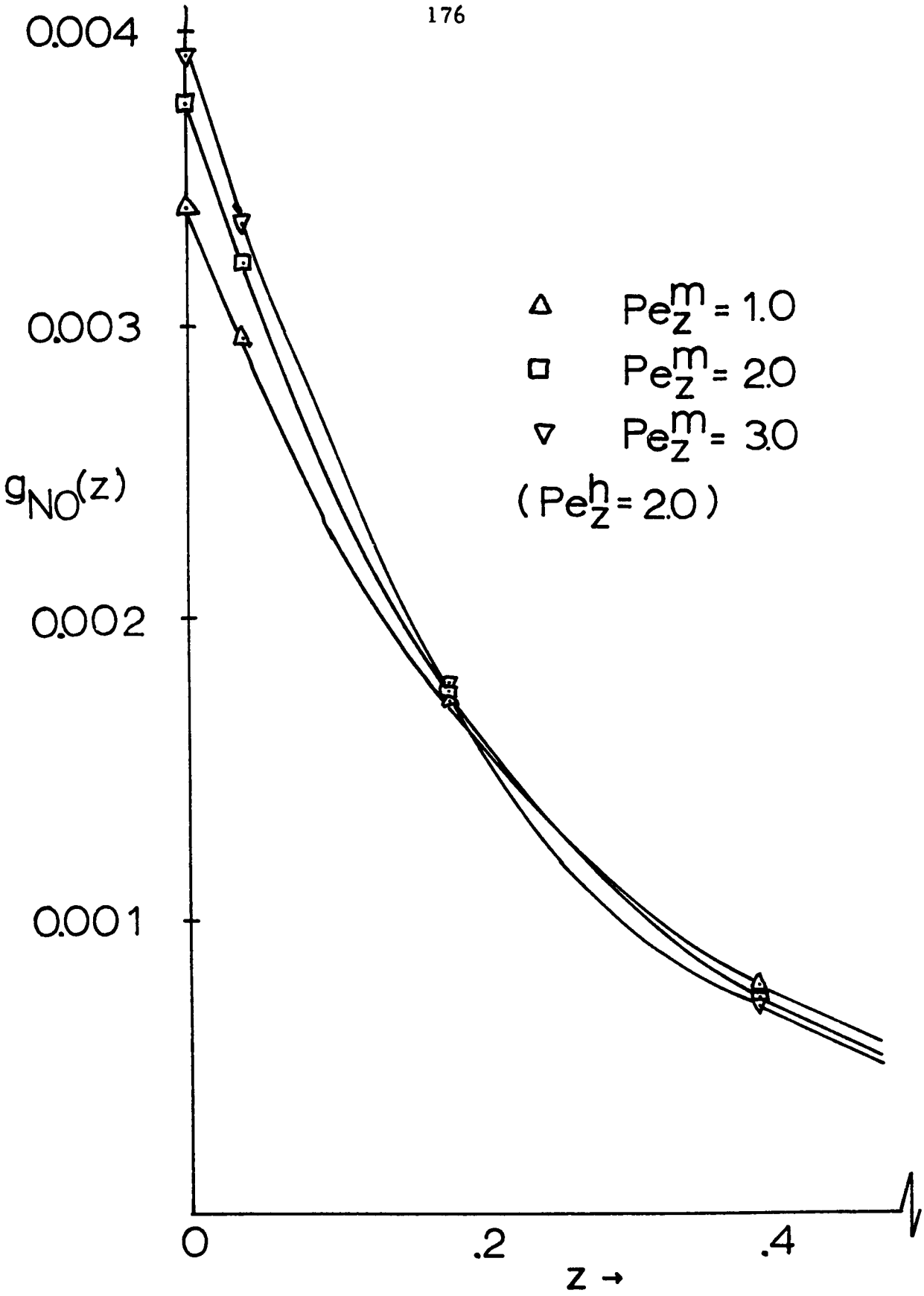

Figure 4. Mass fraction (NO) vs. axial position for 'bulk flow with axial dispersion' model (P_z^e = 2.0) (Case 4 of Table 2)-Re = 87.

increases—the rate of reaction is gm-moles NO/gm-catalyst-minute, so this result is not surprising.

$\rho_s' (1 - \epsilon)$	$g^{NO} (z = .619)$
.75	.00045
.975	.00026
1.461	.00008

All of the results indicate that neither radial or axial dispersion is important. Because of this conclusion, the transient analysis was done using the simpler one-dimensional mixing-cell model. Kuo et al. (21) found that the mixing-cell model represented their experimental data quite well for a carbon monoxide convertor similar to the one of interest here.

4. The Transient Operation of the NO_x Convertor

The nitric oxide convertor encounters inlet conditions which are quite unusual. Industrial packed-bed reactors are designed to handle a given inlet stream and to provide a specified product. The automotive NO_x convertor must be able to handle an inlet stream that varies in temperature from ambient to 1500°F and in composition from 200 to 3500 ppm by volume NO. It must cope with start-up problems daily. The volumetric flow rate varies from zero to 150 SCFM. Additionally, these variations in temperature, composition, and volumetric flow rate occur in no predetermined way. According to Bauerle and Nobe (9), the

variations in composition present one of the most significant problems in the use of catalysts for pollution control.

To analyze such a NO_x convertor, one must know how the exhaust temperature, volumetric flow rate, and composition vary with time. These data have been measured and reported (7, 10, 21) for an operating mode referred to as the Federal Test Procedure (FTP). Due to heat losses throughout the exhaust system, the exhaust temperature actually varies with position in the system—the gas temperatures near the exhaust manifold are considerably hotter than those near the muffler (37). Vardi and Biller (37) studied the thermal response of a packed-bed under the thermal loading conditions of the FTP. They did not include the chemical reactions to be considered here. Their work, both experimental and theoretical, indicates that the thermal inertia of the packing may mean several minutes of heating before the catalyst temperature reaches 500°F. If this is true, then the convertor should be insulated such that the energy contained in the exhaust gases goes directly into heating the catalyst particles. Let us now consider the thermal response for a chemically reacting system.

We previously indicated that the transient analysis would utilize a simple, one-dimensional mixing-cell model. (See appendix for solution of $u_t + u_x = au_{xx}$) Kuo et al. (21) used this model to investigate an automotive carbon monoxide convertor operating under the FTP. Such a model is simply a series of continuous flow, well-stirred tank

reactors. In each mixing-cell (stirred tank), one must consider the additional problem presented by the catalytic reactions,

$$NO + CO \rightleftharpoons CO_2 + \tfrac{1}{2}N_2$$

$$NO + H_2 \rightleftharpoons H_2O + \tfrac{1}{2}N_2$$

Since all particles within a cell experience identical boundary conditions (the bulk fluid temperature and mass fraction within the $i^{\underline{th}}$ cell), we need only consider one catalyst particle for each cell in order to determine the total conversion for the cell. The overall rate expressions for these two reactions are given in the appendix.

In the following, we investigate the heat and mass balances necessary to describe the transient response of the i^{th} mixing-cell. Let us briefly consider the assumptions used to obtain these balances. We consider a series of N equi-volume mixing cells. Each cell is assumed to be adiabatic. Due to heat transfer to and from the solid packing within each cell, the bulk stream temperature differs from one cell to the next. As a simplifying assumption, all physical properties are evaluated (for a given instant in time) for the temperature at the inlet to the convertor. The heat capacity and the mass average molecular weight of the bulk-stream-gas are nearly constant. We assume that the fluid heat capacity is 0.270 cal/(gm-mole °C) and that the average molecular weight is 28 gms/gm-mole. The chemical reactions produce a decrease in the total number of moles and this produces a very small

change in the volumetric flow rate which has been neglected. For a fixed time, the volumetric flow rate is assumed constant throughout the convertor. We are now in a position to state the cell balances.

In writing the cell balances, we incorporate the assumptions of several other authors. As explained by Brian et al. (11), the accumulation of mass is neglected because of the small residence time of the gas in the void space. Similarly, the thermal response of the void space is so much faster than the solid catalyst that the accumulation of enthalpy can be neglected in the void space (22). The enthalpy and mass balances are then

$$G \bar{m} c_f T^g_{i-1} = G \bar{m} c_f T^g_i + \frac{6}{d_p} (1 - \epsilon) V_i h_{ot} (T^g_i - T^s_i) \qquad (11)$$

(heat in) = (heat out) $\qquad (i=1, \ldots N)$

$$\text{and} \quad G \bar{m} g^{NO}_{i-1} = G \bar{m} g^{NO}_i + \rho'_s (1 - \epsilon) V_i m_{NO} \left(\sum_{j=1}^{2} \alpha_{NO,j} \langle |r_j| \rangle_i\right) \qquad (12)$$

(mass in) = (mass out) $\qquad (i=1, \ldots, N)$

$$\langle |r_j| \rangle_i = \frac{3}{R_p^3} \int_o^{R_p} |r_j(T^s_i, g^{NO}_{i,p}, g^{CO}_{i,p}, \ldots)| \, r^2 dr \,, \quad i=1 \ldots, N$$

In the cell heat balance, eq. 11, the change in the heat content of the fluid is matched by the heat transfer to the solid phase. In the cell mass balance, eq. 12, the change in the NO concentration in the bulk fluid is matched by the changes due to the catalytic reactions in the particles.

In the cell balances, eqs. 11 and 12, the first of the N equations would involve inlet temperature, T_0^g, and the inlet mass fractions, g_0^{NO}, g_0^{CO}, and $g_0^{H_2}$. For the numerical investigations, the inlet temperature and volumetric flow rate (related to the mass flux, G), figs. 5 and 6, are from Kuo et al. (21) and the inlet mass fractions for NO and CO, figs. 7 and 8, from Bernstein et al. (10), but are for a hot cycle. We use this data for hot and cold cycles. When an engine is started cold, the inlet carbon monoxide concentration is extremely high because of the low A/F ratio and the NO is low (24). If our inlet data is averaged in accordance with the FTP, we find that the CO concentration is 1.5% by volume and the NO concentration is 850 ppm by volume. In comparing the temperature data of Kuo et al. (21) with that of Vardi and Biller (37), it appears that Kuo et al. have considered a convertor located near the muffler. The hydrogen concentration is difficult to measure under the dynamic conditions of the FTP (21), but can as shown in the appendix be approximated by the following simple relation:

$$g^{H_2} = g^{CO} / 3.8$$

In the following, we investigate the heat and mass balances necessary to describe the transient response of the catalyst particles in the i^{th} mixing-cell. By assuming that the bulk fluid in the i^{th} cell is well-mixed, we need only consider a single particle. The chemical reactions occur within the particle (in a distributed fashion, similar

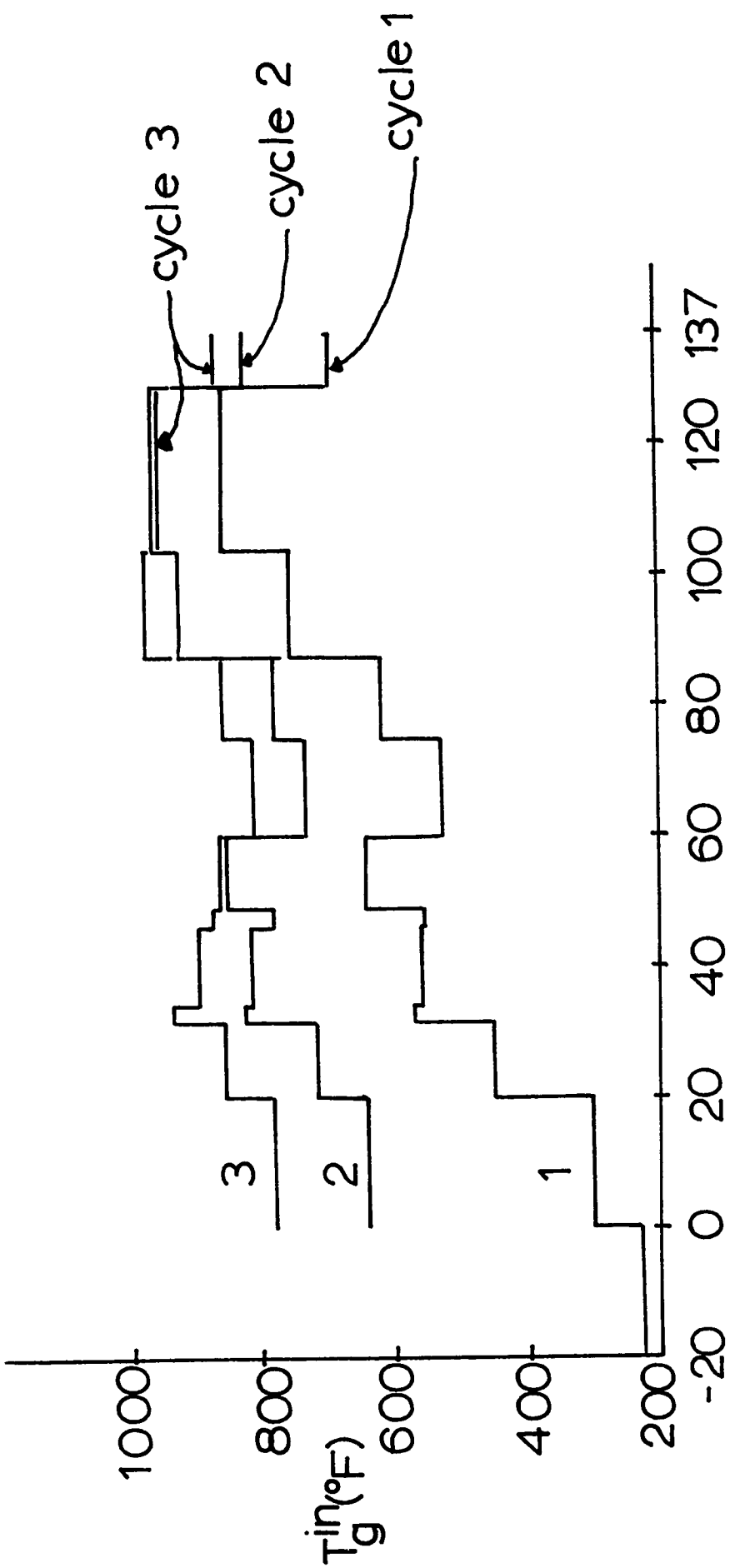

Figure 5. Inlet gas temperature to the convertor versus operating time.

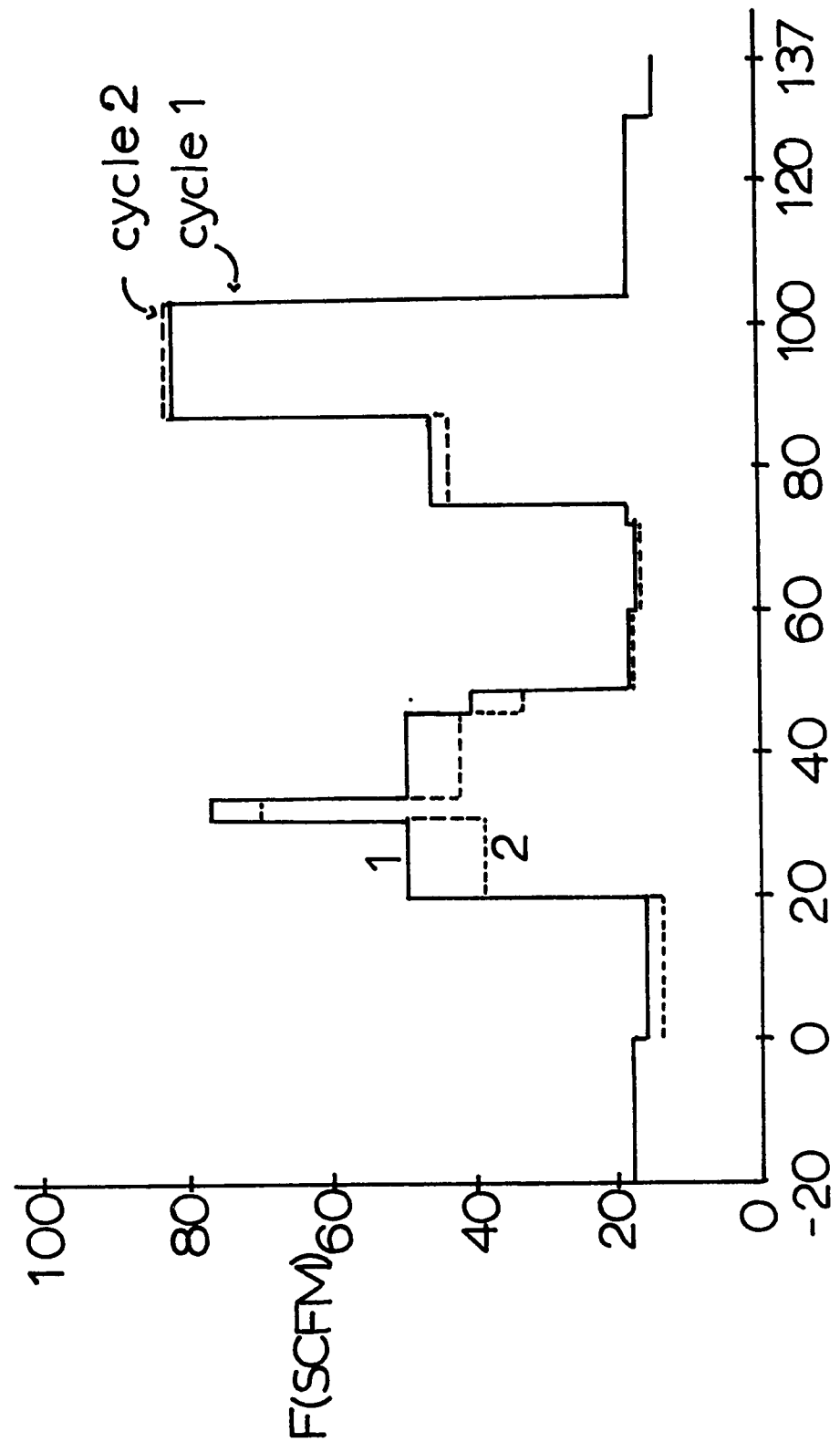

Figure 6. Inlet volumetric flow rate to the convertor versus operating time.

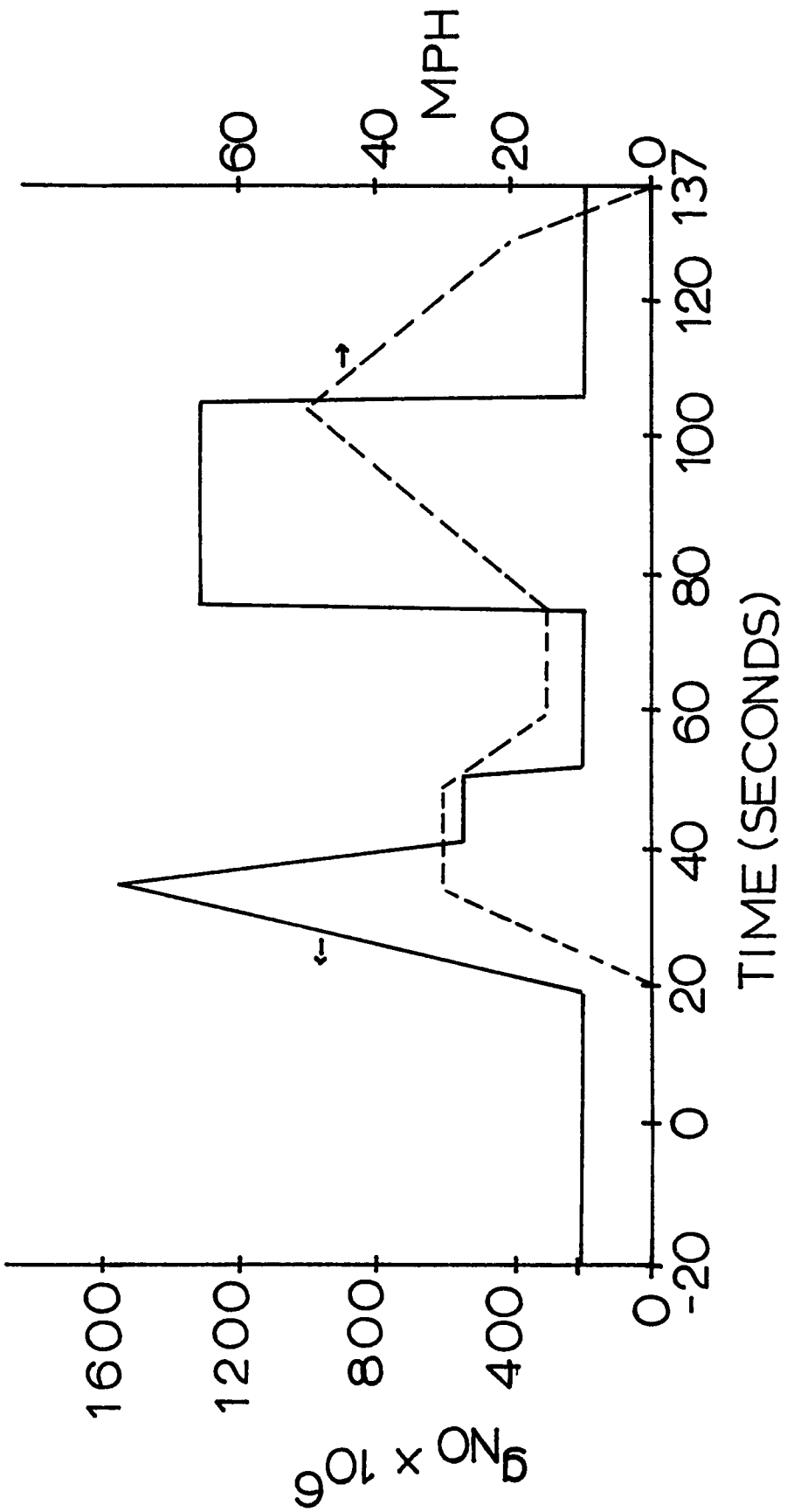

Figure 7. Inlet nitric oxide mass fraction to the convertor versus operating time.

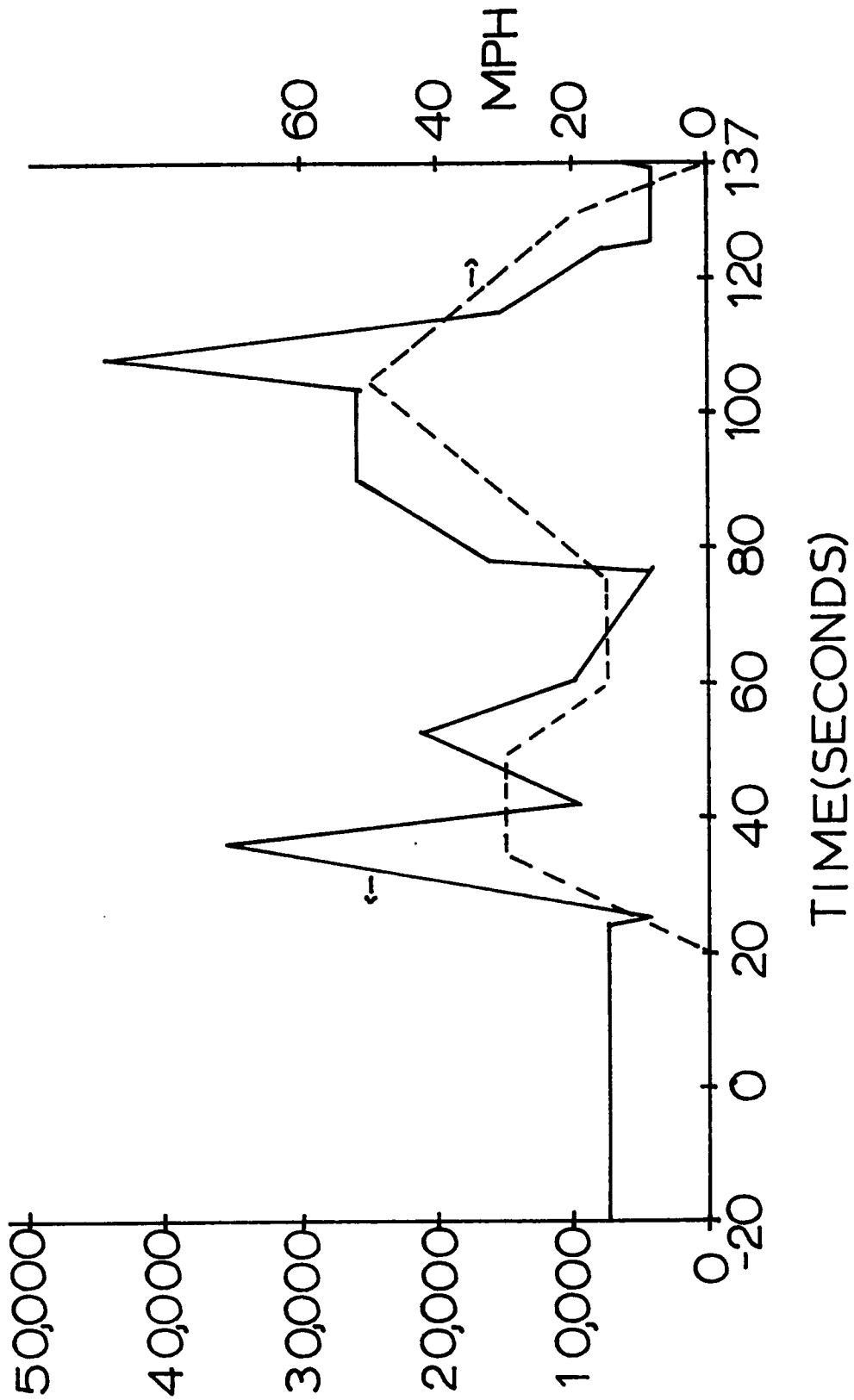

Figure 8. Inlet carbon monoxide mass fraction to the convertor versus operating time.

to eq. 10). The particle effective diffusivity is assumed constant. The heats of reaction are only mildly temperature dependent (refer to appendix) and are taken to be the following constants:

$$\Delta H_{NO+CO} = -89,300 \text{ cal/gm-mole NO}$$

$$\Delta H_{NO+H_2} = -80,500 \text{ cal/gm-mole NO}$$

In obtaining the balance equations, we have considered the results of our preliminary study and those of McGreavy and Thornton (22).

Earlier, we concluded that the catalyst particle was isothermal with respect to the surface temperature under steady-state conditions. For the transient analysis we have assumed that the particle is isothermal with respect to the surface temperature which is a function of time.

$$\rho_s c_s \frac{dT_i^s}{dt} = \frac{6 h_{ot}}{d_p} T_i^g - \left(\frac{6 h_{ot}}{d_p}\right) T_i^s - \sum_{j=1}^{2} (-\Delta H_j) \langle |r_j| \rangle_i \quad (13)$$

(accumulation) = (heat in) - (heat out)

The catalyst temperature is coupled to the bulk fluid temperature through the heat transfer mechanism at the catalyst surface. The overall heat transfer coefficient has been discussed previously. The mass balance for the catalyst particle is similar to eq. 10, that is

$$\rho_f D_s^e \frac{1}{r^2} \frac{\partial}{\partial r} \left(r^2 \frac{\partial g_{i,p}^{NO}}{\partial r}\right) + m_{NO} \sum_{j=1}^{2} \alpha_{NO,j} |r_j| = 0 \qquad (14)$$

with a similar equation for the concentration of carbon monoxide. We have assumed tha the transient response to mass changes is much faster than the response to thermal changes (22). The particle species balance (eq. 14) is coupled to the cell balance (eq. 12) by a boundary condition at the catalyst surface,

$$\rho_f D_s^e \frac{\partial g_{i,p}^{NO}}{\partial r}\Big|_{r=R_p} = \rho_f k_g^{NO} (g_i^{NO}(t) - g_{i,p}^{NO}(R_p, t) \qquad (15)$$

Notice that the NO species balance for the mixing-cell, eq. 12, can be used to replace the boundary condition given by eq. 15 by a nonlinear, integral boundary condition. Assuming that g_{i-1}^{NO}, eq. 12, is known, one sees that $g_i^{NO}(t)$ depends on a nonlinear integral involving $g_{i,p}^{NO}(r,t)$ and $T_i^s(t)$. A little more detail of the overall model is presented in the appendix.

Numerically, we have to solve eqs. 11 through 15 for the cell concentrations, the cell temperature, the solid temperature, and the solid phase concentrations. We use orthogonal collocation to handle eqs. 14 and 15 (and similar equations for the CO balances in the catalyst phase). Let us consider the steps involved in advancing the solutions from t to $t + \Delta t$. We start at the inlet to the convertor where the inlet

conditions are specified functions of time. Based on the old values (at 't'), we predict a new value of T_1^s $(t + \Delta t)$ using the predictor of the improved Euler method for eq. 13.* This predicted value allows the calculation of a corresponding new value for T_1^g $(t + \Delta t)$ using eq. 11. Eq. 12 is used to reduce eqs. 14 and 15 to a problem with a nonlinear boundary condition. Orthogonal collocation reduces this problem then to a system of (n+1) nonlinear algebraic equations where (n) is the number of interior collocation points. With the predicted T_1^s $(t + \Delta t)$, one can then solve for the mass fraction profile within the catalyst particle of the 1^{st} mixing-cell. At this point, one has the requisite numbers to calculate the corrected value of T_1^s $(t + \Delta t)$ (of the improved Euler scheme). Having finished with the first cell, one can proceed to the second. This is repeated through the N^{th} cell. The old values are always saved for the prediction of the new values as we march the solution out in time—$(t + j\,\Delta t)$. As prescribed by the FTP, we must solve these equations for a total of 979 seconds (20 seconds of warm-up followed by 7 cycles of 137 seconds each. We have used a variable step length. For 4 mixing-cells, the total computation time is about $2\frac{1}{2}$ minutes (using three interior collocation points). A computer

---

*It is necessary to include changes in G, h_{ot}, ρ_f, and k_g^{NO} produced by the variation with time of the inlet volumetric flow rate, and the inlet gas temperature. In calculating ρ_f we have assumed the validity of the ideal gas law. The transfer coefficients are calculated from correlations due to Thoenes and Kramer (36) (assuming Pr=0.77 and Sc=0.71).

listing for this program is provided in the appendix.

We have indicated the model for the NO convertor and how it is meant to be used. Let us know consider several specific applications. These enable us to recognize the important variables and the significant difficulties.

Table 3 is a list of values for the designated parameters which have been used for all of the following applications.

Table 3

Fixed Parameter Values

d_p = 0.32cm	V_{total} = 2832 cm^3 (or 0.1 ft^3)
ϵ = 0.35	P_{total} = 1 atm
ϵ_p = 0.45	Sc = 0.71
P_r = 0.77	R_t = 13.97 cms
$\bar{m}$ = 28 gms/gm-mole	$T_i^s(0)$ = 27 °C
k_s^e = 0.00090 cal/(cm-sec-°C)	$T_i^g(0)$ = 27 °C
c_f = 0.27 cal/(gm-°C)	

In addition to these fixed values (Table 3) there are three other parameters of interest: particle effective diffusivity, solid heat capacity, and catalyst density. For these parameter we have investigated three different choices, which correspond to different degrees of difficulty in removing the nitric oxide and are summarized in Table 4.

Table 4

Parameter Values Investigated

	Case A (more favorable)	Case B (standard)	Case C (less favorable)
D_s^e =	0.06 cm^2/sec	0.017 cm^2/sec	0.001 cm^2/sec
c_s =	0.18 cal/(gm-°C)	0.26 cal/(gm-°C)	0.26 cal/(gm-°C)
ρ'_s =	1.5 gms/cm^3	2.9 gm/cm^3	2.9 gms/cm^3

Case A represents a convertor with a thermal inertia which is roughly $\frac{1}{3}$ that of Case B (the standard case). The solid catalyst of Case A should heat up faster than Case B and produce better conversion for short times. When the bed is sufficiently hot, Case B would produce better conversion of NO because of the greater density. Case C (in which the diffusivity approximates that of a micro-porous catalyst rather than a macro-porous catalyst as for Cases A and B) should take as long as Case B to heat up but have lower conversions because of the additional resistance to interparticle mass transport—the diffusivity.

The initial investigation of the nitric oxide conversion involved Case B. Using the inlet conditions from Figures 5-8, one finds the transient responses in T_2^s and g_4^{NO} (for a model with 4 mixing-cells) as given in figs. 9 and 10. This mass fraction represents the exit concentration. The temperature response of the first cell is slightly faster while the response of the third and fourth cells is rather slow. While

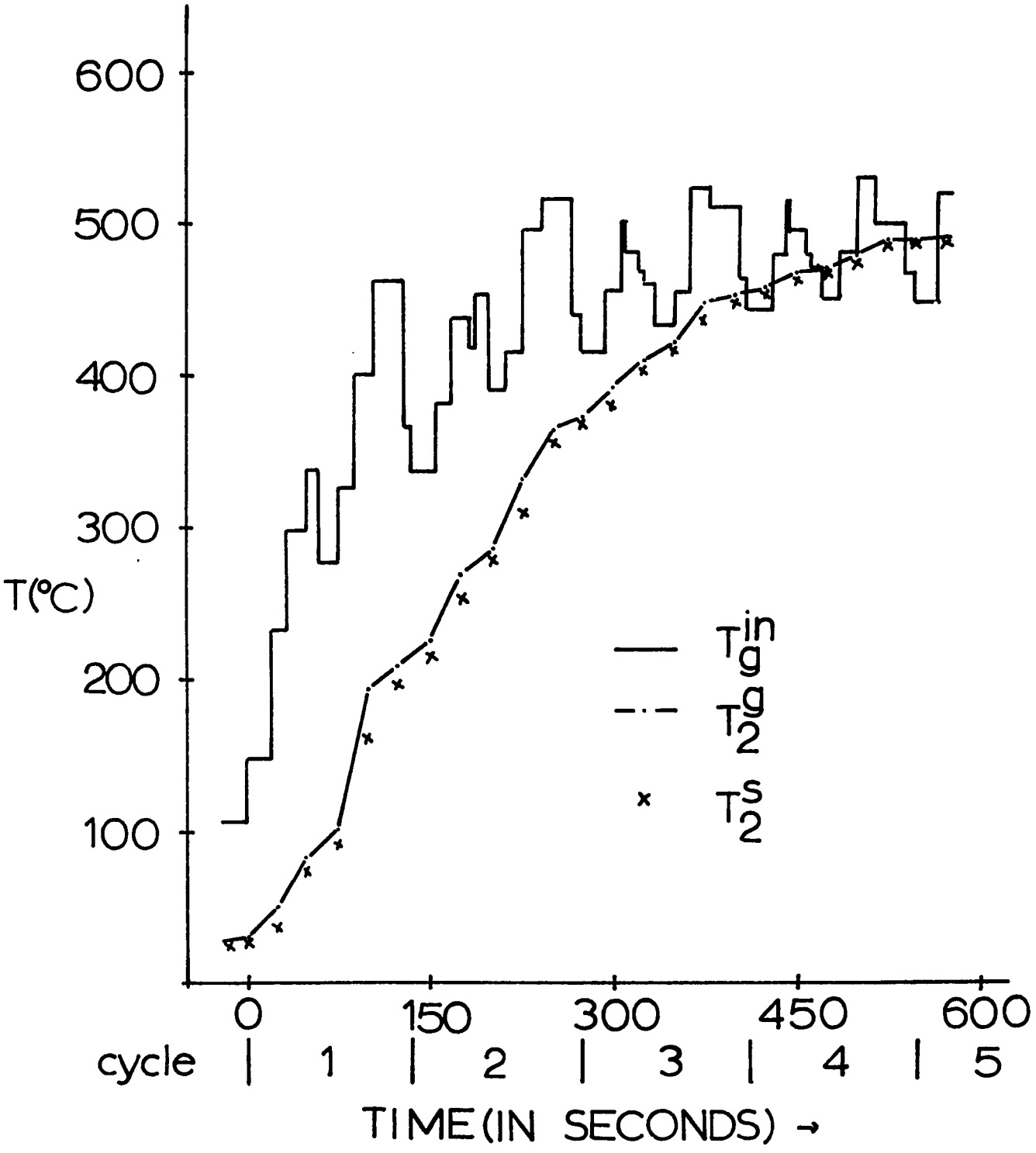

Figure 9. Gas-solid temperatures versus operating time. (Case B of Table 4, second mixing cell of four).

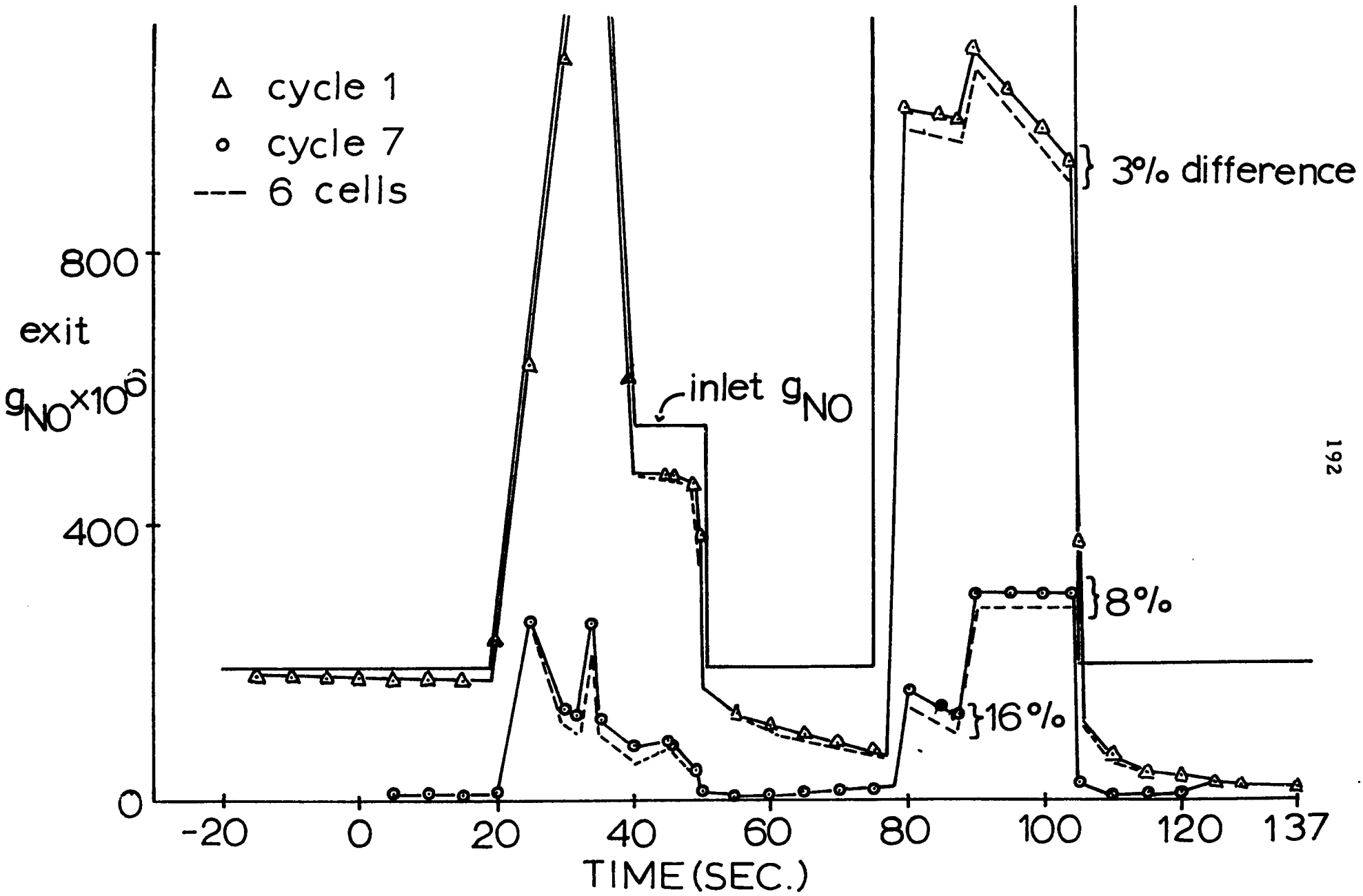

Figure 10. Outlet nitric oxide mass fraction versus operating time. (Cases A and B of Table 4, first mixing cell of four).

the second cell requires roughly 200 seconds to heat up to 300°C, the fourth cell requires roughly 400 seconds. During the first cycle of the FTP, the reaction between NO and H_2 contributes nothing to the conversion of NO while during the seventh and final cycle, this reaction removes between 2 and 9% of the NO. Several conclusions can be drawn from Case B. First, the bed heats up slowly; consequently, the initial conversion is quite low whereas the hot cycle conversion is better. As shown in fig. 10, this model is relatively insensitive to the number of mixing-cells employed (4 cells versus 6 cells) in the model.

It is reasonable to investigate a more favorable set of parameters (Case A) and a less favorable set (Case C). The amount of variability chosen for c_s, ρ'_s, D_s^e is typical of the difference between a supported and an unsupported catalyst (26). For Case C, the conversion was found to be about 30% lower than in Case B. Correspondingly, the lower conversion of NO provides less exothermic heat of reaction, but this never lowers the solid temperature by more than 0.6°C from the standard case (Case B). If we compare the conversion for Case C with that for Case B over the FTP, we find that Case C provides consistently lower conversion (see Table 5) for all times.

Table 5

Instantaneous Percentage Decrease in Conversion for Case C As Compared to Case B

Instantaneous percentage decrease	time (seconds)
5.2%	60
11.4	120
42.1	182
33.3	242
25.0	480
21.4	602
28.2	867
21.2	888
20.5	922
13.0	947

For long times we find that the conversion is roughly 20% lower than for Case B. These results are consistent with what is known about the relation between catalyst efficiency and the interparticle diffusion coefficient (26). As the diffusivity decreases, the effectiveness factor decreases such that the reactor conversion would decrease.

Alternatively, Case A assumes a larger particle effective diffusivity. While the diffusivity of Case A should present an improvement in the NO conversion as compared with Case B, this would only be true for identical solid temperatures. As mentioned previously, a trade-off has been made in selecting Case A. The packed-bed heats up faster for Case A since ρ_s' is smaller—the same amount of energy raises the

temperature of the solid faster for a given length of time. On the other hand, by decreasing ρ'_s, the rate of conversion of NO per unit reactor volume for a fixed temperature is lowered. This trade-off is demonstrated in Table 6 where we show the exit concentration as a function of time for Case A and Case B. For times less than 4 minutes, Case A does provide markedly improved conversion. Table 6 also shows that Case A provides poorer conversion for times longer than 4 minutes. The poorer conversion may be acceptable if the improvement for short times is significant enough to enhance the time average exit conversion over the entire FTP.

Table 6

Instantaneous Exit NO Concentrations for Case A And Case B During the FTP

(seconds)	g^{NO}_{inlet}	g^{NO}_4 (Case A)	g^{NO}_4 (Case B)
60	.000672	.000480	.000615
120	.001307	.000553	.000974
182	.000690	.000146	.000178
242	.001307	.000192	.000321
480	.000546	.000066	.000040
602	.001466	.000368	.000262
867	.000690	.000257	.000259
888	.000546	.000102	.000079
922	.001307	.000214	.000156
947	.001307	.000042	.000022

The different heating capabilities of the two cases are demonstrated in Figs. 11 and 12. For the first mixing-cell (of four), Case A allows the solid catalyst to heat up to 300°C in about 105 seconds while the standard case requires about 140 seconds. Further, the first three mixing-cells in Case A exceed 300°C in about 140 seconds while the standard case requires about 310 seconds. These facts show that a best choice of ρ'_s should minimize the thermal inertial while maximizing the conversion of NO.

It is worth repeating that the interest in this convertor is on the removal of nitric oxide. Any unconverted carbon monoxide would, in practice, be converted in a second packed-bed reactor—along with any HC in the exhaust. Due to the recorded differences in the level of NO and CO in exhaust emissions (17) for different automobiles of the same engine type, the following extremes have been investigated to show how the level of control varies:

CO (volume %)	NO (ppm by volume)
4.3	450
1.3	2880

The standard parameters of Case B are retained,

$$\rho'_s = 2.9 \text{ gms/cm}^3, \quad c_s = 0.26 \text{ cal/(gm-°C)}, \quad \text{and}$$

$$D_s^e = 0.017 \text{ cm}^2/\text{sec}$$

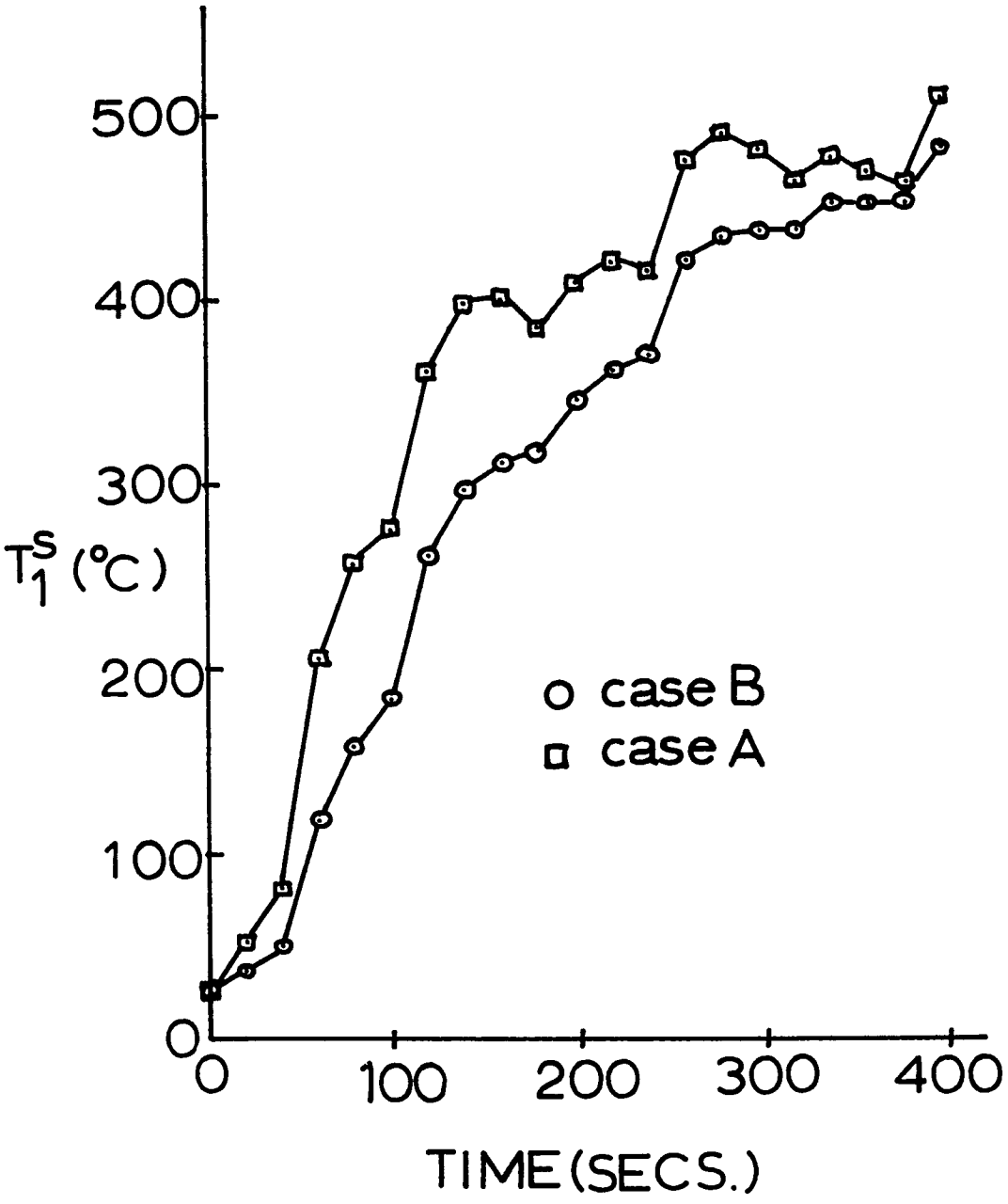

Figure 11. Solid temperature versus operating time. (Cases A and B of Table 4, first mixing cell of four).

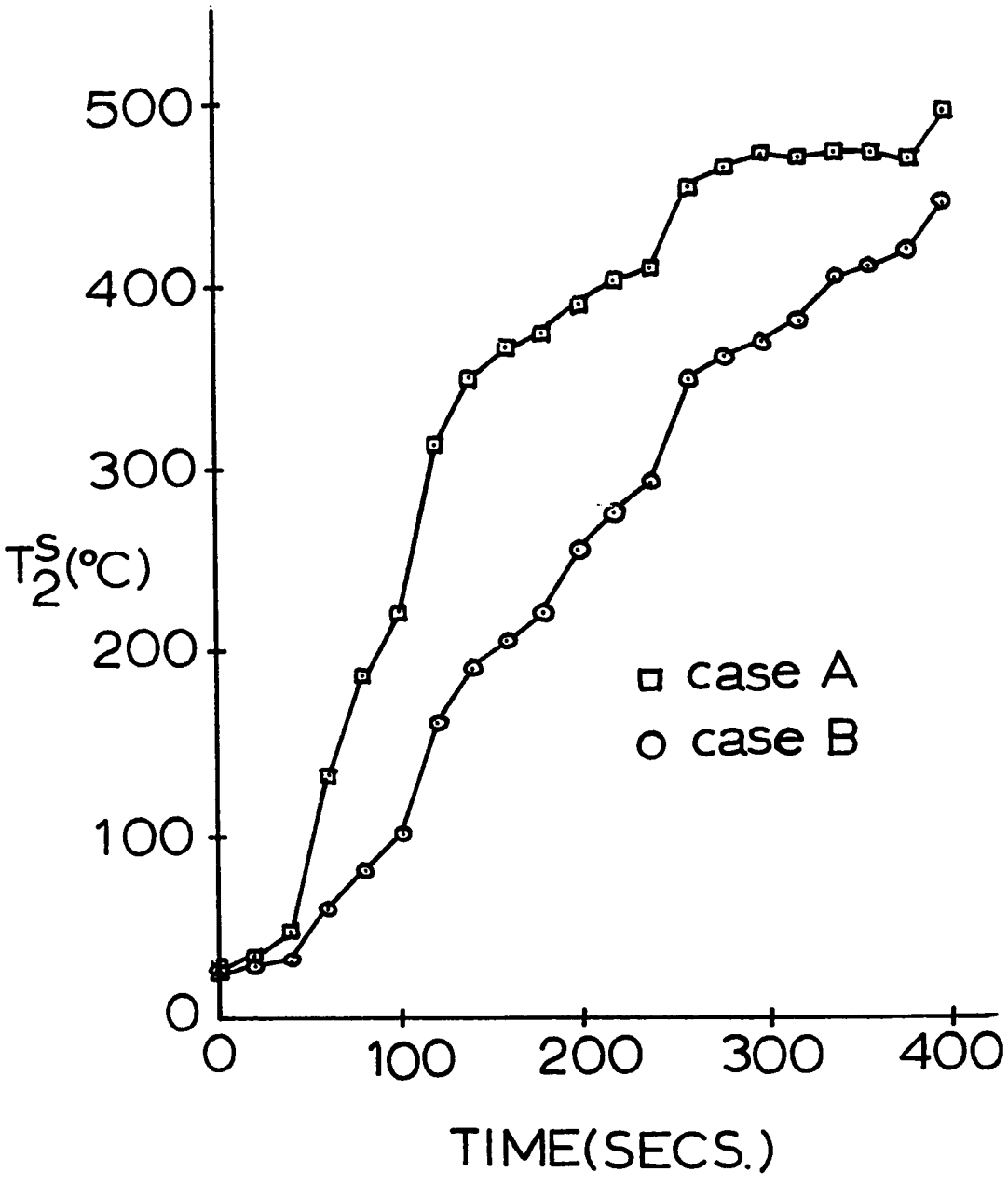

Figure 12. Solid temperature versus operating time. (Cases A and B of Table 4, second mixing cell of four).

and the inlet concentrations are obtained by scaling up or down those previously used (CO of 1.5 volume % and NO of 850 ppm by volume).

The results for these various inlet concentrations, figs. 13 and 14, show clearly that this convertor is unable to successfully control the higher NO_x emissions. Although the percent reduction of NO is relatively constant for all three levels of exhaust emissions, the absolute levels are markedly different,

Inlet NO	Outlet NO (seventh cycle)
450 ppm	75-100 ppm
850	200-250
2880	750-850

Judging by the proposed 1975 standard for NO_x emissions of 225 ppm (over a weighted average of all seven cycles, not just the seventh cycle), the untreated exhaust should have less than 1000 ppm NO_x. This is an obtainable goal but experience (17) shows that more rigid control of individuals and their automobiles may be required.

Let us consider the recommendations which can be drawn from the NO convertor analysis. A truly successful solution to the pollution control problem requires good conversion of the nitric oxide beginning with the first test cycle, not just in the seventh cycle. Because of this the convertor should be placed closer to the exhaust manifold: higher gas temperatures then heat the catalyst more quickly. The analysis shows that a catalyst with a relatively large particle effective diffusivity

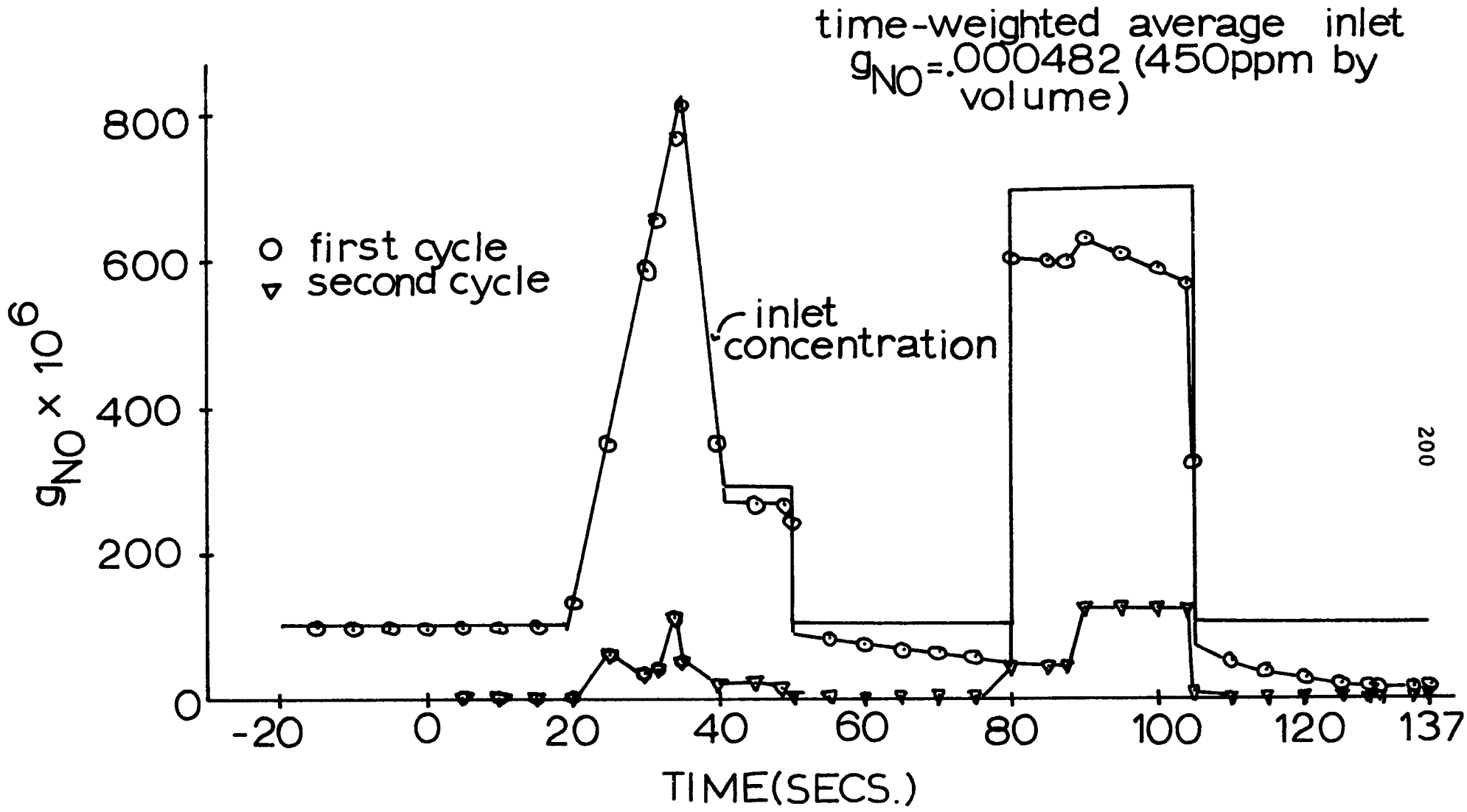

Figure 13. Outlet nitric oxide mass fraction versus operating time. (Low inlet concentrations of nitric oxide).

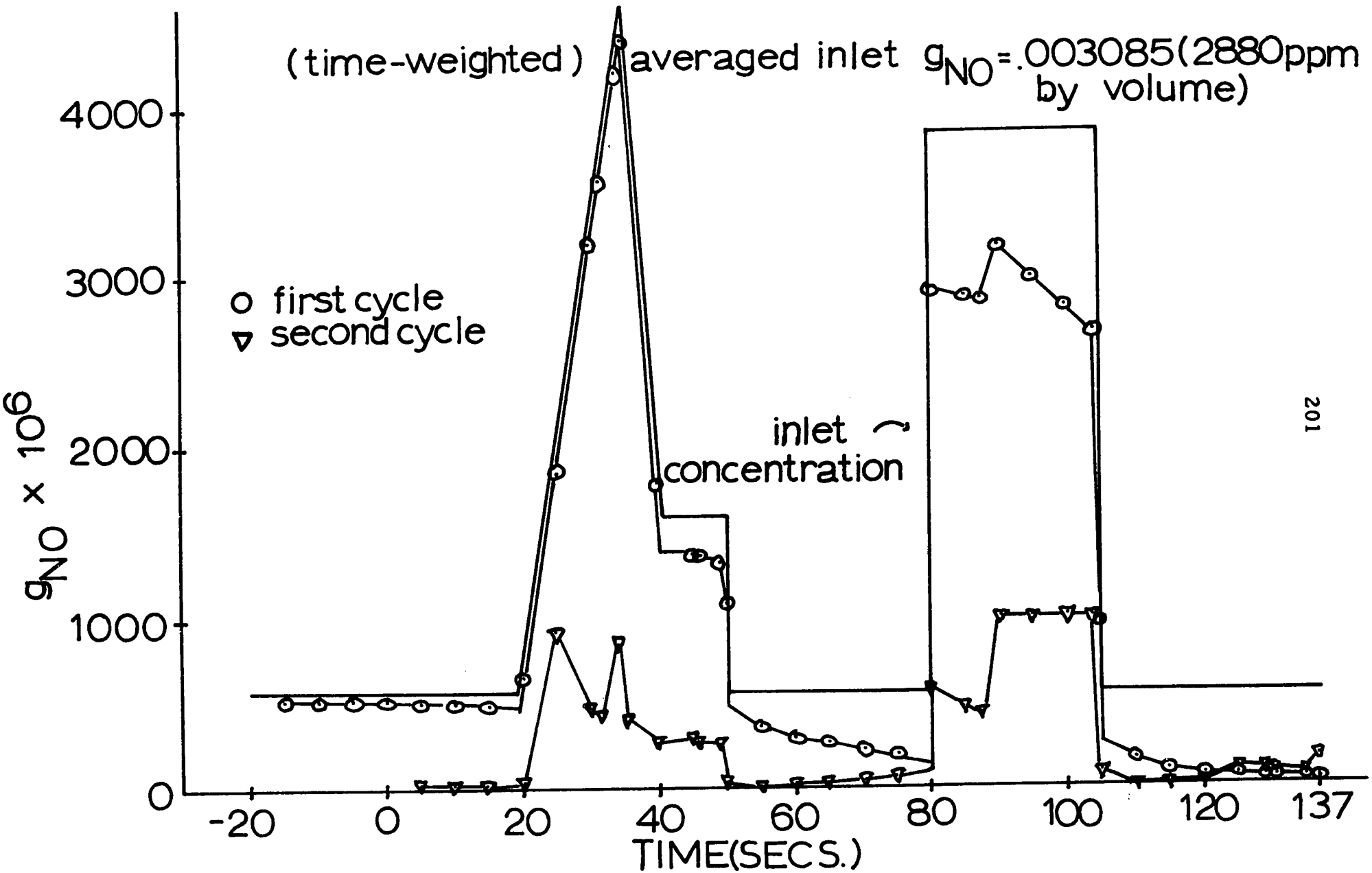

Figure 14. Outlet nitric oxide mass fraction versus operating time. (High inlet concentrations of nitric oxide).

should be used. Good conversion over the entire Federal Test Procedure requires a compromise between a small solid thermal-inertia ($\rho'_s c_s$) for quick heating and a high solid density (ρ'_s) for a high volumetric rate-of-conversion. Additionally, the time average NO concentration of the untreated exhaust gas should be limited to about 1000 ppm. and this seems to be technologically feasible. Conversion of 80% of 1000 ppm NO would satisfy the proposed 1975 standard (225 ppm) while conversion of 80% of 3000 ppm would not.

5. Summary

After discussing the nature of nitric oxide as an air pollutant, we analyzed a catalytic convertor for the reduction of automotive nitric oxide emissions. A brief survey of previous attempts at identifying an acceptable catalyst was presented. From this survey we conclude that the chemical reactions of interest are

$$NO + CO \rightleftharpoons CO_2 + \tfrac{1}{2}N_2$$

and

$$NO + H_2 \rightleftharpoons H_2O + \tfrac{1}{2}N_2$$

Previous studies concluded that these reactions are successfully catalyzed by various copper chromite catalysts. These same studies reported the necessary overall rate expressions to carry-out a packed-bed reactor analysis.

We have limited the mathematical analysis to an axial flow convertor. As part of a preliminary study we concluded that for the operating conditions of interest (1) the effects of dispersion in the bulk fluid could be neglected, (2) the chemical reactions experience transport limitations within the catalyst, and (3) the conversion was sensitive to the catalyst density. This information was used in selecting the model for studying the transient response of such an axial flow convertor. The transient operating conditions are specified by the Federal Test Procedure. The mathematical model chosen consisted of a series of four mixing-cells, each of which contained the separate problem of diffusion limited reactions occurring catalytically. This model was used to study the effects of (1) particle effective diffusivity, (2) catalyst density and heat capacity, and (3) different levels of reactant concentrations. One of the most serious difficulties concerns the length of time required to heat the bed of solid catalyst to a temperature sufficient to produce an acceptable rate of reaction. It is found that a low density catalyst with a low heat capacity heated to 300°C in less than half the time required for a denser catalyst with a higher heat capacity. This difference allows better conversions for shorter times but leads to poorer conversions at longer times, indicating the necessity to make a compromise. Better conversion is also obtained for higher particle effective diffusivities. Eight percent conversion is obtained at three significantly different levels of nitric oxide, but 80% conversion of

concentrations in excess of 3000 ppm leaves too much residual nitric oxide to meet proposed 1975 emission st ards for nitric oxide (225 ppm). Consequently, the untreated e st gas should contain no more than 1000 ppm nitric oxide, which is nically feasible. In the cases studied, it appears that catalytic control of the nitric oxide emissions from automobiles is an obtainable goal.

6. Bibliography

1) The Automobile and Air Pollution, U.S. Department of Commerce, December, 1967.

2) Ayen, R. J. and Amirnazmi, A., Catalytic reduction of nitrogen dioxide by hydrogen, Industrial and Engineering Chemistry, Process Design and Development, 9 (1970) pp. 247-254.

3) Ayen, R. J. and Ng, Y.-S., Catalytic reduction of nitric oxide by carbon monoxide, Air and Water Pollution, 10 (1966) pp. 1-13.

4) Ayen, R. L. and Peters, M. S., Catalytic reduction of nitric oxide, Industrial and Engineering Chemistry, Process Design and Development, 1 (1962) pp. 204-207.

5) Ayen, R. J. and Yonebayashii, T., Catalytic reduction of nitrogen dioxide by carbon monoxide, Atmospheric Environment, 1 (1967) pp. 307-318.

6) Baker, R. A. and Doerr, R. C., U.S. Patent #3,398,101 (Filed, November 22, 1963; Patented, August 20, 1968).

7) Baker, R. A. and Doerr, R. C., Catalytic reduction of nitrogen oxides in automobile exhausts, Journal of the Air Pollution Control Association, 14 (1964) pp. 409-414.

8) Baker, R. A. and Doerr, R. C., Catalyzed nitric oxide reduction with carbon monoxide, Industrial and Engineering Chemistry, Process Design and Development, 4 (1965) pp. 188-191.

9) Bauerle, G. L. and Nobe, K., Design, construction, and testing of catalytic afterburners for removal of air pollutants formed in automobile and stationary combustion processes. In: Project Clean Air. University of California (Los Angeles), School of Engineering and Applied Science, Research Project S-2, 46 p., September 1, 1970.

10) Bernstein, L. S., Kearby, K. K., Raman, A. K. S., Vardi, J., and Wigg, E. E., Application of catalysts to automotive NO_x emissions control. (Presented at the Automotive Engineering Congress, Detroit, January 11-15, 1971, paper #710014,.

11) Brian, P. L. T., Baddour, R. F., and Eymery, J. P., Transient behavior of an ammonia synthesis reactor, Chem. Engr. Sci., 20 (1965) pp. 297-310.

12) Caretto, L. S., McElroy, M. W., Nelson, J. L., and Venturini, P. D., Automotive engine development. Task force assessment. In: Project Clean Air. University of California (Berkeley), Department of Mechanical Engineering, Task Force 1, Volume 1, 68 p., September 1, 1970.

13) Control of air pollution from new motor vehicles and new motor vehicle engines, Federal Register, 33, 108 (June 4, 1968).

14) Control of air pollution from new motor vehicles and new motor vehicle engines, Federal Register, 35 219 (November 10, 1970).

15) Crider, J. E. and Foss, A. S., Computational studies of transients in packed tubular chemical reactors, A. I. Ch. E. Journal, 12 (1966), pp. 514-522.

16) Gross, G. P., Biller, W. F., Greene, D. F., and Kearby, K. K., U. S. Patent #3, 370, 914 (Filed, November 20, 1963; Patented, February 27, 1968).

17) Hocker, A. J., Surveillance of motor vehicle emission in California, Quarterly Progress Report, 21 (July-September, 1970), California Air Resources Board.

18) Hurn, R. W., Comprehensive analyses of automotive exhausts, Archives of Environmental Health, 5 6 (1962) pp. 592-596.

19) Jones, J. H., Weaver, E. E., Kummer, J. T., Otto, K., and Shelef, M., Selective catalytic reaction of hydrogen with nitric oxide in the presence of oxygen. (Presented at the Joint Meeting of the A. I. Ch. E. -I. M. I. Q., Denver, August 30-September 2, 1970).

20) Kohayakawa, T., Control of exhaust gas from internal combustion engine, Nippon Kikai Gakkai-Shi, 73, 612 (1970) pp. 100-111.

21) Kuo, J. C., Lassen, H. G., and Morgan, C. R., Mathematical modelling of catalytic convertor systems. (Presented at the Automotive Engineering Congress, Detroit, January 11-15, 1971, paper #710289).

22) McGreavy, C. and Thornton, J. M., Stability studies of single catalyst particles, Chemical Engineering Journal, 1 (1970) pp. 296-301.

23) Mickley, H.S., and Letts, R.W.M., Yield studies in packed tubular reactors Part 1 Mathematical model for design and analysis, Can. J. Chem. Engng., 41 (1963) pp. 273-279.

24) Preston, T.A., private communication with the Environmental Protection Agency.

25) Roth, J.F., and Doerr, R.C., Oxidation-reduction catalysis, Industrial and Engineering Chemistry, 53, 4 (1961) pp. 293-296.

26) Satterfield, C.N., Mass Transfer in Heterogeneous Catalysis, MIT Press (Cambridge, Massachusetts) 1970.

27) Sehr, R.A., The thermal conductivity of catalyst particles, Chem. Eng. Sci., 9 (1958) pp. 145-152.

28) Shah, K.S. and Rastogi, K.V., Present stand of development in engine exhaust emissions. (Presented at the International Clean Air Congress, 2nd, Washington, D.C., December 6-11, 1970, paper EN-10H; Preprint, International Union of Air Pollution Prevention Associations, 50 p., 1970).

29) Shelef, M., and Kummer, J.T., The behavior of nitric oxide in heterogeneous catalytic reactions. (Presented at the 62nd Annual Meeting of the A.I.Ch.E., Washington, D.C., November 16-20, 1969).

30) Shelef, M. and Otto, K., Appearance of nitrous oxide in the catalytic reduction of nitric oxide by carbon monoxide, J. Catalysis, 10 (1968) pp. 408-412.

31) Shelef, M. and Otto, K., Simultaneous catalytic reaction of O_2 and NO with CO and solid carbon, J. Colloid and Interfacial Science, 31 (1969) pp. 73-78.

32) Shelef, M., Otto, K., and Gandhi, H., The oxidation of CO by O_2 and by NO on supported chromium oxide and other metal oxide catalysts, J. Catalysis, 12 (1968) pp. 361-375.

33) Shelef, M., Otto, K., and Gandhi, H., The heterogeneous decomposition of nitric oxide on supported catalysts, Atmospheric Environment, 3 (1969) pp. 107-113.

34) Sotoodehnia-Korrani, A., and Nobe, K., Reduction of nitric oxide with ethylene on copper-silica catalyst, Industrial and Engineering Chemistry, Process Design and Development, 9 (1970) pp. 455-459.

35) Sourirajan, S., and Blumenthal, J. L., The application of a copper-silica catalyst for the removal of nitrogen oxides present in low concentrations by chemical reduction with carbon monoxide and hydrogen, International J. Air and Water Pollution, 5 (1961) pp. 24-33.

36) Thoenes, D., Jr., and Kramers, H., Mass transfer from spheres in various regular packings to a flowing fluid, Chem. Eng. Sci., 8 (1958) pp. 271-283.

37) Vardi, J., and Biller, W. F., Thermal behavior of an exhaust gas catalytic convertor, Industrial and Engineering Chemistry, Process Design and Development, 7 (1968) pp. 83-90.

38) Wei, J., Catalysis and reactors, Chem. Engr. Prog. Mono. Series, 65, 6 (1969) 19 pp.

39) Yolles, R. S., Wise, H., and Berriman, L. P., Study of catalytic control of exhaust emissions for Otto cycle engines. (Prepared for the National Air Pollution Control Administration, U. S. Department of Health, Education, and Welfare, Durham, North Carolina, April, 1970, Contract No. CPA 22-69-115).

APPENDICES

1. Liu's Explicit Method for Differencing and Solving Parabolic Partial Differential Equations

Explicit methods for differencing and solving quasilinear parabolic partial differential equations avoid the iterations inherent in the implicit methods. Liu(1) develops an explicit finite difference scheme similar to that of Saul'yev(2): the scheme has two finite difference equations for each spatial grid point, $m\Delta x$, in advancing the solution in time from $n\Delta t$ to $(n+1)\Delta t$. One difference equation is solved (explicitly) from $m = 1$ to $m = M$ while the second difference equation is solved from $m = M$ to $m = 1$. These difference equations can be used simultaneously (the average method) or sequentially (the alternating method: alternating the use of one equations for even time steps with the use of the second equation for odd time steps). We refer to the difference equations which can be solved explicitly from $m = 1$ to $m = M$ as part of the L-method. Similarly, the second equation is part of the R-method (this is Liu's terminology).

L-method

$$\frac{\partial u}{\partial t}\Big|_{m,n} = \frac{1}{\Delta t}\,(u(m, n+1) - u(m, n))$$

$$\frac{\partial^2 u}{\partial x^2}\Big|_{m,n} = \frac{1}{2(\Delta x)^2}\,(u(m-1, n) - 4u(m, n) + 3u(m+1, n) - (u(m-2, n+1) - 4u(m-1, n+1) + 3u(m, n+1)))$$

$$\frac{\partial u}{\partial x}\Big|_{m,n} = \frac{1}{4\Delta x}\,(u(m-2, n+1) - 4u(m-1, n+1) + 3u(m, n+1) + (u(m+1, n) - u(m-1, n)))$$

R- method

$$\left.\frac{\partial u}{\partial t}\right|_{m,n} = \frac{1}{\Delta t}\,(u(m, n+1) - u(m, n))$$

$$\left.\frac{\partial^2 u}{\partial x^2}\right|_{m,n} = \frac{1}{2(\Delta x)^2}\,(-u(m+2, n+1) + 4u(m+1, n+1) - 3u(m, n+1) - (-u(m+1, n) + 4u(m, n) - 3u(m-1, n)))$$

$$\left.\frac{\partial u}{\partial x}\right|_{m,n} = \frac{1}{4\Delta x}(-u(m+2, n+1) + 4u(m+1, n+1) - 3u(m, n+1) + (u(m+1, n) - u(m-1, n)))$$

We have presented the difference operators introduced by Liu(1). Notice the indicated groupings of terms—Liu uses extensively the three point forward and backward difference formulas. Liu's method (used as presented) involves "imaginary grid points"—for $m = 1$, the difference operator for the second partial derivative in the L-method introduces $u(-1, n+1)$ which is one spatial step beyond the actual boundary at $m = 0$. Liu suggests that use be made of another difference operator which allows one to solve for $u(-1, n+1)$ in terms of $u(1, n)$, $u(0, n)$, and $u(0, n+1)$. It is necessary to consider the boundary points, such as those discussed, with care.

Liu's method was developed for the following type of nonlinear problem:

$$a_i(x, t, \underline{u})\,\frac{\partial u_i}{\partial t} = b_i(x, t, \underline{u})\,\frac{\partial^2 u_i}{\partial x^2} + c_i(x, t, \underline{u})\,\frac{\partial u_i}{\partial x} + F_i(x, t, \underline{u})$$

where $\underline{u} = (u_1, \ldots, u_n)$ and $(i = 1, \ldots, n)$. Liu's method is numerically stable for all step sizes for the simple linear diffusion equation: $u_t = u_{xx}$.

The use of Liu's method for the problems of Chapter A involves two variations which we describe here. First, our boundary conditions are,

$$\frac{\partial T}{\partial x}(0,t) = 0 \tag{1}$$

and

$$\frac{2}{Nu}\frac{\partial T}{\partial x}(1,t) = g(t) - T(1,t). \tag{2}$$

The following difference approximations were used for the boundary conditions:

$$\frac{\partial T}{\partial x}(0,t) = \frac{T_1^{n+1} - T_0^{n+1}}{\Delta x} = 0 \tag{3}$$

and

$$\frac{2}{Nu}\frac{\partial T}{\partial x}(1,t) = \frac{2}{Nu}\frac{[T_M^{n+1} - T_{M-1}^{n+1}]}{\Delta x} = g^{n+1} - T_M^{n+1} \tag{4}$$

(similarly for $c(x,t)$). Secondly, the image points should depend on the nonlinearity. Consider eq. 46 (of Chapter A) evaluated at $x = 0$:

$$\frac{N_1}{4}\frac{\partial T}{\partial t}(0,t) = 3\frac{\partial^2 T}{\partial x^2}(0,t) + \phi^2\beta\, c(0,t)\exp(-\gamma(1/|T(0,t)| - 1)).$$

Using a forward difference approximation for $\frac{\partial T}{\partial t}(0,t)\Big|_{0,n+1}$ and Saul'yev's difference scheme for $\frac{\partial^2 T}{\partial x^2}\Big|_{0,n+1}$ (see (1)), one obtains the following (using eq. 3):

$$T_{-1}^{n+1} = (1 + \frac{N_1/4}{3\beta})T_1^{n+1} - \frac{1}{3(\Delta x)^2}F(1,n) - \frac{N_1/4}{3\beta}T_1^n$$

where $\beta = \frac{\Delta t}{(\Delta x)^2}$ and $F(1,n)$ is the rate expression evaluated for c_1^n

and T_1^n. T_{-1}^{n+1} is the image point for the L-method. For the R-method, consider the evaluation of eq. 46 (of Chapter A) at $x = (M-1)\Delta x$. When the equation is then approximated using a forward difference for $\frac{\partial T}{\partial t}$ and $\frac{\partial T}{\partial x}$ and Liu's suggested difference scheme for $\frac{\partial^2 T}{\partial x^2}$ (all of these are evaluated at $(M-1)\,\Delta x$),

$$\left.\frac{\partial^2 T}{\partial x^2}\right|_{M-1,\,n+1} = \frac{1}{(\Delta x)^2}\left[T_{M+1}^{n+1} - T_M^{n+1} - T_M^n + T_{M-1}^n\right],$$

one obtains

$$\frac{N_1}{4}\frac{\left[T_{M-1}^{n+1} - T_{M-1}^n\right]}{\Delta t} = \frac{1}{(\Delta x)^2}\left[T_{M+1}^{n+1} - T_M^{n+1} - T_M^n + T_{M-1}^n\right] + \frac{2}{(M-1)\Delta x}\,\frac{\left[T_M^{n+1} - T_{M-1}^{n+1}\right]}{\Delta x}$$

$$+ F(M-1, n). \qquad (5)$$

Eqs. 4 and 5 are then solved for the image point of the R-method.

$$T_{M+1}^{n+1} = -\left(1 + \frac{N_1/4}{\beta}\right) T_{M-1}^n + \left(\frac{2}{M-1} + \frac{N_1/4}{\beta}\right) T_{M-1}^{n+1} + \left(1 - \frac{2}{M-1}\right) T_M^{n+1} + T_M^n - \frac{1}{(\Delta x)^2} F(M-1, n)$$

with

$$T_M^j = \frac{\Delta x \cdot \frac{Nu}{2}\, g(j\Delta t) + T_{M-1}^j}{1 + \Delta x \cdot \frac{Nu}{2}} \qquad (j = n, n+1).$$

References

(1) Liu, S.-L., Stable explicit difference approximations to parabolic partial differential equations, A. I. Ch. E. Journal, 15(1969) pp. 334-338.

(2) Saul'yev, V. K., Integration of Equations of Parabolic Type by the Method of Nets, MacMillan, 1964.

2. A Priori Bounds for the Solution to the Heat Balance of a Transient, Nonisothermal Chemical Reaction

McGuire and Lapidus(3) show that the mass balance for the reactant in a first order chemical reaction is,

$$\epsilon_p \frac{N_2}{4} \frac{\partial c}{\partial t} = \frac{1}{r^2} \frac{\partial}{\partial r} \left(r^2 \frac{\partial c}{\partial r}\right) - \phi^2 c \exp(-\gamma (1/|T| - 1))$$

in dimensionless variables. ϕ is the Thiele modulus and N_2 is the reciprocal of the dimensionless diffusivity. γ is the dimensionless activation energy. Assume the following initial-boundary data:

$$c(r, 0) = \psi(r) \geq 0$$

$$(\text{with } \psi(1) = \phi(0))$$

$$c(1, t) = \phi(t) \geq 0$$

$$\left(\frac{\partial c}{\partial r}(0, t) = 0\right)$$

We are interested in the classical solution which is continuous in $[0, 1] \times [0, t']$ and $C^{2,1}$ in $[0, 1) \times (0, t']$. The following theorem of Protter and Weinberger(4) guarantees that

$$0 \leq c(r, t) \leq \max_{r, t} \{\psi(r), \phi(t)\} :$$

Theorem Let D be a bounded domain in n-dimensional space and let $E = D \times (0, t']$. Suppose that $u(x, t)$ is a solution of

$$L(u) \equiv F(x, t, u, u_x, u_{xx}) - \frac{\partial u}{\partial t} = f(x, t)$$

in E, and that u satisfies the initial and boundary conditions

$$u(x,0) = g_1(x) \text{ in } D$$

$$u(x,t) = g_2(x,t) \text{ on } \partial D \times (0,t')$$

We assume that the functions $z(x,t)$ and $Z(x,t)$ satisfy the inequalities

$$L(Z) \leq f(x,t) \leq L(z) \text{ in } E,$$

and that the operator L is parabolic with respect to the functions $ku + (1-k)z$ and $ku + (1-k)Z$ for $0 \leq k \leq 1$. If

$$z(x,0) \leq g_1(x) \leq Z(x,0) \text{ in } D$$

$$z(x,t) \leq g_2(x,t) \leq Z(x,t) \text{ on } \partial D \times (0,t'),$$

then

$$z(x,t) \leq u(x,t) \leq Z(x,t) \text{ in } E.$$

For the enthalpy balance,

$$\frac{N_1}{4}\frac{\partial T}{\partial t} = \frac{1}{r^2}\left(r^2\frac{\partial T}{\partial r}\right) + \phi^2 \beta c \exp(-\gamma(1/|T| - 1))$$

with

$$T(r,0) = g(r)$$

$$T(1,t) = h(t)$$

$$\left(\frac{\partial T}{\partial r}(0,t) = 0\right)$$

The maximum principle is used to show that

$$\min_{r,t}\{g(r), h(t)\} \leq T(r,t)$$

Let $w \equiv \min_{r,t} \{g(r), h(t)\} = \text{constant}$, and $v(r,t) = T(r,t) - w$.

Then

$$L[T] \equiv F(r,t,T,T_r,T_{rr}) - \frac{\partial T}{\partial t} \quad \text{with}$$

$$F(r,t,T,T_r,T_{rr}) = \frac{4}{N_1}\left[\frac{1}{r^2}\frac{\partial}{\partial r}\left(r^2\frac{\partial T}{\partial r}\right) + \phi^2\beta\, c \exp\left(-\gamma(1/|T|-1)\right)\right]$$

leads to $L[w] \geq 0$. Applying the mean-value theorem of calculus, one finds that $L[T] - L[w] = \frac{4}{N}\frac{1}{r^2}\frac{\partial}{\partial r}\left(r^2\frac{\partial v}{\partial r}\right) + \left[\frac{\partial F}{\partial T}\Big|_{T=kT+(1-k)w}\right] v - \frac{\partial v}{\partial t} \leq 0$

or in cartesian co-ordinates,

$$L[v] = \frac{4}{N_1}(v_{xx} + v_{yy} + v_{zz}) + \left[\frac{\partial F}{\partial T}\Big|_{T=kT+(1-k)w}\right] v - \frac{\partial v}{\partial t} \leq 0$$

Consider the following theorem of Il'in et al. (1).

Theorem Suppose the function v is continuous in $\bar{D}$, that those of its derivatives which enter into the operator L are continuous, and that it satisfies the inequality $L[v] \leq 0$ in $\bar{D} - \Gamma$, where $\frac{\partial F}{\partial T}\Big|_{T=kT+(1-k)w} < M$ and M is some constant. Then $v(x,t) \geq 0$ $\bar{D}$ if $v(x,t) \geq 0$ on Γ.

The theorem of Il'in et al. implies that $T(r,t) \geq w(r,t)$. Let us now consider an upper bound for the function $T(r,t)$.

The motivation for bounding $T(r,t)$ from above stemmed from the form of the Lipschitz condition of the dimensionless rate expression (the nonlinearity) in the enthalpy balance:

$$f(c,T) = c \exp(-\gamma\,(1/|T| - 1)).$$

That is,

$$|f(c_2, T_2)-f(c_1, T_1)| \leq \exp(-\gamma(1/|T_2|-1))|c_2-c_1| + c_1 \max_v \{\frac{\gamma}{2} \exp(-\gamma(1/|v|-1))\} \cdot |T- T_1|$$

or

$$|f(c_2, T_2) - f(c_1, T_1)| \leq a|c_2-c_1| + b|T_2 - T_1|$$

where we are assuming that $T_2 \geq T_1$ and that $c_1 \geq c_2$. If one knows only that

$$T(r,t) \geq 1 \qquad \text{(for typical } g \text{ and } h\text{)}$$

$$1 \geq c(r,t) \geq 0$$

then

$$a = \exp(\gamma)$$

$$b = \frac{4}{\gamma} \exp(\gamma-2), \quad (v = \frac{\gamma}{2})$$

such that for typical values of γ (10 to 30), a and b are quite large. Alternatively, if one can show that

$$T(r,t) \leq m(t)$$

then

$$a = \exp(-\gamma(1/|m| - 1))$$

$$b = \max_{1 \leq v \leq m} \{\frac{\gamma}{2} \exp(-\gamma(1/|v| - 1))\}$$

and a and b may be of 0(1).

Ladyzenskaja et al. (2) proved the following theorem:

Theorem Let $u(x,t)$ be a classical solution of

$u_t - a_{ij}(x, t, u, u_x)\, u_{x_i x_j} + a(x, t, u, u_x) = 0$ in Q_T. Suppose that the functions a_{ij} and a take finite values for any finite u, u_x, and $(x, t) \in \bar{Q}_T$ and that for $(x, t) \in Q_T$ and arbitrary u

$$a_{ij}(x, t, u, 0)\, f_i f_j \geq 0$$

and

$$u\, a(x, t, u, 0) \geq -b_1 u^2 - b_2$$

where b_1 and b_2 are nonnegative constants. Then

$$\max_{Q_T} |u(x, t)| \leq \inf_{\lambda > b_1} \exp(\lambda T) \left\{ \max_{\Gamma_T} |u|, \sqrt{\frac{b_2}{\lambda - b_1}} \right\}.$$

If in place of the condition on a involving b_1 and b_2, one has

$$u\, a(x, t, u, 0) \geq -\Phi(|u|)\, |u| - b_2$$

with b_2 nonnegative and $\Phi(\tau)$ is a nondecreasing positive function of $\tau \geq 0$ satisfying the condition

$$\int_0^\infty \frac{d\tau}{\Phi(\tau)} = +\infty$$

then the estimate

$$\max_{Q_T} |u(x, t)| \leq \inf_{\lambda > 1} \phi(\xi)$$

$$\xi = \exp(\lambda T) \max\left\{1;\ \phi^{-1}\left(\frac{b_2}{(\lambda - 1)\Phi(0)}\right);\ \phi^{-1}\left(\max_{\Gamma_T} |u|\right)\right\}$$

is valid, in which $\phi^{-1}(\ )$ is the inverse of the function $\phi(\ )$ defined by the equation

$$\int_0^{\phi(\xi)} \frac{d\tau}{\Phi(\tau)} = \ell n\, \xi$$

This theorem is modified slightly for the temperature function of the enthalpy balance:

Theorem Let $T(r,t)$ be a classical solution of

$$\frac{N_1}{4}\frac{\partial T}{\partial t} = \frac{1}{r^{a-1}}\frac{\partial}{\partial r}\left(r^{a-1}\frac{\partial T}{\partial r}\right) + (\phi^2\beta)\, c \exp(-\gamma(1/|T| - 1))$$

in $Q_{t'} = [0,1)x(0,t']$. Assume $0 \le c(r,t) \le 1$ and let $1 \le m \le T(r,t)$. $(\phi^2, \beta, \gamma, Le > 0)$. Then with

$$-T\, a(r,t,T,0) \ge \frac{-(\phi^2\beta)4}{N_1} \exp(-\gamma(1/|T| - 1))\, |T|$$

we have

$$\max_{Q_{t'}} |T(r,t)| \le \bar{\phi}(\xi), \qquad \text{where}$$

$$\xi = \exp(t') \max\{1;\ \bar{\phi}^{-1}(\max_{\Gamma_{t'}} |T|)\} \quad \text{with } \bar{\phi}(\ )$$

defined by

$$\frac{N_1}{4(\phi^2\beta)} \int_m^{\bar{\phi}(\xi)} \exp(\gamma(1/|\tau| - 1))\, d\tau = \ell n\,(\xi) \quad \text{with}$$

$$\int_m^{\infty} \exp(\gamma\,(1/|\tau| - 1))\, d\tau = +\infty$$

Proof: If $T(r,t) \equiv \bar{\phi}[v(r,t)]$, then

$$\frac{N_1}{4} v_t - \frac{1}{r^{a-1}} \frac{\partial}{\partial r}\left(r^{a-1} \frac{\partial v}{\partial r}\right) - \frac{\bar{\phi}''}{\bar{\phi}'}(v_r)^2 - \frac{(\phi^2\beta)c}{\bar{\phi}'} \exp(-\gamma(1/|T| - 1)) = 0$$

Let $\tilde{v}(r,t) = v(r,t) \exp(-\lambda t)$, $\lambda > 0$, then

$$\frac{N_1}{4} \tilde{v}_t - \left[\frac{1}{r^{a-1}} \frac{\partial}{\partial r}\left(r^{a-1} \frac{\partial \tilde{v}}{\partial r}\right) + \frac{\bar{\phi}''}{\bar{\phi}'}(\tilde{v}_r)^2 \exp(\lambda t)\right]$$

$$+ \left[\frac{-(\phi^2\beta)c}{\bar{\phi}'} \exp(-\gamma(1/|T| - 1)) \exp(-\lambda t) + \lambda \tilde{v} \frac{N_1}{4}\right] = 0$$

By definition, as ξ goes from 0 to ∞, $\bar{\phi}(\xi)$ goes from $-\infty$ to $+\infty$ monotonically, such that

$$T = \bar{\phi}(v) \leq \bar{\phi}(\bar{v})$$

where $\bar{v}$ is a bound for v: $v \leq \bar{v}$. Now, at any $(r,t) \in \bar{Q}_{t'}$

$$v(r,t) = \tilde{v}(r,t) \exp(\lambda t) \leq \tilde{v}(r_o,t_o) \exp(\lambda t) = v(r_o,t_o) \exp(\lambda(t-t_o))$$

$$= \bar{\phi}^{-1}[T(r_o,t_o)] \exp(\lambda(t-t_o)) \leq \bar{\phi}^{-1}(M) \exp(\lambda(t-t_o))$$

$$\leq \bar{\phi}^{-1}(M) \exp(\lambda t'), \qquad (T(r_o,t_o) \leq M),$$

or, more briefly,

$$v(r,t) \leq \exp(\lambda t') \bar{\phi}^{-1}(M) = \bar{v}$$

Now, the point at which $\tilde{v}(r,t)$ has its maximum, (r_o,t_o), may be

(1) on the boundary, $\Gamma_{t'}$ and positive

(2) interior and positive

or (3) nonpositive

For case (3) we can let $v(r,t) \leq \exp(\lambda t')$, and for case (1) we can let

M be $\max_{\Gamma_{t'}} |T|$. For case (2), we have from the transformed partial differential equation,

$$\frac{-(\phi^2\beta)^4}{N_1} c \exp(-\gamma(1/|T| - 1) + \lambda \bar{\phi}'(v) v \leq 0$$

From the definition of $\bar{\phi}$,

$$\frac{1}{v} = \frac{N_1}{4(\phi^2\beta)} \exp(\gamma(1/|\bar{\phi}| - 1)) \bar{\phi}' \text{ with } \bar{\phi}(1) = m$$

such that

$$v \bar{\phi}'(v) = \frac{4(\phi^2\beta)}{N_1} \exp(-\gamma(1/|\bar{\phi}| - 1))$$

or

$$-(\phi^2\beta) \exp(-\gamma(1/|T| - 1)) + \lambda(\phi^2\beta) \exp(-\gamma(1/|T| - 1)) \leq 0$$

or

$$-1 + \lambda \leq 0$$

such that

$$\lambda \leq 1$$

and we conclude

$$\max |T(x, t)| \leq \bar{\phi}(\xi)$$

$$\xi = \exp(t') \max\{1; \bar{\phi}^{-1}(\max_{\Gamma_{t'}} |T|)\}$$

The integral defining $\bar{\phi}(\ )$ can be evaluated using the exponential integral:

$$J \equiv \frac{N_1}{4(\phi^2\beta)} \int_m^{\bar{\phi}(\xi)} \exp(\gamma(1/|w| - 1)) \, dw$$

$$J = -\frac{\gamma N_1 \exp(-\gamma)}{4(\phi^2\beta)}\left[\frac{\exp(\gamma)}{\gamma} - \frac{\exp(\gamma/\bar{\phi})}{\gamma/\bar{\phi}} + \mathrm{Ei}(\gamma/\bar{\phi}) - \mathrm{Ei}(\gamma)\right]$$

As an example, let the parameters be as follows:

$$\gamma = 20.0$$

$$\phi^2 = 0.25$$

$$\beta = 0.6$$

$$N_1 = 705.0$$

$$a = 3 \quad ,$$

then we have the following upper bounds for $T(r,t)$ (with $m = 1$):

t	Upper bound on $T(r,t)$	Maximum of approximate solution ($n = 6$) $\tilde{T}(r,t)$
1	1.0523	1.0523
5	1.0625	1.0620
10	1.0776	1.0728
100	$0(10^8)$	1.0728

The a priori bound for $T(r,t)$ provides reasonable values up to roughly $t = 25$ ($|T(r,t)| \leq 1.2$).

As with many nonlinear problems, the bound involving an exponential growth in time such that the bound becomes progressively poorer for long times. The bound, for this example, is quite good for short times ($t < 25$).

References

(1) Il'in, A. M., Kalashnikov, A. S., and Oleinik, O. A., Second order linear equations of parabolic type, Russian Mathematical Surveys, 17(1962) pp. 1-144.

(2) Ladyzenskaja, O. A., Solonnikov, V. A., and Ural'ceva, N. N., Linear and Quasilinear Equations of Parabolic Type, American Mathematical Society, 1968.

(3) McGuire, M. L., and Lapidus, L., On the stability of a detailed packed-bed reactor, A. I. Ch. E. Journal, 11(1965) pp. 85-95.

(4) Protter, M. H., and Weinberger, H. F., Maximum Principles in Differential Equations, Prenctice-Hall, Inc., 1967.

3. Specific Equilibrium Constants

For the reactions,

$$NO + CO \rightleftharpoons \tfrac{1}{2}N_2 + CO_2 \qquad (1)$$

$$NO + H_2 \rightleftharpoons \tfrac{1}{2}N_2 + H_2O \qquad (2)$$

the equilibrium constants have been investigated. Using the expressions for the heats of reaction (Appendix 6) in the van't Hoff equation,

$$\frac{d}{dT}\left(\ell n\, K^i_{eq}\right) = \frac{\Delta H^i_{RXN}}{R_g T^2}, \qquad (i = 1, 2)$$

and obtaining the initial condition from standard-state data, one finds that the equilibrium constants are as follows:

$$\ell n(K^1_{eq}) = \frac{1}{R_g}\left(\frac{89,942}{T} + 0.165\,\ell n\, T + 0.000325\, T - \frac{93,500}{T^2} - 26.068240\right)$$

$$\ell n(K^2_{eq}) = \frac{1}{R_g}\left(\frac{78,620}{T} + 2.835\,\ell n\, T + 0.000605\, T - \frac{2,000}{T^2} - 20.740494\right)$$

or,

T(°K)	$\ell n(K^1_{eq})$	$\ell n(K^2_{eq})$
528	73.0484	55.7123
633	58.9114	43.0562
763	46.8011	32.1800
861	40.0920	26.1354
1073	29.7804	16.8067

The extremely large values for the equilibrium constants indicate that the reactants would, in all cases of interest, be entirely converted to the desired products. Unfortunately, there are examples where the

rate of conversion is so small that no changes have been detected for 40-50 years (nitric oxide decomposition). While the above results favor the formation of the products, they do not indicate how fast the conversion is.

4. Rate Expressions for the Chemical Reactions of the NO_x Convertor

Ayen and Ng(1) obtain experimentally the following rate expression for the catalytic chemical reaction between nitric oxide and carbon monoxide:

$$NO + CO \rightleftharpoons \tfrac{1}{2}N_2 + CO_2$$

$$|r_1| = \frac{k^1 K^1_{CO} K^1_{NO} P_{CO} P_{NO}}{(1 + K^1_{CO} P_{CO} + K^1_{NO} P_{NO})^2}$$

where the rate constant, k^1, is

$$k^1 = 48.0 \exp(-9,400/(R_g T)) \frac{\text{gm-moles}}{\text{min-gm catalyst}}$$

and the adsorption-desorption equilibrium constants, K^1_{CO} and K^1_{NO}, are given as,

$$K^1_{CO} = 0.076 \exp(8,200/R_g T)) \text{ atm}^{-1}$$

and

$$K^1_{NO} = 0.064 \exp(7,600/R_g T)) \text{ atm}^{-1}.$$

The catalyst was a combination of BaO, Cr_2O_3, and CuO.

Ayen and Peters(2) obtain experimentally the following rate expression for the catalytic chemical reaction between nitric oxide and hydrogen:

$$NO + H_2 \rightleftharpoons \tfrac{1}{2}N_2 + H_2O$$

$$|r_2| = \frac{k^2 K^2_{H_2} K^2_{NO} P_{H_2} P_{NO}}{(1 + K^2_{H_2} P_{H_2} + K^2_{NO} P_{NO})^2}$$

where the rate constant, k^2, is

$$k^2 = 1.39 \exp(-10,3000/(R_g T)) \frac{\text{gm-moles}}{\text{min-gm catalyst}}$$

and the adsorption-desorption equilibrium constants, $K^2_{H_2}$ and K^2_{NO}, are given as,

$$K^2_{H_2} = 4.5 \times 10^5 \exp(-15,400/(R_g T)) \text{ atm}^{-1}$$

$$K^2_{NO} = 3.1 \times 10^5 \exp(-13,300/(R_g T)) \text{ atm}^{-1}.$$

The catalyst was a combination of $ZnO_3 Cr_2O_3$, and CuO.

Let us consider the relative magnitudes of the two rates for various temperatures (when $p_{NO} = 0.001$, $p_{CO} = 0.015$, and $p_{H_2} = p_{CO}/3.8$).

T(°K)	$\lvert r_1 \rvert$	$\lvert r_2 \rvert$
100	0.00000346	10^{-17}
200	0.00004703	10^{-12}
300	0.00014530	10^{-9}
400	0.00017609	0.00000016
500	0.00014538	0.00000562
600	0.00010899	0.00006805
700	0.00008185	0.00035486
800	0.00006322	0.00064148

Notice that while $\lvert r_2 \rvert$ is insignificant at temperatures below 400°K, it becomes the dominant reaction for temperatures in excess of 700°K.

References

(1) Ayen, R. J., and Ng, N.-S., Catalytic reduction of nitric oxide by carbon monoxide, Air and Water Pollution, 10 (1966) pp. 1-13.

(2) Ayen, R. J., and Peters, M. S., Catalytic reduction of nitric oxide, Industrial and Engineering Chemistry, Process Design and Development, 1 (1962) pp. 204-207.

5. Physical Properties of the Gas Stream to the NO_x Convertor

Assume an exhaust composition of,

CO	6.0 volume %
CO_2	10.0 volume %
NO	0.5 volume %
O_2	0.5 volume %
N_2	77.5 volume %
H_2O	5.0 volume %
H_2	0.5 volume %

and calculate the mixture properties by the following simple empirical equations(2),

$$c_p = \left(\sum_i y_i m_i c_{p,i}\right)/\underline{m}$$

$$\mu = \frac{\left(\sum_i y_i \mu_i (m_i)^{\frac{1}{2}}\right)}{\sum_i y_i (m_i)^{\frac{1}{2}}}$$

$$k_f = \frac{\sum_i y_i k_i (m_i)^{\frac{1}{3}}}{\sum_i y_i (m_i)^{\frac{1}{3}}}$$

where $\underline{m} = 28$ and

$$k_i = \frac{\mu_i}{m_i}(1.25\, R_g + c_{p,i}), \quad \text{(Eucken's equation)}$$

For Eucken's equation, we have calculated the pure component viscosity (μ_i) using the Bromley and Wilke modification of the theoretical

Hirchfelder method(2). According to Perry(2), the average expected errors from these mixture formulas are 2-5%, and the pure component estimates (for μ_i, k_i) are accurate to roughly 3-8%.

We calculated the following values for the mixture Prandtl number, heat capacity, viscosity, and thermal conductivity:

T(°K)	$Pr = c_p\mu/k_f$	$c_p(\frac{cal}{gm-°C})$	μ (poise)	k_f(cal/cm-sec°C)
528	0.754	0.265	0.000253	0.0000889
633	0.761	0.271	0.000288	0.0001026
763	0.765	0.277	0.000328	0.0001188
861	0.766	0.281	0.000355	0.0001303
1073	0.769	0.289	0.000412	0.0001549

If one assumes that the gas mixture behaves as pure nitrogen, one finds the following discrepancies from the mixture properties (for temperatures from 528 to 1073°K),

Property	Discrepancy
Pr	2%
c_p	4%
μ	2%
k_f	2%

As a result of the small differences, the gas mixture physical properties were approximated by those for pure nitrogen gas.

The multi-component diffusivities have been approximated by binary diffusion coefficients. It was found that $D_{N_2\text{-}NO}$ and $D_{N_2\text{-}CO}$ were approximately equal (with in 1.5%). Using the kinetic gas theory(1), one finds the following values for $D_{N_2\text{-}NO}$:

T(°K)	$D_{N_2\text{-}NO}(cm^2/sec)$	$Sc = \frac{\mu/\rho}{D_{N_2\text{-}NO}}$
528	0.550	0.712
633	0.749	0.713
763	1.032	0.711
861	1.256	0.713
1073	1.814	0.714

where the density is calculated from the ideal gas law.

$D_{N_2\text{-}NO}$ was approximated by

$$D_{N_2\text{-}NO} = 0.0000389\,(T)^{1.535}, \quad (T \text{ in } °K)$$

which is within 7% of the above tabulated values.

References

(1) Bird, R. B., Stewart, W. E., and Lightfoot, E. N., Transport Phenomena, John Wiley and Sons, Inc., 1966.

(2) Chemical Engineers' Handbook, Edited by John H. Perry, McGraw-Hill Book Company, 1963.

6. Specific Heats of Reaction—NO_x Convertor

For the reactions of nitric oxide with carbon monoxide and hydrogen,

$$NO + CO \rightleftharpoons \tfrac{1}{2}N_2 + CO_2 \qquad (1)$$

$$NO + H_2 \rightleftharpoons \tfrac{1}{2}N_2 + H_2O \qquad (2)$$

the heats of reaction are mild functions of the absolute temperature. Using the pure component molar heat capacity data of Kelley(1) presented in the form of an empirical series:

$$C_p = a + b\,T + c/T^2$$

the following expressions are obtained for the temperature dependence of the heats of reaction (at a pressure of 1 atmosphere):

$$\Delta H^1_{RXN} = -89,942 - 0.165\,T + 0.000325\,T^2 + \frac{187,000}{T}$$

$$\Delta H^2_{RXN} = -78,620 - 2.835\,T + 0.000605\,T^2 + \frac{4,000}{T}$$

where ΔH_{RXN} [=] cal/gm-mole; T [=] °K.

The variations of ΔH^1_{RXN} and ΔH^2_{RXN} with temperature are quite small:

T(°K)	ΔH^1_{RXN}	ΔH^2_{RXN}
528	-89,410	-79,941
633	-89,412	-80,166
763	-89,382	-80,426
861	-89,342	-80,608
1073	-89,216	-80,962

ΔH^1_{RXN} varies by about 0.2% while ΔH^2_{RXN} varies by about 1.3%.

The following constants have been used for the heats of reaction:

$$\Delta H^1_{RXN} = -89,300 \text{ cal/gm-mole}$$

$$\Delta H^2_{RXN} = -80,500 \text{ cal/gm-mole}$$

Reference

(1) Kelley, K. K., High temperature heat content, heat capacity, and entropy data for the elements and inorganic compounds, U. S. Bur. Mines Bull., 584 (1960).

7. Maximum Temperature Differential Between the Bulk Fluid and the Catalyst Particle Surface

Consider the following enthalpy and mass balances for the chemical reaction between carbon monoxide and nitric oxide, with properties assumed constant:

$$k_s \frac{1}{r^2} \frac{d}{dr} \left(r^2 \frac{dT_s}{dr}\right) + \rho_s \left(-\Delta H^1_{RXN}\right) (1 - \epsilon_p) |r_i| = 0$$

$$\rho D^e_s \frac{1}{r^2} \frac{d}{dr} \left(r^2 \frac{dg^{NO}_p}{dr}\right) - \rho_s (1 - \epsilon_p) m_{NO} |r_1| = 0$$

and the following boundary conditions

$$\frac{dT_s}{dr}(0) = \frac{dg^{NO}_p}{dr}(0) = 0$$

$$k_s \frac{dT_s}{dr}(R_p) = h_t \left(T_{bulk} - T_s(R_p)\right)$$

$$\rho D^e_s \frac{dg^{NO}_p}{dr}(R_p) = \rho k^{NO}_g \left(g^{NO}_{bulk} - g^{NO}_p(R_p)\right).$$

By forming a linear combination of the enthalpy balance and the mass balance, one has

$$\frac{d}{dr} \left(r^2 \frac{d}{dr} \left(k_s T_s + \frac{\rho D^e_s \left(-\Delta H^1_{RXN}\right)}{m_{NO}} g^{NO}_p\right)\right) = 0$$

This is integrated such that

$$k_s \frac{dT_s}{dr}(r) + \frac{\rho D^e_s \left(-\Delta H^1_{RXN}\right)}{m_{NO}} \frac{dg^{NO}_p}{dr}(r) = 0$$

or, using the third and fourth boundary conditions at $r = R_p$,

$$T_s(R_p) = T_{bulk} + \frac{\rho\, k_g^{NO}\,(-\Delta H^1_{RXN})}{h_t\, m_{NO}}\,(g^{NO}_{bulk} - g^{NO}_p(R_p))$$

Physically, the maximum surface temperature occurs when $g^{NO}_p(R_p) = 0$:

$$|T_s(R_p) - T_{bulk}| \leq \frac{\rho\, k_g^{NO}\,(-\Delta H^1_{RXN})}{h_t\, m_{NO}}\, g^{NO}_{bulk}$$

Assume Sh = Nu such that $k_g^{NO}/h_t = D_s^e/k_f = (1.03\ cm^2/sec)/(0.00012$ cal/cm^2-sec-°C), $\rho = (P_t\,\underline{m})/(R_g T) = (1atm \times 28gm/gm\text{-}mole)/$ $(82.06\ atm\text{-}cm^3/(gm\text{-}mole\text{-}°K)) \times 773°K)$, $(-\Delta H^1_{RXN}) = 89,300$ cal/ gm-mole, and that $g^{NO}_{bulk} = \frac{m_{NO}}{(\underline{m})}\, p_{NO} = \frac{30}{28}\,(.001)$. These are typical values. Then,

$$|T_s(R_p) - T_{bulk}| \leq 13.5°C$$

This value is compared with the maximum allowable temperature differential within the particle under identical conditions:

$$T_s(r) - T_s(1) = \int_0^1 G(r, t, Sh)\left[\frac{(-\Delta H^1_{RXN})\rho_s(1-\epsilon_p)}{k_s} R_p^2\right] |r_1|\, t^2 dt$$

where r is dimensionless (length standard used is R_p) and G(r, t, Sh) is the following Green's function:

$$G(r, t, Sh) = \begin{cases} \frac{2}{Sh} + \frac{1}{r} - 1, & t \leq r \\ \frac{2}{Sh} + \frac{1}{t} - 1, & t \geq r \end{cases}$$

The integral equation is reduced to the following inequality:

$$|T_s(r) - T_s(1)| \leq \left[\frac{(-\Delta H^1_{RXN})\rho_s(1-\epsilon_p)R_p^2}{k_s}\right] \xi \; |r_1(\text{bulk})| \; \left|\int_o^1 G\, t^2 dt\right|$$

where ξ is the effectiveness factor and the integral is bounded by,

$$\frac{1}{6} + \frac{1}{3}\,\frac{2}{Sh}, \quad \text{(Table 3 of Chapter B)}$$

Assume $R_p = .159\text{cm}$, $\rho_s = 2.9$ gm-catalyst/cm^3, $\epsilon_p = 0.45$, $k_s = 0.00090$ cal/cm-sec-°C, and $p_{CO} = 0.015$. The rate of reaction for the bulk fluid conditions is then 0.0001454 gm-moles/(gm-catalyst-min) and

$$|T_s(r) - T_s(1)| \leq 9.66\left[\frac{1}{6} + \frac{1}{3}\,\frac{2}{Sh}\right]\xi \; (°C)$$

Then the temperature differential through the catalyst (no more than 2.5°C) is roughly 12% of the temperature differential across the boundary layer film. This comparison justifies the use of a lumped parameter equation to describe heat transfer within the catalyst particle.

8. Effective Radial Thermal Conductivity in a Packed-bed Reactor

The methods and data presented by Yagi, Wakao, Kunii, and Smith (1, 2, 3, 4, 5) are used to calculate effective thermal conductivities in packed-beds. The basic assumption for both axial and radial thermal conductivities is that the coefficient is the sum of a stagnant contribution and a dynamic contribution:

$$\frac{k_{e,R}}{k_f} = \frac{k^o_{e,R}}{k_f} + (\alpha\beta)_H \, Pr \cdot Re$$

$$\frac{k_{e,L}}{k_f} = \frac{k^o_{e,L}}{k_f} + \delta \; Pr \cdot Re$$

Assuming the packed-bed has a random particle structure, the stagnant contributions, $k^o_{e,R}$ and $k^o_{e,L}$, should be identical. Yagi and Kunii(1) and Kunii and Smith(3) propose methods of calculating the stagnant contribution, which include the effect of radiant heat transport mechanisms. The magnitude of radiant heat transport effects depends on the particle diameter, the particle thermal conductivity, and the temperature level.

Let us consider the effective radial thermal conductivity. Assume a solid thermal conductivity, k_s, of 0.00078 cal/(cm-sec-°C), a particle diameter, d_p, of 0.318 cm, a solid emissivity of 1, and a packing void fraction, ϵ, of 0.35. We are interested in the following conditions (see Table 2 of Chapter C):

Bulk fluid temperature (°K)	Bulk fluid thermal conductivity (cal/(cm-sec-°C))	Reynolds number
528	0.0000889	31
633	0.0001026	41
763	0.0001188	52
861	0.0001303	66
1073	0.0001549	87

Kunii and Smith(3) derive the following expression for the stagnant contribution to the effective thermal conductivity for the packed-bed:

$$\frac{k_e^o}{k_f} = \epsilon \left(1 + \beta \frac{h_{rv} d_p}{k_f}\right) + \frac{\beta (1 - \epsilon)}{\gamma (k_f/k_s) + \dfrac{1}{\dfrac{1}{\phi} + \dfrac{d_p h_{rs}}{k_f}}}$$

where h_{rv} and h_{rs} are film coefficients for the radiant transport of energy through the voids (v) and from solid-to-solid (s), β and γ are characteristic lengths associated with the packing(3) which from Kunii and Smith's correlation are both unity, and ϕ is expressed by

$$\phi = \phi_2 + (\phi_1 - \phi_2) \frac{\epsilon - \epsilon_2}{\epsilon_1 - \epsilon_2}$$

with $\epsilon_1 = 0.476$ and $\epsilon_2 = 0.260$. ϕ_1 and ϕ_2 are presented graphically in the work of Kunii and Smith(3).

These expressions and data are used to calculate the effective radial thermal conductivity. The following figure compares the results obtained with (h_{rv}, $h_{rs} = 0$) and with (h_{rv}, $h_{rs} \neq 0$) for $k_{e,R}$ (using $(\alpha\beta)_H = 0.10$):

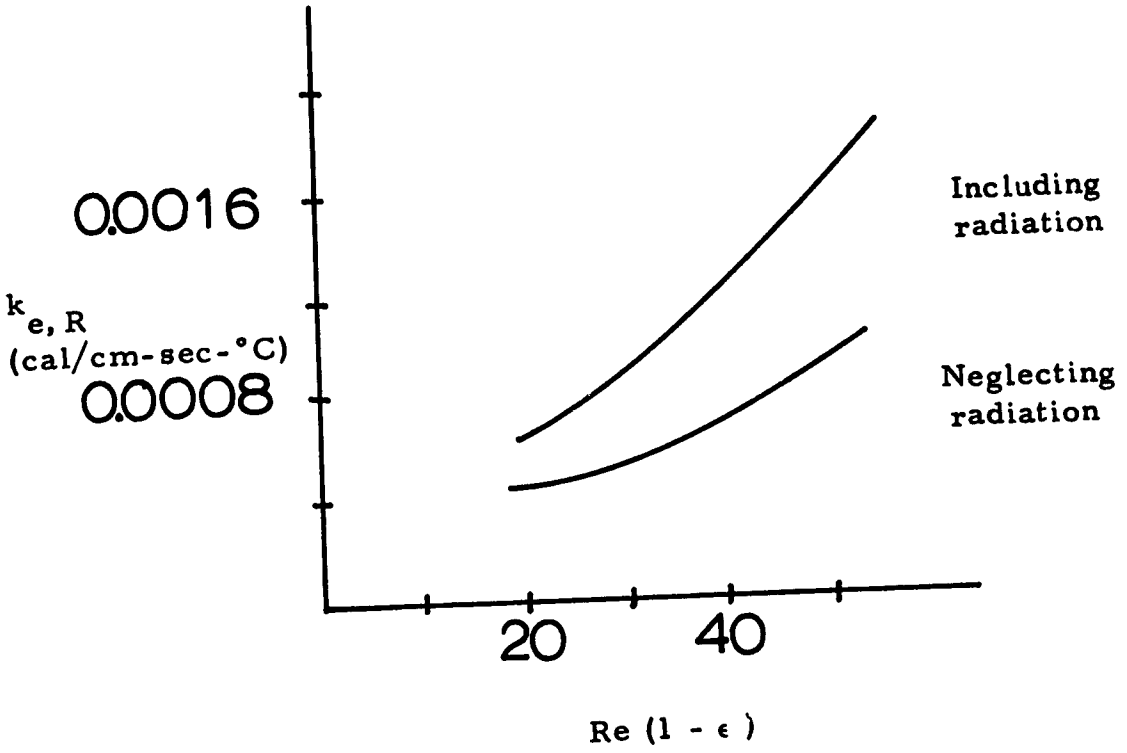

It is interesting to note that radiant transport in packed-beds can become significant at lower temperatures than those normally required for significant black-body radiation(1). This is especially true for low Reynolds numbers—less than 100.

Notation	Remarks
$k_{e,R}$, $k_{e,L}$	effective radial and axial thermal conductivities—cal/cm-sec-°C
$k^{o}_{e,R}$, $k^{o}_{e,L}$	stagnant contributions to the radial and axial thermal conductivities
k_f	thermal conductivity of bulk fluid
$Pr = C\mu/k_f$	Prandtl number
$Re = G\,d\,/\mu$	Reynolds number
$(\alpha\beta)_H$	parameter from Kunii and Smith(3)—usually in the range of 0.10 to 0.14
δ	parameter from Kunii and Smith(3)—usually in the range of 0.7 to 0.8
h_{rs}	heat transfer coefficient for radiation, solid to solid
h_{rv}	heat transfer coefficient for radiation, void to void
ϵ	reactor void fraction

References

(1) Yagi, S., and Kunii, D., Studies of effective thermal conductivities in packed beds, A. I. Ch. E. Journal, 3(1957) pp. 373-381.

(2) Yagi, S., and Wakao, N., Heat and mass transfer from wall to fluid in packed beds, A. I. Ch. E. Journal, 5 (1959) pp. 79-85.

(3) Kunii, D., and Smith, J. M., Heat transfer characteristics of porous rocks, A. I. Ch. E. Journal, 6 (1960) pp. 71-78.

(4) Yagi, S., and Kunii, D., Studies on heat transfer near wall surface in packed beds, A. I. Ch. E. Journal, 6 (1960) pp. 97-104.

(5) Yagi, S., Kunii, D., and Wakao, N., Studies on axial effective thermal conductivities in packed beds, A. I. Ch. E. Journal, 6 (1960) pp. 543-546.

9. Heat Transfer Coefficients

Previous calculations (Chapter C; section 3) indicated that the thermal response of the catalyst particles (for the NO_x convertor) could be modelled quite well by a lumped parameter assumption. A lumped parameter description of such a problem will involve an over-all heat transfer coefficient rather than a heat transfer coefficient. We give three ways to calculate an over-all heat transfer coefficient, h_{ot}. The three values for h_{ot} are obtained by comparing (1) the average particle temperature to the surface temperature (both temperatures are calculated from the first term of the exact series solution), (2) the average particle temperature and the surface temperature (both temperatures are calculated from a one-term orthogonal collocation solution), and (3) a lumped parameter temperature and the temperature at the interior collocation point of a one-term orthogonal collocation solution. The three values for h_{ot} are discussed in the above order.

Consider the following description of the distributed parameter problem: a constant inlet temperature (for example, a gas stream) is introduced into a well-stirred mixing cell. In the mixing cell there is a spherical particle, which at time equal to zero has a specified constant temperature distribution. There is a film resistance to heat transfer at the particle surface. For this problem we have the following dimensional equations:

$$\text{Bulk: } h_t(T_{cell} - T_s(R_p, t)) = K(T_{inlet} - T_{cell}) \qquad (1)$$

$$\text{where } K = \frac{F \bar{m} c_f}{(1 - \epsilon) V_i \frac{6}{d_p}} \tag{2}$$

Solid: $$\rho_s c_s \frac{\partial T_s}{\partial t} = k_s \frac{1}{r^2} \frac{\partial}{\partial r} \left(r^2 \frac{\partial T_s}{\partial r}\right) \tag{3}$$

$$\frac{\partial T_s}{\partial r} (0, t) = 0 \tag{4}$$

$$k_s \frac{\partial T_s}{\partial r} (R_p, t) = h_t (T_{cell} - T_s(R_p, t)) \tag{5}$$

$$T_s(r, 0) = T_{initial}, \text{ a constant} \tag{6}$$

Nondimensionalize the temperatures by using the $T_{initial}$ as the standard. Eq. 1 is solved for T_{cell},

$$T_{cell} = \frac{1 + f\, T_s(R_p, t)}{1 + f} \tag{7}$$

$$\text{where} \quad f = \frac{h_t}{K} \tag{8}$$

Using eq. 7, one is able to replace eq. 5 by the following:

$$k_s \frac{\partial T_s}{\partial r} (R_p, t) = \frac{h_t}{1 + f} (1 - T_s(R_p, t)) \tag{9}$$

Nondimensionalize eqs. 3, 4, and 9 using R_p as the length standard and $k_s/(R_p^2\ \rho_s\ c_s)$ as the time standard. The resulting equations have the following solution (in the dimensionless variables):

$$T_s(r, t) = 1 - \frac{2}{r} \frac{Nu}{2} \sum_{n=o}^{\infty} \frac{y_n^2 \sin(y_n r) \exp(-y_n^2 t)}{\sin(y_n) \left(y_n^2 + \left(\frac{Nu}{2} - 1\right) \frac{Nu}{2}\right)} \tag{10}$$

where

$$Nu = \frac{h_t d_p}{k_s} \cdot \frac{1}{1+f} \tag{11}$$

and y_n's are the roots of,

$$y_n \cos(y_n) + \sin(y_n)\left(\frac{Nu}{2} - 1\right) = 0 \tag{12}$$

This solution, eqs. 10 and 12, was obtained using Laplace transform methods. Eq. 10 is truncated to one term of the indicated summation—this represents the asymptotic solution (valid for large t). We then define the following over-all heat transfer coefficient:

$$h_{ot}(T_{cell}(t) - T_s(t)_{ave.}) = h_t(T_{cell}(t) - T_s(1, t)) \tag{13}$$

All of the temperatures occurring in eq. 13 are obtained from the truncated series; $T_s(t)_{ave.}$ is the mean value of the asymptotic temperature distribution. When the required algebra is performed, one obtains the following result:

$$\frac{h_t}{h_{ot}} = \frac{3Bi}{y_1^2} - f \tag{14}$$

where $$Bi = \frac{h_t R_p}{k_s}$$

This completes the definition of an over-all heat transfer coefficient (eq. 14) based on the asymptotic behavior of the distributed parameter temperature.

Let us now consider an over-all heat transfer coefficient based on the mean value of the distributed parameter temperature. The

dimensionless equations for the heat transfer problem are,

$$\frac{\partial T_s}{\partial t} = \frac{1}{r^2} \frac{\partial}{\partial r} \left(r^2 \frac{\partial T}{\partial r}\right) \tag{15}$$

$$\frac{\partial T_s}{\partial r}(0, t) = 0 \tag{16}$$

$$\frac{\partial T_s}{\partial r}(1, t) = \frac{Nu}{2} (1 - T_s(1, t)) \tag{17}$$

If we apply orthogonal collocation to eq. 15,

$$\frac{dT_{s,1}}{dt} = B_{11} T_{s,1} + B_{12} T_{s,2} = -B_{12}(T_{s,1} - T_{s,2}) \tag{18}$$

and to eq. 17 (assuming eq. 16 is satisfied by the choice of polynomials),

$$A_{21} T_{s,1} + A_{22} T_{s,2} = \frac{Nu}{2} (1 - T_{s,2}) \tag{19}$$

or,

$$\left(A_{22} + \frac{Nu}{2}\right) T_{s,2} = \frac{Nu}{2} + A_{22} T_{s,1} \tag{20}$$

Using eq. 20, one can reduce eq. 18 to the following:

$$\frac{dT_{s,1}}{dt} = - \frac{\left(B_{12} \frac{Nu}{2}\right)}{A_{22} + \frac{Nu}{2}} (T_{s,1} - 1) \tag{21}$$

Eqs. 7 and 13 are combined and rearranged to define the following overall heat transfer coefficient (where the temperatures are now the collocation solution):

$$\frac{h_t}{h_{ot}} = \frac{((T_s)_{ave.} - 1)(1 + f)}{T_{s,2} - 1} - f \tag{22}$$

but

$$\frac{(T_s)_{ave.} - 1}{T_{s,2} - 1} = \frac{w_1}{w_1 + w_2} \frac{(T_{s,1} - 1)}{(T_{s,2} - 1)} + \frac{w_2}{w_1 + w_2} \tag{23}$$

and

$$\frac{T_{s,1} - 1}{T_{s,2} - 1} = 1 + \frac{Nu}{2} \frac{1}{A_{22}} \text{ , (from eq. 19)} \tag{24}$$

For the Legendre polynomials, $A_{22} = 5$, $w_2 = 0$, $w_1 = \frac{1}{3}$, and the final relation between h_t and the defined h_{ot} is,

$$\frac{h_t}{h_{ot}} = 1 + \frac{Bi}{5} \tag{25}$$

As our final over-all heat transfer coefficient, we consider the following description of the original heat transfer problem:

$$\rho_s c_s \frac{dT'_s}{dt} = \frac{3h_{ot}}{3R_p} (T_{cell} - T'_s) \tag{26}$$

with

$$h_{ot}(T_{cell} - T'_s) = K(T_{inlet} - T_{cell}) \tag{27}$$

If we nondimensionalize eqs. 26 and 27 using the time standard introduced previously,

$$\frac{dT'_s}{dt} = \frac{3h_{ot} R_p}{k_s} (T_{cell} - T'_s) \tag{28}$$

$$(T_{cell} - T'_s) = f(T_{inlet} - T_{cell}) \tag{29}$$

If eq. 17 is written in terms of T_{cell}, one obtains an equation similar to eq. 21 but with 1 replaced by T_{cell}. If we identify $T_{s,1}$ of this equation (similar to eq. 21) with T'_s of eq. 28, then the following equation results:

$$\frac{h_t}{h_{ot}} = \frac{3(A_{22} + Bi)}{B_{12}} \tag{30}$$

(we have required that T_{cell} be identical for the two equations). For the Jacobi polynomials, we have (from eq. 30),

$$\frac{h_t}{h_{ot}} = 1 + \frac{Bi}{3.5} \tag{31}$$

We have derived three different expressions for the over-all heat transfer coefficient: eq. 14, eq. 25, and eq. 31. A comparison of the three (using eq. 14 as our standard) shows that eq. 31 is better than eq. 25 for large Biot numbers. For other values of the Biot number, we must specify the value of f (eq. 8). One is interested in the following parameters:

ϵ	= 0.35	$\bar{m}$	= 28.
V_i	= 43.2 in^3	d_p	= 0.125 in
F	= 50 SCFM	k_s	= 0.00006 BTU/sec-ft-°F
c_f	= 0.26 BTU/lb-°F	k_f	= 0.00000876 BTU/sec-ft-°F

with Re = 43 and Pr = 0.766. Thoenes and Kramer(1) give the following correlation for h_t:

$$h_t = \frac{k_f}{d_p} \left(2.42 \left(Re \cdot Pr\right)^{\frac{1}{3}} + 0.129\, Re^{0.8}\, Pr^{0.4} + 1.4\, Re^{0.2}\right) \qquad (32)$$

such that $h_t = 0.011$ BTU/sec-ft^2-°F. As a result, one finds that $f = 6.1$, or $Bi = 0.954$ ($y_1 = 0.63$, the first eigenvalue of eq. 12). The asymptotic over-all transfer coefficient is then

$$h_{ot} = 0.00980 \text{ BTU/sec-ft}^2\text{-°F} .$$

Eq. 25 (orthogonal collocation with the average temperature related to the surface temperature as the definition of h_{ot}) gives

$$h_{ot} = 0.00923 \text{ BTU/sec-ft}^2\text{-°F} .$$

As the following table shows, eq. 25 is better for low Bi numbers and eq. 31 is better for high Bi numbers.

(for $f = 6.1$)		h_t/h_{ot}		
Bi	y_1	eq. 14	eq. 25	eq. 31
0.0355	0.1224	1.0086	1.0071	1.0101
0.071	0.1730	1.0168	1.0142	1.0203
0.71	0.5423	1.14	1.14	1.20
7.1	1.5708	2.53	2.42	3.02
78.1	2.8628	22.5	16.6	23.3
717.1	3.1105	216.	144.	206.

For the transient analysis of the NO_x convertor, the Bi numbers were low (of order 1) and eq. 25 was used to calculate the corresponding over-all heat transfer coefficient as the inlet conditions to the convertor changed.

References

(1) Thoenes, D., and Kramers, H., Mass transfer from spheres in various regular packings to a flowing fluid, Chem. Eng. Sci., 8 (1958) pp. 271-283.

10. Transient Mixing-cell Model for the NO_x Convertor

The presentation of the mixing-cell model in Chapter C is intentionally brief. Here we provide an expanded presentation of the explicit equations and define various constants as they are used in the computer program.

Consider a series of three mixing-cells as in the following sketch

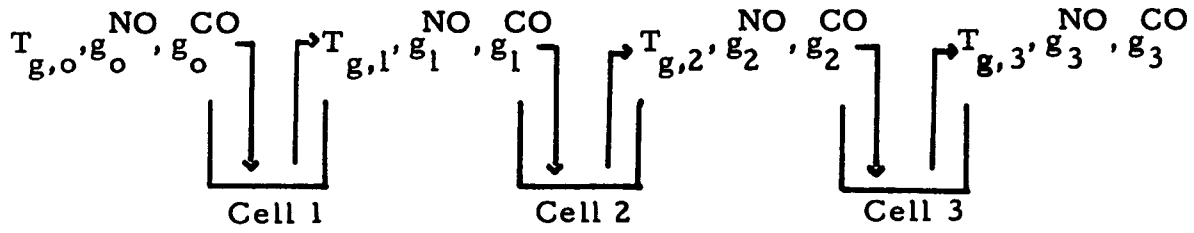

The volume of each cell, V_n, is then simply $V_{total}/3$. The heat balance for the solid phase in the i-th cell is,

$$\frac{dT_{s,i}}{dt} = \frac{6h_{ot}}{d_p \rho_s c_s}[T_{g,i} - T_{s,i}] + \frac{(-\Delta H^1_{RXN})}{60\,\rho_s c_s}\langle|r_1|\rangle_i + \frac{(-\Delta H^2_{RXN})}{60\,\rho_s c_s}\langle|r_2|\rangle_i$$

(where we have included conversion factors: units of seconds, grams, centimeters, and calories) and the heat balance for the gas phase in the i-th cell is,

$$T_{g,i} = \frac{\dfrac{F\,\bar{m}\,c_f}{(60 \times 359.05/453.59)}\,T_{g,i-1} + \dfrac{6(1-\epsilon)V_i\,h_{ot}}{d_p}\,T_{s,i}}{\dfrac{F\,\bar{m}\,c_f}{(60 \times 359.05/453.59)} + \dfrac{6(1-\epsilon)\,V_i\,h_{ot}}{d_p}}$$

Define

$$w_1 = \frac{6(1-\epsilon)V_i}{d_p} \quad ; \quad w_2 = \frac{\bar{m}\, c_f}{(60 \times 359.05/453.59)}$$

$$A_s = \frac{\bar{m}\, c_f}{(60 \times 359.05/453.59)\,(1-\epsilon)\, V_i \rho_s c_s}$$

and

$$\langle |r_1| \rangle_i = \frac{\rho_s \int_o^{R_p} |r_1(T_{s,i}, g^{NO}_{p,i}(r), g^{CO}_{p,i}(r))|\, r^2 dr}{\int_o^{R_p} r^2 dr}$$

$$\langle |r_1| \rangle_i \; [=] \; \frac{\text{gm-moles NO}}{\text{min-cm}^3 \text{ catalyst}}$$

such that the enthalpy balance for the solid phase is re-written as,

$$\frac{dT_{s,i}}{dt} = \frac{(w_1 A_s) h_{ot} F}{w_1 h_{ot} + w_2 F} (T_{g,i-1} - T_{s,i}) + \frac{(-\Delta H^1_{RXN})\, k^1(T_{ref})}{60\, c_s} \langle |r'_1| \rangle_i$$

$$+ \frac{(-\Delta H^2_{RXN})\, k^2(T_{ref})}{60\, c_s} \langle |r'_2| \rangle_i \qquad (1)$$

where $\langle |r'_1| \rangle_i$ and $\langle |r'_2| \rangle_i$ are dimensionless rates of reaction (with respect to the rate constant evaluated at $T_{ref} = 380°K$). For low temperatures the reactions proceed at such low rates that the solid heating is essentially governed by

$$\frac{dT_{s,i}}{dt} = \frac{(w_1 A_s) h_{ot} F}{w_1 h_{ot} + w_2 F} (T_{g,i-1} - T_{s,i})$$

The nitric oxide mass balance for the solid phase (catalyst particle of i-th cell) is

$$\rho D_e^s \frac{1}{r^2} \frac{\partial}{\partial r}\left(r^2 \frac{\partial g_{p,i}^{NO}}{\partial r}\right) = m_{NO}\left[\frac{\rho_s k'(T_{ref})}{60}(r_1')_i + \frac{\rho_s k^2(T_{ref})}{60}(r_2')_i\right]$$

or

$$\frac{1}{(r')^2} \frac{\partial}{\partial r'}\left((r')^2 \frac{\partial g_{p,i}^{NO}}{\partial r'}\right) = m_{NO} T_{s,i}\left[\frac{\rho_s k'(T_{ref}) R_p^2 R_g}{D_e^s P_t \bar{m}\ 60}\right](r_1')_i$$

$$+ m_{NO} T_{s,i}\left[\frac{\rho_s k^2(T_{ref})\ R_p^2\ R_g}{D_e^s P_t \bar{m}\ 60}\right]\ (r_2')_i$$

where $r' = r/R_p$. Define

$$b_s^1 = \frac{\rho_s k^1(T_{ref})\ R_p^2 R_g}{D_e^s P_t \bar{m}\ 60}$$

$$b_s^2 = \frac{\rho_s k^2(T_{ref})\ R_p^2\ R_g}{D_e^s P_t \bar{m}\ 60}$$

such that

$$\frac{1}{r^2} \frac{\partial}{\partial r}\left(r^2 \frac{\partial g_{p,i}^{NO}}{\partial r}\right) = m_{NO}\ T_{s,i}\ b_s^1\ \langle |r_1'| \rangle_i + m_{NO} T_{s,i} b_s^2 \langle |r_2'| \rangle_i \tag{2}$$

with the boundary conditions,

$$\left.\frac{\partial g_{p,i}^{NO}}{\partial r}\right|_{r=1} = \frac{k_g^{NO} d_p}{D_s^e}\left(g_i^{NO} - g_{p,i}^{NO}\right)\Big|_{r=1} \tag{3}$$

$$\left.\frac{\partial g_{p,i}^{NO}}{\partial r}\right|_{r=0} = 0 \tag{4}$$

But from the mass balance for nitric oxide in the i-th cell,

$$g_i^{NO} = g_{i-1}^{NO} - \frac{(1-\epsilon)V_i m_{NO}(359.05/453.59)\rho_s}{F\,m}\{k^1(T_{ref})\langle|r_1'|\rangle_i + k^2(T_{ref})\langle|r_2'|\rangle_i\} \quad (5)$$

Similar results hold for carbon monoxide, while hydrogen concentrations are describable in terms of nitric oxide and carbon monoxide.

$$g_i^{H_2} = g_{i-1}^{H_2} - \frac{m_{H_2}}{m_{NO}}(g_{i-1}^{NO} - g_i^{NO}) + \frac{m_{H_2}}{m_{CO}}(g_{i-1}^{CO} - g_i^{CO})$$

$$g_{p,i}^{H_2}(r) = g_i^{H_2} + \frac{m_{H_2}}{m_{NO}}(g_{p,i}^{NO}(r) - g_i^{NO}) - \frac{m_{H_2}}{m_{CO}}(g_{p,i}^{CO}(r) - g_i^{CO})$$

Numerically, a differencing scheme is applied to eq. 1 while eqs. 2-5 are solved by orthogonal collocation. By including eq. 5 in the boundary condition of eq. 3, we obtain a nonlinear boundary condition. Using the improved Euler (explicit) method, one finds that the procedure of obtaining the solution numerically presents no problems.

11. Series Solution to: $u_t + u_x = a\, u_{xx}$

Problem: $\frac{\partial u}{\partial t} + \frac{\partial u}{\partial x} = \frac{1}{Pe}\left(\frac{d}{L}\right)\frac{\partial^2 u}{\partial x^2}$

$$\frac{\partial u}{\partial x}(1, t) = 0$$

$$1 = u(0, t) - \frac{1}{Pe}\left(\frac{d}{L}\right)\frac{\partial u}{\partial x}(0, t)$$

---

let $v = 1 - u$, then

$$\frac{\partial v}{\partial t} = \frac{1}{Pe}\left(\frac{d}{L}\right) e^{Pe(\frac{L}{d})x}\, \frac{\partial}{\partial x}\left[e^{-Pe(\frac{L}{d})x}\, \frac{\partial v}{\partial x}\right]$$

$$\frac{\partial v}{\partial t}(1, t) = 0$$

$$v(0, t) - \frac{1}{Pe}\left(\frac{d}{L}\right)\frac{\partial v}{\partial x}(0, t) = 0$$

(can solve by separation of variables)

$$v(x, t) = \bar{X}(x)\, T(t)$$

$$\frac{T^1}{T} = \frac{1}{Pe}\left(\frac{d}{L}\right)\frac{1}{\bar{X}} e^{Pe(\frac{L}{d})x}\, \frac{1}{dx}\left[e^{-Pe(\frac{L}{d})x}\, \frac{d\bar{X}}{dx}\right] = -\mu_n^2$$

such that $T_n = A_n e^{-\mu_n^2 t}$

and $\frac{d}{dx}\left[e^{-Pe(\frac{L}{d})x}\, \frac{d\bar{X}_n}{dx}\right] + Pe\left(\frac{L}{d}\right)\mu_n^2 e^{-Pe(\frac{L}{d})x}\, \bar{X}_n = 0$

$$\bar{X}_n(0) - \frac{1}{Pe}\left(\frac{d}{L}\right)\bar{X}_n^1(0) = 0$$

$$\bar{X}_n^1(1) = 0$$

let $a = \frac{1}{Pe}\left(\frac{d}{L}\right)$

$$\bar{X}_n = e^{\frac{x}{2a}}\left[2a\sqrt{\left|\frac{1}{4a^2} - \frac{\mu_n^2}{a}\right|}\cos\sqrt{\left|\frac{1}{4a^2} - \frac{\mu_n^2}{a}\right|}\,x + \sin\sqrt{\left|\frac{1}{4a^2} - \frac{\mu_n^2}{a}\right|}\,x\right]$$

with $\int_o^1 \bar{X}_n \bar{X}_m e^{-\frac{x}{a}}\,dx = 0 \qquad n \neq m$

$$\int_o^1 \bar{X}_n^2 e^{-\frac{x}{a}}\,dx = \frac{1}{2}\left\{4a\left(a\left|\frac{1}{4a^2} - \frac{\mu_n^2}{a}\right| + 1\right) + 1\right\}$$

$$\int_o^1 \bar{X}_n e^{-\frac{x}{a}}\,dx = \frac{8a^2\left|\frac{1}{4a^2} - \frac{\mu_n^2}{a}\right|}{4a^2\left|\frac{1}{4a^2} - \frac{\mu_n^2}{a}\right| + 1}$$

such that

$$u(x,t) = 1 - \sum_{n=o}^{\infty} \frac{\left(\frac{\mu_n^2}{a} - \frac{1}{4a^2}\right)}{\mu_n^2(\mu_n^2 + 1)}\,\bar{X}_n\,e^{-\mu_n^2 t}$$

with μ_n^2 determined from

$$2a\sqrt{\frac{\mu_n^2}{a} - \frac{1}{4a^2}}\cos\sqrt{\frac{\mu_n^2}{a} - \frac{1}{4a^2}} + (1 - 2a\,\mu_n^2)\sin\sqrt{\frac{\mu_n^2}{a} - \frac{1}{4a^2}} = 0$$

The series solution is poorly behaved for small a,

$$a = \frac{1}{Pe} \left(\frac{d}{L}\right) = 0 \left[\frac{d}{L}\right]$$

or, in other words, for large L/d.

12. H_2 Concentration in Automobile Exhaust

In the dynamic model for the catalytic convertor, the effect of the reaction between nitric oxide and hydrogen are included as,

$$NO + H_2 \rightleftharpoons \tfrac{1}{2}H_2 + H_2O$$

but as mentioned by Kuo et al. (2), the molecular hydrogen in the exhaust gas is very difficult to measure during the transient driving conditions. An assumption usually made is that the hydrogen concentration is simply the equilibrium concentration for the water-gas shift reaction:

$$CO_2 + H \rightleftharpoons CO + H_2O$$

Gross et al. (1) mention that the equilibrium constant is usually between 3 and 4 for automobile exhaust and that a value of 3.8 is commonly accepted.

Given a fuel composition (viz., iso-octane, C_8H_{18}) and the air/fuel ratio (viz., 15), the hydrogen concentration can be found as a function of the carbon monoxide concentration. Assuming the fuel contributes the only hydrogen and carbon to the exhaust, eq. 1 represents the conservation of H and C atoms (using the ideal gas law). Eq. 2 is the sum of the partial pressures (neglecting oxygen) and eq. 3 is the equilibrium condition.

$$(2p_{H_2} + 2p_{H_2O}) : (12p_{CO_2} + 12p_{CO}) = (18m_H) : (8m_C) \qquad (1)$$

$$p_{H_2} + p_{H_2O} + p_{CO_2} + p_{CO} + p_{N_2} = 1 \qquad (2)$$

$$(p_{CO}\, p_{H_2O})/(p_{CO_2}\, p_{H_2}) = 3.8 \qquad (3)$$

Eqs. 1-3 are solved to give the following equation which expresses the hydrogen partial pressure as a function of the carbon monoxide and nitrogen partial pressures:

$$p_{H_2} = \frac{\frac{9}{17}(1 - p_{N_2})}{\frac{8}{17}\frac{3.8}{p_{CO}}(1 - p_{N_2}) - 2.8} \qquad (4)$$

If the nitrogen partial pressure is assumed to be approximately constant, eq. 4 relates the carbon monoxide partial pressure (for which data is available) to the hydrogen partial pressure (for which data is not available). For an air/fuel ratio of 13 the nitrogen partial pressure is 0.775 while for an air/fuel ratio of 17 the nitrogen partial pressure is 0.779. We have assumed that the nitrogen partial pressure is constant and has a value of 0.777. Eq. 4 then yields the following results:

p_{CO}	p_{H_2} (eq. 4)	$p_{H_2} = p_{CO}/3.8$
0.01	0.0032	0.0026
0.02	0.0069	0.0053
0.04	0.0165	0.0105
0.06	0.0307	0.0158
0.08	0.0540	0.0211

We used the approximate expression (column 3 of the above table) to calculate the hydrogen concentration. At low values of p_{CO} the

approximation is roughly 20% lower than that of eq. 4. The approximation is conservative: lower p_{H_2} values represent lower rates of reaction with nitric oxide and, consequently, lower conversions of the pollutant, nitric oxide.

References

(1) Gross, G. P., Biller, W. F., Greene, D. F., and Kearby, K. K., U. S. Patent #3,370,914 (Filed: November 20, 1963; Patented: February 27, 1968).

(2) Kuo, J. C., Lassen, H. G., and Morgan, C. R., Mathematical modelling of catalytic converter systems. (Presented at the Automotive Engineering Congress, Detroit, January 11-15, 1971, paper #710289).

13. Computer Listing of Mathematical Model for the Transient Operation of the NO_x Convertor

```
      PROGRAM TEST(INPUT,OUTPUT)
      REAL MBAR,MNO,MCO,MH2,K1TREF,K2TREF,KRATIO,KGMIX,KPEFF,KGM,NU
      COMMON/FCU/AS,W1,W2,AS1,AS2
      COMMON/PAR/MNO,MCO,BS1,BS2,DRAT,MH2,ABORT,CS1,CS2
      COMMON/RXNS/TREF,GAMM1,GAMM2,EPSIC1,EPSIN1,EPSIH2,EPSIN2,ALPHN1,
     1 ALPHC1,ALPHN2,ALPHH2
      DIMENSION TICONL(13),GINO(10),GICO(10),GIH2(10),TGNEW(10),
     1 GVECTO(7,13,2),TSOLD(10),AR1OLD(10),AR2OLD(10),RTOLD(10),
     2 GNOG(3,7),GCOG(3,12),TSNEW(10),TGOLD(10)
      FCN(RE,C1,C2,C3) = C1*(RE)**.333 + C2*(RE)**.8 + C3*(RE)**.2
      CPNO(T) = (6.83 + .00090*(T+273.1) - 12000./((T+273.1)*(T+273.1)))
     1 /28.
      KGMIX(VIS,CPN) = VIS*(CPN + 2.48/28.)
      DIF(T) = .0000389*(T+273.1)**1.535
      CALL PARTIC(0.0,0.0,0.0,0.0,0.0,0.0,0.0,0)
      TIME = VISCOS(0,0.0)
      DO 2 K=1,7
      READ 1,(GVECTO(K,J,1),GVECTO(K,J,2),J=1,11)
    1 FORMAT(5X,F5.0,5X,F10.2)
    2 CONTINUE
      DO 3 J=1,7
      DO 3 K=1,11
    3 GVECTO(J,K,1) = (GVECTO(J,K,1) - 32.)*5./9.
      READ 4,(GNOG(1,J),GNOG(2,J),GNOG(3,J),J=1,7)
```

```
4 FORMAT(5X,F10.4,5X,F10.4,5X,F10.4)
  READ 4,(GCOG(1,J),GCOG(2,J),GCOG(3,J),J=1,12)
  TREF = 380.
  DELTH1 = -89300.
  DELTH2 = -80500.
  CS = .260
  EPSBED = .35
  DPART = .3175
  VTOTL = 2832.
  MBAR = 28.
  KPEFF = .00090
  CF = .270
  RHOP = 2.9
  DIFFEP = .017
  EPSPAR = .45
  P = 1.0
  RG = 82.06
  MNO = 30.
  MCO = 28.
  MH2 = 2.
  T = 1.987*TREF
  GAMM1 = 9400./T
  GAMM2 = 10300./T
  EPSIC1 = 8200./T
  EPSIN1 = 7600./T
  EPSIH2 = -15400./T
  EPSIN2 = -13300./T
  ALPHN1 = .064*P*EXP(EPSIN1)*MBAR/MNO
  ALPHC1 = .076*P*EXP(EPSIC1)*MBAR/MCO
  ALPHN2 = 310000.*P*EXP(EPSIN2)*MBAR/MNO
  ALPHH2 = 450000.*P*EXP(EPSIH2)*MBAR/MH2
  PR = .766
  C1 = 2.42*(PR)**.333
  C2 = .129*(PR)**.4
  C3 = 1.4
  SC = .713
```

```
      D1 = 2.42*(SC)**.333
      D2 = .129*(SC)**.4
      D3 = 1.4
      K1TREF = 48.*EXP(-GAMM1)
      K2TREF = 1.39*EXP(-GAMM2)
      KRATIO = K2TREF/K1TREF
      AS1 = -DELTH1*K1TREF/(60.*CS)
      AS2 = -DELTH2*K2TREF/(60.*CS)
      READ 5,CELLN,DELTT,NPRINT
    5 FORMAT(F6.3,5X,E15.8,5X,I8)
      NSTEP = 248
      RPART = DPART/2.
      NSTEP = NSTEP + 1
      VN = VTOTL/CELLN
      W1 = 6.*(1. - EPSBED)*VN/DPART
      W2 = MBAR*CF/(60.*359.05/453.59)
      AS = W2/((1. - EPSBED)*VN*RHOP*CS)
      BS1 = RHOP*K1TREF*RPART*RPART*RG
      BS1 = BS1/(60.*DIFFEP*P*MBAR)
      BS2 = BS1 *KRATIO
      DS1 = (1. - EPSBED)*VN*359.05*MNO*RHOP*K1TREF
      DS1 = DS1/(453.59*MBAR)
      DS2 = DS1*KRATIO
      RTUBE = 13.97
      AREA = 3.1415926*RTUBE*RTUBE
      REC = 453.59*MBAR/(60.*359.05*AREA)
      G = 18.11
      CS1 = DS1/G
      CS2 = DS2/G
      TGNEW(1) = 107.
      TSNEW(1) = 0.0
      VIS = VISCOS(1,TGNEW(1))
      RE = REC*(G*DPART/VIS)
      CPN = CPNO(TGNEW(1))
      NU = FCN(RE,C1,C2,C3)
      KGM = KGMIX(VIS,CPN)
```

```
      HT = KGM*NU/DPART
      HOT = 1./HT + DPART/(10.*KPEFF)
      HOT = 1./HOT
      SH = FCN(RE,D1,D2,D3)
      DIFFE = DIF(TGNEW(1))
      DRAT = DIFFE/DIFFEP
      NCELL = CELLN + 1.
      X1 = W1*HOT + W2*G
      X2 = G*HOT*AS*W1/X1
      ITINO = 1
      ITICO = 1
      ANO = GNOG(2,1)*MNO/MBAR
      BNO = GNOG(3,1)*MNO/MBAR
      ANO = ANO/1.E+06
      BNO = BNO/1.E+06
      ACO = GCOG(2,1)
      BCO = GCOG(3,1)
      ACO = ACO/100.
      BCO = BCO/100.
      READ 6,(TICONL(J),J=1,11)
    6 FORMAT(5X,F5.1)
      ICYCL1 = 1
      TIME = 0.0
      ITIM1 = 0
      TCHEK = 0.0
      READ 7,(TSOLD(J),J=1,NCELL)
    7 FORMAT(E15.8)
      TGOLD(1) = TGNEW(1)
      DO 28 J=2,NCELL
   28 TGOLD(J) = TSOLD(J)
      DO 8 I=1,NCELL
      AR1OLD(I) = 0.0
    8 AR2OLD(I) = 0.0
      TKO = -20.
      CALL SECOND(TSTAR1)
      DO 25 I=1,NSTEP
```

```
      DELT = DELTT
      IF(TKO .EQ. 30.) DELT=1.5
      IF(TKO .EQ. 31.5) DELT = 2.5
      IF(TKO .EQ. 34. .OR. TKO .EQ. 45. ) DELT = 1.0
      IF(TKO .EQ. 49. .OR. TKO .EQ. 104.) DELT = 1.0
      IF(TKO .EQ. 129.) DELT = 1.0
      IF(TKO .EQ. 46.) DELT = 3.0
      IF(TKO .EQ. 85. .OR. TKO .EQ. 87.5) DELT = 2.5
      IF(TKO .EQ. 100. .OR. TKO .EQ. 125.) DELT = 4.0
      IF(135. .EQ. TKO ) DELT = 2.
      TIME = TIME + DELT
      KT = (TIME - 20.)/137.
      TK = (TIME-20.) - FLOAT(KT)*137.
      IF(TIME .LE. 20.) GO TO 11
      IF(TK-TKO .LT. 0.0) GO TO 9
      TKO = TK
      IF(TK .LE. TCHEK) GO TO 71
      ITIM1 = ITIM1 + 1
      TCHEK = TICONL(ITIM1)
      GO TO 10
    9 ICYCL1 = ICYCL1 + 1
      TKO = TK
      ITIM1 = 1
      TCHEK = TICONL(ITIM1)
      ITINO = 1
      ITICO = 1
      ACO = GCOG(2,ITICO)
      BCO = GCOG(3,ITICO)
      ACO = ACO/100.
      BCO = BCO/100.
      ANO = GNOG(2,ITINO)*MNO/MBAR
      BNO = GNOG(3,ITINO)*MNO/MBAR
      ANO = ANO/1.E+06
      BNO = BNO/1.E+06
   10 G = GVECTO(ICYCL1,ITIM1,2)
      CS1 = DS1/G
```

```
      CS2 = DS2/G
      TGNEW(1) = GVECTO(ICYCL1,ITIM1,1)
      TGOLD(1) = TGNEW(1)
      VIS = VISCOS(1,TGNEW(1))
      RE = REC*(G*DPART/VIS)
      NU = FCN(RE,C1,C2,C3)
      CPN = CPNO(TGNEW(1))
      KGM = KGMIX(VIS,CPN)
      HT = KGM*NU/DPART
      HOT = 1./HT + DPART/(10.*KPEFF)
      HOT = 1./HOT
      SH = FCN(RE,D1,D2,D3)
      DIFFE = DIF(TGNEW(1))
      DRAT = DIFFE/DIFFEP
      X1 = W1*HOT + W2*G
      X2 = G*HOT*AS*W1/X1
   71 IF(TK .LT. GNOG(1,ITINO)) GO TO 20
      ITINO = ITINO + 1
      ANO = GNOG(2,ITINO)*MNO/MBAR
      BNO = GNOG(3,ITINO)*MNO/MBAR
      ANO = ANO/1.E+06
      BNO = BNO/1.E+06
   20 IF(TK.LT. GCOG(1,ITICO)) GO TO 11
      ITICO = ITICO + 1
      ACO = GCOG(2,ITICO)
      BCO = GCOG(3,ITICO)
      ACO = ACO/100.
      BCO = BCO/100.
   11 IF(TK .LT. 0.) TK = 0.0
      FCO = .233
      FNO = 3.69
      GICO(1) =(ACO + BCO*TK)*FCO
      GINO(1) =(ANO + BNO*TK)*FNO
      GIH2(1) = GICO(1)/3.8*MH2/MCO
      IZERO = 0
      DO 12 IV=2,NCELL
```

```
      IF(IZERO .EQ. 1) GO TO 40
      RTOLD(IV) = RIGHT(G   ,HOT ,TGOLD(IV-1),TSOLD(IV),AR1OLD(IV),
     1 AR2OLD(IV))
      TSP = TSOLD(IV) + RTOLD(IV)*DELT
      CALL PARTIC(TSP,GINO(IV-1),GICO(IV-1),GIH2(IV-1),SH,AR1INT,AR2INT,
     1 1)
   29 TSPP = RIGHT(G,HOT,TGNEW(IV-1),TSP,AR1INT,AR2INT)
      TSNEW(IV) = TSOLD(IV) + DELT /2.*(TSPP+RTOLD(IV))
      TSOLD(IV) = TSNEW(IV)
      CALL PARTIC(TSNEW(IV),GINO(IV-1),GICO(IV-1),GIH2(IV-1),SH,
     1 AR1OLD(IV),AR2OLD(IV),1)
      GINO(IV) = GINO(IV-1) - (CS1*AR1OLD(IV) + CS2*AR2OLD(IV))
      IF(GINO(IV) .LT. 0.0) GINO(IV) = 0.0
      GICO(IV) = GICO(IV-1) - MCO/MNO*CS1*AR1OLD(IV)
      GIH2(IV) = GIH2(IV-1) - MH2/MNO*(GINO(IV-1) - GINO(IV)) + MH2/MCO*
     1 (GICO(IV-1) - GICO(IV))
      IF(GINO(IV) .EQ. 0.0) IZERO = 1
   31 TGNEW(IV) = (W1*HOT*TSNEW(IV) + W2*G*TGNEW(IV-1))/X1
      GO TO 12
   40 AR1OLD(IV) = 0.0
      AR2OLD(IV) = 0.0
      RTOLD(IV) = RIGHT(G   ,HOT ,TGOLD(IV-1),TSOLD(IV),0.0,0.0)
      TSP = TSOLD(IV) + RTOLD(IV)*DELT
      GINO(IV) = GINO(IV-1)
      GICO(IV) = GICO(IV-1)
      GIH2(IV) = GIH2(IV-1)
      TSPP = RIGHT(G,HOT,TGNEW(IV-1),TSP,0.0,0.0)
      TSNEW(IV) = TSOLD(IV) + DELT/2.*(TSPP + RTOLD(IV))
      TSOLD(IV) = TSNEW(IV)
      TGNEW(IV) = (W1*HOT*TSNEW(IV) + W2*G*TGNEW(IV-1))/X1
   12 CONTINUE
      DO 30 IV=1,NCELL
   30 TGOLD(IV) = TGNEW(IV)
      IF(MOD(I,NPRINT) .NE. 0) GO TO 25
      CALL SECOND(TSTAR2)
      TSTAR3 = TSTAR2 - TSTAR1
```

```
26 PRINT 21,TIME
   PRINT 21,TSTAR3
21 FORMAT(1H0,5X,7HTIME = ,F7.2)
   DO 24 J=1,NCELL
   PRINT 22,J,TGNEW(J),GINO(J),GICO(J)
22 FORMAT(1H0,5X7HCELL = ,I6,5X,5HTG = ,F9.2,5X,6HGNO = ,F8.6,5X,
  1 6HGCO = ,F7.6)
   PRINT 23,TSNEW(J),AR1OLD(J),AR2OLD(J)
23 FORMAT(1H0,5X,5HTS = ,F9.2,9HAVE. R1 = ,E15.8,5X,9HAVE. R2 = ,
  1 E15.8)
24 CONTINUE
   TSTAR1 = TSTAR2
   IF(ABORT .EQ. 1.) GO TO 27
25 CONTINUE
27 STOP
   END
```

```
      FUNCTION VISCOS(I,T)
      DIMENSION VI(10),TP(10),C(4)
      IF(I .GT. 0) GO TO 5
      READ 1,NPT
    1 FORMAT(I8)
      READ 2,(VI(K),TP(K),K=1,NPT)
    2 FORMAT(E15.8,2X,F8.2)
      DO 3 K=1,4
    3 C(K) = 0.0
      DO 4 K=1,NPT
      C(1) = C(1) + VI(K)
      C(2) = C(2) + TP(K)
      C(3) = C(3) + VI(K)*TP(K)
    4 C(4) = C(4) + TP(K)*TP(K)
      DETM = NPT*C(4) - C(2)*C(2)
      A = (C(4)*C(1) - C(2)*C(3))/DETM
      B = (-C(2)*C(1) + NPT*C(3))/DETM
      GO TO 6
    5 VISCOS = A + B*T
    6 RETURN
      END
```

```
      FUNCTION RIGHT(G,HOT,TGIM1,TIS,AR1,AR2)
      COMMON/FCU/AS,W1,W2,AS1,AS2
      RIGHT = (G*HOT*AS*W1)*(TGIM1 - TIS)/(W1*HOT + W2*G) + AS1*AR1 +
     1 AS2*AR2
      RETURN
      END
```

```
      SUBROUTINE PARTIC(TSI,GINO,GICO,GIH2,SH,AR1,AR2,IT)
      COMMON/PAR/WNO,WCO,BS1,BS2,DRAT,WH2,ABORT,CS1,CS2
      DIMENSION G(12,12),A(6),B(6,6),WT(6),FVEC(12),GNO(6),GCO(6),GH2(6)
     1,SAVE(6,6),X(6)
      EPS = 1.E-3
      SWT = 1./3.
      ABORT = 1.0
      IF(IT.EQ. 1) GO TO 4
      READ 1,NPTS
    1 FORMAT(I8)
      NS = NPTS + 1
      KS = 2*NS
      DO 3 I=1,NS
      READ 2,(B(I,J),J=1,NS)
    2 FORMAT(4E20.9)
    3 CONTINUE
      READ 2,(A(I),I=1,NS)
      READ 2,(WT(I),I=1,NS)
      READ 2,(X(I),I=1,NS)
      GO TO 15
    4 CON = SH/2.*DRAT
      CALL RXN1(R1,RNO1,RCO1,GINO,GICO,TSI,2)
      ARG = SQRT(R1/GINO*BS1*WNO*(TSI+273.1))
      X1 = EXP(ARG)
      X2 = 1./X1
      COSHO = (X1+X2)/2.
      SINHO = (X1-X2)/2.
      CONST = GINO*CON/(ARG*COSHO+SINHO*(CON-1.))
      DO 16 I=1,NS
      X1 = EXP(ARG*X(I))
      X2 = 1./X1
      SINHR = (X1-X2)/2.
   16 GNO(I) = CONST*SINHR/X(I)
      ISLIP = 0
      DO 5 I=1,NS
      GCO(I) = GICO -WCO/WNO*(GINO - GNO(I))
```

```
5 GH2(I) = GIH2 + WH2/WNO*(GNO(I) - GINO) - WH2/WCO*(GCO(I) - GICO)
  DO 14 ITER=1,20
  DO 6 I=1,KS
  DO 6 J=1,KS
6 G(I,J) = 0.0
  DO 7 I=1,NS
  G(NS,I) = A(I)
7 G(KS,NS+I) = A(I)
  G(NS,NS) =  G(NS,NS) + CON
  G(KS,KS) = G(NS,NS)
  FVEC(NS) = CON*GINO
  FVEC(KS) = CON*GICO
  DO 8 I=1,NPTS
  DO 8 J=1,NS
  G(I,J) = B(I,J)
8 G(NS+I,NS+J) = B(I,J)
  DO 9 I=1,NS
  CALL RXN1(R1,RNO1,RCO1,GNO(I),GCO(I),TSI,ISLIP)
  CALL RXN2(R2,RNO2,RCO2,GNO(I),GH2(I),TSI,ISLIP)
  ISLIP = 1
  SAVE(1,I) = R1
  SAVE(2,I) = R2
  SAVE(3,I) = RNO1
  SAVE(4,I) = RCO1
  SAVE(5,I) = RNO2
  SAVE(6,I) = RCO2
  IF(I .EQ. NS) GO TO 9
  G(I,I) = G(I,I) - WNO*(TSI+273.1)*(BS1*RNO1+BS2*RNO2)
  G(I,NS+I) = -WNO*(TSI+273.1)*(BS1*RCO1+BS2*RCO2)
  FVEC(I) = WNO*(TSI+273.1)*(BS1*(R1-RNO1*GNO(I)-RCO1*GCO(I))+BS2*(
 1 R2-RNO2*GNO(I)-RCO2*GCO(I)))
  G(NS+I,I) = -WCO*(TSI+273.1)*BS1*RNO1
  G(NS+I,NS+I) = G(NS+I,NS+I) - WCO*(TSI+273.1)*BS1*RCO1
  FVEC(NS+I) = WCO*(TSI+273.1)*BS1*(R1-RNO1*GNO(I)-RCO1*GCO(I))
9 CONTINUE
  SUM1 = 0.0
```

```
      SUM2 = 0.0
      DO 17 I=1,NS
      SUM1 = SUM1 + WT(I)*SAVE(1,I)
   17 SUM2 = SUM2 + WT(I)*SAVE(2,I)
      FVEC(NS) = FVEC(NS) - CON*CS1/SWT*SUM1 - CON*CS2/SWT*SUM2
      FVEC(KS) = FVEC(KS) - CON*CS1/SWT*SUM1*WCO/WNO
      SUM1 = 0.0
      SUM2 = 0.0
      SUM3 = 0.0
      SUM4 = 0.0
      DO 18 I=1,NS
      SUM1 = SUM1 + WT(I)*SAVE(3,I)*GNO(I)
      SUM2 = SUM2 + WT(I)*SAVE(4,I)*GCO(I)
      SUM3 = SUM3 + WT(I)*SAVE(5,I)*GNO(I)
      SUM4 = SUM4 + WT(I)*SAVE(6,I)*GCO(I)
      G(NS,I) = G(NS,I) + CON*(CS1/SWT*WT(I)*SAVE(3,I) + CS2/SWT*WT(I)*
     1 SAVE(5,I))
      G(NS,NS+I) = CON*(CS1/SWT*WT(I)*SAVE(4,I) + CS2/SWT*WT(I)*SAVE(6,I
     1))
      G(KS,I) = CON*CS1/SWT*WT(I)*SAVE(3,I)*WCO/WNO
   18 G(KS,NS+I) = G(KS,NS+I) + CON*CS1/SWT*WT(I)*SAVE(4,I)*WCO/WNO
      FVEC(NS) = FVEC(NS) + CON/SWT*(CS1*(SUM1+SUM2) + CS2*(SUM3+SUM4))
      FVEC(KS) = FVEC(KS) + CON/SWT*CS1*(SUM1+SUM2)*WCO/WNO
      CALL INVR(G,KS,FVEC,1,DETERM,12,12)
      DO 10 I=1,NS
      IF(ABS(FVEC(I)-GNO(I)).GT.EPS*ABS(FVEC(I)))GO TO 12
      IF(ABS(FVEC(NS+I) - GCO(I)) .GT. EPS*FVEC(NS+I)) GO TO 12
   10 CONTINUE
      AR1 = 0.0
      AR2 = 0.0
      DO 11 I=1,NS
      AR1 = AR1 + WT(I)*SAVE(1,I)
   11 AR2 = AR2 + WT(I)*SAVE(2,I)
      AR1 = AR1/SWT
      AR2 = AR2/SWT
      ABORT = 0.0
```

```
      GO TO 15
   12 DO 13 I=1,NS
      GNO(I) = FVEC(I)
      GCO(I) = FVEC(NS+I)
   13 GH2(I) = GIH2 + WH2/WNO*(GNO(I)-GINO) - WH2/WCO*(GCO(I)-GICO)
   14 CONTINUE
   15 RETURN
      END
```

```
      SUBROUTINE RXN1(R1,RNO1,RCO1,GNO,GCO,TSI,ISLIP)
      COMMON/RXNS/TREF,GAMM1,GAMM2,EPSIC1,EPSIN1,EPSIH2,EPSIN2,ALPHN1,
     1 ALPHC1,ALPHN2,ALPHH2
      IF(ISLIP .EQ. 1) GO TO 1
      X1 = EXP((-GAMM1+EPSIC1+EPSIN1)*(TREF/(TSI+273.) - 1.))
      X2 = EXP(EPSIC1*(TREF/(TSI+273.) - 1.))
      X3 = EXP(EPSIN1*(TREF/(TSI+273.) - 1.))
    1 R1 = ALPHN1*ALPHC1*X1*GNO*GCO
      X4 = 1. + ALPHC1*X2*GCO + ALPHN1*X3*GNO
      X5 = X4*X4
      R1 = R1/X5
      IF(ISLIP .EQ. 2) GO TO  2
      RNO1 = R1/GNO-2.*R1/X4*ALPHN1*X3
      RCO1 = R1/GCO-2.*R1/X4*ALPHC1*X2
    2 RETURN
      END
```

```
      SUBROUTINE RXN2(R2,RNO2,RCO2,GNO,GH2,TSI,ISLIP)
      COMMON/RXNS/TREF,GAMM1,GAMM2,EPSIC1,EPSIN1,EPSIH2,EPSIN2,ALPHN1,
     1 ALPHC1,ALPHN2,ALPHH2
      IF(ISLIP .EQ. 1) GO TO 1
      X1 = EXP((-GAMM2+EPSIH2+EPSIN2)*(TREF/(TSI+273.) - 1.))
      X2 = EXP(EPSIN2*(TREF/(TSI+273.) - 1.))
      X3 = EXP(EPSIH2*(TREF/(TSI+273.) - 1.))
    1 R2 = ALPHN2*ALPHH2*X1*GNO*GH2
      X4 = 1. + ALPHN2*X2*GNO + ALPHH2*X3*GH2
      X5 = X4*X4
      R2 = R2/X5
      IF(ISLIP .EQ. 2) GO TO  2
      X6 = R2/GNO - 2.*R2/X4*ALPHN2*X2
      X7 = R2/GH2 - 2.*R2/X4*ALPHH2*X3
      RNO2 = X6 + X7*2./30.
      RCO2 = -X7*2./28.
    2 RETURN
      END
```

```
      SUBROUTINE INVR(A,N,B,M,DETERM,ISIZE,JSIZE)
      DIMENSION IPIVOT(100),A(ISIZE,JSIZE),B(ISIZE,M),INDEX(100,2),
     1PIVOT(100)
      EQUIVALENCE (IROW,JROW),(ICOLUM,JCOLUM),(AMAX,T,SWAP)
C
   10 DETERM=1.0                                                    INVR  10
   15 DO 20 J=1,N                                                   INVR  11
   20 IPIVOT(J)=0                                                   INVR  12
   30 DO 550 I=1,N                                                  INVR  13
C                                                                   INVR  14
C     SEARCH FOR PIVOT ELEMENT                                      INVR  15
C                                                                   INVR  16
   40 AMAX=0.0                                                      INVR  17
   45 DO 105 J=1,N                                                  INVR  18
   50 IF (IPIVOT(J)-1) 60, 105, 60                                  INVR  19
   60 DO 100 K=1,N                                                  INVR  20
   70 IF (IPIVOT(K)-1) 80, 100, 740                                 INVR  21
 80   IF(ABS(AMAX)-ABS(A(J,K)))85,100,100                          INVR  22
   85 IROW=J                                                        INVR  23
   90 ICOLUM=K                                                      INVR  24
   95 AMAX=A(J,K)                                                   INVR  25
  100 CONTINUE                                                      INVR  26
  105 CONTINUE                                                      INVR  27
  110 IPIVOT(ICOLUM)=IPIVOT(ICOLUM)+1                               INVR  28
C                                                                   INVR  29
C     INTERCHANGE ROWS TO PUT PIVOT ELEMENT ON DIAGONAL             INVR  30
C                                                                   INVR  31
  130 IF (IROW-ICOLUM) 140, 260, 140                                INVR  32
  140 DETERM=-DETERM                                                INVR  33
  150 DO 200 L=1,N                                                  INVR  34
  160 SWAP=A(IROW,L)                                                INVR  35
  170 A(IROW,L)=A(ICOLUM,L)                                         INVR  36
  200 A(ICOLUM,L)=SWAP                                              INVR  37
  205 IF(M) 260, 260, 210                                           INVR  38
  210 DO 250 L=1, M                                                 INVR  39
  220 SWAP=B(IROW,L)                                                INVR  40
                                                                    INVR  41
```

```
  230 B(IROW,L)=B(ICOLUM,L)                                          INVR  42
  250 B(ICOLUM,L)=SWAP                                               INVR  43
  260 INDEX(I,1)=IROW                                                INVR  44
  270 INDEX(I,2)=ICOLUM                                              INVR  45
  310 PIVOT(I)=A(ICOLUM,ICOLUM)                                      INVR  46
  320 DETERM=DETERM*PIVOT(I)                                         INVR  47
C                                                                    INVR  48
C     DIVIDE PIVOT ROW BY PIVOT ELEMENT                              INVR  49
C                                                                    INVR  50
  330 A(ICOLUM,ICOLUM)=1.0                                           INVR  51
  340 DO 350 L=1,N                                                   INVR  52
  350 A(ICOLUM,L)=A(ICOLUM,L)/PIVOT(I)                               INVR  53
  355 IF(M) 380, 380, 360                                            INVR  54
  360 DO 370 L=1,M                                                   INVR  55
  370 B(ICOLUM,L)=B(ICOLUM,L)/PIVOT(I)                               INVR  56
C                                                                    INVR  57
C     REDUCE NON-PIVOT ROWS                                          INVR  58
C                                                                    INVR  59
  380 DO 550 L1=1,N                                                  INVR  60
  390 IF(L1-ICOLUM) 400, 550, 400                                    INVR  61
  400 T=A(L1,ICOLUM)                                                 INVR  62
  420 A(L1,ICOLUM)=0.0                                               INVR  63
  430 DO 450 L=1,N                                                   INVR  64
  450 A(L1,L)=A(L1,L)-A(ICOLUM,L)*T                                  INVR  65
  455 IF(M) 550, 550, 460                                            INVR  66
  460 DO 500 L=1,M                                                   INVR  67
  500 B(L1,L)=B(L1,L)-B(ICOLUM,L)*T                                  INVR  68
  550 CONTINUE                                                       INVR  69
C                                                                    INVR  70
C     INTERCHANGE COLUMNS                                            INVR  71
C                                                                    INVR  72
  600 DO 710 I=1,N                                                   INVR  73
  610 L=N+1-I                                                        INVR  74
  620 IF (INDEX(L,1)-INDEX(L,2)) 630, 710, 630                       INVR  75
  630 JROW=INDEX(L,1)                                                INVR  76
  640 JCOLUM=INDEX(L,2)                                              INVR  77
```

```
650 DO 705 K=1,N                                                    INVR  78
660 SWAP=A(K,JROW)                                                  INVR  79
670 A(K,JROW)=A(K,JCOLUM)                                           INVR  80
700 A(K,JCOLUM)=SWAP                                                INVR  81
705 CONTINUE                                                        INVR  82
710 CONTINUE                                                        INVR  83
740 RETURN                                                          INVR  84
     END                                                            INVR  85
```

The following is a complete set of typical input data for the mathematical model of the NO_x convertor:

```
   2
-.156699620E+002     .200348780E+002    -.436491670E+001
 .996512165E+001    -.443300380E+002     .343649170E+002
 .269328550E+002    -.869328550E+002     .600000000E+002
 .169677300E+001    -.106967730E+002     .900000000E+001
 .949059000E-001     .190808400E+000     .476190500E-001
 .468849000E+000     .830224000E+000     .100000000E+001
   5
.25300000E-003    255.
.28800000E-003    360.
.32800000E-003    490.
.35500000E-003    588.
.41200000E-003    800.
     298.          16.12
     450.          49.24
     570.          76.84
     560.          49.24
     558.          40.41
     642.          18.33
     530.          17.62
     619.          45.48
     753.          81.69
     863.          18.33
     693.          14.79
```

642.	13.91
719.	38.64
826.	69.55
818.	41.95
783.	33.34
850.	17.88
733.	17.09
780.	43.06
924.	82.80
961.	18.33
825.	14.79
781.	13.91
854.	44.82
935.	73.75
897.	42.39
875.	33.12
861.	18.11
811.	15.72
853.	38.86
976.	81.03
952.	18.11
869.	14.79
831.	13.91
894.	37.76
960.	64.69
925.	44.16
894.	33.12
881.	17.88
845.	17.05
899.	43.06
987.	77.28
932.	18.77
874.	14.79
841.	14.28
895.	39.08
968.	66.24

```
926.          40.41
904.          30.25
884.          18.33
855.          16.82
909.          40.85
988.          77.06
929.          18.77
875.          14.79
844.          14.35
896.          38.64
962.          65.13
930.          37.09
900.          31.57
890.          18.11
865.          15.59
898.          42.39
982.          76.17
925.          18.11
881.          14.79
848.          14.35
895.          40.41
970.          65.13
915.          40.63
904.          33.12
891.          18.33
858.          17.00
908.          40.41
983.          76.17
924.          18.77
887.          14.79
  19.2000       180.0000     00000.0000
  35.0000     -1368.5000     00080.5000
  41.0000     07227.0000      -165.0000
  52.0000     00510.0000
  76.0000     00180.0000
 106.0000     01220.0000
```

```
      137.0000      00180.0000
       25.0000      00000.74
       36.0000         -6.726          .285
       42.             19.0944        -.432
       52.2            -3.8418         .114
       60.              9.6336        -.144
       77.1             3.0341        -.0339
       90.             -4.6045         .0798
      105.0000          2.5800
      107.8           -70.5048          .696
      114.6            51.7278         -.438
      124.8            10.6475         -.0794
      137.0000           .4200
4.          5.00000000E+000              1
     20.
     31.5
     34.
     46.
     49.
     60.
     75.
     87.5
    104.
    129.
    137.
.27000000E+002
.27000000E+002
.27000000E+002
.27000000E+002
.27000000E+002
```